PHD

Reactor design: compact and catalytic for speciality chemicals

Al Badran, Firas

Award date:
2011

Awarding institution:
University of Bath

REACTOR DESIGN: COMPACT & CATALYTIC FOR SPECIALITY CHEMICALS

FIRAS AL BADRAN

A thesis is submitted for the degree of Doctor of Philosophy

University of Bath

Department of Chemical Engineering

October 2011

Dedicated to the memory of Assistant Prof. Elham Hashem

بسم الله الرحمن الرحيم

لَقَدْ مَنَّ اللَّهُ عَلَى الْمُؤْمِنِينَ إِذْ بَعَثَ فِيهِمْ رَسُولًا مِنْ أَنْفُسِهِمْ يَتْلُو عَلَيْهِمْ آيَاتِهِ وَيُزَكِّيهِمْ وَيُعَلِّمُهُمُ الْكِتَابَ وَالْحِكْمَةَ وَإِنْ كَانُوا مِنْ قَبْلُ لَفِي ضَلَالٍ مُبِينٍ

صدق الله العلي العظيم

ال عمران ﴿١٦٤﴾

In the name of Allah, the Most Gracious, the most Merciful

Allah did confer a great favour on the Believers when He sent among them a Messenger from among themselves, rehearsing unto them the Signs of Allah, sanctifying them, and instructing them in Scripture and Wisdom, while before that, they had been in manifest error.

Quran: AL-I-Imran (3:164)

Abstract

When speciality chemicals are manufactured within the pharmaceutical industry, they are often produced in stirred batch/semi-batch reactors. A 'methodology' was explored, to help with the development of continuous fixed-bed catalytic reactors for this sector. This was tested on two different types of model reactions:

(a) In the first, the viability of producing tertiary amines *via* 'borrowing hydrogen' was explored, and the reaction of morpholine and benzyl alcohol was studied, on Ru and Pt catalysts. This provided an opportunity for an early involvement in small-scale batch testing of catalysts, and then experiments were performed with the catalyst supported on granules in a packed bed (i.d. = 7 mm, length = 300 mm). Although it was shown that continuous processing is viable, and that high conversions (e.g. 73 to 98%, at 150 ºC) could be achieved, unfortunately further work was necessary to identify a more robust catalyst system, before moving on to pilot-scale trials.

(b) In the second, the partial oxidation of benzyl alcohol to benzaldehyde was studied, using a Pt catalyst on a carbon support. This proved to be successful, and the reaction was finally demonstrated at pilot-scale. Carbon monoliths were used as catalyst supports (monolith o.d. = 19 mm; length = 50 mm long; square 0.7 mm x 0.7 mm channels; catalyst loading 2.5 and 2.7 wt% Pt). With a liquid flow of 1 L h^{-1} and a reactant concentration of ~1 mol L^{-1}, operating at 110 ºC, conversion ranged from 80 to 90% and selectivity from 65 to 99%. The catalyst system was tested for 160 h of operation, and retained its performance.

While testing the 2nd reaction, a pilot-scale reactor was also developed, which could be used for a variety of novel reactions. The design was flexible and it was easy to insert and remove the catalytic monoliths.

Acknowledgments

First and before everything, I would like to express my great thanks to Allah for his mercy and blessing.

I would like to express my sincere gratitude to my supervisor Professor Stan Kolaczkowski for his over-seeing, guidance, commitment, patience and suggestions which were of great value to myself and were very helpful for the this work so it can be done.

I would like to extend my grateful thanks to the following people for their help in compiling this thesis:

- Dr. Gareth Lamb and Professor Jonathan Williams for all their help in the work described in Chapter 3.
- Dr. Pawel Plucinski for advice in catalyst coating methods and using the GC apparatus.
- Professor Gary Hawley, Heatric (Division of Meggitt) UK Ltd., Great Western Research (GWR) Project 387, and the Ministry of Higher Education and Scientific Research in Iraq for financial support.
- F. Acosta, J. Bishop, R. Brain, S. Hurley, R. Bull, and P. Frith for their kind technical support in helping with the experimental work.
- U. Potter, A. O' Reilly, J. Mitchell in CEOS, for work on SEM and TEM imaging.
- MAST Carbon Ltd. (UK), for supplying the carbon monoliths.

I would also like to express my appreciation to the research team; Dr Serpil Awdry, Dr. Y.H Yap, and Dr. Umi Asli for their useful discussion, advice and friendship over the period I was in Bath.
Finally, my special gratitude to my beloved family and friends for their precious encouragement and support.

List of Figures

Chapter 1

Chapter 2

Chapter 3

Chapter 4

Chapter 5

Chapter 6

List of Tables

Chapter 4

Chapter 5

Nomenclature

a	external surface area, m^2.
A	Pre-exponential factor, units vary.
C_A	concentration of alcohol , mol L^{-1}.
$c_{A_\circ}$	initial concentration of alcohol, mol L^{-1}.
c_{Ae}	final concentration of alcohol, mol L^{-1}.
C_{b-ald}	concentration of benzaldehyde, mol L^{-1}.
$[Cat]_{tot}$	total catalyst sites.
$C_{BA,s}$	benzyl alcohol concentration at the catalyst surface, mol L^{-1}.
$C_{BA,b}$	benzyl alcohol concentration in the bulk liquid, mol L^{-1}.
$C_{O_2,s}$	oxygen concentration at the catalyst surface, mol L^{-1}.
$C_{O_2,b}$	oxygen concentration in the bulk liquid, mol L^{-1}.
C_{BA}	concentration of benzyl alcohol, mol L^{-1}.
C_{BH}	concentration of benzaldehyde, mol L^{-1}.
$C(t)$	concentration of the tracer as function of time, g L^{-1}.
D_{BA}	diffusivity of benzyl alcohol, m^2 s^{-1}.
E_a	Activation energy, J mol^{-1}.
$E(t)$	residence time distribution function, s^{-1}.
F_L	volumetric flow rate of liquid, L h^{-1}.
h	total length of the reactor, m.
H	Henry's constant, bar.
k_s	reaction rate constant, mol^{1-n} m^{n-1} s^{-1}.
k	rate constant, units vary.
k	rate of catalyst deactivation, h^{-1}.
k_{Am}	mass transfer coefficients in the liquid phase, mol s^{-1}.
K_A	the adsorption equilibrium constant of alcohol at the catalytic surface.
m_{cat}	weight of the catalyst, g.
Mw_{Ru}	atomic weight of ruthenium, g mol^{-1}.
Mw_{pt}	atomic weight of platinum, g mol^{-1}.
m_{Pt}	mass of metallic platinum, g.
m_{Ru}	mass of metallic ruthenium, g.
n	over all reaction order.

n_{BA}	number of moles of benzyl alcohol, mol.
$n_{BA,in}$	initial number of moles of benzyl alcohol, mol.
$n_{BA,out}$	final number of moles of benzyl alcohol, mol.
N_{tracer}	amount of the tracer, g.
$N``_{BA}$	mass flux of benzyl alcohol, mol m^{-2} s^{-1}.
N_{BA}	mass transfer rate of benzyl alcohol, mol s^{-1}.
P_T	total pressure, bar.
P_{O_2}	partial pressure of oxygen, bar.
r	radius of the catalyst support particle, m.
$-r_A$	reaction rate, mol g^{-1} s^{-1}.
$-r_{BA}$	surface reaction rate, mol m^{-3} s^{-1}.
$-r_{BA}$	experimental reaction rate, mol g_{cat}^{-1} s^{-1}.
R	universal gas constant (8.314), J mol^{-1} K.
t	time, s.
t_m	mean residence time, s.
T	temperature, K.
u_s	superficial velocity of the liquid phase, m s^{-1}.
v	volumetric flow rate, L s^{-1}.
V	reactor volume, L.
x_{O_2}	mole fraction of oxygen in the liquid phase.
X_{BA}	fractional conversion of benzyl alcohol.
y_{O_2}	mole fraction of the oxygen in the gas phase.
z	actual lenth of the reactor, m.

Greek symbols

ρ_b	bulk density of the catalyst in a channel, g L^{-1}.
ρ_m	molar density of liquid feed stock, mol L^{-1}.
τ	average residence time, s.
α	reaction order with respect to benzyl alcohol.
β	reaction order with respect to oxygen.

CHAPTER 1

INTRODUCTION

Speciality chemicals are used in the pharmaceutical industry and these types of chemical are also produced by them (as drugs are developed).

In this chapter the motivation and resistance faced in moving from batch to continuous processing in the pharmaceutical industry is explored. This leads to a consideration of methodologies to facilitate that process, which is an important consideration in this PhD thesis.

1.1 Background

The pharmaceutical industry is a highly regulated industry and all production must be carried out in accordance with good manufacturing practice (Plumb, 2005).

Pharmaceutical products are organic or inorganic which are chemicals synthesized and then converted into an easily administrable dosage form for human consumption. This conversion can involve combining the active ingredient with inert materials to facilitate dispensing of the drug (Girish 2005).

According to Girish (2005):

> For safety reasons, active pharmaceutical ingredients (APIs) have to be manufactured using methods outlined in the FDA's (Food and Drug Administration) "Guideline on General Principles of Process Validation". A review of these guidelines indicates a basic assumption that most APIs are produced by batch processes.

The slant in these guidelines is toward batch processes rather than continuous processes, there is no mention of continuous processes in the FDA guidelines (Girish 2005). Therefore, the pharmaceutical industry has relied traditionally on stirred tank reactors, generally operated in batchwise mode (Stitt, 2002), in spite of cost disadvantages and the fact that in many cases continuous processing could lead to the manufacture of a purer product (Plumb, 2005).

Pellek and Van Arnum (2009), mentioned that the current Food and Drug Administration (FDA) regulations do not distinguish between batch and continuous manufacturing because the world 'batch' can mean either the mode of manufacturing or the quantity of material being processed, where the regulations specify:

> *"A batch means a specific quantity of a drug or other material that is intended to have uniform character and quality, within specified acceptance limits, and is produced according to a single manufacturing order during the same cycle of manufacture".*

This means that the definition of 'batch' refers to the quantity of material and does not specify the mode of manufacturing, therefore the manufacturer should not be dissuaded from applying continuous processing based on the prevalence of the word 'batch' in the regulation.

Given the regulatory framework for continuous processing, the key question is whether it offers technical and economic benefits compared with batch manufacturing.

According to Roberge *et al.,* (2005), there are two major advantages that can be associated with batch or semi-batch processes over the continuous counterpart:

(i) The flexibility and versatility of the equipment: a reaction vessel is flexible because it can easily accommodate miscellaneous reaction kinetics.
(ii) The reaction time can be adjusted as a function of kinetics.

However, batch processes have a number of problems, notably inefficient mixing, relatively high capital cost and poor heat and mass transfer (Stitt, 2002), in addition to difficulties with scaling-up and producing homogenous processing conditions (Plumb, 2005).

Based on information from different sources (e.g. AstraZeneca and GlaxoSmithKline), the benefits of using continuous flow reactors in the pharmaceutical sector are summarized in Lamb *et al*., (2010) as follows:

- The risks associated with process scale-up could be reduced (as the process is developed from laboratory bench-top, to pilot-scale, to plant-scale).
- Scale-up to plant production could be faster.
- Significant savings could be achieved in plant capital and operating costs.
- The environmental footprint could be reduced.
- The reactor inventory could be reduced, and hence containment hazards reduced.
- A faster response to market demand could be achieved, and product inventory reduced.

According to Thomas (2005), Foster Wheeler (in June 2003) considered the conversion of an existing batch API plant to operate in continuous flow mode and the following advantages were identified:

- Moving to continuous processing opens up chemical and physical processing opportunities that cannot be achieved in batch equipment.
- More efficient processing is achieved as reactors can be designed to give a greater degree of freedom to segregate competing reactions, thereby giving higher yields and selectivity.
- The variation of conditions is greatly reduced, thus reducing the variation in reactor product.
- Counter-current extractions maximise extraction efficiency while minimising extracting solvent usage.
- Where the process returns to operate batch-wise for crystallisation, isolation and drying, the scale of the equipment is greatly reduced, thus reducing process variation and giving a more robust process.

In the literature, there are also many examples that show that there is real interest in the pharmaceutical sector to introduce 'continuous processing' as an alternative to 'batch processing'. To illustrate this level of interest, in the sections that follow, descriptions of activity from a number of sources are presented as direct quotes:

For example in Pellek and Van Arnum (2009):

(i) **Novartis:** *Novartis Pharma AG (Basel, Switzerland) is proceeding with what it terms its "Blue Sky Vision" for continuous processing, in which process steps are reduced to a minimum, and a product is made from start to finish, from drug substance to finished drug-product, on a continuous basis in one facility. Novartis has teamed up with the Massachusetts Institute of Technology (MIT) to help realize that goal. As part of a 10-year collaborative effort, Novartis is investing $65 million in the Novartis-MIT Center for Continuous Manufacturing, which was formed in September 2007.*

(ii) **Pfizer:** *Pfizer (New York) is evaluating continuous processing for drug-substance, biologics, and drug-product manufacturing where the manufacturing division is working with the research and development group for:*

- *Development of internal capabilities by working with vendors and academia to develop methodology and continuous processes.*
- *Expanding expertise in chemical engineering and in laboratory and pilot facilities.*
- *Adopting new process-design methodology. For example, Pfizer is a member of Britest, a 21-member company consortium developing innovative approaches to manufacturing and process design, including continuous manufacturing.*
- *Identifying continuous unit operations that could be applicable to a wide range of manufacturing processes and developing expertise in their applications and capabilities in R&D and manufacturing.*

(iii) **C-SOPS:** *The Centre for Structured Organic Particulate Systems (C-SOPS), a multi-university consortium consisting of Rutgers University, Purdue University, the New Jersey Institute of Technology, and the University of Puerto Rico at Mayaguez, is developing a test bed for continuous manufacturing. C-SOPS was founded in 2006 with a $15-million grant from the National Science Foundation and is also funded by industrial partners, which include pharmaceutical manufacturers and equipment producers. C-SOPS is focused on three areas:*

- *Manufacturing science.*
- *Composite synthesis and characterization.*
- *Particle formation and functionalization.*

The centre is developing a test bed to show the feasibility of continuous technology for sequential blending, dry-granulating, lubricating, and tableting of dry powders and granules.

These three examples from Pellek and Van Arnum (2009), demonstrate that there is real interest from industry in the development of continuous processing.

Then, according to Mollan and Lodaya (2010):

> *The pharmaceutical industry is poised to change radically in the next 5-10 years in response to a changing marketplace. New risk models will need to be implemented to stay competitive and rapidly respond to these changing dynamics. The urgent need to dramatically improve efficiency and productivity within the pharmaceutical manufacturing sector will be a requirement for the future. The design of new production facilities utilizing new technology and implementing continuous processing strategies will be one way to remain competitive as the industry undergoes the next wave of change.*

Recently, Lamb *et al*., (2010), concluded that the trick with the introduction of continuous processing into the pharmaceutical industry rests with:

(i) *The introduction of a methodology and apparatus that could be used at the laboratory bench scale, which could easily be scaled-up to pilot, and then plant scale. This methodology would then be used in the development of new drug molecules.*

(ii) *The application of continuous processing technology to an established drug that may now be manufactured as a generic drug. The motivation for this would need to be financial and the ability to apply a cleaner method of manufacture. Regulatory approval would then need to be sought for this new pathway/reacting environment. However, at least there is no uncertainty about the market for such a drug, and the presence of any undesirable reaction intermediates could be relatively easily assessed and adjustments made to the process, before the drug was tested in clinical trials.*

Therefore, from this introduction, it is clear that there is plenty of interest (and motivation) in the development of 'continuous processing' as an alternative to 'batch processing' in the pharmaceutical industry. This view is also reflected in many technical publications where an opportunity for process intensification, or for the implementation of a cleaner process, may also be taken (e.g. Grasemann *et al*., 2010; Kolaczkowski *et al*., 2007; Plucinski *et al*., 2005 a; Stankiewicz and Moulijn, 2000; Cybulski *et al*., 1999).

1.2 The motivation for the work and the structure of the thesis

The motivation behind this work is to develop environmentally friendly chemical conversion processes, which create the possibility of utilizing a continuous process for the manufacture of speciality chemicals which lead to the production of APIs.

In simple terms there are two novel aspects to this work. The first is the selection of appropriate reaction chemistry, and the second is the design of a novel reacting environment in which the novel chemistry may proceed. In this thesis there was an opportunity to make progress with both of these aspects, and two different types of reactions were selected to act as model reactions:

Case Study 1: This is based on a new reaction pathway known as "Borrowing Hydrogen", where tertiary amines are produced by reacting alcohols with secondary amines using an immobilised ruthenium complex catalyst (e.g. Lamb *et al*., 2009) this chemistry has been studied in detail in the Department of Chemistry at the University of Bath.

Case Study 2: This builds on earlier work (2002 to 2005) started in the Department of Chemical Engineering at the University of Bath. This involves the use of gaseous oxygen as an oxidant in a selective oxidation reaction. In this reaction, benzaldehyde is produced by the partial oxidation of benzyl alcohol, using a mixture of 90 vol% dioxane and 10 vol% water as solvent and a platinum on activated carbon (Pt/C) as catalyst (e.g. Kolaczkowski *et al*., 2007).

The emphasis in this thesis when the term 'continuous processing' is used, is on the design of the reactor and not the associated processing steps (e.g. product crystallization).

Chapter 2 starts with a review of literature, concentrating on work that encourages a continuous approach in the pharmaceutical industry. Then in **Chapter 3**, Case Study 1 is progressed, following the first two Steps illustrated in Figure 1.1. Unfortunately, it was not possible to progress this reaction to Step 3 (the pilot-scale testing step), as problems were identified with the system and these could not be resolved within the scope of this thesis. However, this showed the value of testing in the Step 2 phase. Also, work on this case study was important, as it provided an opportunity to be involved at an early phase with the development of some novel chemistry. As a 'model system', the reaction between morpholine and benzyl alcohol was studied on different types of catalyst (i.e. Ru and Pt), and this involved collaboration with Dr Gareth Lamb working on a separate EPSRC funded project. This work led to a joint publication, which is included in Appendix A.

In **Chapter 4** the work now moves to exploring Case Study 2, where the partial oxidation reaction of benzyl alcohol to benzylaldehde over Pt/C catalyst is studied. This builds on earlier work (2002 to 2005) at the University of Bath and CNRS (Lyon), where suitable conditions had been identified for this model reaction, and the results of work had been published on the development of a continuous process in which the catalyst in the form of small spherical beads was held in a fixed bed. However, based on ideas expressed in a recent patent application (Kolaczkowski 2008, *priority date Oct 2006*), this chapter starts with the selection of a carbon monolith as a catalyst support (rather than spherical beads), and it is shown that this structure overcomes many of the problems identified in earlier work. Preliminary experiments are performed in a batch autoclave reactor to measure some of the chemical kinetics for this partial oxidation of benzyl alcohol (Step 1, in Figure 1.2), and this helps with the interpretation of data obtained in Chapter 5.

In **Chapter 5**, a variety of experiments are performed to help assess the viability of using a carbon monolith as a catalyst support (Step 2 in Figure 1.2). The experiments are performed in a Single Tube Monolith Reactor (STMR), which contains a number of Pt/carbon monoliths. This is shown to be effective, and this overcomes one of the major problems (of rapidly increasing pressure drop with time) which made the earlier design based on spherical beads in-operable. This is a major break-through as it provides supporting scientific evidence for the ideas expressed in the patent (Kolaczkowski 2008), and also enables a pilot-scale reactor to be designed and built with confidence.
Experiments are then described in the pilot-scale reactor (see Step 3 in Figure 1.2), known as the Radiator Monolith Reactor (RMR), and these are performed, probably for the first time at this scale in the pharmaceutical industry, using a monolith supported catalyst system in a fixed bed. Visitors to the laboratory both from Lilly (USA), and GSK (UK), confirmed that this work was clearly innovative and in advance of anything they had yet seen.

Finally in **Chapter 6** conclusions and recommendations for further work are presented.

Throughout this thesis the word 'methodology' is used to highlight features that are important in the development of techniques that will help the pharmaceutical & fine chemicals industry to progress with the development of continuous processes (where appropriate).

At the end of each chapter, a list of supporting references is provided.

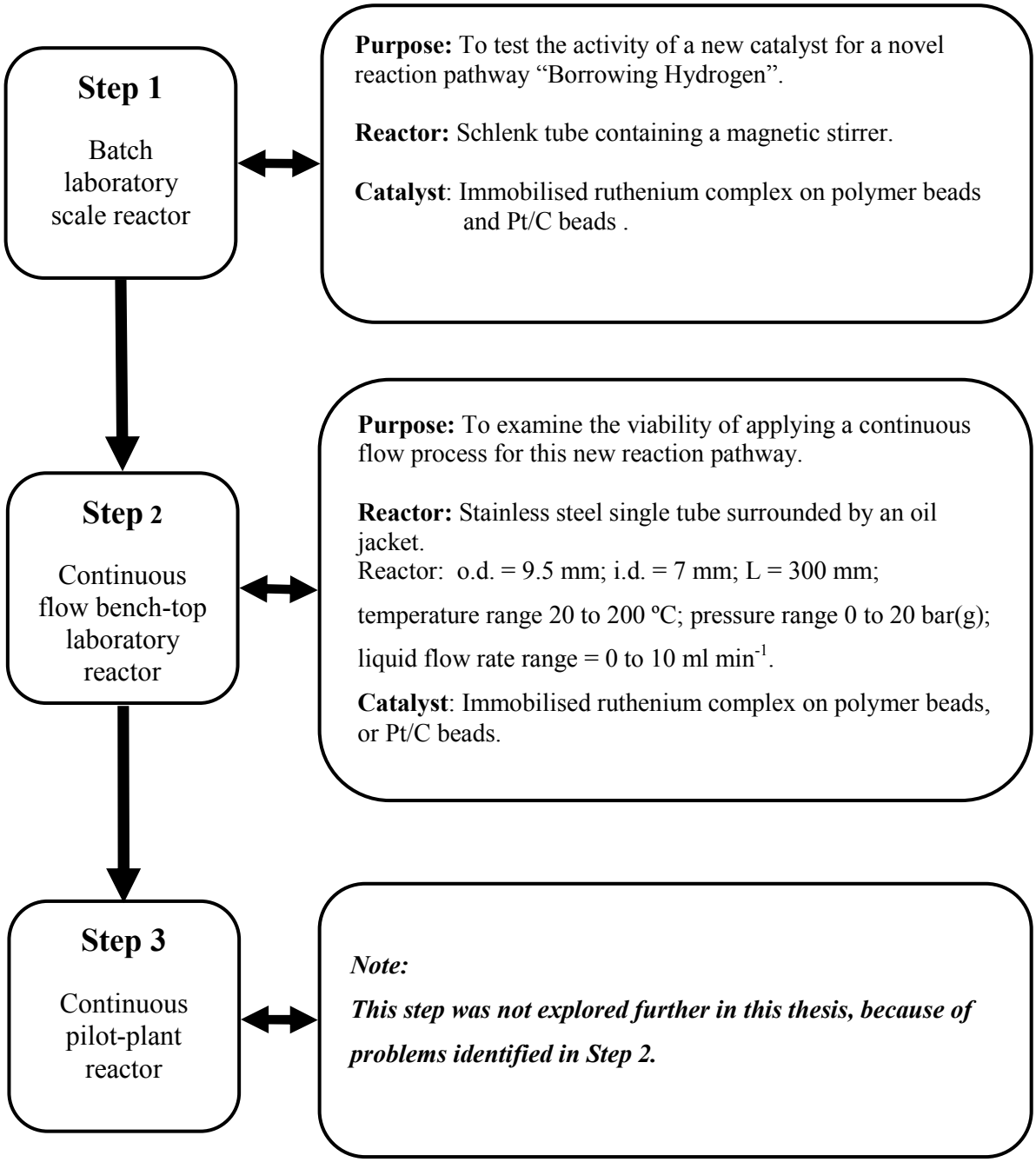

Figure 1.1: The scheme followed to explore the application of a novel reaction pathway "Borrowing Hydrogen".

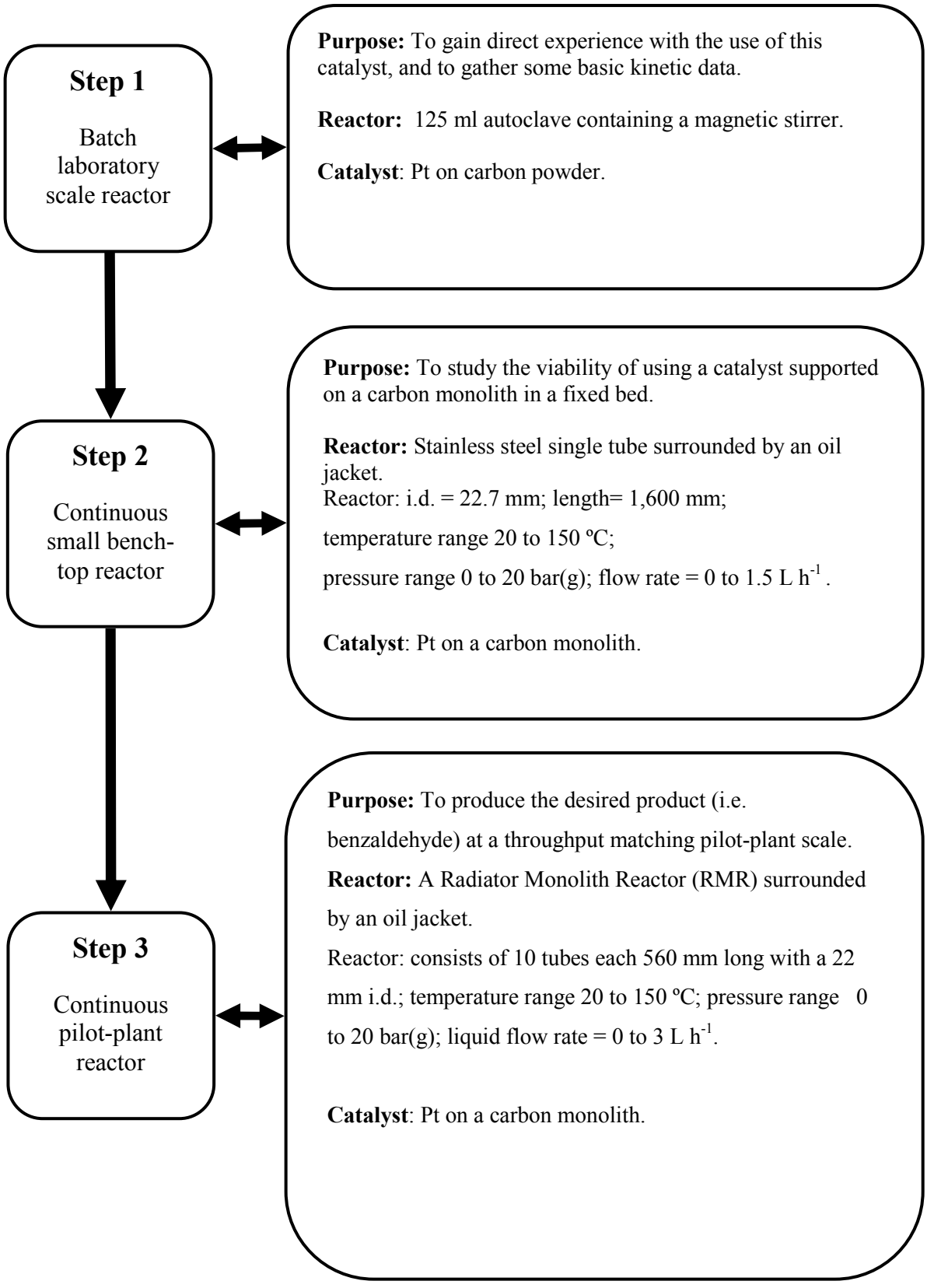

Figure 1.2: The scheme followed for the partial oxidation of benzyl alcohol.

References

Cybulski, A., Albers, R.E.A. and Moulijn, J.A., 2006. *Monolithic Catalysts for Three-Phase Processes*. In: 'Structured catalysts and reactors' Cybulski, A. and Moulijn J.A., ed. United States: Taylor and Francis Group, LLC, pp. 355-391.

Girish, M., 2005. Pharmaceutical Processing - Batch or a Continuous Process: A Choice, http://www.pharmpro.com/ShowPR.aspx?PUBCODE=021&ACCT=0000100&ISSUE=0503&RELTYPE=PR&Cat=0&SubCat=0&ProdCode=0000&PRODLETT=H&SearchText=girish%20malhotra&CommonCount=0. (Accessed 15 October 2009).

Grasemann *et al*., 2010. A novel compact reactor for three-phase hydrogenations. *Chemical Engineering Science*. 65, pp. 364-371.

Kolaczkowski, S.T., Pluncinski, P., and Lapkin, A.A., 2007. Selective Oxidation of Benzyl Alcohol in a Pilot Scale Multichannel Reactor. *Proceedings of the 1st International Congress on Green Process Eng.*, 24 – 26 April 2007, Toulouse. France, pp. 1-8.

Kolaczkowski, S.T, 2008. Priority Date 6 October 2006. *Apparatus and Process for use in three-Phase Catalytic Reactions.* International Application Published Under The Patent Cooperation Treaty (PCT), WO2008/040999 A2.

Lamb G., Al Badran F.A., Williams J. M. J., and Kolaczkowski S.T, 2010. Production of pharmaceuticals: amines from alcohols in a continuous flow fixed bed catalytic reactor, *Chemical Engineering Research and Design*. 88, pp. 1533-1540.

Lamb G., and Watson A., 2009. Borrowing hydrogen methodology for the conversion of alcohols into *N*-protected primary amines and in situ deprotection. *Tetrahedron Lett*. **50**, pp. 3374-3377.

Mollan M., and Lodaya M., 2010. Continuous Processing in Pharmaceutical Manufacturing. http://www.ieor.berkeley.edu/~shen/ieor298/pdd/ContinuousProcessinginPharmaManufacturing.doc (Accessed 12 May 2011).

Plumb, K., 2005. Continuous Processing in the Pharmaceutical Industry Changing the Mind Set. *Trans IChemE, Chemical Engineering Research and Design*, 83 (A6), pp. 730-738.

Plucinski, P.K., Bavykin, D.V., Kolaczkowski, S.T., and Lapkin, A.A., 2005 a. Application of a structured multifunctional reactor for the oxidation of a liquid organic feedstock. *Catalysis Today*, 105, pp. 479-483.

Pellek A., and Arnum V., 2009. Continuous Processing: Moving with or against the Manufacturing Flow. http://www.pharmtech.findpharma.com/pharmtech/Regulation+Article/Continuous-Processing-Moving-with-or-against-the-M/ArticleStandard/Article/detail/549164 (Accessed 8 November 2010).

Roberge, D.M., Ducry, L., Bieler, N., Cretton P., and Zimmerman, B., 2005. Microreactor Technology: A Revolution for the Fine Chemical and Pharmaceutical Industries. *Chem. Eng. Technology*, 28 (3), pp. 318-323

Stankiewicz, A.J. and Moulijn, J.A, 2000. Process Intensification: Transforming Chemical Engineering. *Chemical Engineering Progress*, January, pp. 22-34.

Stitt, E.H., 2002. Alternative multiphase reactors for fine chemicals A world beyond stirred tanks. *Chemical Engineering Journal*, 90, pp. 47-60.

Thomas, H., 2005. The Reality of Small Scale Continuous Processes,.http://www.fwc.com/publications/tech_papers/files/Reality%20HT%20Edited%20Rev%2002.doc (Accessed 29 June 2010)

CHAPTER 2

BATCH TO CONTINUOUS PROCESSING IN THE PHARMACEUTICAL INDUSTRY

In this chapter, a literature review is provided of work that supports the conversion of batch into continuous processes in the pharmaceutical sector.

2.1 Stirred tank reactor systems

Traditionally, medicines have been manufactured using batch vessels. Painted leaves that were traced back to the thirteenth century from the Baghdad School in Iraq show evidence of using a simple form of batch reactor (with a man-powered mixer) to make a cough medicine from honey, see Figure 2.1. The resemblance between some of the devices shown in the pictures (for instance, the stirred vessels and the stirrers) and the basic equipment in today's chemical process industries is striking.

Figure 2.1: Leaves from an Arabic translation of the Materia Medica of Dioscorides showing (a) preparation of medicine from honey, and (b) The Pharmacy , dated 1224 A.D. Iraq, Baghdad School, Colours and gold on paper. Ettinghausen *et al*., (1978), (*copied from Image for Academic Publishing (IAP) with permission from a scholar's licence at the metropolitan museum*).

A good discussion of pharmaceutical reactors is available in Stitt (2002), from which the following observations are made:

a) The stirred tank reactor is considered to be the workhorse of the intermediate scale and fine chemicals industries. They are used at the small scale (< 1 m^3) and/or in the bulk chemicals industry for continuous production units at the very large scale, 15 to 30 m^3, (e.g terephthalic acid and aniline production plants).

b) The catalyst that is used may be in the form of slurry, or as a homogeneous catalyst. Slurry catalyst particle sizes vary from one catalyst to another, and significantly from one support material to another, but diameters in the range of 20–250 μm are typical. The gas may be sparged, or pulled in from the bulk gas–liquid interface using a gas inducing type of impeller.

c) Heat transfer (cooling or heating) may be provided by an external jacket, or by internal coils, or tubes. The internal fittings provide the opportunity for a higher heat transfer area, but make cleaning more difficult (in fouling or multi-product applications) and disrupt the fluid mixing patterns within the vessel. External jackets are generally inevitable if the reactor is lined, for example with glass. In the case of poor mixing design (or operation), or insufficient heat transfer (area or heat transfer coefficient), then one or more of these transfer processes may limit the rate of the reaction. This can result in variable concentrations of chemical species in the liquid phase, and variations in the adsorbed amount on the catalyst surface. This can impact on the selectivity of the reaction and in some cases the stability of the catalyst itself. Inadequate heat transfer can result in overheating (for an exothermic reaction) and can thus change the selectivity. Alternatively, a lower temperature (for an endothermic reaction) can result in low activity and longer batch times.

A flow visualisation based on the mathematical reconstruction of data measured by tracking the motion of a radioactive particle was studied using two techniques (a γ-ray emitting particle and a positron-emitting particle). Stitt (2002), noted that there were a number of general observations that could be made from such flow visualisations studies, namely:

- There were large variations in local velocities.
- There was high shear and there were high velocities in the impeller region.
- Impeller induced up-end and down-drafts may not progress far past the plane of the impeller.
- Areas of low velocity and near stagnation were seen.
- There was uncertain inter-penetration between the upper and the lower circulation patterns of both the fluid and the catalyst.

Stitt (2002) concluded that:

- In addition to the uncertainty on scale-up, stirred tank reactors are fundamentally poor mixers, and the larger they get the worse they get.
- It remains difficult especially for multiphase systems, to predict mixing heterogeneity with any certainty, even after significant improvements have been made to the mixing devices.

2.2 Micro-channel reactors system

Micro-channel reactors are considered a new kind of reactor. Their novelty dictates a new approach in design, which requires the development of new manufacturing techniques and materials, and more understanding of the difference in fluid behaviour and dominant phenomena at the micro-scale.

Micro-channel reactors are defined in Ehrfeld *et al.,* (2000) as follows:

> *"Miniaturized reaction system fabricated by using some methods of micro-technology and precision engineering".*

The development history of micro-channel reactors has been summarised in Gavriilidis *et al.,* (2002), and the origins of micro-reaction technology can be traced back almost half a century ago to the manufacturing of the first silicon sensors and actuators.

In the literature, there is evidence of work to use micro-channel reactors as a tool for transition from batch to continuous processes in both pharmaceutical and fine chemicals industries (e.g.; Kockmann *et al*., 2008; Zanfir and Gavriilidis 2007; Roberge *et al*., 2005; Watts and Haswell 2003).

In a comprehensive review, Gavriilidis *et al.,* (2002) described many advantages, which include the following:

a) Micro-channel reactors have the potential of altering the chemical engineering landscape by: expanding the tools available to the reaction engineer, and increasing the manufacturing speed of processes (and the rate of information generation).

b) Due to the ability of providing high heat and mass transfer, micro-channel reactors allow reactions to be performed safely, under more aggressive conditions and with higher yield, than can be achieved by conventional reactors, and more importantly, with new reaction pathways deemed too difficult in a conventional reactor.

However, micro-channel reactors also have drawbacks and these are summarized in Gavriilidis *et al.,* (2002) include:

a) The fact that micro-channel reactors generally do not tolerate particulates well, often clogging. Clogging has been identified by a number of researchers as the biggest hurdle for micro-channel reactors.

b) They have a high manufacturing cost.

Xiuyan and Asterios (2008) demonstrated the use of a scalable micromesh reactor as an efficient tool to move from a batch to a continuous process. They studied a homogenous catalytic system involving asymmetric transfer hydrogenation of acetophenone. A comparative study was made between the performance of a batch and a micromesh continuous flow reactor, and it was shown that the micromesh reactor is an efficient device for acetone stripping from isopropanol.

Roberge *et al*., (2005) determined the percentage of twenty-two large scale processes performed at Lonza Exclusive Synthesis that could benefit from a continuous production process. In addition, they discussed the appropriate type of continuous reactor. They noticed that 50% of the reactions in the pharmaceutical industry would benefit from the use of a continuous process. For many of them (44%), a micro-channel reactor would be the preferred reaction device. A large proportion of these reactions, however, cannot be performed in a micro-channel reactor since the devices currently available cannot handle solids, at least not with the flexibility and versatility required in multi-purpose equipment.

Stitt (2002) looked into the world beyond the stirred tank reactor (for the pharmaceutical and fine chemical industries) by considering different types of continuous multiphase reactors. The reactors were categorised into two types:

- Fixed bed catalysis (e.g. trickle bed, packed bubble column, pulsed trickle bed, structured catalysis and monolith catalysis).
- Mobile catalysis (e.g. stirred tank, three phase fluidized bed, slurry bubble column and loop/jet reactor).

When considering the concept of a micro-channel reactor, Stitt (2002) concluded that there were potential problems which related primarily to the robustness of the operation. The key potential gremlin was fouling, because real process liquids do foul the surfaces, and filtration processes are never perfect. Therefore, even 50 μm particles could easily be admitted to the reactor and eventually cause plugging.

2.3 Compact mm-scale multifunctional system

The idea of exploiting the advantages of reactors with small channels, but avoiding some of the problems with the use of very small channels (micro-channels) has been promoted by researchers at the University of Bath, and this is known as the 'mm-scale multifunctional reactor'. In this type of reactor, the channels are at the mm-scale e.g. between 1 to 20 mm. Then, depending on the diameter of the channel, advantages in terms of improved rates of heat transfer to the walls of the channel may still be very significant, and benefit reactions within the channel. It is also possible to pack such channels with fine catalyst particles, or to even make use of monolith structures as supports. If monoliths are used, the catalyst is deposited on the surface of the monolith support, or is an integral part of the monolith structure.
Unfortunately, in the literature there is very little published on the possibility of using such reactors for pharmaceutical reactions at this mm-scale.

2.3.1 Partial oxidation reactions in mm-scale multi-functional reactors

The group at the University of Bath have published the following papers, and features from them are summarised as follows:

2.3.1.1 Plucinski *et al*., (2005 a)

In this paper, early work on the hydrodynamic characterization of a single channel bench top reactor was described. The reactor consisted of 3 mm x 3 mm square channels that were 100 mm long. The channels were packed with catalytic beads and a static mixer section was placed at the inlet of each channel (for oxygen and liquid mixing). The neighbouring channels contained a heat transfer fluid, which maintained a relatively uniform temperature along the length of the reaction zone. This sustained the reaction and maintained selectivity, for the model reaction studied (benzyl alcohol to benzaldehyde). It was shown that in a short 100 mm length of packed bed (in 3 mm x 3 mm channel) with powdered catalyst (0.9 wt% Ru on Al_2O_3, 150 μm), a product yield of 25% (with 99.7% selectivity) could be obtained.

In the study the following key points were made:

a) At pressure up to 8 bars, the yield of benzaldehyde is independent of pressure i.e. independent of oxygen concentration. This means that the oxidation of benzyl alcohol to benzaldehyde on Ru/Al_2O_3 catalyst was zero order with respect to oxygen and that result agreed with Yamaguchi and Mizuno (2003). In addition, it was suggested that the reaction was in the kinetic regime, and was not influenced by gas-liquid mass-transfer resistance.

b) Isothermal reaction conditions needed to maintained as the oxidation of benzyl alcohol is an exothermic reaction ($\Delta H_R^\circ = -183$ kJ mol^{-1}) and if the reactor was operated at adiabatic conditions with a 55 % aldehyde yield, this could raise the temperature by 180 K.

c) The apparent kinetic constant k = 3.38 x 10^{-6} kmol kg_{cat}^{-1} s^{-1} and the activation energy, ΔE_A = 79.3 kJ mol^{-1}.

In addition, a mathematical model was presented of the reactor, which was used to evaluate kinetic data. The following were assumed:

- At a high operating pressure the oxygen was completely dissolved in the toluene solvent.
- Plug flow conditions prevailed in the reactor.
- Operation was in the saturation region of the Langmuir-Hinshelwood isotherm.
- The reaction was not limited by inter or intra-particle diffusion (effectiveness factor η=1).

The design equation for the reactor (based on reactant concentration and homogeneous approach) was written (Plucinski *et al*., (2005 a)) as follows:

$$-u_s \frac{d_{C_A}}{d_z} = \rho_b(-r_A) \tag{2.1}$$

where:

u_s is the the superficial velocity of the liquid phase, m s^{-1},

C_A is the concentration of alcohol , mol L^{-1},

z is the actual lenth of the reactor, m,

ρ_b is the bulk density of the catalyst in a channel, g L^{-1}, and

$-r_A$ is the reaction rate, mol g^{-1} sec^{-1}.

If the rate of reaction was independent of alcohol concentration (high concentration used of alcohol feed-stock), then:

$$-r_A = k \tag{2.2}$$

where:

k is the apparent rate constant.

In equation (2.2), account was taken of the high concentration of alcohol in the feed, when the adsorption term in the Langmuir-Hinshelwwod kinetic expression was given by :

$$K_A c_A >> 1 \qquad (2.3)$$

where:

K_A is the adsorption equilibrium constant of alcohol at the catalytic surface.

is the adsorption equilibrium constant of alcohol at the catalytic surface

As isothermal conditions were maintained along the channel, then the integration of equation (2.1) and the incorporation of fractional conversion X resulted in:

$$X = \frac{c_{A_\circ} - c_{A_e}}{c_{A_\circ}} = \frac{k\, h\, \rho_b}{u_s\, c_{A_\circ}} \qquad (2.4)$$

where:

h is the total length of the reactor, m,

$c_{A_\circ}$ is the initial concentration of alcohol at z = 0, mol L^{-1}, and

c_{Ae} is the final concentration of alcohol at z = h, mol L^{-1}.

2.3.1.2 Bavykin *et al*., (2005)

Further studies were done on the same Ru/Al_2O_3 catalyst and reaction system that been used in Plucinski *et al*., (2005 a) to investigate the performance of a multichannel compact reactor by studying the following aspects:

- Product yield, selectivity and heat transfer efficiency.
- Testing the concept of multiple injection of oxygen as a possible method of improving selectivity.
- Gas-liquid and liquid-liquid mass transfer efficiency was investigated to confirm the range of operating conditions.

It was concluded that:

a) The catalyst had a high activity (TOF = 300 h^{-1}, at 388 K, 1 mol L^{-1} feed alcohol concentration and 25% conversion for a single pass through reactor), high selectivity (99.5%) and good stability (rate of catalyst deactivation k = 0.018 h^{-1}). The turnover frequency (TOF) was defined as the number of moles of product per number of moles of catalyst per time,

$$\text{TOF} = \frac{C_{b-ald}.F_L.Mw_{Ru}}{m_{\text{Ru}}} \qquad (2.5)$$

where:

C_{b-ald}	is the concentration of product benzaldehyde in the product stream, mol L^{-1}.
F_{L}	is the volumetric liquid flow rate, L h^{-1},
m_{Ru}	is the mass of metallic ruthenium, g,
Mw_{Ru}	is the atomic weight of ruthenium, g mol^{-1}

and

$$TOF_{(t)} = TOF_{(0)} \times e^{-kt} \quad (2.6)$$

where:

$TOF_{(t)}$	is the turnover number at (time = t), h^{-1},
$TOF_{(0)}$	is the turnover number at (time = 0), h^{-1},
k	is the rate of catalyst deactivation, h^{-1}, and
t	is the reaction time, h.

b) The reaction occurs in the kinetic regime over a broad range of operating conditions due to the intensified mass-transfer regime in the reactor.

c) The reactor was also shown to operate isothermally despite a significant heat effect.

d) Staged injection of oxygen was shown to be beneficial, however, in the case of benzyl alcohol oxidation, the positive effect is likely to be only due to a better control over residence time.

e) Favoured operating conditions for a 1.0 mol L^{-1} concentrated feed of benzyl alcohol were found be as follows: operating pressure, P = 8 bar; flow rate of liquid, F_l = 2 mL min^{-1}; flow rate of gas, F_g = 6.7 mL (STP) min^{-1}; and temperature, T = 115 ºC.

2.3.1.3 Plucinski *et al*., (2005 b)

Then further studies were done on a Ru/Al_2O_3 catalyst in a 100 mm long single channel reactor to examine the effect of solvent type, channel size, reactor orientation (horizontal and vertical), and direction of flow (co-current upward flow, and downward flow) on the reactor performance. It was shown that:

a) The choice of solvent was shown to affect the yield of desired product.

b) The reaction rate was found to vary in the three different channel sizes studied, i.e. 2 mm x 2 mm, 3 mm x 3 mm, and 5 mm x 5 mm. The best performance was obtained in the 3 mm x 3 mm channels.

c) The performance of the reactor was not affected strongly by the orientation of the channels (horizontal or vertical), or by the direction of fluid flow (co-current upward flow, or downward flow).

d) In a preliminary experiment using a Pt on carbon catalyst with dioxane as a solvent, it was shown that a two fold increase in the rate of oxidation could be achieved.

2.3.1.4 Kolaczkowski *et al*. (2007)

In further work, the application of the knowledge gained was demonstrated in a pilot-scale reactor to explore the effect of using a spherical shaped Pt/C catalyst (160 microns, Pt 3 wt%) packed in channels. The pilot-scale reactor consisted of four individual segments, which could operate separately, in parallel, or even in series. Each segment consisted of 48 channels (3 mm hydraulic diameter, total length 500 mm). The reaction experiments were carried out at a temperature of 95 ºC and 8 to 17 bar gauge pressure. The partial oxidation of benzyl alcohol to benzaldehyde was studied (as a model reaction) and benzyl alcohol in a mixture of 90 vol% dioxane and 10 vol% water was fed into the reactor at 4.2 L h^{-1}. It was shown that with an effective overall bed length of 500 mm, it was possible to achieve a high conversion of benzyl alcohol to benzaldehyde (70% was obtained) with 95% selectivity to benzaldehyde. However, problems where encountered with a rapidly increasing pressure drop across the bed.

2.3.1.5 Kolaczkowski (2008)

Clues on how to overcome some of the problems were then presented in a patent application. The following is a summary of some the problems that need to be overcome in such a packed bed system:

a) It was proposed that the increase in pressure drop (up to 0.63 bar h^{-1}) was caused by the deposition of by-products (e.g. benzoic acid) in the packed sections of the reactor. This may have also accurred in the gas-liquid mixing section.

b) It was difficult to ensure a uniform distribution of gas and liquid across the channels, especially with such a low linear velocity in the bed.

c) The packing of multiple channels with powdered catalyst, and then after use, the emptying and replacing of such catalyst would be very labour-intensive.

In the patent application, it was claimed that the problem of pressure drop could be overcome by using monoliths in short sections of the bed. Before each catalytic section there would be a gas-liquid mixing zone and then a heat transfer zone to maintain a uniform temperature alone the reactor. At the base of the reactor, a pulsating device (e.g. piston, a diaphragm) could be attached, to create pulsatile flow. The advantages that could be achieved by using such a device were listed as follows:

a) The pulsating action would promote mixing of gas and liquid in zones upstream/downstream of respective reaction zones, thereby dispersing the gas in the form of very fine bubbles throughout the liquid phase, increasing the surface area of gas to liquid mass transfer of gas, and promoting mass transfer of gas from the gas phase to the liquid phase.

b) The pulsating action would cause displacement of the liquid inside the reaction zones at a greater linear velocity than that which would arise if no pulsating action was generated. This in turn would increase rates of mass transfer of

reactants and products, and the transfer of heat both to, and from, the catalytic surface.

c) The displacement of the liquid at a higher velocity in the reaction zones would have a very important washing action on the surface of the catalyst. This in turn would reduce the rate at which pressure drop would build up across the reactor.

2.4 Monolith reactor

The monolith honeycomb structure is widely used as catalyst support in many gas treatment applications (e.g. cleaning of automotive exhaust gases and industrial off-gases), however, in the last few decades, the use of monoliths has been extended to include applications in which multiphase reactions are performed, such as: hydrogenation and oxidation (Cybulski and Moulijin 2006). In many cases monolithic reactors are an attractive alternative to conventional multi-phase reactors due to their advantages of: low pressure drop, the absence of need for a catalyst separation step, and a large geometrical surface area (Nijhuis *et al*., 2001).

In contrast to the traditional structured catalyst systems, the vast majority of fixed bed reactors used in industry consist of randomly packed beds with catalyst particles of different shapes, which normally exhibit some problematic aspects in fluid flow such as high resistance to heat transfer, stagnated zones and high pressure drop (Campos and Ferreira 2001).

In the literature, there are many examples of work where monolith reactors are proposed as an alternative from the traditional reactors employed in the pharmaceutical and fine chemicals industries (e.g. Campos and Ferreira 2001; Irandoust 1988; Edvinsson 1994; Nijhuis *et al*., 2001; Cybulski and Moulijin 2006; etc.). In this section information from two of these sources will be considered.

2.4.1 Nijhuis *et al*., (2001)

A pilot-scale set-up for hydrogenation reactions was constructed and a comparison was made between a monolith and a trickle bed reactor. Two hydrogenation reactions were

studied, the first reaction was the hydrogenation of α-methylstyrene, and the second reaction was the hydrogenation of benzaldehyde to benzyl alcohol with a consecutive reaction (unwanted) to toluene.

The monolithic supports were washcoated with a layer of γ-alumina using a sol-gel method (to increase the surface area of cordierite monolith ~ 0.7 m^2 g^{-1}), then an egg-shell-type of nickel catalyst was made by deposition precipitation. Scanning electron micrographs (SEM) and transmission electron micrographs were made to evaluate the deposition of washcoat and nickel catalyst. Nijhuis *et al*., (2001), concluded that:

a) Monolithic reactors are promising systems to replace catalyst in conventional multiphase reactors. Not only do monoliths have advantages (catalyst separation, pressure drop, etc.), but also the performance of a monolith has been demonstrated to be better.

b) Pilot-scale experiments to compare a monolith and a trickle-bed catalyst system have demonstrate higher productivity in the monolithic reactor for mass transfer limited reaction, and also higher selectivity for the selective hydrogenation of benzaldehyde.

2.4.2 Cybulski and Moulijin (2006)

The following description of a recycle monolith reaction system was provided which was investigated by Smits *et al*., (1995):

a) An extensive investigation was carried out on the potential of monolith reactors for the competitive hydrogenation of mixtures containing alkenes, alkadienes, aromatics, and functionalized aromatics. Mixtures of styrene and 1-octene were chosen as model ones for pyrolysis gasoline (Pygas) from steam crackers. It was reported that the hydrotreating of such mixtures was performed in trickle-bed reactors using Pd/Al_2O_3 or Ni/Al_2O_3 catalysts. Because intrinsic hydrogenation rates are very high, intraparticle diffusion plays an essential role in such a process. Therefore, monolithic catalysts seemed to be promising for applications in that process.

b) To assess the potential of monolith reactors, model experiments were performed. A typical example was the competitive hydrogenation of styrene and 1-octene in toluene over a monolithic Pd catalyst. The experiments were carried out in a bench-scale loop reactor.

c) The simultaneous hydrogenation of styrene/1-octene mixtures over Pd in such a monolithic loop reactor was found to proceed at high rates, considerably higher than those reported so far in the literature for other reactors. Therefore, monolith reactors were considered to be very promising.

2.5 Exploiting homogenous catalysis

A useful discussion is presented in Stevens *et al*., (2005 a), from which the following points are drawn:

a) Homogeneous catalysts offer some important advantages over their heterogeneous counterparts. Such catalysts can usually be dissolved in reaction media making all catalytic sites accessible to the reactants in the solution.

b) Many homogeneous catalysts demonstrate high selectivity.

c) In spite of these advantages and progress, homogeneous catalysis features in less than 20% of industrial processes.

d) One major disadvantage with the use homogeneous catalysis, is that it can be difficult to separate the reaction products from the catalyst, and from the reaction solvent especially when heavy metal contamination of a product is undesirable and must be limited to ppm or lower levels.

e) Many transition metals used in homogeneous catalytic systems are also expensive. Industrial processes based on these new inventions are less attractive unless a new and practical strategy for recycling active catalysts can be found.

2.5.1 Immobilization of homogenous catalysts

Immobilization of homogenous catalyst (e.g precious metal) can be achieved by two methods:

2.5.1.1 Immobilization on insoluble supports

Immobilization of homogenous catalysts on various insoluble supports, especially porous materials with high surface area, is usually the method of choice since the immobilized catalysts can be recovered *via* a simple filtration process (Stevens *et al*., 2005 b).

In the work by Lamb *et al*., (2008), a ruthenium complex catalyst was immobilised on the surface of a triphenylphosphine bound (1.6 mmol g^{-1} of phosphine) resin and the reaction of morpholine with benzyl alcohol to form amines was studied. The reaction was performed in a batch reactor (sealed Schlenk tube) in an atmosphere of argon gas. Toluene was used as a solvent. Operating at 110 ºC, it was shown that high conversions of 77 % and 95 % can be achieved, within 6 h and 12 h respectively.

However, there are drawbacks in the immobilization of homogenous catalysts on insoluble supports, and theses were summarized in Stevens *et al*., (2005 b) as follows:

a) A substantial decrease in activity and selectivity of the immobilized catalysts is frequently observed due to the heterogeneous nature of these support materials in the reaction media.

b) With such loaded catalyst systems other problems are also encountered such as non linear kinetic behaviour, unequal access to chemical reactions, and synthesis difficulties in transferring standard solution-phase reactions to the solid phase.

2.5.1.2 Immobilization on soluble magnetic nanoparticles supports

The development of novel soluble matrixes for supporting solution-phase organic reactions (e.g magnetic nanoparticles) has received a great deal of research attention as many of the aforementioned problems associated with heterogeneous insoluble matrixes can be addressed by adopting a soluble support. In one approach, magnetic nanoparticles can be used and their use is discussed in Stevens *et al*., (2005 b) from which the following information has been selected:

a) Magnetic nanoparticles usually have a core/shell structure consisting of a magnetic iron oxide core surrounded by a layer of lightly cross-linked polymeric shell wall. The organic polymer shells stabilize the nanoparticles by preventing aggregation of inorganic cores and offer a platform for the immobilization of the catalyst. The shell walls are usually thin (~ nm) and the shell polymers are preferred to have low molecular weights. Iron oxide cores will respond to a magnetic field but retain no magnetization properties when the field is removed.

b) The following advantages were stated:

- As the size of the support materials is decreased to the nm scale, the surface area of nanoparticles will increase dramatically.
- Unlike other soluble matrixes, recovery of the catalyst immobilized on partially soluble magnetic nanoparticles could be achieved using an external permanent magnet.
- There was no significant loss in the activity of the immobilized catalyst, even after several reaction cycles.

2.5.2 Biphasic reaction systems

Another approach that has received significant attention is to constrain the catalytic species in an organic immiscible liquid such as water. Information from two sources is presented in these sections.

2.5.2.1 Shaughnessy (2009)

a) In a biphasic reaction system, the products and catalyst reside in different immiscible phases, which are usually both liquid. The two phases are brought into contact by stirring, allowing the reaction to proceed upon completion of the reaction the two phases can be separated by simple decantation.

b) Because the catalyst remains in solution, it often retains its reactivity and selectivity properties. Provided there is sufficient interaction between the substrate phase and the catalyst phase, good activity can be achieved.

In this work an overview was provided of a wide range of hydrophilic ligand structures that had been prepared and their application in aqueous-phase metal-catalyzed processes was described. The review focused on advances over the past 10-15 years, providing examples of aqueous-phase catalysis. In the paper, the following conclusions were presented:

a) The major driver for the development of aqueous-phase catalyst systems was to simplify the separation of catalytic active species from the hydrophobic product stream, especially as the majority of metals used in catalysis (Ru, Rh, Ir, Pd, Pt) are expensive and rare. This makes their recovery an important requirement of their large-scale use. In addition, product specifications typically require low levels of metal, or ligand derived impurities.

b) By simplifying the catalyst separation (by the use of an aqueous biphasic catalyst system) this can lower the economic and environmental costs associated with separation of the catalyst from the product.

c) Water is potentially a more environmentally benign solvent than traditional organic solvents. For water to be a truly green replacement, issues related to the handling of water which has been contaminated with organic impurities must be addressed.

d) Aqueous phase catalyst systems that provide comparable activity and selectivity to homogeneous processes have the potential to provide significant savings if implemented.

2.5.2.2 Anson *et al*., (1998)

A heterogeneous catalyst system was developed making use of the hydrophilic nature of the surface of controlled pore glasses. To this a layer of water (or another suitable polar solvent) was attached in which a hydrophilic catalyst could be anchored (Figure 2.2). This allowed a large surface area of catalyst (~ 77 m^2 g^{-1}) to be formed, whilst the catalyst retained mobility within the polar solvent on the surface of the glass bead.

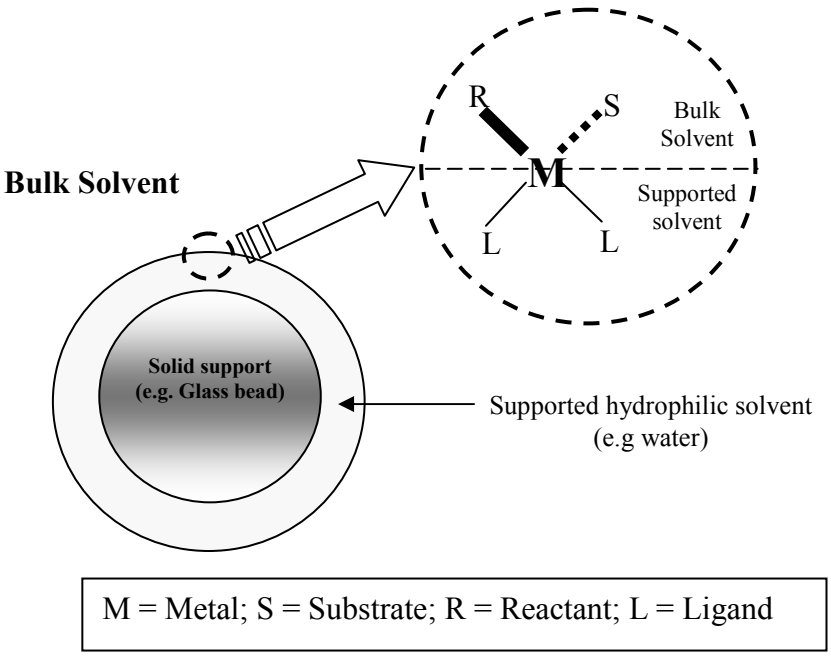

Figure 2.2: A schematic of the supported aqueous phase catalyst, adapted from (Anson *et al*., 1998).

Such a support structure was considered possible for the following applications:

(i) Palladium catalysed Heck reaction.

(ii) Palladium catalysed allylic substitution.

(iii) Palladium catalysed Suzuki couplings.

(iv) Glass beads as sponges for transition metals.

It was also considered to have been successfully used in the following applications:

(i) Cobalt hydroformylation catalysts.

(ii) Platinum hydroformylation catalyst.

(iii) Asymmetric hydrogenation.

(iv) Hydrogenation of α,β-unsaturated aldehydes.

(v) Wacker oxidation.

From an operational perspective:

- The constitution of the glass bead/palladium catalyst system could have significant effect on the reaction rate.

- Low levels of transition metal leaching were generally observed, which represent an economically and sound environmentally friendly approach to transition metal catalyzed reactions.

2.6 Conclusions

Having reviewed the literature, the following conclusions have now been drawn.

(a) There is much interest in the transformation of batch into continuous processes; however, this is a very challenging task.

(b) The way in which reactions are performed at the discovery stage influences the way in which they are scaled-up to mini-pilot-plant, then pilot-plant, and finally production plant scale.

(c) The use of micro-channel reactors is clearly promising, but these narrow channels are prone to blockage, either by the by-products formed, or contaminants in the feed.

(d) Fixed bed reactors that have fine spherical beads of catalyst at the micron scale are also prone to blockage, and deposition can cause pressure drop to rise across the reactor.

(e) Work on magnetic catalyst particles seems very promising, and magnetic nanoparticles could be an attractive soluble support for the immobilization of industrial homogeneous catalysts.

(f) There is a need for apparatus and methodology which allow the effective manufacture of compounds in three-phase catalytic reaction systems.

(g) Monolith reactors, with mm scale channels have been used in a number of applications (e.g. recycle monolith systems) and this type of support structure will be considered in the thesis.

Therefore, to investigate and illustrate the methodology for transforming a batch into a continuous process, the following two model chemical reactions, have been selected for the reasons described:

(i) The 'borrowing hydrogen' example reaction between morpholine and benzyl alcohol to form amines: This is selected as Case Study 1, as this builds on work in the Department of Chemistry at the University of Bath, and it was possible to become involved in the early phases of catalyst selection and development.

(ii) The partial oxidation of benzyl alcohol to benzylaldehde: This is selected as Case Study 2, as this reaction had previously been studied in a project in the Chemical Engineering Department at the University of Bath, so the chemistry was well known. This had also been studied at a pilot-scale, however, problems were encountered. If these could be overcome, then that would be a significant achievement. Based on information in the literature, it was also decided to perform experiments in a reactor where the catalyst is supported on a carbon monolith.

References

Anson, M.S., Leese, M.P., Tonks, L., and Williams J.M.J., Transition metal catalysed reaction using glass bead technology. *J. Chem. Soc. Dalton Trans*., pp. 3538-3529.

Bavykin, D.V., Lapkin, A.A., Kolaczkowski, S.T. and Plucinski, P.K., 2005. Selective Oxidation of Alcohols in a Continuous Multifunctional Reactor: Ruthenium Oxide Catalysed Oxidation of Benzyl Alcohol. *Applied Catalysis A: General,* 288, pp. 175-184.

Cybulski, A., Albers, R.E.A. and Moulijn, J.A., 2006. *Monolithic Catalysts for Three-Phase Processes*. In: 'Structured catalysts and reactors' Cybulski, A. and Moulijn J.A., ed. United States: Taylor and Francis Group, LLC, pp. 355-391.

Campos, V.J.M., and Ferreira, and R.M.Q., 2001. Structured catalysts for partial oxidations. *Catalysis Today*, 69, pp. 121-129.

Edvinsson, R., 1994. Monolith Reactors in Three-Phase Processes. Thesis (PhD). Delft University of Technology, Holland.

Ehrfeld, W., Hessel, V., and Lowe, H., 2003. Microreactors: New Technology for Modern Chemistry. 1st ed, 2nd reprint. Germany: WILEY-VCH.

Ettinghausen, R., and Marie, L.S., 1978. "Islamic Painting." *The Metropolitan Museum of Art Bulletin*, v. 36, no. 2. http://www.metmuseum.org/toah/works-of-art/13.152.6. (Accessed 2 Augest 2011).

Irandoust, S., 1988. The Monolithic Catalyst Reactor. Thesis (PhD), Chalmers University of Technology, Sweden.

Kolaczkowski, S.T., Pluncinski, P., and Lapkin, A.A., 2007. Selective Oxidation of Benzyl Alcohol in a Pilot Scale Multichannel Reactor. *Proceedings of the 1st International Congress on Green Process Eng.*, 24 – 26 April 2007, Toulouse. France, pp. 1-8.

Kockmann, N., Gottsponer, M., Zimmerann, B., and Roberge, D.M., 2008. Enabling continuous-flow chemistry in microstructured devices for pharmaceutical and fine-chemical production. *Chemistry Eur. J*., 14, pp. 7470-7477.

Lamb, G.W., and Williams J.M.J., 2008. Borrowing hydrogen - C - N bond formation from alcohols. *Chimica Oggi-Chemistry Today*, 26 (3), pp. 17-19.

Lamb, G.W., Al Badran, F.A., Williams, J.M.J., and Kolaczkowski, S.T, 2010. Production of pharmaceuticals: amines from alcohols in a continuous flow fixed bed catalytic reactor, *Chemical Engineering Research and Design*. 88, pp. 1533-1540.

Nijhuis, T., Kreutzer, M., Romijn, A., Kapteijn, and F., Moulijn, J., 2001. Monolithic catalysts as efficient three-phase reactors. *Chemical Engineering Science*. 56, pp. 823-829.

Plucinski, P.K., Bavykin, D.V., Kolaczkowski, S.T., and Lapkin, A.A., 2005 a. Application of a structured multifunctional reactor for the oxidation of a liquid organic feedstock. *Catalysis Today*, 105, pp. 479-483.

Plucinski, P.K., Bavykin, D.V., Kolaczkowski, S.T., and Lapkin, A.A., 2005 b. Liquid-Phase Oxidation of organic Feedstock in a Compact Multichannel Reactor. Ind. *Eng.Chem. Res*., 44, pp. 9683-9690.

Roberge, D.M., Ducry, L., Bieler, N., Cretton P. and Zimmerman, B., 2005. Microreactor Technology: A Revolution for the Fine Chemical and Pharmaceutical Industries. *Chem. Eng. Technology*, 28 (3), pp 318-323

Shaughnessy, K., 2009. Hydrophilic Ligands and Their Application in Aqueous-Phase Metal-Catalyzed Reactions. *Chem. Rev*, 109, 643–710.

Stitt, E.H., 2002. Alternative multiphase reactors for fine chemicals A world beyond stirred tanks. *Chemical Engineering Journal*, 90, pp.47-60.

Stevens, P.D., Fan J., Gardimalla, H.M.R., Yen, M., and Gao,Y., 2005 a.Superparamagnatic nanoparticals-supported catalyst of Suzuki cross-coupling reactions. *Organic Letters*., 7, 11, pp. 2085-2088.

Stevens, P.D., Guifeng, L., Fan, j., Yen, M., and Gao, Y., 2005 b, Recycling of homogeneous Pd catalysts using superparamagnetic nanoparticles as novel soluble supports for Suzuki, Heck, and Sonogashira cross-coupling reactions, *Chem. Commun*., pp. 4435-4437.

Watts, P. and Haswell, S.J., 2003. Continuous flow reactors for drug discovery. *Drug discovery today*, 8, 13, pp. 286-293

Xiuyan, S. and Asterios, G., 2008. Scalable Reactor Design for Pharmaceuticals and Fine Chemicals Production. 3: A Novel Gas-Liquid Reactor for Catalytic Asymmetric Transfer Hydrogenation with Simultaneous Acetone Stripping. *Organic Process Research & Development*, 12, pp. 1218-1222.

Zanfir, M. and Gavriilidis, A., 2007. Scalable Reactor Design for Pharmaceuticals and Fine Chemicals Production. 2: Evaluation of Potential Scale-up Obstacles for Asymmetric Transfer Hydrogenation. *Organic Process Research & Development*, 11, pp. 699-971.

CHAPTER 3

CASE STUDY 1: "BORROWING HYDROGEN" THE *N*-ALKYLATION OF MORPHOLINE WITH BENZYL ALCOHOL

This part of the study involved collaboration with Dr Gareth Lamb, in the Department of Chemistry, who was studying the chemistry aspects of borrowing hydrogen. However, the work that forms part of this thesis concentrates on the engineering aspects of how to translate the novel chemistry into a continuous reacting process. Some of the work described in this chapter has now been published in Lamb *et al*., (2010), and a copy of the paper is included in Appendix A

3.1 Introduction

There is a significant interest from the pharmaceutical industry in the alkylation of amines by alcohols to produce a range of components including antihistamines drugs (e.g. chlorpheniramine Piriton®). Traditionally, synthetic methods for the *N*-alkylation of amines have involved the use of potentially environmentally damaging reagents such as alkyl halides, which can also lead to the wasteful formation of by-products due to over-alkylation (Lamb and Williams, 2008).

In addition, the reductive amination of aldehydes and ketones is another well-known method, which had been developed as a useful tool in the synthesis of various amines (Fujita *et al*., 2003). However, this method requires the use of strong reducing reagents or high pressure hydrogen gas and is not always selective for monoalkylation of primary amines (Fujita and Yamaguchi 2005).

The use of alcohols instead of alkyl halides to produce N-alkyl amines is an attractive method because it produces only water as a by-product and does not need special equipment. A variety of transition metal complexes such as ruthenium, iridium, rhodium, platinum, gold, nickel, copper, and iron catalysts are known to be good catalysts for the *N*-alkylation of amines and alcohols (Zhang *el al*., 2011).

Therefore a model reaction based on the *N*-alkylation of a secondary amine (i.e. morpholine) using an alcohol (i.e. benzyl alcohol) has been chosen for this chapter. This reaction is based on some novel chemistry known as ‘borrowing hydrogen’, and this will be described in more detail in the section that follows.

As a reminder, there are three development steps in the proposed 'methodology', and these are illustrated in Figure 3.1. The work in this chapter will focus on Step 1 with an attempt to move on to Steps 2 and 3.

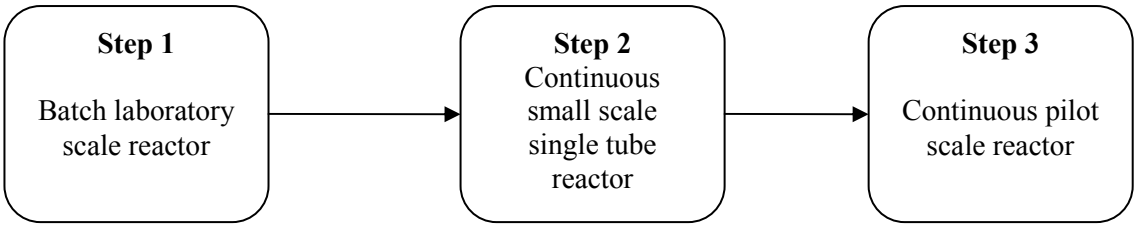

Figure 3.1: Outline scheme for the development of a continuous pharmaceutical process.

3.2 Background on 'Borrowing Hydrogen'

The *N*-alkylation of primary and secondary amines by reaction with alcohols can be achieved under forcing conditions by a number of metal catalysts, e.g. nickel, nickel-rhenium compounds, thorium salts, silica-alumina, metal alloy catalysts, and mixed oxides of copper, barium, and chromium Grigg *et al*., (1981).

According to Hamid *et al*., (2009), it appears that Grigg *et al*., (1981) and Watanabe (1984), were the first to employ the use of metal phosphine complexes as homogenous catalysts for the alkylation of amines by alcohol.

The use of alcohols as alternative alkylating agents for amines (Figure 3.2) has recently received considerable attention in Lamb *et al*., (2008) and Lamb *et al*., (2009).

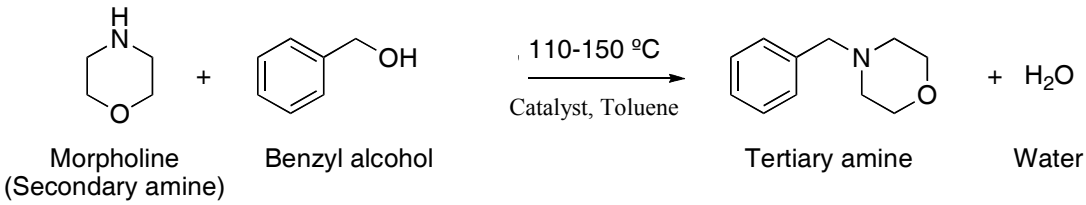

Figure 3.2: Reaction scheme for the model reaction between morpholine and benzyl alcohol (adapted from Lamb *et al*., (2009)).

A good description of the way in which "borrowing hydrogen" works is presented in Lamb *et al*., (2009) from which the following has been obtained:

> *The metal-catalysed pathway involves the temporary removal of hydrogen from an alcohol to form an aldehyde, which undergoes imine formation prior to return of the hydrogen to generate a new C–N bond. Rather than trying to force direct substitution reactions between the amine and the weakly electrophilic alcohol, the borrowing hydrogen approach involves the temporary removal of hydrogen from an alcohol to form an intermediate aldehyde (Figure 3.3). The aldehyde readily undergoes reaction with an amine to form an imine, and the borrowed hydrogen is then returned to provide the amine with no net loss or gain of hydrogen. Whether or not the imine-forming step takes place whilst the substrate is co-ordinated to the metal has not been established.*

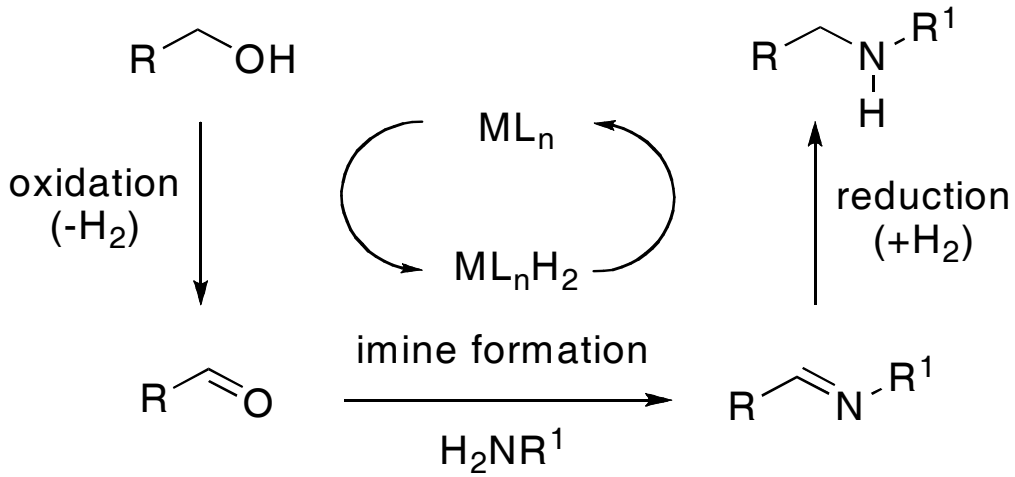

Figure 3.3: Conversion of alcohols into amines by 'borrowing hydrogen' (adapted from Lamb *et al*., (2009)).

There are a number of relevant papers on the topic of "borrowing hydrogen" which where helpful in the selection of experimental conditions in this chapter, and from which the following information has been selected:

3.2.1 Lamb and Williams (2008)

Based on a review of work in this area, the advantages of using "borrowing hydrogen" were listed as follows:

(a) The alkylation of amines by alcohols using the borrowing hydrogen strategy provides an alternative approach to the synthesis of amines.

(b) With only water as a by-product the reaction appeared to be more environmentally friendly.

(c) The traditional alkylating agents, including potentially mutagenic alkyl halides, can be avoided.

3.2.2 Hamid *et al*., (2006)

Based on a review of work on this area the following conclusions were formed:

(a) The Borrowing hydrogen strategy has been exploited in the synthesis of C-C and C-N bonds from alcohols, allowing alcohols to be employed as benign alkylating agents.

(b) Reactions proceed by oxidation of the alcohol to an intermediate carbonyl compound, which can form alkenes or imines *in-situ* before reduction occurs.

(c) Temporary oxidation of an alcohol into a carbonyl compound also allows access to enol/enolate chemistry, before restoration of the alcohol moiety

3.2.3 Hamid *et al.,* (2007 a)

The utility of the combination of $[Ru(p\text{-cymene}Cl_2)]_2$ catalysts with different supported ligands (e.g. dppf, PCy_3 (10 mol%), pph3 (10 mol%), dippf) for the *N*-alkylation of tert-butylamine with phenethyl alcohol was investigated. It was found that the alkylation of tert-butylamine with alcohol could be achieved at good yields by using the combination of $[Ru(p\text{-cymene}Cl_2)]_2$ complex with dppf (diphenylphosphinoferrocene) 5 mol% ligand in toluene media.

3.2.4 Hamid *et al*., (2007 b)

They investigated the benzylation of a range of heterocyclic and aliphatic amines as well as preparing a series of *N*-substituted morpholines using $[Ru(p\text{-cymene})Cl]_2$ in combination with bidentate phosphine ligands as catalysts to produce Piribedil, where Piribedil is a dopamine agonist used in the treatment of Parkinson's disease.

They performed experiments in an atmospheric batch system as follows:

(a) Benzyl alcohol was chosen as a model starting material and was reacted with a range of secondary amines (e.g. morpholine) using 1.25 mol% [Ru(*p*-cymene)Cl_2]$_2$ (2.5 mol% Ru) with either dppf or DPEphos, bis(2 diphenylphosphinophenyl) as the diphosphine ligand.

(b) The products were isolated and purified by column chromatography in good yields.

(c) It was shown that the combination of [Ru(*p*-cymene)Cl_2]$_2$ with dppf provides a useful catalyst for the alkylation of secondary amines with alcohols and therefore the use of potential harmful alkyl halides was avoided. This chemistry was successfully applied to the synthesis of Piribedil (2-[4-(benzo[1,3]dioxol-5-ylmethyl) piperazin-1-yl] pyrimidine).

3.2.5 Hamid *et al*., (2009)

The alkylation of amines by alcohols was studied using 0.5 mol% [Ru(p cymene)Cl_2]$_2$/PPh_3 as a homogeneous catalyst. A conversion of 100% was achieved during the first 6 h.

3.2.6 Preliminary conclusions

In conclusion, N-alkylation reactions based on metal-catalysed hydrogen transfer have become attractive because:

(a) It may enable the development of safer drug products.

(b) The overall reaction is atom efficient consuming all of the starting material with the only other by-product being water

(c) Many alcohols are environmentally benign as well as being readily available compared with their alkyl halide counterparts, highlighting the potentially green credentials of such an approach.

(d) This reaction can effectively be considered as a "one pot" reaction scheme, and if the metal catalyst can be retained within the reactor (e.g using structured support), then the system can be turned into a continuous process benefiting from the associated advantages.

In addition, it is important to emphasize that in general, pharmaceutical reactions are very temperature sensitive, so the use of a structured multi-functional reactor, where good temperature control can be achieved, would clearly be beneficial in this type of process (Cybulski 2006).

However, before a structured reactor can be designed, a suitable catalyst had to be identified that could be used on a structured support. With this aim in mind, in the following sections the viability of fixing the catalyst onto a support (i.e Ru/polymer and Pt/C) is explored.

3.3 Batch laboratory scale reactor

The batch experiments were performed by Dr. Gareth Lamb, however, the author was involved in this aspect, selection of catalysts and discussions about the outcome. They are described in this thesis, as they provide information on how the novel chemistry was developed, and how this leads into the next phase of work as the viability of a continuous process is explored.

In order to assess the viability of using a Ru/polymer and Pt/C catalyst, a series of small-scale experiments were first performed in a batch reactor (Pyrex glass vessel in Radley's carousel). In some of the experiments, *p*-xylene was used instead of toluene as a solvent, as it had a higher boiling point. The reactor assembly is illustrated in Figure 3.4. A 20 mm i.d. (15 ml) proprietary Pyrex glass vessel was used in a Radley's carousel, which was set upon a stirrer hot plate. The top of the vessel was sealed using a Young's tap, retaining the vapour inside the vessel. This type of apparatus is considered relatively standard chemistry bench-top laboratory equipment for reaction studies.

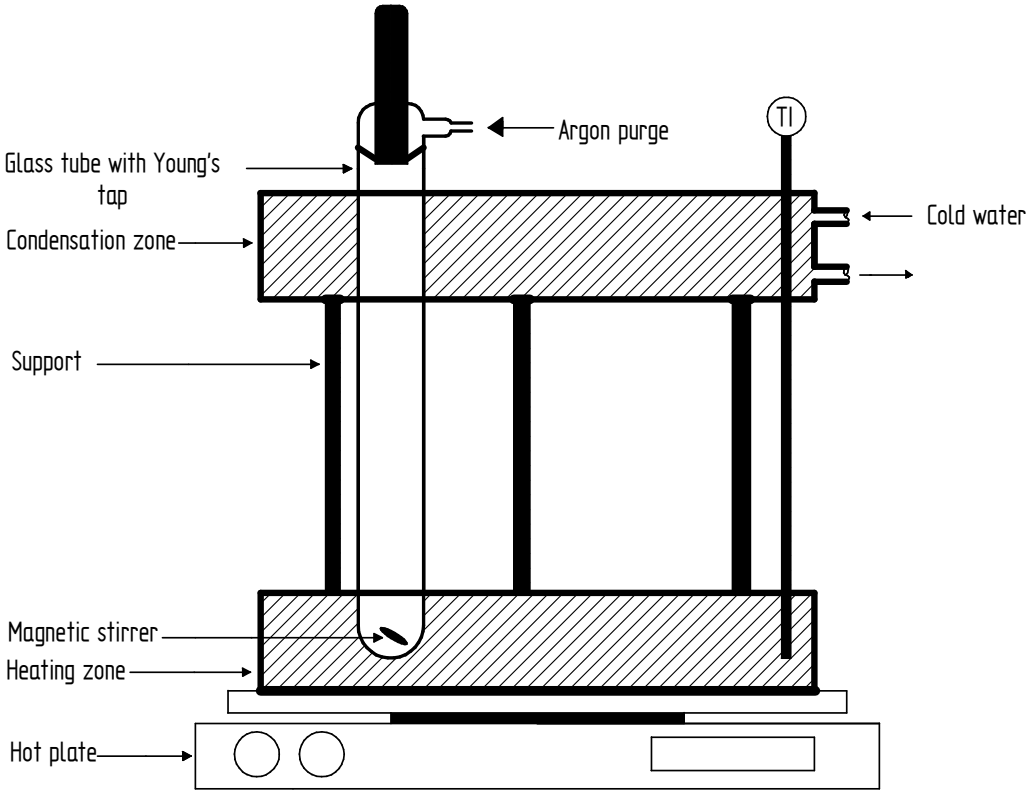

Figure 3.4: Schematic of the Radley's carousel used for the batch experiment.

3.3.1 Experiments on Ru supported polymer in a batch reactor

Based upon the ruthenium systems developed by (Hamid *et al.,* 2007 b), it was decided to develop a polymer-supported system (heterogeneous catalyst) to improve catalyst recovery, and further increase the green credentials of the 'borrowing hydrogen' methodology.

The procedure consisted of the following steps:

(a) Initially, the supported system used a triphenylphosphine bound polymer (1.6 mmol g^{-1} of phosphine) which was complexed in a 2:1 ratio of P:Ru with [Ru(*p*-cymene)Cl_2]$_2$.

(b) The Ru precursor and the polymer bound phosphine were added to a glass vessel containing a magnetic stirrer.

(c) The tube was then purged with argon before adding benzyl alcohol (1 mmol), morpholine (1 mmol) and toluene (1 ml). A molar ratio of 1:1 for alcohol to amine was chosen in order to highlight the atom efficiency of the reaction. This was to ensure that all of the starting material was consumed, with the only other by-product being a stoichiometric amount of water. Previous studies have shown that increasing the amount of amine can increase the percentage conversion; however, it was believed that the advantages of atom efficiency outweighed the 'quick fix' for a higher conversion.

(d) The glass vessel was then sealed and heated to 110 ºC and stirred at this constant temperature for a further 24 h.

Visual observation: As the reactor consisted of a glass tube, it was possible to observe the rapid complexation of the ruthenium precursor with the polymer bound phosphine. Initially, upon stirring the solution turned red as the Ru dissolved in the toluene, then over the course of the next hour the solution became colourless with the polymer turning a deep red colour showing that the Ru was now supported on the polymer. In this type of reactor, as the liquid is heated and a vapour starts to be formed, the vapour

condenses at the top of the reactor (in the condensation zone), and the liquid droplets then trickle back into the base of the reactor.

Analysis: An aliquot of each individual reaction was taken and analysed using ^{1}H NMR to measure the overall conversion of the starting materials into the desired product. NMR spectra were run in $CDCl_3$ on either a Bruker Avance 250 (250 MHz) or a Bruker Avance 300 (300 MHz). Structural assignments were achieved with comparisons from analogous literature compounds. The overall conversion into the desired product was calculated from the ratio of specific product to starting material ^{1}H NMR signals with an expected margin of error of $\pm 5\%$.

Example calculation No 1: To determine the conversion of benzyl alcohol from a ^{1}H NMR spectrum.

The possible ^{1}H NMR protons for the reaction of benzyl alcohol and morpholine are presented in Figure 3.5 a.

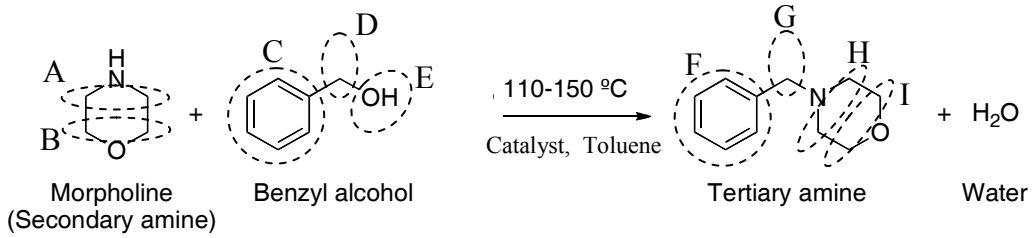

Figure 3.5 a: The locations of ^{1}H NMR protons for the reaction of morpholine and benzyl alcohol.

In Figure 3.5(b) the equivalent peaks for those protons are illustrated. The peak D at 4.5 ppm was identified as the proton in the benzyl alcohol peak, and then the peak G at 3.3 ppm was identified as the proton in the tertiary amine peak. By doing the integration in the software provided within the NMR machine. The results were:

I_D (is the integration value of the benzyl alcohol) = 1.00

I_G (is the integration value of the tertiary amine) = 2.65

Making use of:

$$\text{Conversion of benzyl alcohol} = \frac{I_G}{I_G + I_D} \times 100 \qquad (3.1)$$

Then substituting values:

$$\text{Conversion of benzyl alcohol} = \frac{2.65}{2.65 + 1} \times 100$$

$$= 72 \pm 1\%$$

End of example

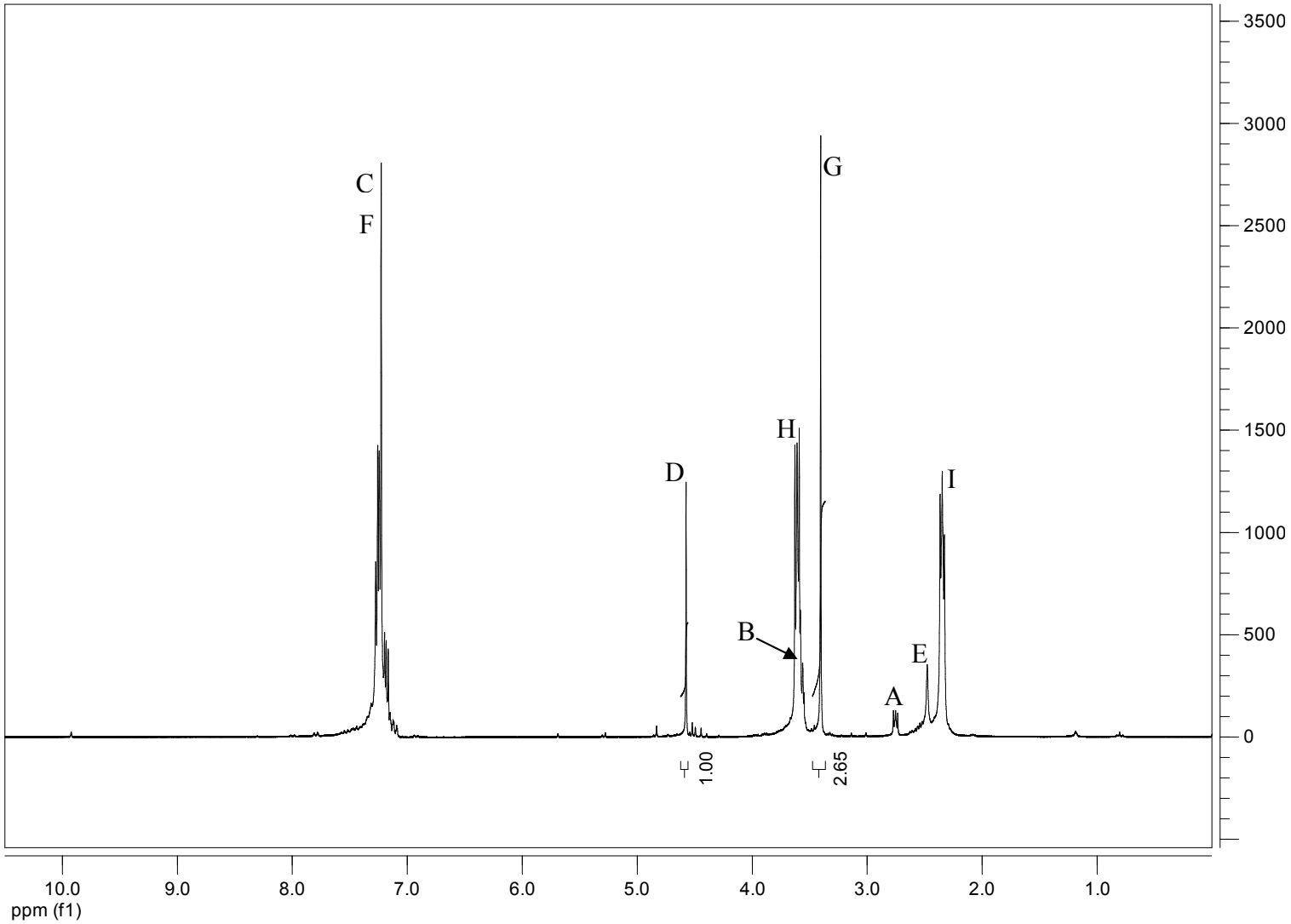

Figure 3.5 b: ^{1}H NMR spectrum of the reaction product sample.

3.3.2 Results from experiments on Ru supported polymer in a batch reactor

After testing two different forms of Ru/polymer catalyst (i.e. Ru(1.6) and Ru(3.2)), a comparison was made with a homogeneous catalyst that had been prepared according to a procedure described in Hamid *et al*., (2009).

The results of the key experiments are summarised in Figure 3.6. It is encouraging to observe that very high conversions could be achieved, indicating that the reaction had not been limited by the thermodynamic equilibrium of the reaction. Figure 3.6 clearly shows that although slower in comparison to the homogeneous system of [Ru(p-cymene)Cl_2]$_2$/PPh_3 (Ru/PPh_3), the polymer-supported systems are still highly active for the *N*-benzylation of morpholine with almost complete conversion being achieved within 24 h (98%). Although very similar in composition the two phosphine bound polymers differ in activity. The polystyrene polymer with a lower loading (containing 1% divinyl benzene (DVB) co-polymer and 1.6 mmol of phosphine g^{-1} (Ru (1.6))) was shown to be considerably more active than the polystyrene polymer with higher loading (containing 2% DVB and 3.2 mmol of phosphine g^{-1} (Ru (3.2))). For example, after a period of 6 hours the 1.6 mmol g^{-1} polymer gave a high conversion of 77% in comparison to 38% when the high loading polymer was used.

.

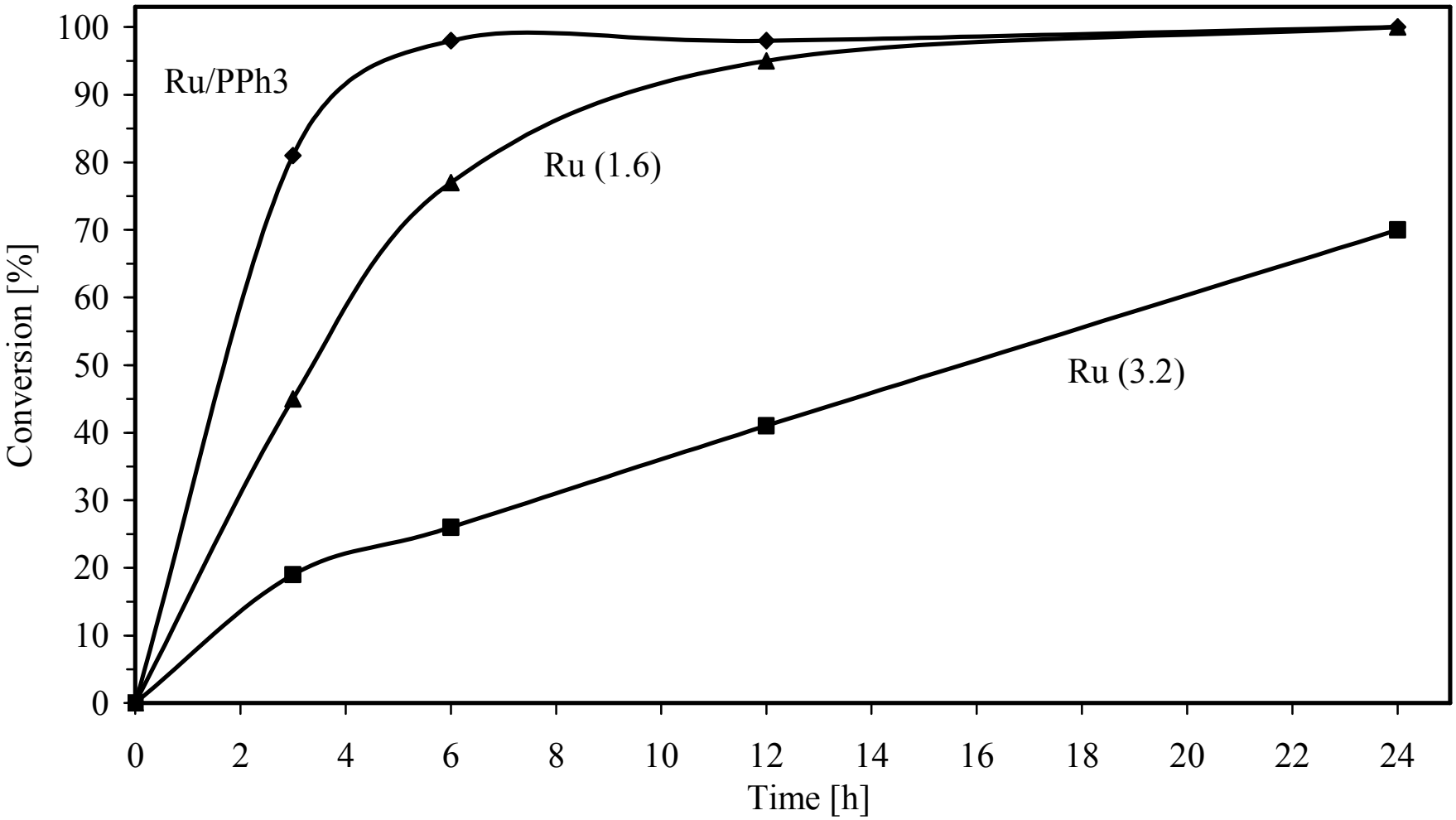

Figure 3.6: The screening of homogeneous (Ru/PPh_3) and supported systems (using 1.6 and 3.2 mmol g^{-1} of polymer-supported phosphine) in the batch reactor for the *N*-alkylation of morpholine at 110 ºC sampled over 24 h.

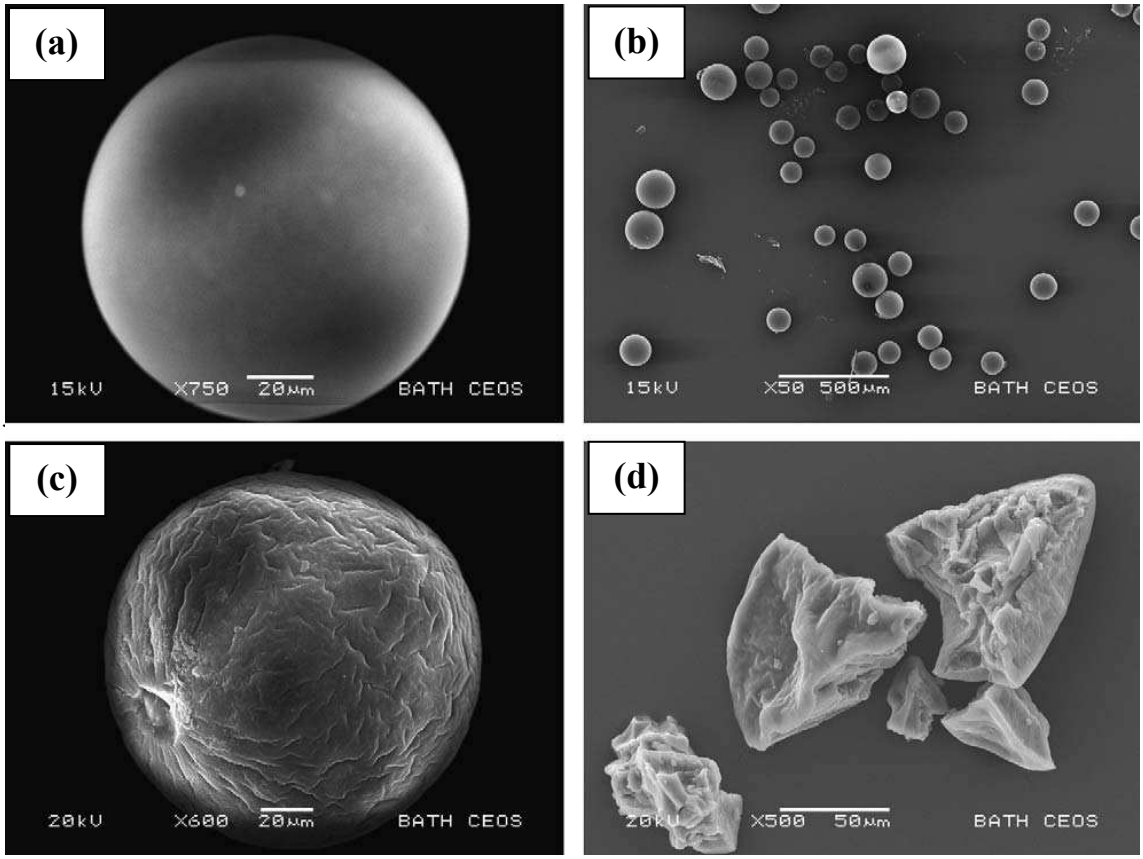

Figure 3.7: SEM images of the polymer beads: (a) 1.6 mmol g^{-1} of phosphine before , and (b) after complexing with ruthenium. Then in (c), 3.2 mmol g^{-1} of phosphine before, and (d) after complexing with ruthenium.

The SEM images in Figure 3.7 show the slight differences between the two types of polystyrene support. Figure 3.7a shows the polymer containing 1.6 mmol g^{-1} of phosphine before being complexed with the ruthenium precursor, $[Ru(p\text{-cymene})Cl_2]_2$. The image shows smooth spherical beads (average particle size 120 µm). On complexing with ruthenium (which involved stirring at 110 ºC in toluene for 3 h under argon), the particles maintain their structural integrity, see Figure 3.7 b. When looking at the uncomplexed polymer containing 3.2 mmol g^{-1} of phosphine (see Figure 3.7 c), the beads although spherical in nature, have many more surface abnormalities in comparison to the polymer with the lower phosphine loading. When these beads went through the same procedure (in order to support the ruthenium precursor) they seemed to disintegrate into much smaller pieces with highly defined jagged edges (see Figure 3.7 d). The average particle size was 70 µm.

Stability of catalyst: The same experimental procedure was followed, however, after 24 h the colourless liquor was extracted and replaced with a fresh aliquot. This was repeated over the course of 5 days. For the first 3 days (72 h) the catalyst remained stable and active giving 3 consecutive results of 100% conversion. However, after 4 days (96 h) the activity dropped off to 73%, and then on the fifth day the conversion dropped further to 50%. Although the solution remained colourless, even after the fifth day the decline in catalytic activity suggested a very low level of catalyst leaching. However, the condition of the polymer itself was seen to deteriorate over the course of the experiment, possibly due to the presence of the water being formed.

It was hoped that in a continuous flow system this would lead to increased catalyst stability as the water produced would be removed with the product and therefore not allow for the build up of water within the system.

3.3.3 Experiments on Pt supported carbon in a batch reactor

The carbon support that was used in this experiment consisted of regular spherical activated carbons with particle sizes of 90 to 150 μm, see Figure 3.8. The Brunauer Emmett Teller (BET) surface area was found to be equal to 750 m^2 g^{-1} with an average mesopore size of 18 nm (Korovchenko et al., 2007). These beads had been prepared in a European project, where the partial oxidation of primary alcohols with air on carbon-supported platinum catalysts was studied (Donze *el al*., 2007).

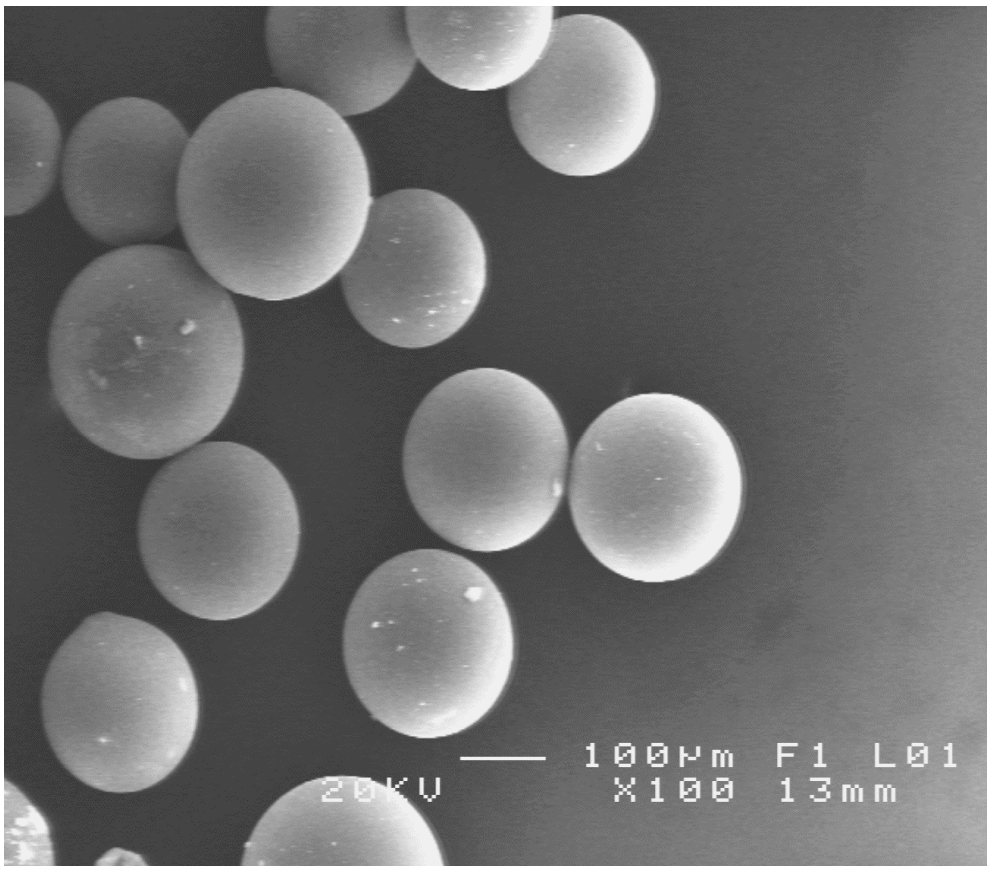

Figure 3.8: SEM showing spherical shaped catalyst beads.

To establish the viability of using Pt/C catalyst in the "borrowing hydrogen" reaction, a series of preliminary experiments were first performed in sealed Schlenk tubes under an atmosphere of argon, in the apparatus illustrated earlier in Figure 3.4. The procedure consisted of the following steps:

(a) The Pt/C catalyst beads (3%wt Pt, 5 mol% loading) were added to the vessel containing a magnetic stirrer.

(b) The vessel was then purged with argon before adding benzyl alcohol (103 µL, 1 mmol), morpholine (87 µl, 1 mmol) and toluene (1 ml).

(c) The vessel was sealed and then heated to 110 ºC and stirred for a further 24 h.

(d) An aliquot of the resulting solution was taken and analysed using ^{1}H NMR to measure the overall conversion into the desired product.

Along with the Pt/C beads (3 wt% Pt) used for the selective oxidation studies, a range of other Pt/C catalyst systems was also screened, several of which are commercially available:

(a) (CP97) 5 wt% Pt on carbon from Engelhard. Other samples from Engelhard:

E1 has a particle size of 250 µm and was activated in CO_2 at 200 ºC.
E2 has a slightly larger particle size of 500 µm and was activated in a similar manner; whilst
E3 also has a particle size of 500 µm, however, it did not undergo activation under CO_2.

(b) 10 wt% Pt/C from Sigma-Aldrich.

(c) Pt on cordierite.

3.3.4 Results from experiments on Pt supported carbon in a batch reactor

The results from a series of batch experiments run at 110 ºC are summarised in Figure 3.9 and clearly show that the Pt/C beads (made in European project) have a far superior activity over many of the commercially available samples. After 24 h at 110 ºC, the Pt/C beads gave a conversion into the desired product of 70% and selectivity of 100% as water is the only by-product.

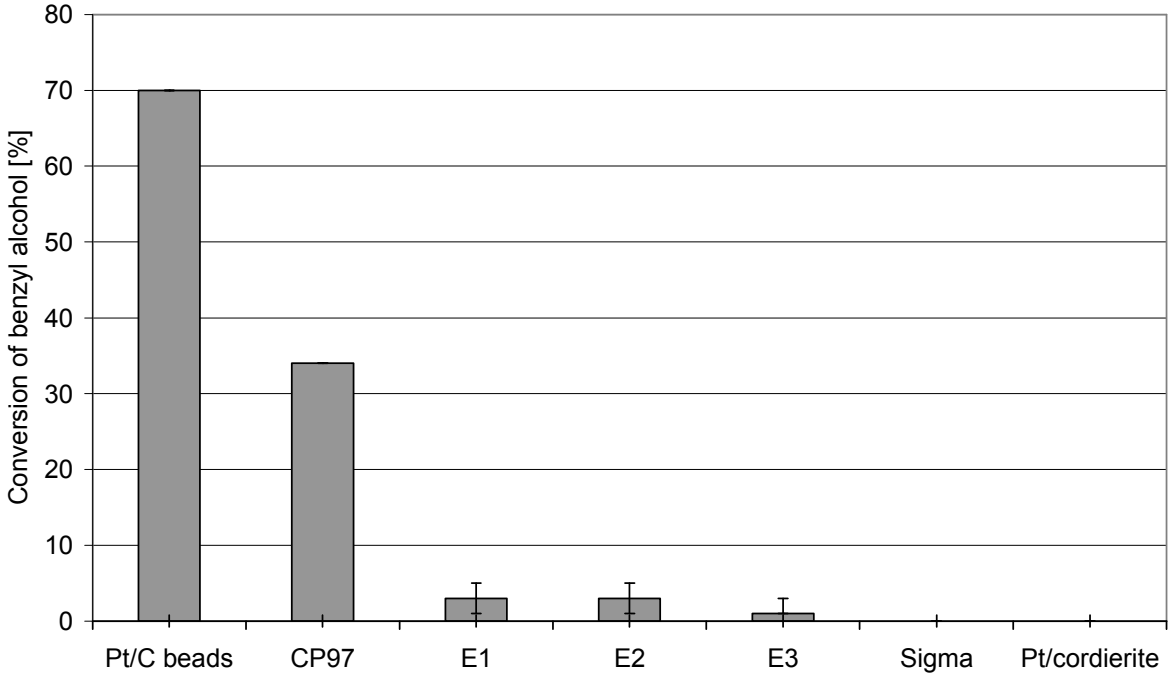

Figure 3.9: Results from batch experiments. A catalytic loading of 5 mol% was used for each of the Pt/C samples in the batch reactions. The Pt/C beads contained 3 wt% Pt, whilst the Englhard samples were 5 wt% Pt, with the Sigma-Aldrich sample being 10 wt% Pt.

When the temperature was increased to 150 ºC, the conversion improved still further to 89%, with only a small amount of by-product ester ($PhCO_2CH_2Ph$) being detected.

3.4 Continuous flow small scale reactor

This Case Study, enabled experiments to be developed for Step 2, in the methodology described earlier in Figure 3.1. Work on this type of reactor is described in this section, and this work was led by the author of this thesis. The chemist (Dr Lamb), who was working on the chemistry, was also involved in this set of experiments, and this aspect helped with recognition of the interface between the two disciplines, and the resulting challenges that have to be overcome, if the proposed 'methodology' is to work.

It was postulated that by moving to a continuous flow system, then this could lead to increased catalyst stability (as the water produced would immediately be removed and not accumulate within the system).

The continuous flow experiments were performed in the following system (see Figure 3.10):

(a) A 300 mm long stainless steel single-tube (7 mm i.d.) acted as the reaction vessel.

(b) The tube was packed with catalyst to a depth of 250 mm, and contained ~ 7 g of catalyst powder.

(c) The reactor was surrounded by an oil jacket, and the heat transfer fluid (Julabo Thermal HC20S) was circulated using a Grant GP200 circulating oil bath. This ensured that a constant temperature could be maintained.

(d) The reactants were premixed with the solvent in a container, and then the solution was pumped into the reactor using a HPLC pump (ConstAMetric LDC Model III G) at a predetermined flow rate.

(e) The pressure was measured at the top and the bottom of the reactor using pressure gauge.

(f) At the outlet from the reactor a 16-turn needle valve was positioned, which was used to maintain the desired back-pressure, this was used to suppress vaporisation of liquid in the reactor. After this valve, the line was left un-insulated so the temperature of the fluid dropped rapidly allowing the liquid to be collected for analysis.

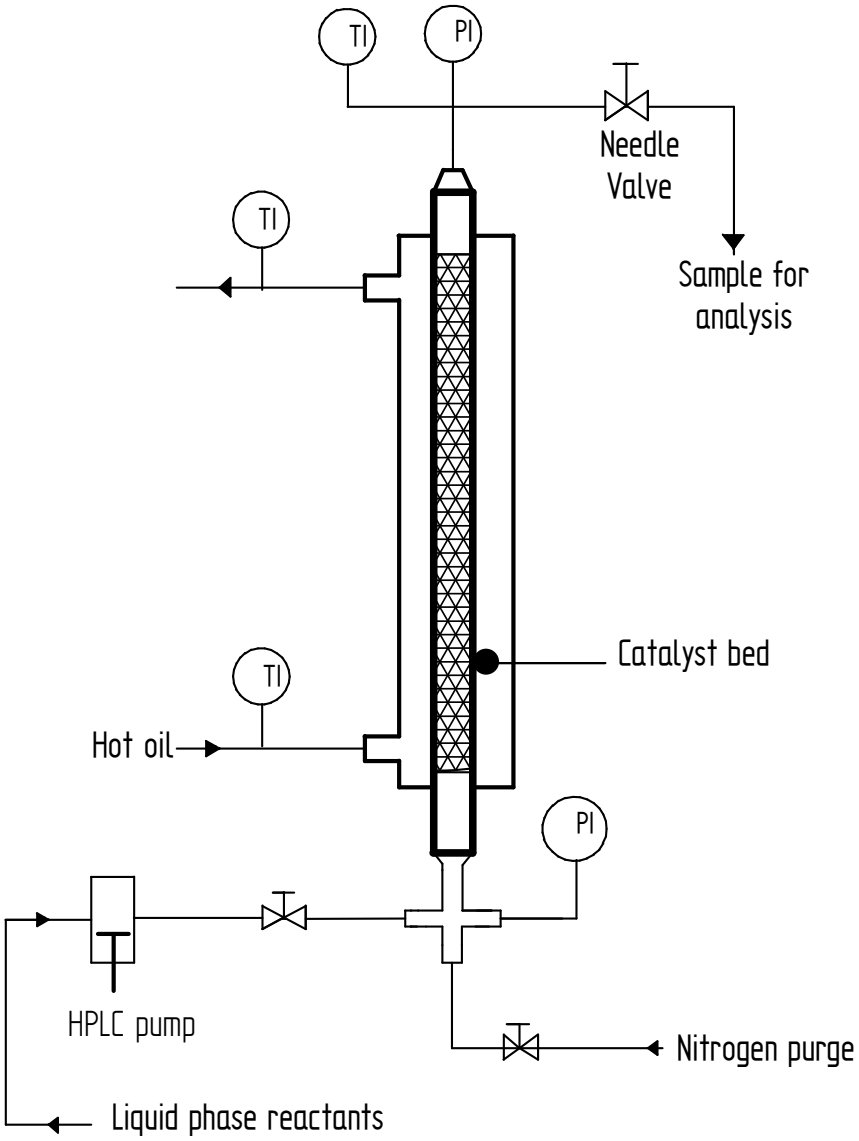

Figure 3.10: Schematic of the small-scale continuous flow experiment.

3.4.1 Experiments on Ru catalyst in a continuous reactor

Based on the results described in Section 3.3.2., experiments were performed with a supported system which used a triphenylphosphine bound polymer (1.6 mmol g^{-1} of phosphine) which was complexed in a 2:1 ratio of P:Ru with $[Ru(p\text{-cymene})Cl_2]_2$.
Two different approaches were tried in order to prepare the catalyst and they were as follows:

(a) In situ catalyst preparation: The catalyst bed was first packed with the polystyrene beads containing 1.6 mmol of phosphine g^{-1} with an average particle size of 150 μm. Then by maintaining the heat transfer fluid in the annular tube at 110 ºC a solution containing the ruthenium precursor, $[Ru(p\text{-cymene})Cl_2]_2$ (0.025 M solution in toluene) was pumped through the reactor, in an endeavour to support the metal (*via* the polymer bound phosphine) on the polymer beads in the bed. Unfortunately, although this was an interesting approach, this technique was not successful, as the pressure-drop across the bed soon became 25 bar(g). The resin had swelled and blocked the voidage between the particles in the bed. ***Therefore, this approach was abandoned, and an alternative approach was considered***.

(b) External catalyst preparation: To a 50 ml round bottom flask under an atmosphere of argon, $[Ru(p\text{-cymene})Cl_2]_2$ (500 mg, 0.816 mmol) polystyrene beads containing 1.6 mmol of phosphine g^{-1} (2.04 g, 3.264 mmol phosphine) and 20 ml of dry, degassed toluene were added. The solution was then heated to 110 ºC for 3 h until the solution was colourless. The supported catalyst was then cooled and filtered. This was then loaded into the packed bed, whilst the filtered particles were still wet-this was to avoid any expansion due to swelling of the resin. ***This technique worked well***

3.4.1.1 Experiments on Ru at atmospheric pressure

Initially, the reactor was operated with the needle valve in the fully opened position corresponding to approximately atmospheric pressure, as the pressure drop across the catalytic bed was assumed to be negligible (pressure gauge at the bottom of the reactor was 0.0 bar(g)). The first set of experiments was performed to ascertain a desirable set of operating conditions and procedures. Sampling every 15 minutes, the activity of the supported catalyst was examined at a range of two different temperatures with a constant flow rate. This was then repeated for two different ranges of flow rates and temperatures. The results of the main experiments are presented in Figure 3.11 and Figure 3.12.

It is interesting to note that even in this relatively short catalytic bed (250 mm), high conversions could be achieved. As expected the conversion into the desired product increases with increasing temperature and decreasing flow rate.
For example, at 110 ºC and a flow rate of 0.25 ml min^{-1} with toluene solvent, a low conversion of 15% to the desired product was achieved (see Figure 3.11), whilst at 150 ºC and a flow rate of 0.1 ml min^{-1}, a conversion of 98 % was obtained (see Figure 3.12).

In the earlier experiment performed in the batch reactor (Section 3.3.1), although the reactor was operated at atmospheric pressure, vaporised material would have been condensed and retained in the reactor. However, when the continuous flow reactor was operated at near atmospheric pressure, then it is likely that vaporised material would have created a two-phase gas–liquid mixture, which would have flowed through the bed. Using a proprietary package known as Aspen Plus, equilibrium flash calculations on the mixture were performed and the vapour pressure of the feed mixture was also estimated. This confirmed, that at 150 ºC, as the vapour pressure was 2.6 bar (see top curve in Figure 3.13) and hence greater than atmospheric, then two-phase flow would have occurred inside the reactor.

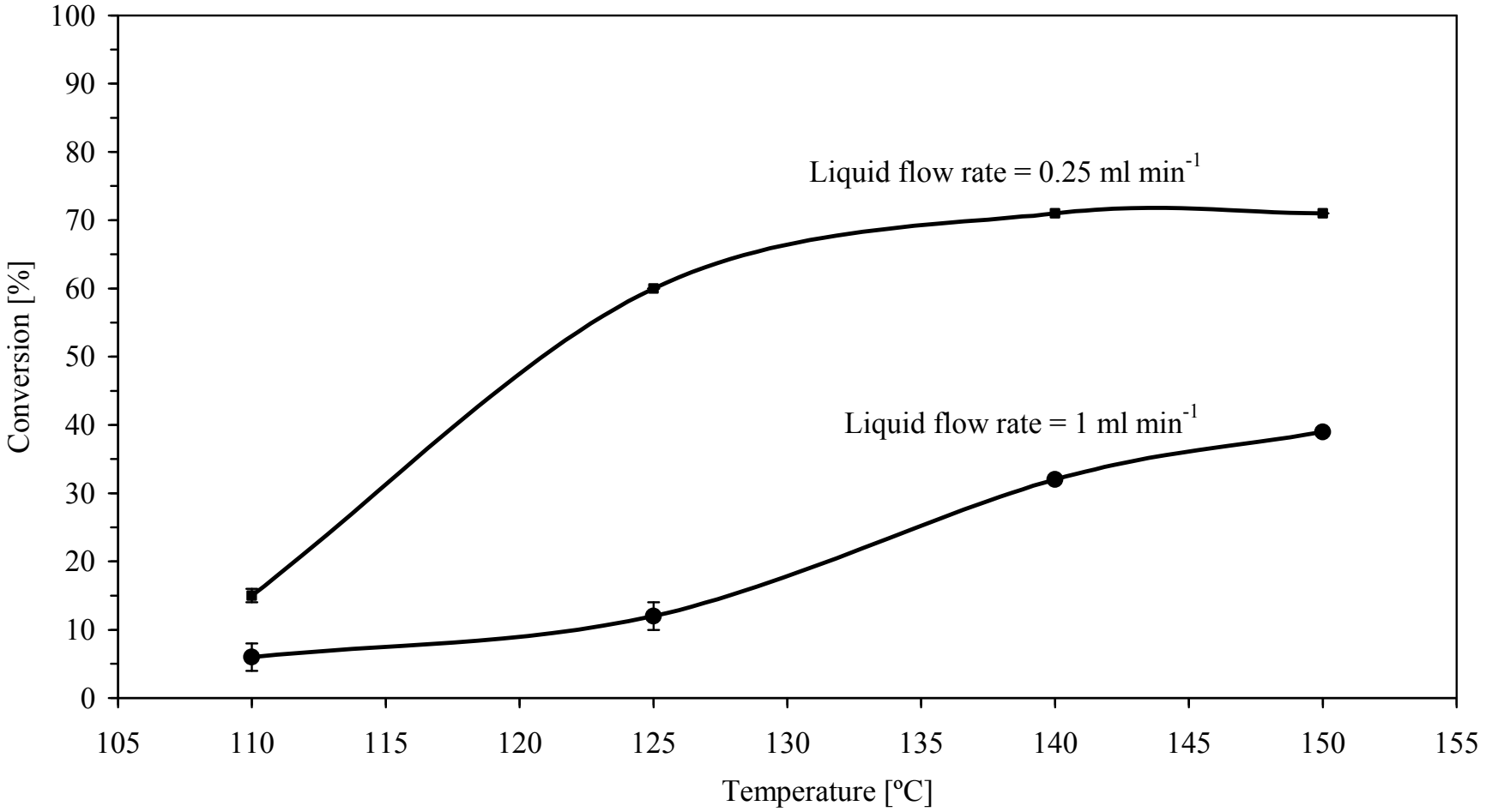

Figure 3.11: Influence of reaction temperature on the conversion of benzyl alcohol at different liquid volumetric flow rates, with a reactant concentration of 1 mol L^{-1} of benzyl alcohol in toluene.

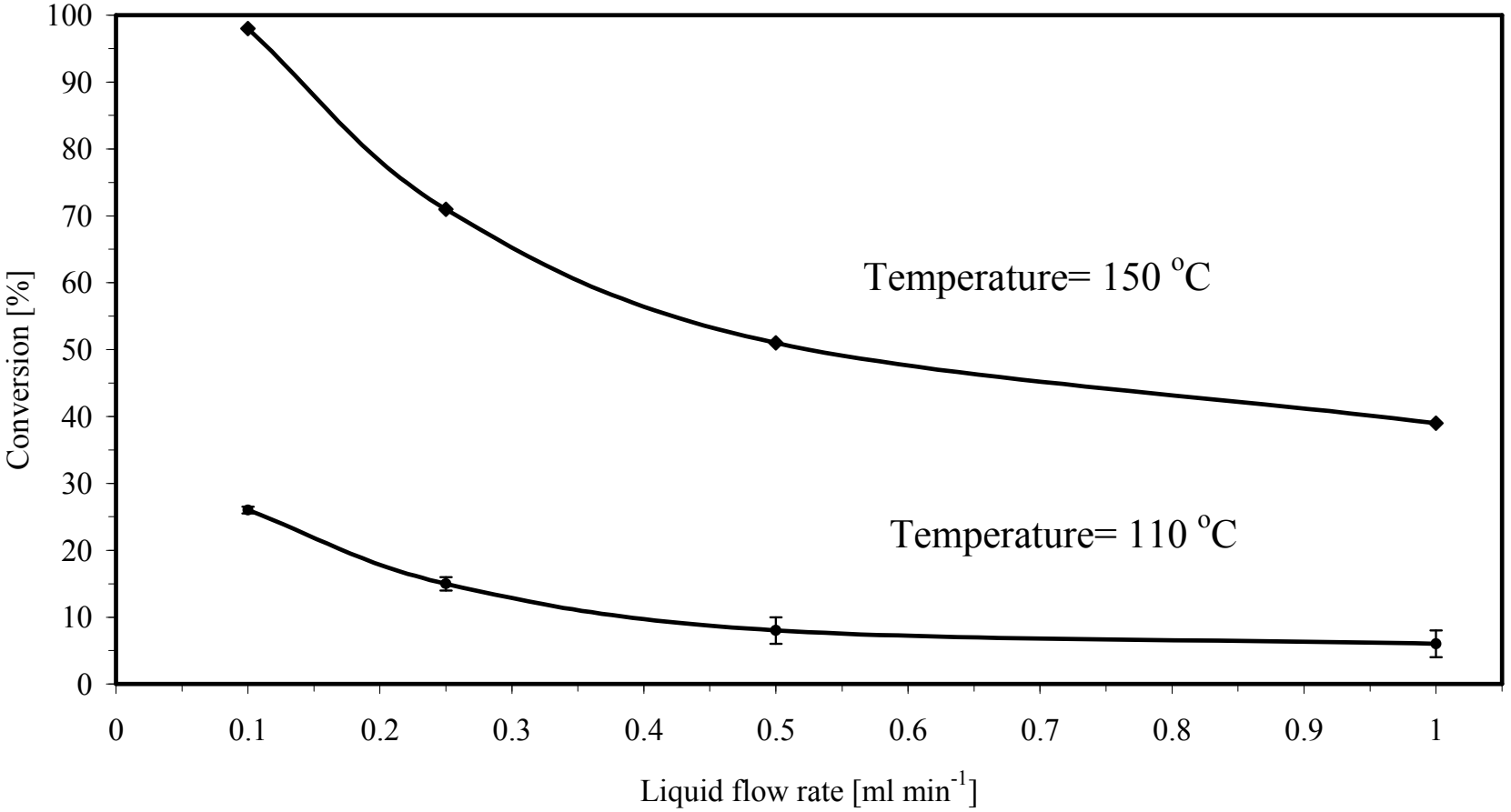

Figure 3.12: Influence of the liquid flow rate on the conversion of benzyl alcohol at different temperatures, with a reactant concentration of 1 mol L^{-1} of benzyl alcohol in toluene.

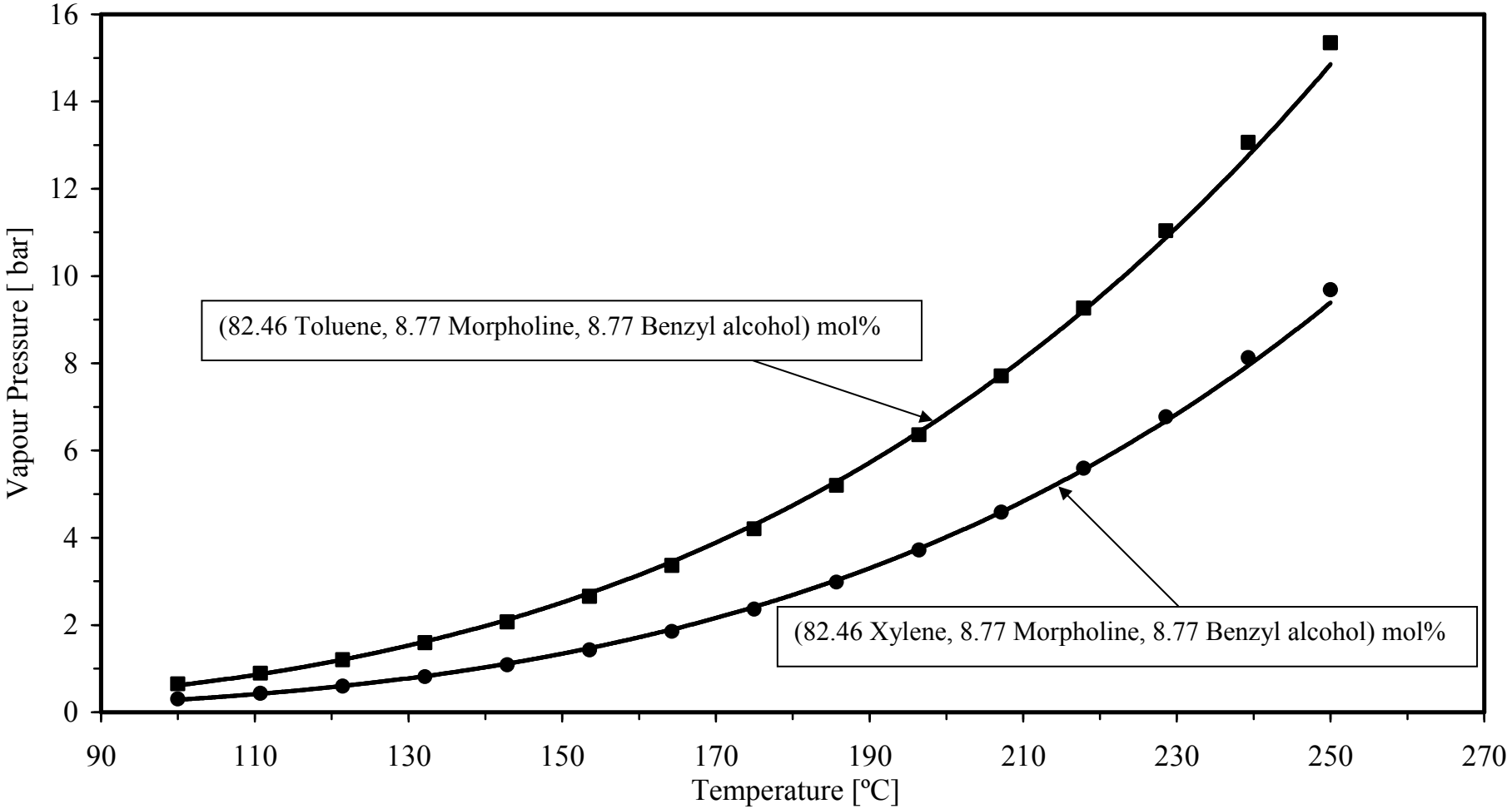

Figure 3.13: Influence of temperature on the vapour pressure for two different organic mixtures.

3.4.1.2 Experiment on Ru at 5 bar(g)

In order to see what effect a back-pressure would have, the reactor was run at 150 ºC, 0.1 ml min^{-1} in toluene solvent with ~5 bar(g). The back-pressure was controlled using a needle valve positioned at the end of the reactor. Suppressing the vaporisation of the mixture (solvent, reactant and product) in this manner led to a slight decrease in activity, whilst still achieving a high conversion of 88% to the desired tertiary amine. This decrease is believed to be as a direct result of the loss of Ru from the system. With the introduction of a back-pressure, catalyst leaching was observed visually as the liquid from the outlet of the reactor turned from a clear colourless solution to dark red.

In order to reduce the loss of Ru from the system, and yet maintain vapour suppression, a decision was made to use a higher boiling solvent, and hence *p*-xylene was used instead of toluene. When the reactor was then run at 150 ºC and 0.1 ml min^{-1} under atmospheric pressure, high conversions (>98%) were again achieved with no visible catalyst leaching. With a boiling point of 138 ºC, *p*-xylene limited the degree to which vaporisation occurred in the reactor. Therefore it was not necessary to add a back-pressure, as with a vapour pressure of 1.36 bar (see lower curve in Figure 3.13) it was only fractionally above atmospheric pressure.

3.4.1.3 Ru Catalyst Stability

When a new catalytic pathway is considered, it is important to explore catalyst stability. In order to draw a comparison with a possible novel homogeneous catalytic pathway, the catalytic turnover number (TON) (van Leeuwen 2005) for the continuous flow fixed bed catalytic reactor was calculated, and this was compared with a possible novel catalytic homogeneous system. The TON was defined as:

$$\text{TON} = \frac{\text{mole of limiting reactant}}{\text{mole of catalyst}} \times \text{fractional conversion}$$

The TON illustrates for how long the same catalyst system can be used, before it needs to be replaced (fixed bed application), or before it has to be recovered from the product solution (homogeneous catalytic system). Although several homogeneous catalytic routes have already been proposed in publications, they are not in use as a commercial process. A disadvantage of the homogeneous system is the need to recover the homogeneous catalyst from the reactor effluent stream. This may be possible to reuse, however, it may not be practicable to do so. Comparisons may also be drawn in the relative catalytic loading of the homogeneous and supported systems. Even a highly active homogeneous system using 1 mol% catalyst loading, the system is ultimately limited by its inability to be recovered and recycled efficiently. However, if it is possible to support a catalyst with a continuous supply of fresh feed, then the TON is only limited by the lifetime of the catalyst.

The fixed bed catalytic reactor was run at 150 ºC, 0.1 ml min^{-1} with a feed solution of 16 vol% of reactants in *p*-xylene. The reactor was run continuously for 72 h processing nearly 500 ml of feed. The TON was calculated to be 515. This compared very favourably with an active homogeneous system operating at 1 mol% catalyst loading having a TON of 100 (experiment described in Section 3.3.2).

3.4.1.4 Preliminary conclusions

It is clear that for this fixed bed reactor, a higher TON is achievable if, for example, the run time was increased, but at this stage in this work enough has been done to show the viability of this approach. However, the stability of the Ru beads catalyst clearly needs to be examined more closely in further work, and a more stable catalyst system needs to be found before progressing to Step 3 in Figure 3.1.
This then led to exploring if a Pt/C catalyst system could be more robust.

3.4.2 Experiments on Pt catalyst in a continuous reactor

Based on the results described in Section 3.3.3., experiments were performed with a supported system which used an activated carbon beds made in a European project, where the partial oxidation of primary alcohols with air on carbon-supported platinum catalysts was studied (Donze *et al*., 2007).

3.4.2.1 Experiments on Pt catalyst at atmospheric pressure

Using the apparatus illustrated in Figure 3.10, the initial set of experiments was performed with the needle valve in the fully opened position, corresponding to approximately atmospheric pressure in the bed. Running at 150 ºC, with a flow rate of 0.25 ml min^{-1}, a 15% conversion to the desired product was achieved. At higher temperatures of between 175 to 225 ºC, leaching of Pt from the reactor was observed visually as the liquid from the outlet of the reactor turned from a clear colourless solution to dark brown.

Experiment was then performed with a fresh catalyst bed, the flow rate was then reduced to 0.05 ml min^{-1} (at 150 ºC) in order to achieve a greater conversion. At the outlet from the reactor, samples of the fluid were collected every hour over a period of 6 h. Analysis of the samples collected (using ^{1}H NMR) showed that after 6 h a conversion of 53% appeared to have been achieved. However it was believed that two phase flow was occurred as the solvent (toluene) can be vaporised at such a condition of 150 ºC (see Figure 3.13).

3.4.2.2 Experiments on Pt catalyst at elevated pressure of 5 bar(g)

The experiment was then repeated using a back-pressure of 5 bar(g) in order to suppress solvent vaporisation. Unfortunately, once again very little of the tertiary amine passed through the column. Only when the pressure was released did the absorbed product begin to flow. Analysis of this solution showed a high conversion of around 73% into the desired product.

Although the experiments with Pt/C did show some interesting initial results, the scale-up of this particular system (from batch to continuous) under the current operating

conditions was found to have complications. It was also postulated that the metal may be forming an association with the amine increasing its solubility in the feed solution as one possible explanation for the visually observed leaching as the liquid from the outlet of the reactor turned from a clear colourless solution to dark brown.

3.5 General discussion of experimental errors

In this section experimental errors are reviewed, so that their impact on the key conclusions presented at the end of this chapter may also be taken into account.

3.5.1 Experiments in the batch reactor

Temperature: This was measured in the Radley's carousel reactor with a temperature probe, and when measuring 110 ºC, this type of measurement is generally considered to be within ± 1.5 ºC which corresponds ±1.4% of the reaction temperature. This error would have no significant impact on the conclusions formed.

Analysis of the composition of the liquid phase: This was performed using ^{1}H NMR, and as discussed in Section 3.3.1, the expected margin of error in the integration value (i.e. I_G, see Figure 3.5 b) was <5%. This value was then used to calculate the conversions. The error in the conversion could vary from ±1 at low conversion (10%), to ±0.1 at high conversion (98%).
These errors would have no significant impact on the conclusions formed.

Volumes of fluid used in the reactor: The errors uncertainty in measuring these volumes are in the region of ±0.01 ml of the volume measured, which corresponds ±1% of the liquid volume and this would have no significant impact on the conclusions formed.

3.5.2 Experiments in the continuous flow reactor

Temperature: This was measured with K type thermocouples, and when measuring 110 ºC, this type of measurement is generally within ± 2.2 ºC which corresponds ±2% of the reactor temperature. This error would have no significant impact on the conclusions formed.

Analysis of the composition of the liquid phase: This was performed using ^{1}H NMR, and as discussed in Section 3.3.1, the expected margin of error in the integration value (i.e. I_G, see Figure 3.5 b) was <5%. This value was then used to calculate the conversions. The error in the conversion could vary from < ±2 at low conversion (10%), to < ±1 at high conversion (98%).
These errors would have no significant impact on the conclusions formed.

Liquid flow in the reactor: The fluid was pumped into the reactor, by a HPLC pump, at a prescribed setting on the pump. At that setting, a quantity of liquid was collected in a measuring cylinder over a known interval of time, and the liquid flow rate was calculated. For example, at a flow of 1 ml min^{-1}, the error was estimated to be ±0.01 ml, which corresponds to ±1 % of the liquid flow. This would have no significant impact on the conclusions formed.

Pressure: For a very early set of experiments, as the outlet valve on the reactor was left open, it was assumed that the pressure in the reactor was above, yet close to atmospheric. This assumption was not checked with an actual pressure measurement. However, for subsequent experiments a pressure gauge was installed, and experiments were then performed with a partially closed valve resulting in a back-pressure on the reactor. A reported pressure of 5 bar(g) would be reading within ±0.2 bar which corresponds to ±4 % of the total pressure. These errors would have no significant impact on the conclusions formed.

3.6 Conclusions

From this chapter, where several experiments on batch and continuous systems were performed and analysed, and the following important conclusion have been formed:

(a) It was shown, that a novel homogeneous catalytic pathway, based on 'borrowing hydrogen' could be extended and used to make amines in a continuous process, with the catalyst retained and fixed in a packed bed. This is clearly a major achievement and one on which other researchers working on pharmaceutical applications can build.

(b) In the batch experiments, it was not easy to detect if catalyst leaching was going to be a major problem. This is an important observation from a 'methodology' perspective.

(c) In the batch experiments, it was not intuitive from a chemistry perspective that vaporisation was occurring, but because of the way the vapours were condensed and returned into the reactor, the reaction took place mainly in the presence of a liquid phase. This is another important observation from a 'methodology' perspective.

(d) The Ru catalyst was clearly very active, although catalyst leaching also occurred under certain conditions. It was postulated that this was due to interaction between morpholine and Ru in the liquid phase, hence it was influence by operating pressure as at 5 bar(g) solvent vapour is suppressed (liquid flow only) while two phase flow was expected to accrue at atmospheric pressure Figure 3.13.

(e) There are some interesting and unexpected results in this work, as it was found that the system works well when the liquid phase reactants are allowed to partially/completely vaporise. This is completely counter-intuitive, and once again this could lead to some interesting 'methodology' in the future.

(f) For applications in the pharmaceutical industry, this approach is clearly very promising, as it provides a greener and more atom efficient route for the production of secondary and tertiary amines. However, it is recognized that further work is necessary to optimize the system, and quantify longer term catalyst stability.

(g) In batch experiments, the reaction with Pt/C showed some interesting initial results, however, the transfer of this particular system from batch to continuous under current operating conditions was found to have complications and catalyst leaching.

Finally, it important to conclude that a point had been reached with this reacting system, where it was not possible to proceed further to Step 3 (pilot-scale), as the chosen combination of catalyst/support and reactants/solvent was shown to be insufficiently robust. This also reflects the reality of developing a system in a batch reactor which appears to work, and then problems are noticed at the Step 2 (small continuous-flow) stage. It is far better to realize the problem in Step 2, rather than in Step 3, where the costs are higher.

References

Cybulski, A., Albers, R.E.A., and Moulijn, J.A., 2006. *Monolithic Catalysts for Three-Phase Processes*. In: 'Structured catalysts and reactors' Cybulski, A. and Moulijn J.A., ed. United States: Taylor and Francis Group, LLC, pp. 355-391.

Donze, C., Korovchenko, P., Gallezot, P., and Besson, M., 2007. Aerobic selective oxidation of (hetro) aromatic primary alcohol to aldehydes or carboxylic acids over carbon support platinum. *Applied catalysis B: Environment,* 70, pp. 621-629.

Fujita, K., Ozeki Li, N., and Yamaguchi, R., 2003. N-Alkylation of amines with alcohols catalyzed by a Cp*Ir complex. *Tetrahedron Letters,*44, pp. 2687-2690.

Fujita, K., and Yamaguchi, R., 2005. Cp*Ir complex-catalyzed hydrogen transfer reactions directed toward environmentally benign organic synthesis Synlett, 2005, *Organic Chemistry*, pp. 560-571

Grigg, R., Mitchell, T., Sutthivaiyakit, S., and Tongpenyai, N., Transition Metal catalysed N -Alkylation of Amines by Alcohols. *J.C.S. CHEM. COMM.*, 1981, pp. 611-612.

Hamid, M., Slatford P., Williams, J.M.J., 2006. Borrowing Hydrogen in the Activation of Alcohol. *Adv. Synth. Catal.*, 349, pp. 1555-1575.

Hamid, M.H.S.A., and Williams, J.M.J., 2007 a. Ruthenium Catalysed N-alkylation of amines with alcohols. *Chem. Commun.,* 7, pp.725-727.

Hamid, M.H.S.A., and Williams, J.M.J, 2007 b. Ruthenium-catalysed sunthesis of tertiary amines from alcohol. *Tetahedron Letters*., 48, pp. 8263-8265.

Hamid M.H.S.A., Allen, C.L., Lamb, G.W., Maxwell, A.C., Hannah, C.M., Andrew, J.A., and Williams J.M.J., 2009. Ruthenium-Catalyzed N-Alkylation of Amines and Sulfonamides Using Borrowing Hydrogen Methodology. *Journal of the American chemical society*.131(5), pp. 1766-1774.

Korovchenko, P., Donze, C., Gallezot, P. and Besson, M., 2007. Oxidation of primary alcohol with air on carbon-supported platinum catalyst for the synthesis of aldyhied or acids. *Catalysis Today*, 121, pp. 13-21.

Lamb, G.W. and Williams, J.M.J., 2008. Borrowing hydrogen - C - N bond formation from alcohols. *Chimica Oggi-Chemistry Today*, 26 (3), pp. 17-19.

Lamb, G.W., Al Badran, F.A, Williams, J.M.J., and Kolaczkowski S.T, 2010. Production of pharmaceuticals: amines from alcohols in a continuous flow fixed bed catalytic reactor, *Chemical Engineering Research and Design*. 88, pp. 1533-1540.

Lamb, G.W., and Watson, A., 2009. Borrowing hydrogen methodology for the conversion of alcohols into *N*-protected primary amines and in situ deprotection. *Tetrahedron Lett*., 50, pp. 3374-3377.

Zhang, Yan., Xiujuan, Qi., Xinjiang, Cui., Feng Shi., Youquan, D., 2011. Palladium catalyzed N-alkylation of amines with alcohols. *Tetrahedron Letters*, 52, pp. 1334-1338.

CHAPTER 4

CASE STUDY 2: REACTION KINETICS FOR THE PARTIAL OXIDATION OF BENZYL ALCOHOL TO BENZYLALDEHDE OVER A PLATINUM ON CARBON CATALYST.

Chemical reaction kinetic experiments were performed with a platinum catalyst supported on an activated carbon powder in an autoclave batch reactor. In a set of preliminary experiments appropriate experimental conditions are established. Experiments were then performed to achieve a better understanding of the effect of the key variables.

4.1 Theoretical background

Catalytic selective oxidation in the liquid phase is a developing research area due to industrial interest in these types of reactions and the increasing need to substitute conventional stoichiometric oxidising reagents, such as nitric acid, organic peroxides and metal oxides, with environmentally benign oxidants, such as air or molecular oxygen (Bavykin *et al*., 2005).

4.1.1 Yamaguchi and Noritaka (2003)

They explored the kinetic aspects of the aerobic oxidation of benzyl alcohol to benzaldehyde in the presence of a ruthenium catalyst (2.5 mol% Ru on Al_2O_3) in a trifluorotoluene solvent. The effect of varying conditions (i.e. alcohol concentration, pressure of molecular oxygen, and amount of the catalyst) on the reaction rate expression was investigated using a batch reactor. Based on their work, they found:

(a) A first-order dependence of the rate of oxidation on the amount of the catalyst.

(b) A zero-order dependence of the rate of oxidation on the pressure of molecular oxygen.

(c) A first-order dependence on alcohol concentration at low concentration and zero-order dependence at higher concentration.

(d) The following parameters were found: ΔE_A= 51.4 kJ mol^{-1}; lnA=15.1; ΔH_{298K} = 48.9 kJ mol^{-1}.

(e) The reaction rate ($r_{alcohol}$) was as follow:

$$r_{alcohol} = -d[alcohol]/dt = k[catalyst]^{1}[alcohol]^{1\rightarrow 0} \qquad (4.1\ a)$$

where

$$k = 3.44\times 10^{6} \exp\left(-6.18\times 10^{3}/T\right) \qquad (4.1\ b)$$

4.1.2 Plucinski *et al*., (2005 a)

They studied the reaction kinetics of the partial oxidation of benzyl alcohol to benzylaldehde over a heterogeneous catalyst consisting of 0.9 wt% Ru on Al_2O_3 (150 μm particle size). A single channel bench-top reactor was used where the reactor consisted of 3 mm x 3 mm square channels and was 100 mm long. The channels were packed with 150 μm catalytic beads and a static mixer section was at in the inlet of each channel (for oxygen and liquid mixing). They found that the apparent kinetic constant $k = 3.38 \times 10^{-6}$ kmol kg_{cat}^{-1} s^{-1}, and $\Delta E_A = 79.3$ kJ mol^{-1}.

4.1.3 Zotova *et al*., (2010)

They describe the use of a commercially-available XCube^{TM} reactor, in which they performed experiments on the partial oxidation of benzyl alcohol to aldehydes. The reactor had a small volume (6 ml), and the catalyst was loaded into one or two cylindrical cartridges (each measuring 4 mm × 70 mm) that could be heated and pressurised (Figure 4.1). In a typical experiment:

(a) A solution of the alcohol (0.1 to 1.0 mol L^{-1} in toluene) was delivered by a piston pump to a gas mixer, where it was pre-mixed and saturated with the gaseous reactant (O_2 or air) before it was passed through the catalyst bed.

(b) A gas bubble detector maintained a 19:1 liquid-to-gas ratio; thus, the system was not subjected to gas–liquid mass transfer resistance and the small reactor volume also ensured very little, if any, pressure drop.

(c) Residence times of up to 180 s could be achieved by controlling the flow rate (normally 1 ml min^{-1}), and the product stream could then be collected as separate fractions (for single-pass experiments), or, if desired, re-circulated in continuous flow until the reaction was complete.

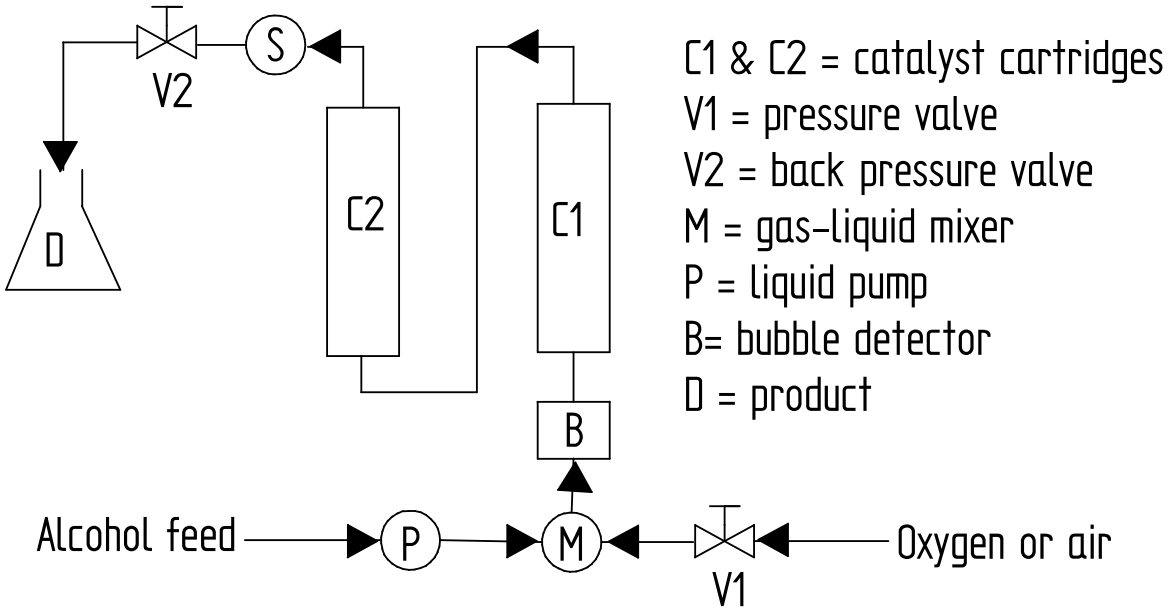

Figure 4.1: General schematic of the Xcube™ flow reactor (adapted from Zotova *et al*., (2010)).

Zotova *et al*., (2010) also derived a global rate equation to model the kinetic behaviour of the partial oxidation reaction of benzyl alcohol and provided the following explanations in their paper:

(a) The active catalyst species was believed to be ruthenium hydroxide (see Figure 4.2), which reacted with the alcohol to generate a ruthenium-alkoxide species that dehydrogenates *via* a b-H elimination process. The insertion of a dioxygen molecule into the resultant Ru–H species forms an unstable peroxide complex, which eliminates an oxygen atom to complete the catalytic cycle. Thus, the overall process consumes an oxygen atom and produces a water molecule as a side product.

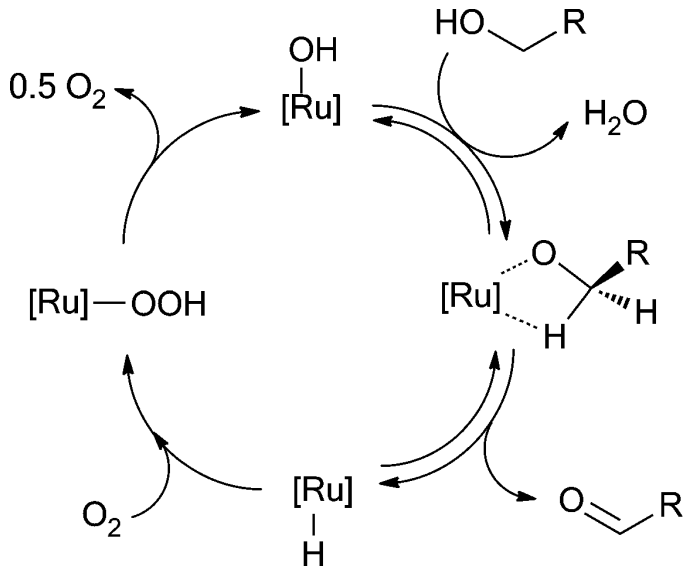

Figure 4.2: The Proposed mechanism for the Ru/Al2O3-catalyzed aerobic oxidations of alcohols (adapted from in Zotova *et al*., (2010)).

(b) Assuming that the overall rate is governed by surface reactions, there are essentially two processes that operate in the catalytic system: (i) the conversion of benzyl alcohol to benzaldehyde with the concomitant formation of a water molecule (equation 4.2), and (ii) the regeneration of the active catalyst site by dioxygen (equation 4.3). From these, a Mars–van Krevelen-type of rate equation can be derived (equation 4.4) as follows:

$$PhCH_2OH + [Ru-OH] \xleftrightarrow{k_1} PhCHO + H_2O + [Ru-H] \tag{4.2}$$

$$[Ru-OH] + 0.5O_2 \xleftrightarrow{k_2} [Ru-H] \tag{4.3}$$

$$\text{rate} = A\frac{[PhCH_2OH][O_2]^{0.5} - [PhCHO][H_2O]/k_1k_2}{1+[O_2]^{0.5}k_2} \tag{4.4}$$

where $A = k_1k_2[Cat]_{tot}$, and $[Cat]_{tot}$ = total catalyst sites.

(c) They tested the validity of equation 4.3 by following the oxidation of benzyl alcohol at two different initial concentrations (0.1 and 0.2 mol L^{-1}). Under such dilute conditions, the reaction was found to be pseudo-first-order with respect to benzyl alcohol.

(d) By increasing the O_2 pressure from 5 to 25 bar the reaction rate was significantly enhanced, restoring the first-order rate of consumption of benzyl alcohol; therefore, O_2 is integral to the kinetics of the reaction in equation 4.3.

(e) Although the selectivity of the reactions was >99% in most cases, a trace amount of benzoic acid (<1%), which they considered to be a catalyst poison, could often be detected by GC in the reaction streams. Indeed, the catalyst lost about 20% of its activity when it was reused, even though the selectivity of the reaction was maintained. However, it was claimed that the catalytic activity could be restored by washing the supported catalyst with an aqueous NaOH solution.

4.1.4 Interim conclusions from literature

Having reviewed some of the more relevant literature, the following conclusions were formed:

(a) There is an interest in studying the reaction kinetics of partial oxidation of benzyl alcohol to benzylaldehde, however many of the previous studies were on a Ru/Al_2O_3 catalytic system.

(b) Some work has been done on a Pt/C catalyst, but there is a lack of information on kinetics.

(c) A batch reactor is a suitable system in which mass transfer and diffusion resistances can explored.

(d) To study the catalytic kinetics of benzyl alcohol to benzylaldehde on the Pt/C catalyst system, an autoclave (Parr Instrument, Model 425 HC) would be used.

(e) Power low kinetic was considered in this chapter to express the kinetic of benzyl alcohol reaction. This type of kinetic was applied successful in Yamaguchi and Noritaka (2003).

4.1.5 Three phase reaction system

Liquid phase oxidation employing heterogeneous catalysts are multi-phase (gas-liquid-solid) systems containing concentration gradients (Fogler, 2006). In order to obtain a true measure of reaction kinetics, gas absorption, external mass transfer, and internal diffusion resistances need to be understood and minimized as the mass transfer resistance effects can alter reaction time, reaction selectivity and product yields.

For the partial oxidation reaction of benzyl alcohol to benzaldehyde to take place in a three phase heterogeneous system, the following sequence must occur, see also Figure 4.3:

(S1) Transport of the oxygen reactant into the liquid phase. It could be assumed that this step is controlled by Henry's law:

$$P_T \, y_{O_2} = H \, x_{O_2} \tag{4.5}$$

where:

y_{O_2} is the mole fraction of the oxygen in the gas phase,

x_{O_2} is the mole fraction of the oxygen in the liquid phase,

H is the Henry's constant of oxygen in reaction mixture, bar, and

P_T is the system pressure, bar.

(S2) Transport of the dissolved gaseous oxygen and the benzyl alcohol through the bulk liquid to the surface of a catalyst particle. The rate of mass transfer N_{BA} is represented by:

$$N_{BA} = k_{Am} a (C_{BA,b} - C_{BA,s}) \tag{4.6}$$

where:

N_{BA} is the mass transfer rate of benzyl alcohol, mol s^{-1},

$C_{BA,s}$ is the benzyl alcohol concentration at the catalyst surface, mol L^{-1},

$C_{BA,b}$ is the benzyl alcohol concentration in the bulk liquid, mol L^{-1},

k_{Am} is the mass transfer coefficients in the liquid phase, mol s^{-1}, and

a is the external surface area, m^2.

(S3) Diffusion of the reactants into the pore structure of the catalyst particle. the diffusion mass transfer step is controlled by:

$$N``_{BA} = -D_{BA} \frac{dC_{BA}}{dr} \tag{4.7}$$

where:

$N``_{BA}$ is the mass flux of benzyl alcohol, mol m^{-2} s^{-1},

D_{BA} is the diffusivity of benzyl alcohol, m^2 s^{-1},

C_{BA} is the benzyl alcohol concentration, mol L^{-1},

r is the radius of the catalyst support particle, m, and

$\frac{dC_{BA}}{dr}$ is the concentration gradient of benzyl alcohol inside the catalyst particle.

(S4) Chemical reaction. The surface reaction step is controlled by the rate of reaction, which could be of the following form:

$$r_{BA} = -\frac{dC_{BA}}{dt} = k_s[C_{BA,s}]^{\alpha}[C_{O_2,s}]^{\beta} \tag{4.8}$$

where:

r_{BA} is the surface reaction rate, mol m^{-3} s^{-1},

k_s is the reaction rate constant, mol^{1-n} m^{n-1} s^{-1},

$C_{BA,s}$ is the benzyl alcohol concentration at the catalyst surface, mol L^{-1},

$C_{O_2,s}$ is the oxygen concentration at the catalyst surface, mol L^{-1},

α and β are the individual reaction order, and

n is the overall reaction order, $n = \alpha + \beta$.

(S5) Diffusion of the products out of the pore structure of the catalyst particle is controlled by a similar form of equation 4.7.

(S6) External mass transfer of the product back to bulk liquid from the catalyst surface is controlled by a similar form of equation 4.6.

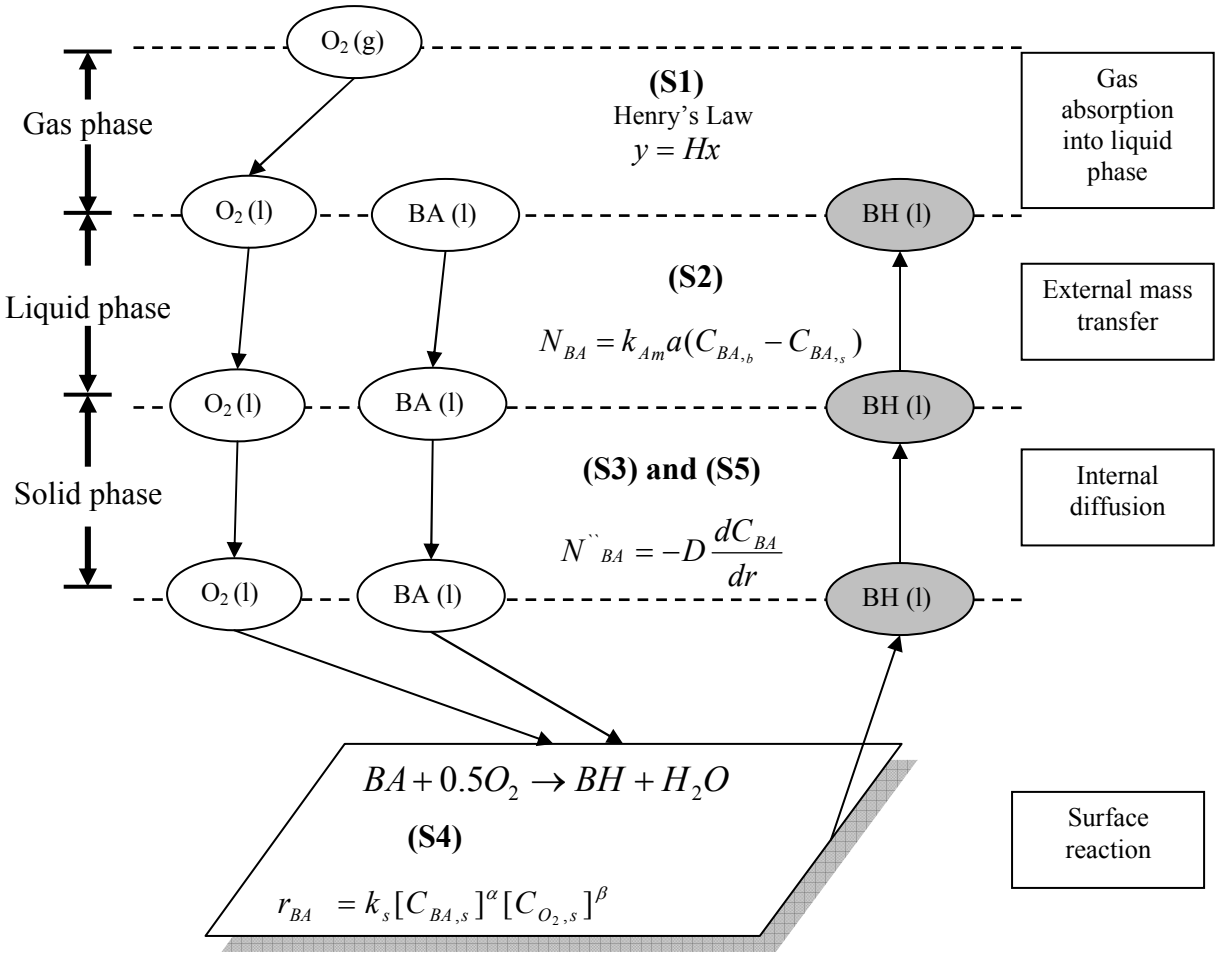

Figure 4.3: Schematic to illustrate the sequence of steps in a heterogeneous catalytic reaction involving a gas, liquid and solid phase.

4.2 Experimental Studies

4.2.1 Description of the experimental apparatus

The experiments were performed in a 115 ml autoclave. The autoclave (Model 425 HC) was made by Parr Instrument from type 316 stainless steel to operate within a pressure range of 0 to 200 bar(g), and temperatures up to 300 ºC. The autoclave was immersed in a paraffin oil bath (heated by a magnetic stirred hot plate) to provide isothermal conditions with good mixing control. The temperature was controlled using a digital thermostat. A schematic diagram of the apparatus is illustrated in Figure 4.4 a and an image is shown in Figure 4.4 b.

The platinum on carbon catalyst was made following the method that was described in the sections that follow, and the feedstock consisted of 10 vol% benzyl alcohol in a solvent mixture of 90 vol% dioxane and 10% water. A pure oxygen gas stream was connected to the autoclave.

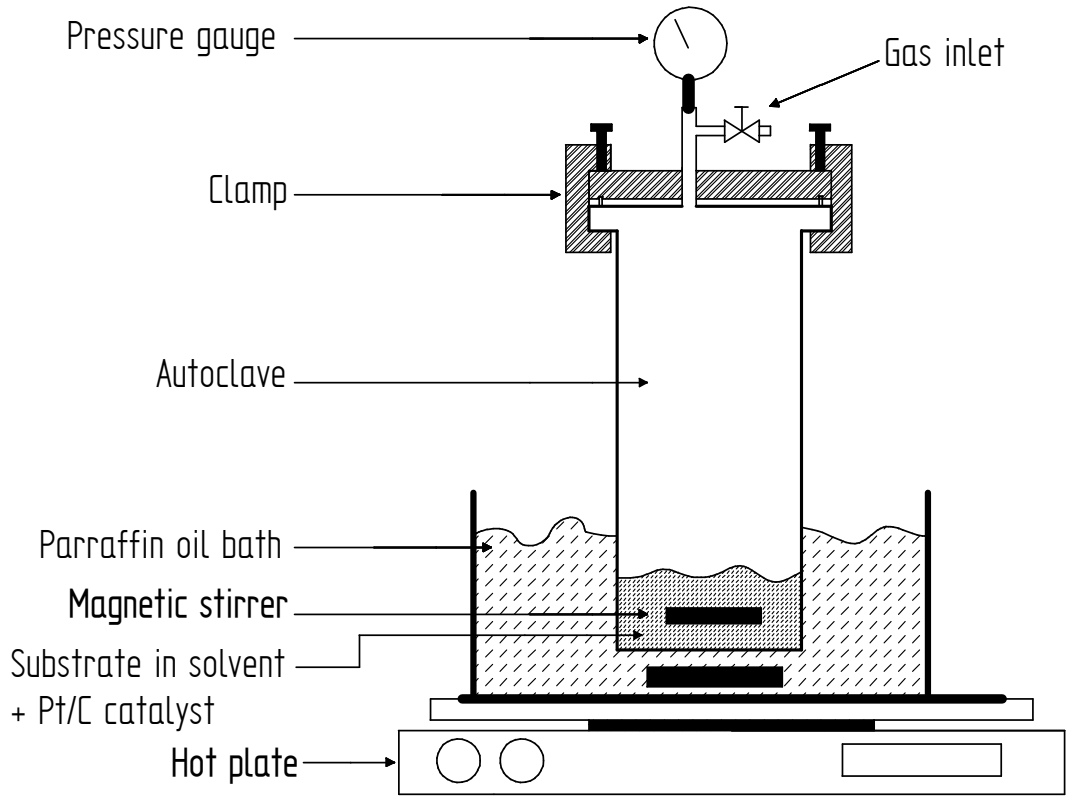

Figure 4.4 a: Schematic of the autoclave that was used for the kinetic experiments.

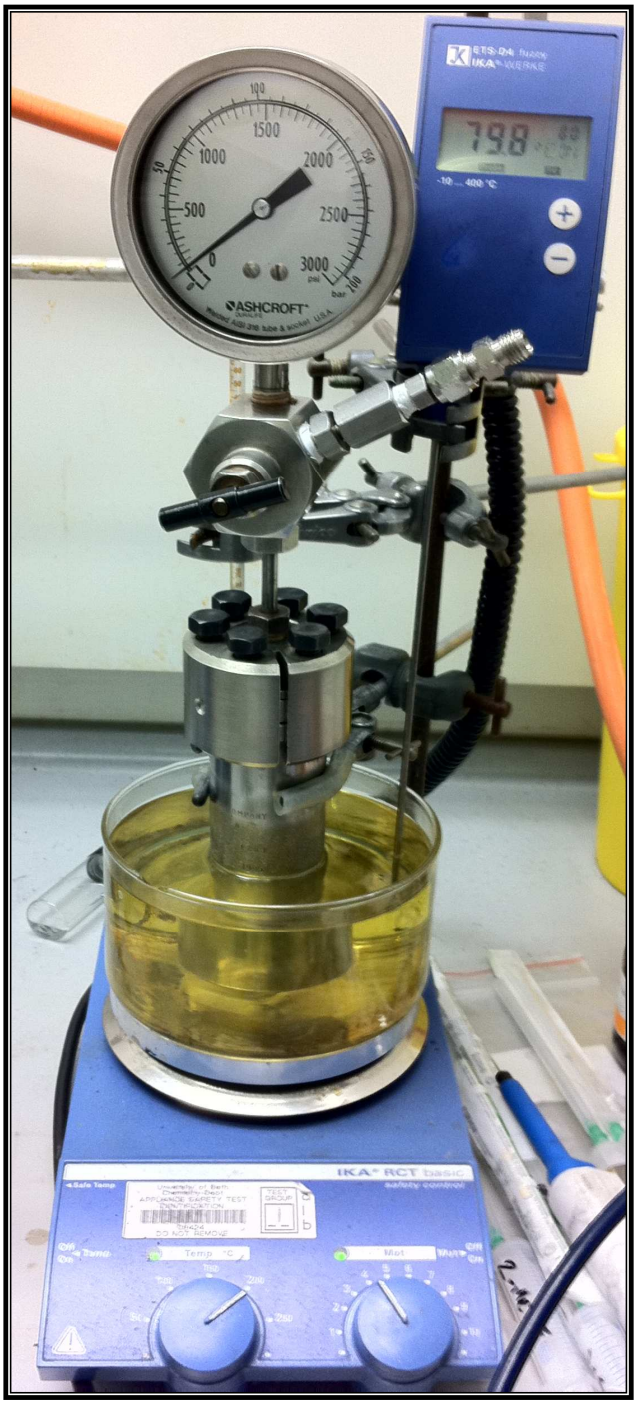

Figure 4.4 b: Experimental set-up for kinetic experiments.

4.2.2 Pt/C Catalyst

In the experments that follow, activated carbon monoliths were used as support for the Pt catalyst. The monoliths were supplied by MAST Carbon Ltd. (UK). In this chapter, experments are performed on particles obtained from milling four pieces of carbon monolith, each piece was 50 mm in length and 22 mm o.d. and ~ 11 g in weight.

In the sections that follow, the following tasks are described:

- Manufacturing aspect of carbon monoliths.
- Possible methods of coating with Pt are reviewed.
- A coating method is selected, and then the method of coating is described.

4.2.2.1 Manufacture of activated carbon monoliths

The carbon monoliths were manufactured by MAST Carbon Ltd. (UK) from a Novolac resin (Novacarb™), and the author observed this process. The carbon was made into the form of a monolith using conventional extrusion techniques. The procedure that was used is described in Figure 4.5. Although each step has an effect on the final product, the activation step is considered to be a key factor in controlling the value of the BET surface area. It was found that the longer the activation time applied, then the higher value of the BET surface area was achieved. However, there was a reduction in the mechanical strength of the monolith structure. For example, with an activation time:

(a) >12 h, this can lead to a 1300 $m^2 g^{-1}$ BET surface area, and it is recommended for carbon beads.

(b) Up to 12 h can lead to a 1000 $m^2 g^{-1}$ BET surface area, and this is recommended for monoliths.

(c) Up to 8 h can lead to a 800 $m^2 g^{-1}$ BET surface area.

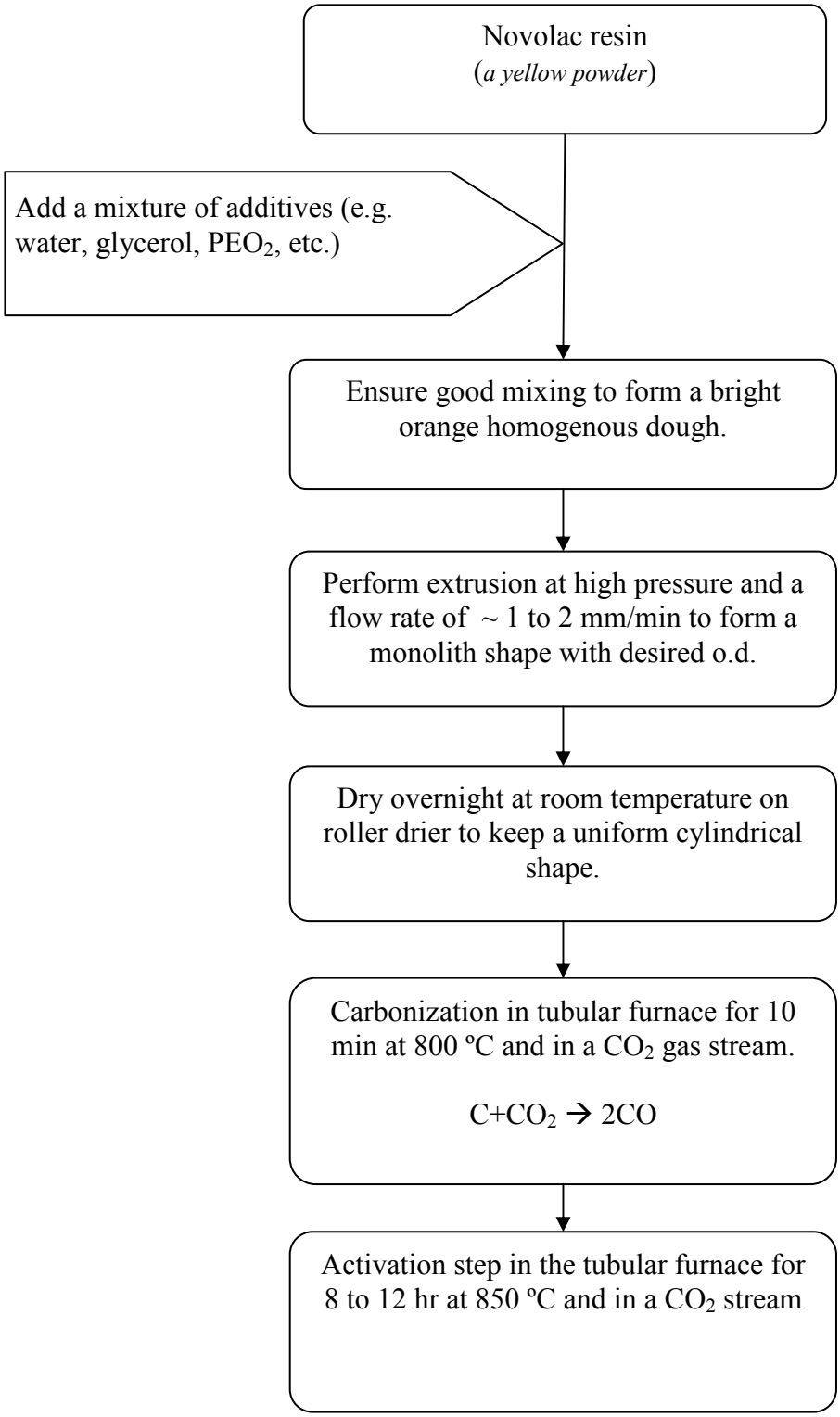

Figure 4.5: An outline flow chart showing the manufacturing steps for carbon monoliths from polymer resin performed by MAST Carbon Ltd. (UK).

4.2.2.2 Catalyst preparation – Pt on carbon

Carbon material as a support for noble metal catalysts (e.g. Pt , Au, and Pd) already has many applications due to it is unique properties, such as the existence of various forms of surface functional groups, strong corrosion resistance, and relatively high surface area (Van Dam and Van Bekkum, 1991). Carbon-supported platinum catalysts were shown to be highly stable heterogeneous catalysts for the selective oxidation of various types of primary alcohols to the corresponding aldehydes and carboxylic acids (Korovchenko *et al*., 2007).

In the sections that follow, extracts are presented from three key publications where information is useful for this thesis:

(a) Li Jia *et al*., (2006)

As described in their paper, the impregnation-reduction method is the most popular way to get highly dispersed platinum particles on carbons. The method includes the following steps:

(i) Adsorption of the platinum precursor ions on the surface of the carbon support.

(ii) Subsequent reduction with hydrogen flow at an appropriate temperature.

The authors highlighted a number of important aspects:

(a) During the impregnation step, the interactions of the carbon support surface with both the metal precursor and the solvent greatly influence metal uptake and dispersion. These interactions are governed by the polarity of the solvent, the pH value of the impregnating solution, the cationic or anionic nature of the metal precursor and the surface charge in the solution of the carbon support.

(b) The surface chemistry of the carbon greatly depends on various functional groups on the surface (e.g. carboxylic and hydroxyl groups), which can act as the adsorption sites for the metal precursor. These groups can be obtained by oxidation treatments, or progressively destroyed by thermal treatments which make the support more hydrophilic, allowing better accessibility of the impregnating aqueous solution to the carbon surface.

(c) In an aqueous solution, the carboxylic or hydroxyl groups behave as the amphoteric species being dissociated or protonated, depending on the pH value of the solution. Thus, the impregnation with an anionic precursor like $PtCl_6^{-2}$ is favoured in an acidic solution, whereas the cationic precursors such as $[Pt(NH)4]^{2+}$ should be used in basic solutions.

In their paper the Pt/C catalysts were prepared by the impregnation of the supports with aqueous solution of $H_2PtCl_6.6H_2O$ (Grikin, Beijing) at room temperature. The procedure was as follows:

(i) The carbon support (0.2 g) was immersed in 10 ml of aqueous $H_2PtCl_6.6H_2O$ solution under agitation for 48 h.

(ii) Then the suspension was filtered to remove the excess of the solution, and the remained solid was washed with 500 ml of distilled water.

(iii) The catalyst samples were dried at 110 ºC in air, and then reduced in a hydrogen flow at 180 ºC for 4 h.

The amount of platinum was determined as follows:

(i) A sample of carbon supported platinum catalyst was calcined in air at 800 ºC until the carbon support was burnt away, and then the platinum residue was dissolved in aqua regia.

(ii) The obtained solution was heated, and the platinum complex solids were diluted with distilled water.

(iii) The analysis of the dilute platinum solution was carried out using an inductively coupled plasma optical emission spectrometry (ICP-OES, VISTA-MPX).

(b) Donze *et al*., (2007)

A synthetic carbon (MAST) was used as the metal support and it was prepared by polycondensation of Novolac resin at 800 ºC, and activated by a ‘‘burn-off’’ technique using CO_2 at 850 ºC. The carbon consists of regular spherical particles with an average particle size of 150 μm. Platinum was deposited according to the conventional method of impregnation in liquid phase using $H_2PtCl_6.6H_2O$ as follows:

(i) A slurry of several grams of carbon was prepared (~10 ml H_2O per 1 g of carbon) and was stirred at a moderate rate for 30 min under nitrogen.

(ii) The aqueous solution with the required amount of platinum to obtain 3 wt% Pt was then added drop-wise while the solution was stirred.

(iii) After 5 h of impregnation, the slurry was cooled to 0 ºC, and drop-wise addition of formaldehyde (37 wt.%, 5 ml g^{-1} of carbon) followed by KOH (30 wt.%, 2 ml g^{-1} of carbon) was performed to achieve reduction of the metal complex.

(iv) After overnight stirring under nitrogen at ambient temperature, the suspension was filtered, washed with water until neutrality was obtained and then dried overnight under a N_2 atmosphere at 100 ºC.

(v) The experimental Pt percentage was verified by elemental chemical analysis using AES-ICP (1.95 wt.% Pt instead of 3 wt.% nominal content). The platinum dispersion was evaluated by CO chemisorption and it was found to be equal to 44%.

(c) Korovchenko *et al*., (2007)

In their paper, the Pt/C catalyst was made by an impregnating method as follows:

(i) An aqueous solution of $H_2PtCl_6.6H_2O$ containing the required amount of platinum was added drop-wise under stirring to an aqueous suspension of the carbon.

(ii) After 5 h impregnation, the slurry was cooled down in an ice bath and a 37 wt.% solution of formaldehyde was added drop-wise, and then a 30 wt.% KOH solution.

(iii) After stirring under nitrogen overnight, the suspension was filtered, and washed with water.

(iv) The catalyst was dried under nitrogen atmosphere at 100 ºC for 1 day.

(v) The platinum content was determined by analysing the solution by ICP **(**Inductively Coupled Plasma Mass Spectrometry), after dissolution of the solid in aqua regia (1:3 volumetric ratio of nitric acid and concentrated hydrochloric acid) at 250 to 300 ºC, then in HCl.

4.2.2.3 UV spectroscopy for metal tracking

In Korovchenko *et al*., 2007), the platinum content of the catalyst was determined by analysing the solution by ICP **(**Inductively Coupled Plasma Mass Spectrometry) However, it was necessary to find an alternative method to estimate the amount of Pt that was loaded on the carbon because of the difficulties of applying that method in our laboratory.

The UV spectrophotometer was found to be as an attractive method to determine the concentration of platinum in the form of $PtCl_6^{-2}$ in hydrochloric acid solution because it is simple, rapid and sensitive Georgieva and Andonovski (2003). A method was therefore developed in which the UV spectrophotometer was used to monitor the concentration of the $PtCl_6^{-2}$ ion in the solution during the coating process.

In order to apply this method, 5 samples of known concentrations were prepared by dissolving a known amount of $H_2PtCl_6.6H_2O$ in ethanol. The samples were then scanned using a UV-visible spectrophotometer SHIMADZU (UV-1601). The UV spectra were recorded between 190 to 900 nm to indentify all of the possible peaks and/or dips, see Figure 4.6. The measurements were performed using a 1 cm quartz cell.

In Figure 4.6, it was easy to recognize peaks at 460 nm and a dip at 440 nm, which indicate the difference in the Pt ion in solution. The absorbance at 460 nm was chosen to track the concentration of platinum ion in the form of $PtCl_6^{-2}$ in ethanol solution, and a calibration curve was then made, see Figure 4.7. For better accuracy three extra calibration samples (5.0, 6.0 and 8.0 g L^{-1}) were prepared and added to the calibration curve.

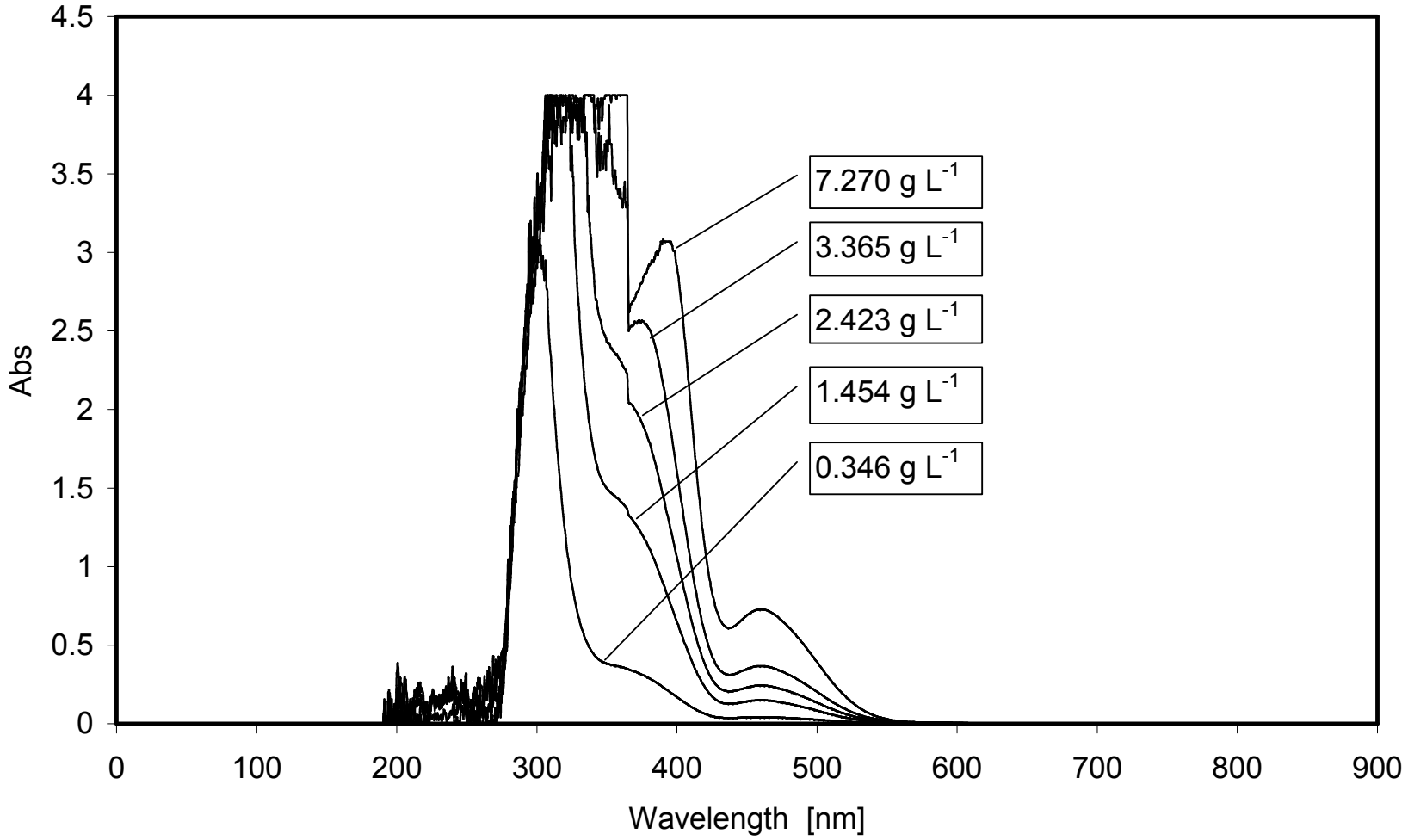

Figure 4.6: UV spectra at different Pt concentration. Solution made by dissolving $H_2PtCl_6.6H_2O$ in ethanol.

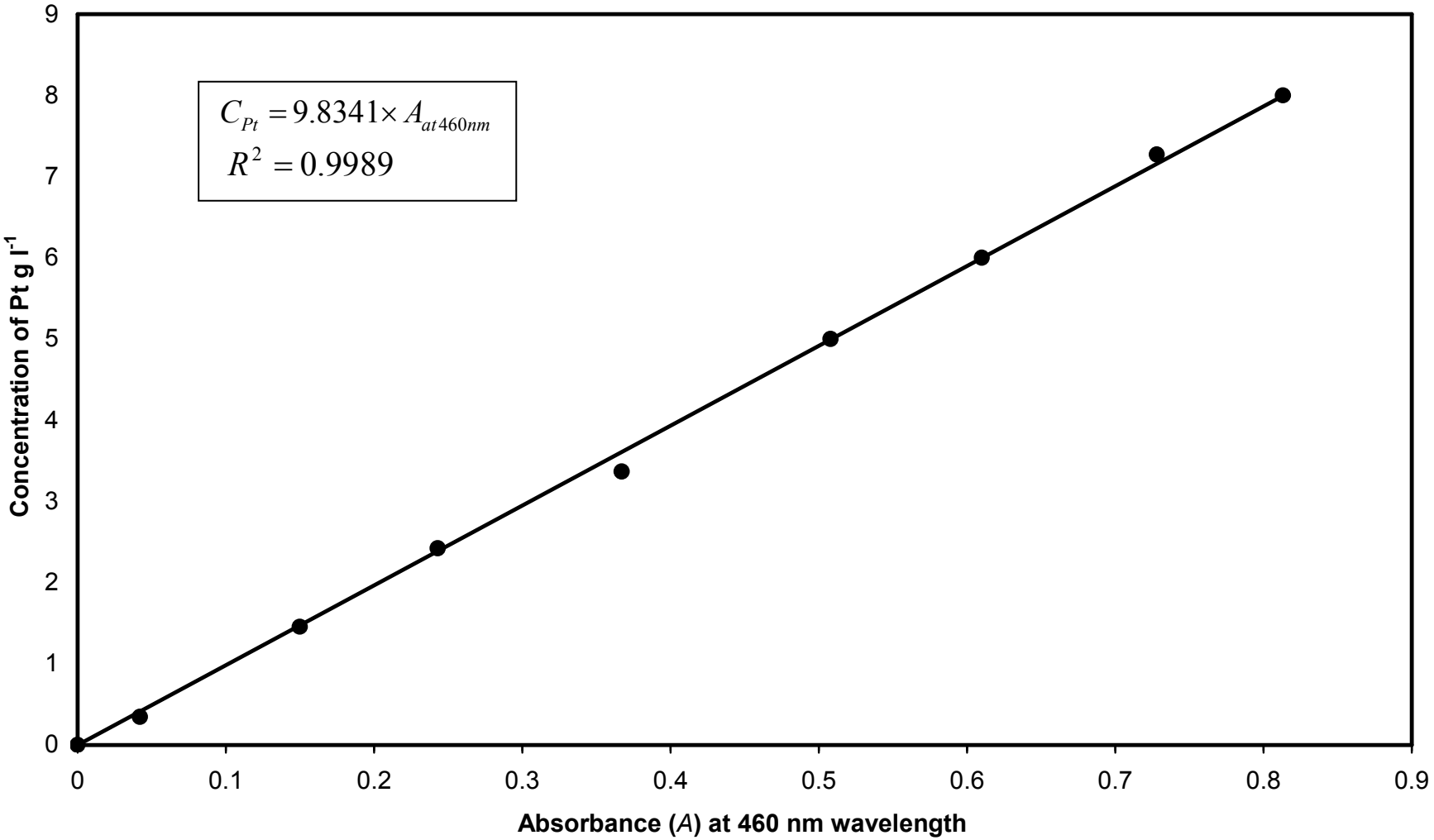

Figure 4.7: Experimental calibration curve between UV spectra at 460 nm and the concentration of Pt in solution. Solution made by dissolving $H_2PtCl_6.6H_2O$ in ethanol at room temperature.

4.2.2.4 Catalyst coating

After reviewing the literature, it was decided to coat the carbon powder with platinum metal using the impregnation-reduction method in an ethanol media to overcome a surface wetability problem.

The carbon powder was made by crushing 4 pieces of carbon monoliths ~ 40 g. The crushed monoliths were then separated into four different particle size ranges using a sieve, see Table 4.1. The carbon powder was then coated by impregnating the platinum metal as follows:

(i) A known quantity consisting of 2.2 g of $H_2PtCl_6 \cdot (H_2O)_6$ (molar mass = 517.92 g mol^{-1}) was added to 44 ml ethanol to create a stock solution. Then a 25 ml of 30 wt% potassium hydroxide solution (reducing agent) was also prepared.

(ii) The milled carbons of varying sizes were split into four groups based on particles size, and ethanol was added as shown in Table 4.1.

(iii) The flasks were fixed to a bench shaker, and shaken gently for 20 minutes under vacuum condition. This allowed the liquid to penetrate the carbon beads.

(iv) The flasks had an inert nitrogen atmosphere, and the platinum solution prepared earlier was added drop-wise, in the same proportion as the ethanol. Again, exact values are given in Table 4.1.

(v) Once the platinum solution was added, a sample was taken immediately from each (as the initial reading) and then the flasks were returned to the inert atmosphere whilst being shaken.

(vi) The samples were then tested in the UV spectrophotometer, with absorbance being measured at 460 nm, although a range from 190-900 nm was used. All samples were returned to the flasks after measurement and an inert atmosphere was re-established.

(vii) The initial concentration was approximately 8.3 g L^1 in each of the four flasks, and samples were taken for UV measurement at intervals over 10 days. The approximate loading capacities are shown in Table 4.2.

(viii) When coating was complete, the flasks were cooled in an ice bath for 15 minutes, and then formaldehyde was added drop-wise.

(ix) Next potassium hydroxide (reducing agent) was added drop-wise and an inert atmosphere was restored.

(x) Reduction took place over two days whilst the flasks were gently shaken.

(xi) The carbon powder was removed after reduction, and it was filtered and washed with fresh ethanol twice during this process. Then the powder was dried overnight in ambient conditions.

Table 4.1: Quantities added as the four different samples were prepared.

Particles Size [µm]	**Batch No**	**Weight of carbon [g]**	**Ethanol added [ml]**	**$H_2PtCl_6(H_2O)_6$ Stock solution added [ml]**	**Formalde-hyde added [ml]**	**Potassium hydroxide (30 wt% solution) added [ml]**
< 38	**(A)**	2.48	200	4	2	2
38-125	**(B)**	13.20	106.5	21.3	10.65	10.65
125-250	**(C)**	3.72	30	6	3	3
250-500	**(D)**	7.88	63.5	12.7	6.45	6.45

Table 4.2: Calculated Pt loading on carbon.

Group	**(A)**	**(B)**	**(C)**	**(D)**
Particles size [µm]:	> 38	38-125	125-250	250-500
% of the Pt adsorbed on the carbon support	90	90	80	80
Pt loaded wt%:	2.7	2.7	2.4	2.4

4.2.3 Analytical Technique

During the kinetic experiments, samples of the liquid were taken from the autoclave and these were analysed with a GC (Agilent 6890N Network) based in the Department of Chemistry. The GC was equipped with a 30 m HP-5 × 0.32 mm × 0.25 μm film column. The method was developed in a previous project (to detect similar boiling point range of components).

4.2.3.1 Calibration method for gas chromatography

The calibration process consisted of three stages.

Stage 1: At this stage, the retention time (t_R) for each component was recognized and identified, making sure that there were no interactions between the peaks. To achieve this target, three samples were made with relatively high concentrations, which were then tested in the GC. The GC output chromatograms from this experiment are presented in Figures 4.8. This figure shows three different retention times (benzylaldehde t_R = 2.719 min, benzyl alcohol t_R = 3.031 min, and benzoic acid t_R = 3.931 min). The well spaced peaks show no interaction between the components t_R values while the dioxane appears at a retention time of t_R = 1.985 min.

Stage 2: At this stage, the Multiple Point Internal Standard Method was used to calibrate the GC. Dodecan (Supplied by Sigma-Aldrich) was used as the internal standard. In Figure 4.9, a relation between the ratio of the area of the benzyl alcohol to the area of the internal standard is plotted *vs,* the ratio of the concentration of the benzyl alcohol to the concentration of internal standard.

Stage 3: A comparison between the values of the % conversion which had been calculated using Multiple Point Internal Standard Method and Area Percentage Method was made to identify the possible % error Table 4.3.

Table 4.3: A range of expected error for selected samples which were been tested using Area Percentage Method and Multiple Point Internal Standard Method.

% Conversion		
Area Percentage Method	Multiple Point Internal Standard Method	% error
50.76	48.8	4
44.20	41.9	5
50.56	47.6	6
80.69	76.9	5
83.11	78.1	6
84.49	80.5	5
52.91	50.7	4
12.89	11.79	9
12.51	11.54	8

Although the method has been used in this thesis (Area Percentage Method) to calculate the % conversion of benzyl alcohol is not the most accurate one. This method gives a very good estimate with an average of error of 5% for the value of % conversion compared to the value of the % conversion that has been calculated using Multiple Point Internal Standard Method with Dodecan (Supplied by Sigma-Aldrich) as the internal standard.

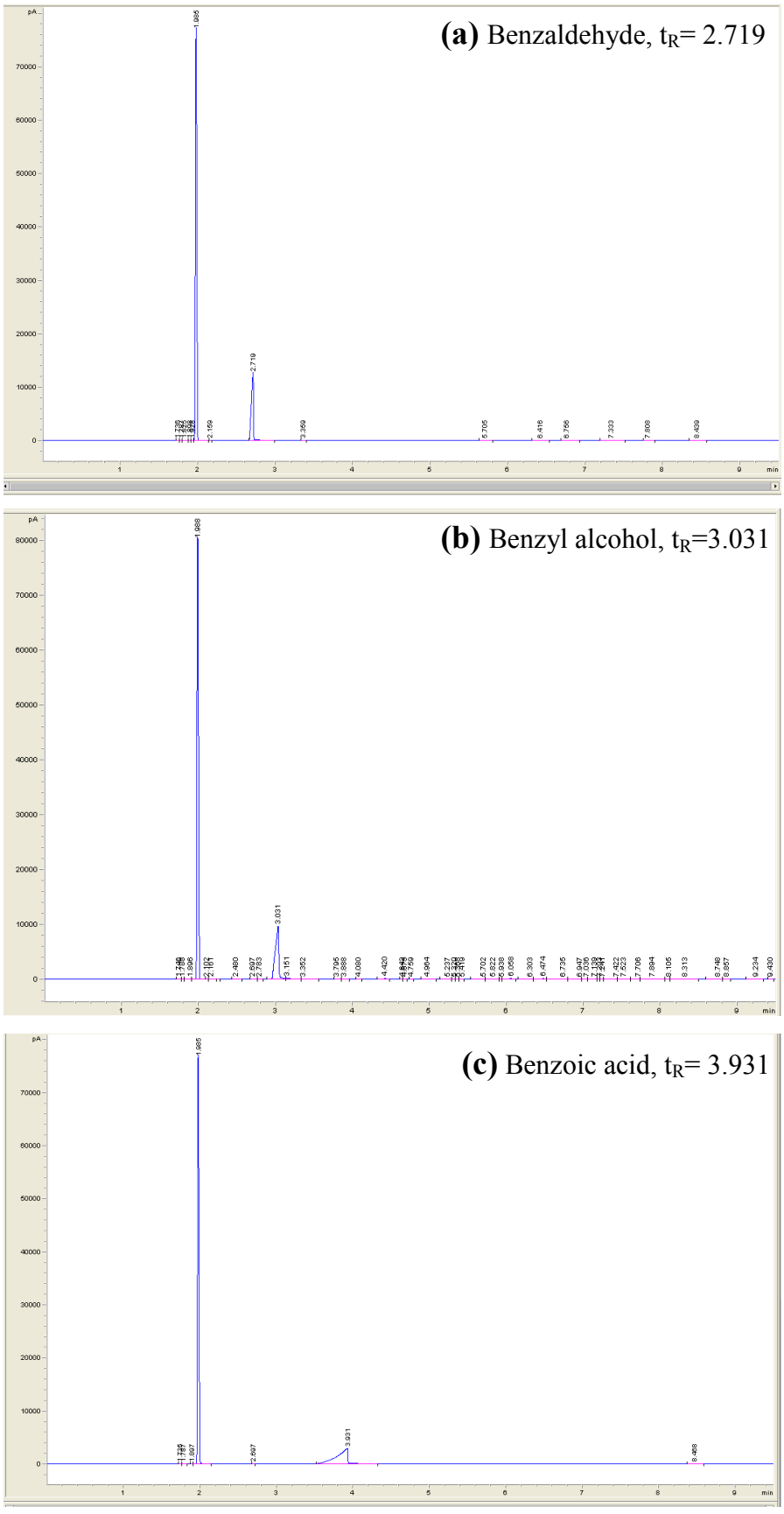

Figure 4.8: Chromatograms of the expected species.

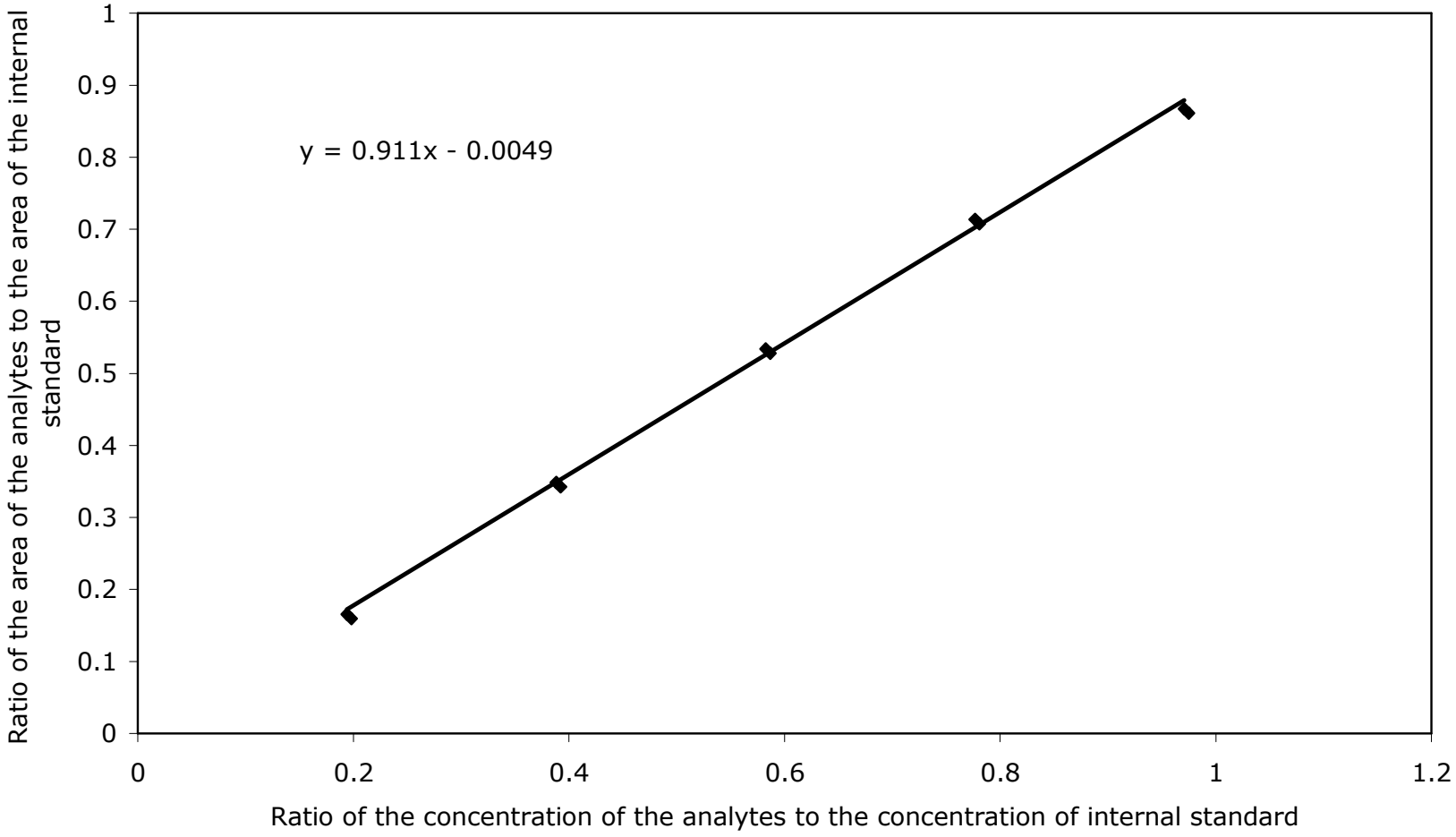

Figure 4.9: Calibration curve for benzyl alcohol using an internal standard (Dodecan).

4.2.4 Experimental procedure for the kinetic experiments

The following experimental procedure was followed:

(i) Ensure that the autoclave is dry and clean.

(ii) Place 0.1 g of the carbon coated catalyst into the autoclave.

(iii) Place 20 ml of feedstock into the autoclave.

(iv) The autoclave was then capped and tightened with the screws.

(v) Switch on the magnetic stirred hot plate and set the digital thermostat to 110 ºC.

(vi) Immerse the autoclave in the oil bath and leave it there for 5 minutes while mixing until it reached the required temperature.

(vii) When the reactor temperature was reached (e.g. 110 ºC), the autoclave was then charged with pure oxygen up to the desired pressure.

(viii) The autoclave was then left for 1 h at contestant temperature and pressure before it was removed from the oil bath and cooled down, and then the remaining pressure was released.

(ix) A sample was taken after each run and analysed with the GC. Figure 4.10 shows a typical GC chromatogram for a selected sample.

An example calculation both for the % conversion, and the % selectivity is shown in the example that follows.

Example calculation No 2 To determine the conversion of benzyl alcohol and the selectivity of the desired benzylaldehde product from the GC chromatogram.

In Figure 4.10 there are four peaks and the integral value for the area *I* under the curve at each peak. These peaks represent the solvent (dioxane at t_R= 1.986), reactant (benzyl alcohol at t_R=2.984), the desired product (benzylaldehde at t_R=2.711), and the by-product benzoic acid (at t_R=3.819).
The conversion of benzyl alcohol is calculated as follows:

$$\% \text{ conversion} = \frac{I_A + I_C}{I_A + I_B + I_C} \times 100$$

where I_A represent the integral area for species A. Hence,

$$\% \text{ conversion} = \frac{17105.4 + 12197.6}{17105.4 + 1046.1 + 12197.6} \times 100$$

$$= 79 \pm 2\%$$

The selectivity is determined from:

$$\% \text{ selectivity} = \frac{I_A}{I_A + I_C} \times 100$$

$$\% \text{ selectivity} = \frac{17105.4}{17105.4 + 12197.6} \times 100$$

$$= 58 \pm 2\%$$

End of the Example

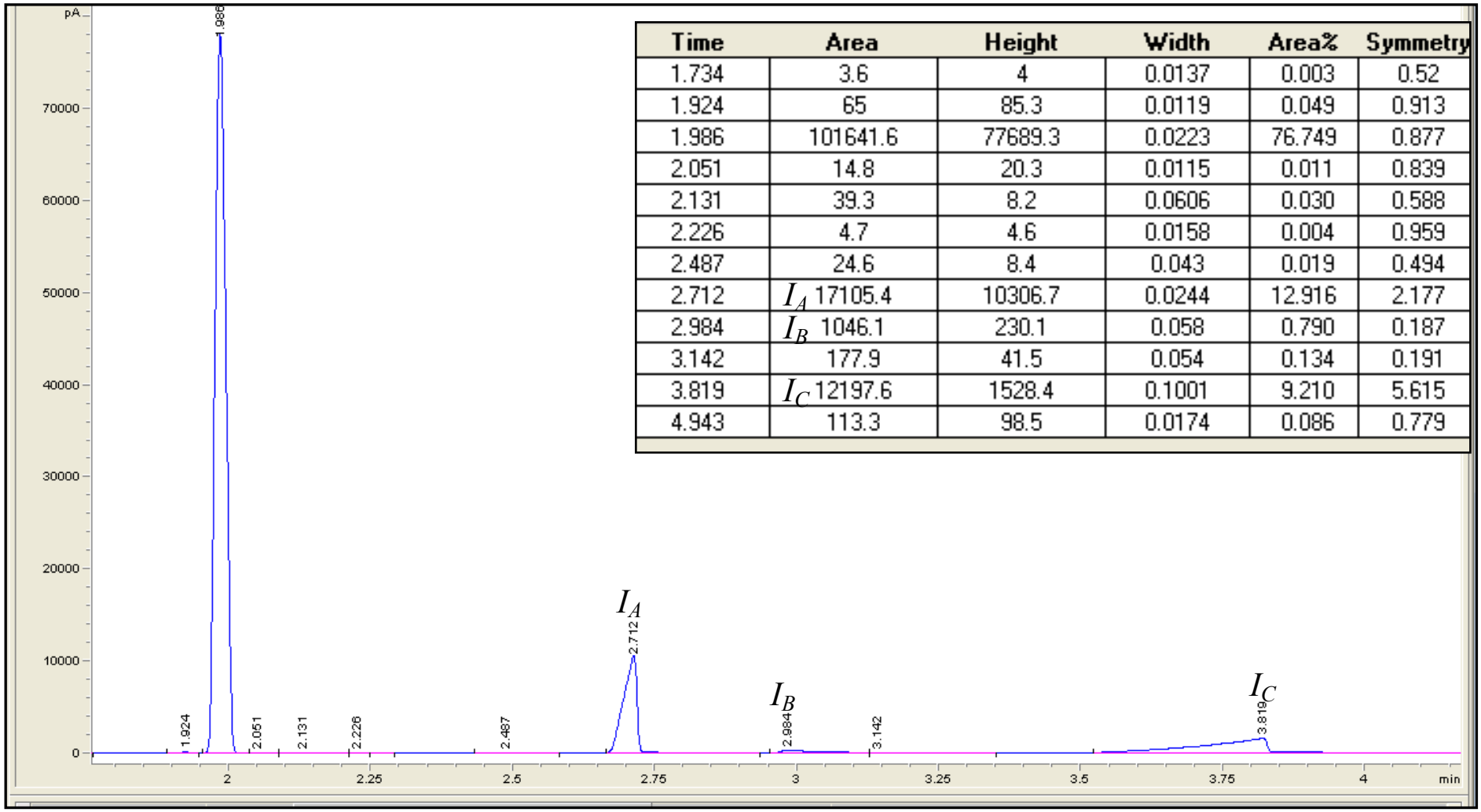

Time	Area	Height	Width	Area%	Symmetry
1.734	3.6	4	0.0137	0.003	0.52
1.924	65	85.3	0.0119	0.049	0.913
1.986	101641.6	77689.3	0.0223	76.749	0.877
2.051	14.8	20.3	0.0115	0.011	0.839
2.131	39.3	8.2	0.0606	0.030	0.588
2.226	4.7	4.6	0.0158	0.004	0.959
2.487	24.6	8.4	0.043	0.019	0.494
2.712	I_A 17105.4	10306.7	0.0244	12.916	2.177
2.984	I_B 1046.1	230.1	0.058	0.790	0.187
3.142	177.9	41.5	0.054	0.134	0.191
3.819	I_C 12197.6	1528.4	0.1001	9.210	5.615
4.943	113.3	98.5	0.0174	0.086	0.779

Figure 4.10: The GC chromatogram for a selected sample.

4.2.5 Preliminary experiments trials

The intrinsic rate of the surface chemical reaction r_{BA} can easily be obscured when the reaction involves: gas absorption, external mass transport, and internal diffusion. Therefore, a set of preliminary experiments were performed to establish the experimental conditions for the acquisition of kinetic data.

4.2.5.1 Effect of gas absorption rate

For the experimental batch reactor system, the mole fraction of oxygen in the liquid phase was calculated using Henry's Law (equation 4.9) as the liquid phase was assumed to be in equilibrium with gaseous oxygen (Perry and Green, 2008), hence:.

$$P_{O_2} = H\, x_{O_2} \tag{4.9}$$

where:

P_{O_2} is the partial pressure of oxygen, bar,

H is the Henry's Law constant of oxygen in the reaction mixture at specified temperature, bar, and

x_{O_2} is the mole fraction of oxygen in reaction mixture.

Equation (4.9) can be written in terms of oxygen concentration:

$$C_{O_2,b} = \frac{P_{O_2}\rho_m}{H} \tag{4.10}$$

where:

$C_{O_2,b}$ is the oxygen concentration in the bulk liquid, mol L^{-1}, and

ρ_m is the molar density of liquid feed stock, 11.789 mol L^{-1}.

Henry's constant, *H,* is different for every gas, temperature and solvent (Seader and Henley, 2006). The units of *H* depend on the units used for concentration and pressure.

Values of *H* and ρ_m were calculated (see Table 4.4) using the property method in the chemical engineering simulation package known as ASPEN+ for a feed mixture:

Benzyl alcohol (BA) = 6 mol%
Dioxane (DX) = 64 mol%
Water (W) = 30 mol%

Table 4.4 Henry's constant and molar volume for a solvent mixture of (6 BA, 64 DX, and 30 W) mol%. Results calculated using the property method in the chemical engineering simulation package ASPEN+ (see Appendix B).

Run no.	**Temperature [ºC]**	ρ_m **Molar density [mol L^{-1}]**	**Henry's constant [bar]**
1	90	11.789	1413.23
2	100	11.789	1319.49
3	110	11.789	1231.74
4	120	11.789	1149.74
5	130	11.789	1032.45

4.2.5.2 Effect of external mass transfer

As described in Section 4.1.1, the transport benzyl alcohol through the bulk liquid to the catalyst surface is represented by equation 4.6 and at steady-state the concentration of benzyl alcohol at the catalyst surface, and the rate of mass transfer (N_{BA}) depends on the mass transfer coefficient (k_{Am}), which is affected by the speed of mixing.

$$N_{BA} = k_{Am} a (C_{BA,b} - C_{BA,s}) \tag{4.6}$$

A similar expression could also be written for the transfer of dissolved oxygen

To distinguish between the liquid phase mass transfer regime and the kinetic reaction regime, the reaction was studied at a range of mixing speeds between 200 to 1000 revolutions per minutes (rpm). It was found that increases in mixing had no significant effect above 600 rpm, showing that at this range of mixing, the reaction was not controlled by the external liquid phase mass transfer step. The results of such an experiment are presented in Figure 4.11.

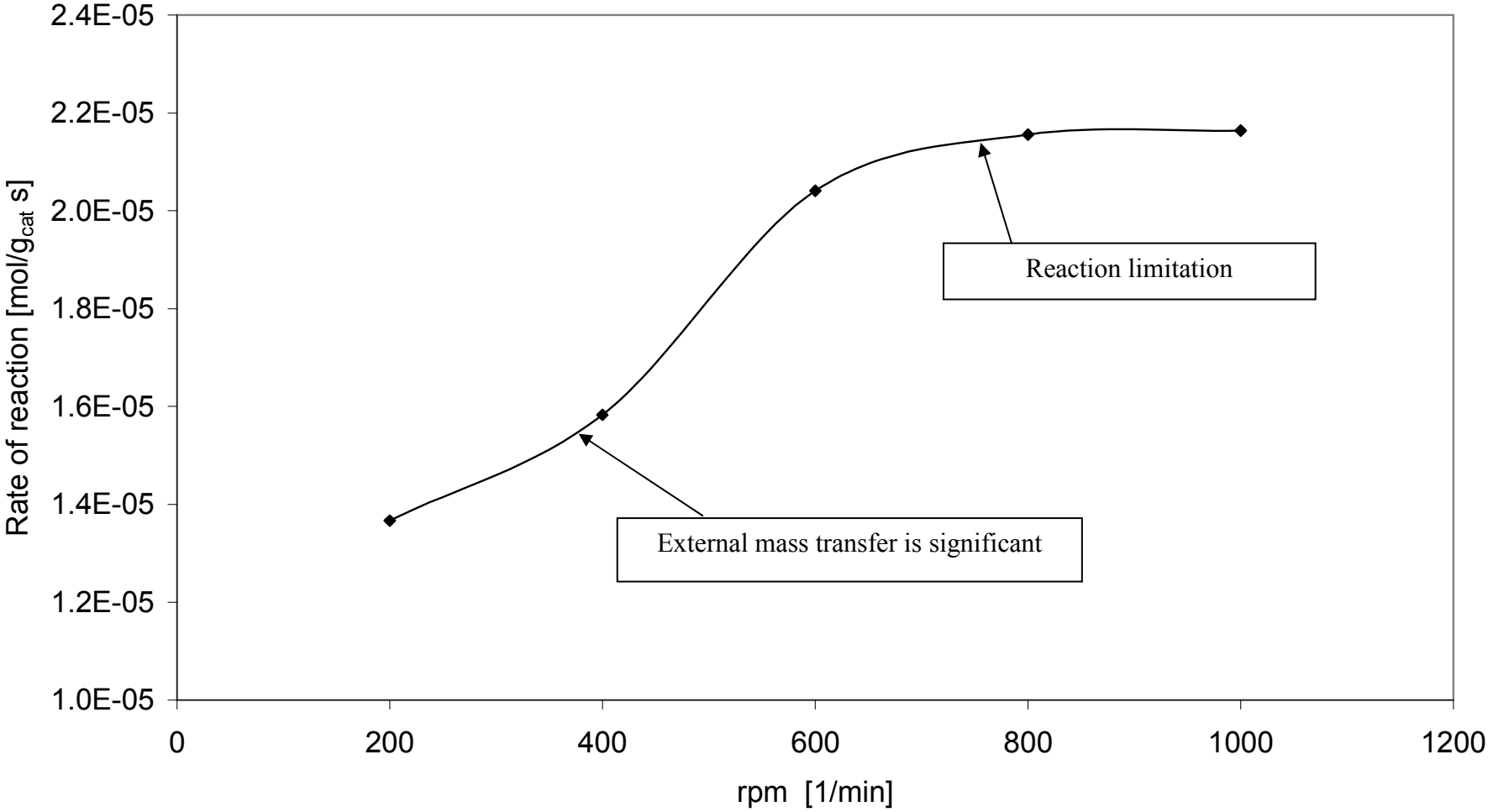

Figure 4.11: Dependence of the rate of reaction on mixing speed. Results obtained at: pressure of 80 bar(g) oxygen; temperature of 110 ºC; reaction time equal to 1 h; 10 vol% of benzyl alcohol in a solvent mixture of 90 vol% dioxane in water; mass of carbon coated catalyst = 0.1 g; Pt loading 2.7 wt%; particle size = 38 -125 μm.

4.2.5.3 Effect of internal diffusion

The effect of internal diffusion (in the catalyst) can be distinguished by performing experiments with different particle sizes of catalyst. As the diffusion rate depends on the particle radius, then from equation 4.7.

$$N''_{BA} = -D_{BA}\frac{dC_{BA}}{dr} \tag{4.7}$$

By varying the diameter of the particles (as illustrated in Table 4.5), the effect of particle size on reaction rate may be evaluated.

Table 4.5: Variation in particle size for different samples.

Batch No:	**A**	**B**	**C**	**D**
Particles size μm	< 38	38-125	125-250	250-500

It is well know that the crushing process leads to a mixture of spherical and slab shaped particles. However, in similar practical applications it was shown that the degree of deviation caused by such shape variation is sufficiently small to be ignored (Christian *et al*., 1966).

Reaction experiments were then performed and the results are shown in Figure 4.12. The size of the particles clearly has a significant effect on the rate of reaction, especially at the size between 38-125 μm to 250-500 μm. However, it clear that the effect is small for particles between < 38 μm to 38-125 μm. So the 38-125 μm range was selected for the kinetic study. Particles < 38 μm were fine powder, which could coagulate and form a dead zone in the reactor.

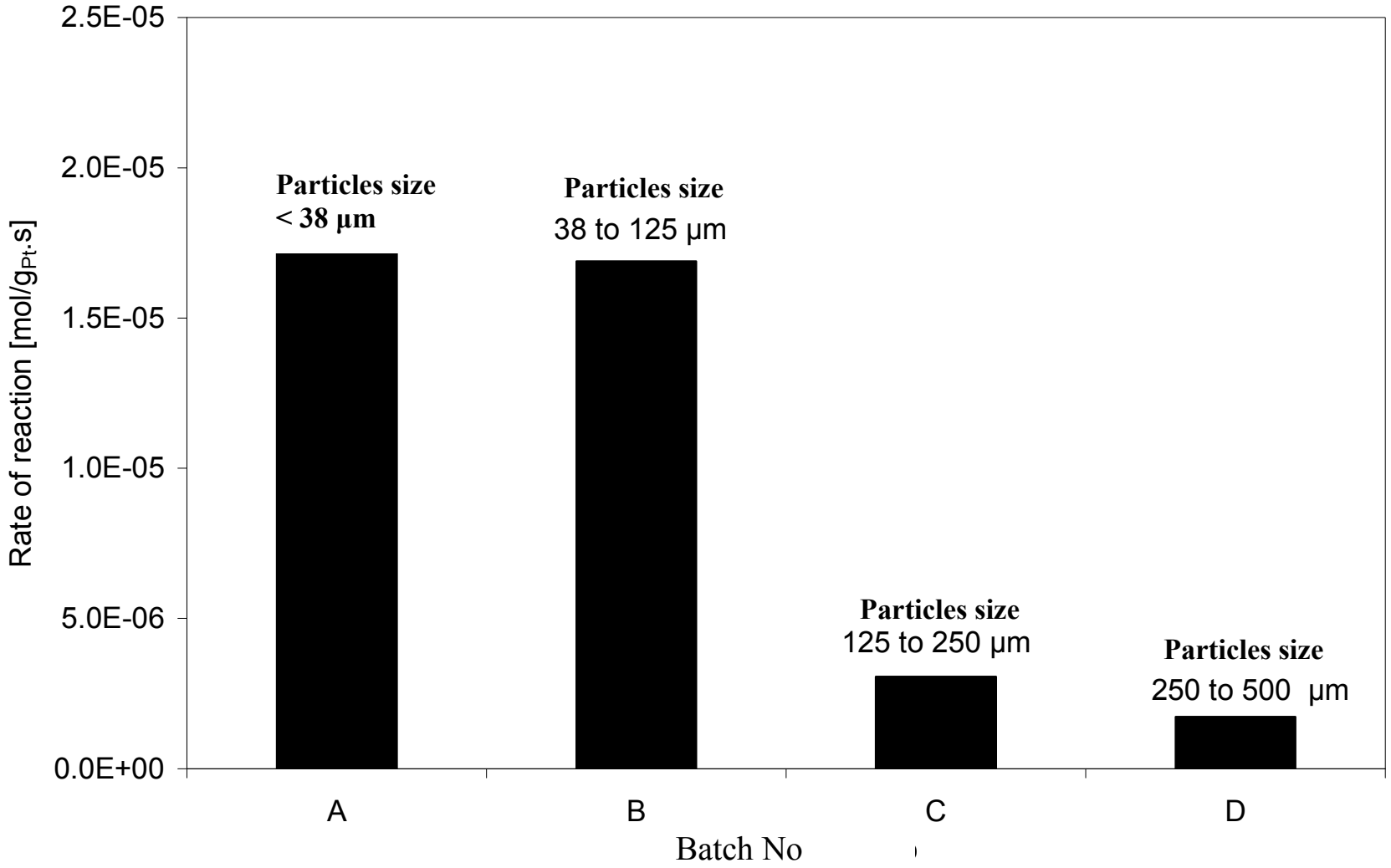

Figure 4.12: Dependence of the rate of reaction on particle size. Results obtained at pressure of 80 bar(g) oxygen; temperature of 110 ºC; reaction time equal to 1 h; and 10 vol% of benzyl alcohol in a solvent mixture of 90 vol% dioxane in water; mass of carbon coated catalyst = 0.1 g; Pt loading: (A) = 2.7 wt%, (B) = 2.7 wt%, (C) = 2.4 wt%, (D) = 2.4 wt%.

4.2.6 Kinetic model

To evaluate a set of kinetic parameters, the following assumptions were made:

(a) The autoclave is operated in batch mode at a specified set of conditions for each run.

(b) The partial oxidation reactions take place in the liquid phase on the catalytic Pt sites.

(c) Isothermal conditions were maintained in the reactor (constant temperature). The autoclave was surrounded by an oil jacket and the temperature was controlled by a digital thermostat.

(d) By operating the stirrer at 1,000 rpm, mass transfer resistance at the gas/liquid face, liquid phase, and the liquid/solid interface were minimized.

(e) Internal diffusion resistance within the particles was minimised, by using small catalyst particles in the 38-125 micron range.

(f) The reaction was assumed to be irreversible.

The reaction scheme may be represented by:

$$C_2H_5CH_2OH_{(l)} + 1/2O_{2\ (g)} \rightarrow C_6H_5CHO_{(l)} + H_2O_{(l)} \quad \Delta H_R \approx -210\ \text{kJ mol}^{-1} \qquad (4.12)$$

$$\text{BA} \quad + \quad \tfrac{1}{2}\ O_2 \longrightarrow \quad \text{BH} \quad + \quad \text{W} \qquad (4.13)$$

As described in Section 4.1.1 in S4, the reaction rate was represented by a power law term:

$$r_{BA} = -\frac{dC_{BA}}{dt} = k_s[C_{BA,s}]^{\alpha}[C_{O_2,s}]^{\beta} \qquad (4.8)$$

From batch experiments, the r_{BA} term can be determined from the initial rate equation:

$$r_{BA,\text{exp}} = \frac{n_{BA}}{m_{cat}} \cdot \frac{dX_{BA}}{dt}\ \Big|_{t=0} \qquad (4.14)$$

where

r_{BA} is the calculated reaction rate, $\text{mol g}_{\text{cat}}^{-1}\ \text{s}^{-1}$,

n_{BA} is the number of moles of benzyl alcohol in the feed, mol,

dX_{BA} is the fractional conversion of benzyl alcohol,

m_{cat} is the weight of the catalyst, g,

dt is the reaction time, s,

and the X_{BA} calculated from:

$$X_{BA} = \frac{n_{BA,in} - n_{BA,out}}{n_{BA,in}} \tag{4.15}$$

where:

$n_{BA,in}$ is the initial number of moles of benzyl alcohol, mol and

$n_{BA,out}$ is the final number of moles of benzyl alcohol, mol.

For an irreversible reaction it may be possible to determine the reaction order α and β, and the reaction rate constant k_s by applying a nonlinear regression method of analysis, and making use of the software package Polymath 5.1 (Fogler, 2006).

The value of the Arrhenius constant and the activation energy could be obtained from:

$$k_s = A \exp\left(-\frac{E_a}{RT}\right) \tag{4.16}$$

where:

A is the pre-exponential factor or frequency factor, same units as k_s,

E_a is the activation energy, J mol^{-1},

R is the gas constant (8.314), J mol^{-1} K, and

T is the absolute temperature, K.

For the technique to be truly valid, such experiments need to be performed such that X_{BA} is relatively small (i.e between 10 to 20% conversion). However, care must be taken as a large error could occur at very low conversion.

4.2.6.1 Kinetic experiments

The experiments were performed at the following conditions:

Catalyst particle size range: 38-125 μm;

Temperature: 80 ºC to 130 ºC;

Reaction time: 900 to 3600 s;

Speed of mixing: 1,000 rpm;

Volume of batch (substrate + solvent): 20 ml; and

Catalyst weight: 0.1 g of Pt/C, with 2.7 wt% Pt.

The experimental results are presented in Table 4.6.

- **Runs 1 to 11:** these were performed at a constant temperature but at various concentrations of BA and O_2. These could then be used to estimate the α and β coefficients in the rate expressions.
- **Run 12-17**: these could then be used to determine the coefficients in the rate constant.

Table 4.6: A set of experiments to determine the kinetics parameter constants.

#	C^*_{BA} [mol L^{-1}]	n_{BA} [mol]	$C^*_{O_2}$ [mol L^{-1}]	P [bar(g)]	X_{BA} [%]	Time [s]	Temp. [ºC]	$r_{BA,\exp}$ [10^{-6} mol g^{-1}_{cat} s^{-1}]
1	0.050	0.001	0.766	80	21.30	900	110	2.367
2	0.100	0.002	0.766	80	14.30	900	110	3.178
3	0.250	0.005	0.766	80	9.34	900	110	5.189
4	0.500	0.010	0.766	80	11.95	1800	110	6.639
5	1.000	0.020	0.766	80	8.23	1800	110	9.144
6	0.500	0.010	0.287	30	12.48	1800	110	6.933
7	0.500	0.010	0.239	25	12.50	1800	110	6.944
8	0.500	0.010	0.191	20	12.62	1800	110	7.011
9	0.500	0.010	0.144	15	12.81	1800	110	7.117
10	0.500	0.010	0.096	10	11.41	1800	110	6.339
11	0.500	0.010	0.048	5	11.82	1800	110	6.567
12	0.500	0.010	0.766	80	17.54	1800	130	9.744
13	0.500	0.010	0.766	80	14.15	1800	120	7.861
14	0.500	0.010	0.766	80	11.98	1800	110	6.656
15	0.500	0.010	0.766	80	8.96	1800	100	4.978
16	0.500	0.010	0.766	80	11.75	3600	90	3.263
17	0.500	0.010	0.766	80	7.24	3600	80	2.012

* Concentration of the reactant at time = 0

4.2.6.2 Experimental results

4.2.6.2.1 Estimating the order of the reaction coefficients (α and β)

For this analysis Runs 1 to 11 were used.
The experimental data was analyzed using a nonlinear regression method, the software package known as "Polymath 5.1" is used (Fogler, 2006) and following was determined:

The reaction order with respect to benzyl alcohol was found to be equal to $\alpha = 0.442$ at 95% confidence of ± 0.055.

The reaction order with respect to oxygen was found to be equal to $\beta = 0.005$ with 95% confidence of ± 0.001.

The over all reaction order, n = 0.447.

Rate constant at 110 ºC, was found to be equal to k_s = 9.28 × 10^{-6}, $mol^{0.553}\ L^{0.447}\ g_{cat}^{-1}\ s^{-1}$ with 95% confidence of $\pm 5.52 \times 10^{-7}$.

Then the reaction rate equation at 110 ºC can be written as follows:

$$r_{BA} = -\frac{dC_{BA}}{dt} = 9.28 \times 10^{-6} \times [C_{BA,s}]^{0.442} \times [C_{O_2,s}]^{0.005} \qquad (4.17)$$

4.2.6.2.2 Evaluating an expression for the reaction rate constant

Equation 4.16 may be expressed as:

$$\ln k_s = \ln A - \frac{E_a}{R} \times \frac{1}{T} \qquad (4.18)$$

By solving for values of k_s (for Runs 12-17), and then plotting $\ln k_s$ *vs* $\frac{1}{T}$, then E_{aT_1} (for Runs 12-14) and E_{aT_2} (for runs 15-17) were determined:

For ΔT_1: E_{aT_1} = 24.4 kJ mol^{-1} and A_{T_1} = 0.019 see Figure 4.13.

For ΔT_2: E_{aT_2} = 49.6 kJ mol^{-1} and A_{T_2} = 0.016 see Figure 4.13.

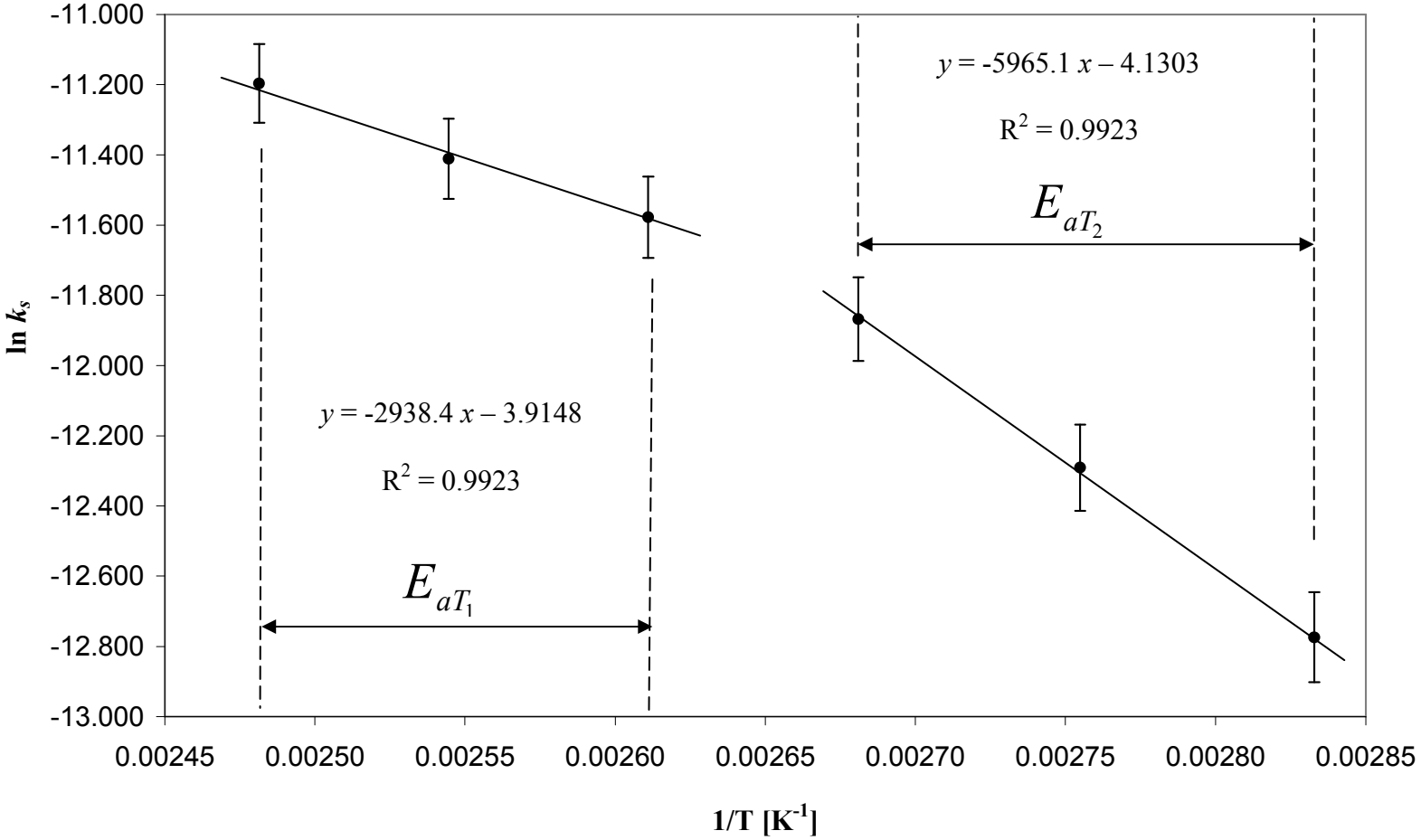

Figure 4.13 Temperature effect on the reaction rate constant (using data from Runs 12 to 14 and 15-17).

4.3 General discussion of experimental errors

In this section experimental errors are reviewed, so that their impact on the key conclusions presented at the end of this chapter may also be taken into account.

4.3.1 Experiments in the batch reactor

Temperature: This was measured in the autoclave reactor with a temperature probe, and when measuring 110 ºC, this type of measurement is generally considered to be within ± 2.2 ºC which corresponds ±2% of the reaction temperature.

Analysis of the composition of the liquid phase: This was performed using a GC and as discussed in Section 4.2.3.1, The integral areas ($I_{A,}$ $I_{B,}$ and I_C in Example calculation No 2) were then used to calculate the conversions. The resulting error in the value reported could for example, at a low conversion of 10%, be expressed as a value =10 ±1%

Volumes of fluid used in the reactor: The errors in measuring these volumes are in the region of ±0.05 ml which corresponds 0.25 % of the volume measured.

Quantity of catalyst used: This was weighed and a quantity of 0.1 ± 0.005 g of Pt/C was used. This would influence the pre-exponential factor in the rate equation.

These errors would have an impact on the calculated values of: the order of reaction, activation energy, and pre-exponential factor, and these are indicated in the conclusions.

4.4 **Conclusions on reaction kinetics**

(a) For the Pt/C catalyst (with a loading of 2.7 wt% Pt) and for the reaction conditions studied, the reaction rate expression is of the following form:

$$r_{BA} = -\frac{dC_{BA}}{dt} = k_s \times [C_{BA,s}]^{0.442} \times [C_{O_2,s}]^{0.005}$$

where:

$$k_s \Big|_{atT_1} = 0.019 \exp\left(-\frac{24.4 \times 10^3}{RT}\right) \qquad T \text{ range from 130 ºC to 110 ºC}$$

or

$$k_s \Big|_{atT_2} = 0.016 \exp\left(-\frac{49.6 \times 10^3}{RT}\right) \qquad T \text{ range from 100 ºC to 80 ºC}$$

(b) An activation energy of 24.4 ± 0.1 kJ mol^{-1} (for a temperature range 130 ºC to 110 ºC) and 49.6 ± 0.1 kJ mol^{-1} (for a temperature range 100 ºC to 80 ºC) were determined for the Pt, which are lower than the value of 79.3 kJ mol^{-1} determined by Plucinski *et al*., (2005 a) for a 0.9 wt% Ru on Al_2O_3 catalyst.

(c) As excess oxygen was present in the gas phase, then it is not surprising to find that the liquid phase concentration would also be high, and the order of reaction with respect to oxygen, $\beta = 0.005 \pm 0.0001$, which is close to zero.

(d) It was useful to find that the reaction order with respect to benzyl alcohol, $\alpha = 0.442 \pm 0.005$. The pre-exponential factor was found to be 0.019 ± 0.005 (for a temperature range 130 ºC to 110 º C) and 0.016 ± 0.005 (for a temperature range 100 ºC to 80 º C), (units to match the equation).

(e) Despite the complexities of the three phase reaction system, it was shown that it is possible to estimate the form of the rate expression, and further studies could be performed using these techniques.

(f) When the catalyst particle size was $\leq$ 38 to 125 μm, the reaction did not appear to be limited by intra-particle diffusion.

References

Bavykin, D.V., Lapkin, A.A., Kolaczkowski, S.T. and Plucinski, P.K., 2005. Selective Oxidation of Alcohols in a Continuous Multifunctional Reactor: Ruthenium Oxide Catalysed Oxidation of Benzyl Alcohol. *Applied Catalysis A: General,* 288, pp. 175-184.

Christain, W., Knudsen, George, W., Roberts, and Charles, N., Satterfield, 1966. Effect of Geometry on Catalyst effectiveness factor. I & EC Fundamentals, 5, 3, pp. 325-326.

Donze, C., Korovchenko, P., Gallezot, P. and Besson M., 2007. Aerobic selective oxidation of (hetro) aromatic primary alcohol to aldehydes or carboxylic acids over carbon support platinum. *Applied catalysis B: Environment,* 70, pp. 621-629.

Fogler, H.S. 2006. *Elements of Chemical Reaction Engineering*. 4th ed. United States of America: Pearson Education International.

Georgieva, M., and Andonovski, B., 2003. Determination of platinum (IV) by UV spectrophotometer. *Anal Bioanal Chem*, 375, pp. 836-839.

Seader, J.D., Henley, E.J., and., 2006. *Equilibrium-stage separation operations in chemical engineering.* 2nd ed. United states of America: John Wiley & Sons,Inc.

Korovchenko, P., Donze C., Gallezot P. and Besson M., 2007. Oxidation of primary alcohol with air on carbon-supported platinum catalyst for the synthesis of aldyhied or acids. *Catalysis Today*, 121, pp. 13-21.

Li Jia, R.., Wang, C.Y., and Wang, S.M., 2006. Preparation of carbon supported platinum catalysts: role of π sites on carbon support surface. *Journal of Material Science*, 41, pp. 6881-6888.

MAST Carbon, http://www.mastcarbon.co.uk/, (Accessed 1st April 2011)

Plucinski, P.K., Bavykin, D.V., Kolaczkowski, S.T and and Lapkin, A.A., 2005 a, Application of a structured multifunctional reactor for the oxidation of a liquid organic feedstock. *Catalysis Today*, 105, pp. 479-483.

Perry, R. H. and Green, D.W. 2008. *Perry's Chemical Engineering Handbook*. Physical and chemical data, 8th ed. United States of America: McGraw-Hill.

Yamaguchi, and Noritaka, 2003. Scope, Kinetics, and Mechanistic Aspects of Aerobic Oxidations Catalyzed by Ruthenium Supported on Alumina. *Chem. Eur. J.* 9, pp. 4353-4361.

Van Dam, H.E., and Van Bekkum, H., 1991. Preparation of Platinum on Activated Carbon. *Journal of Catalysis,* 131, pp. 335-349.

Zotova, N., Hellgardt, K., Kelsall, H.G., Jessimna, A.S., and Mimi, K.K., 2010. Catalysis in flow: the practical and selective aerobic oxidation of alcohols to aldehydes and ketones. *Green Chemistry*, 12, pp. 2157-2163

CHAPTER 5

CASE STUDY 2: THE PARTIAL OXIDATION OF BENZYL ALCOHOL TO BENZALDEHYDE USING PLATINUM COATED MONOLITHS

In this chapter, the second of the two selected reactions is considered in more detail. Experiments are performed using Pt impregnated carbon monoliths in a small scale flow reactor (Step 2), and then a pilot-scale flow reactor (Step 3).

5.1 Background

The background to earlier work on this reaction has already been described in Section 2.3. In this chapter the objectives for this Case Study are summarised, and a report is provided of progress made.

As a reminder the reaction stoichiometry is represented by:

$$C_6H_5CH_2OH_{(l)} + 1/2O_{2\ (g)} \rightarrow C_6H_5CHO_{(l)} + H_2O_{(l)} \qquad \Delta H_R \approx -210\ \text{kJ mol}^{-1} \qquad (5.1)$$

The following features are important in the design of this reacting environment, and this is important to identify as the 'methodology' for this process is developed:

Temperature control: As the reaction proceeds favourably at a temperature of 110 ºC, it is necessary to raise the temperature of the reactants up to that point and to keep them there. As this is an exothermic reaction, then if isothermal conditions are to be maintained, heat must be removed. "K" type thermocouples were used in the experiments to measure temperature.

Oxygen supply: Oxygen needs to be supplied in gaseous form. This means that a three-phase system exists in the reactor (gas, liquid and solid). The oxygen needs to dissolve in the liquid phase, before it can react on the catalytic sites. In order to ensure an adequate supply of oxygen, excess oxygen above the stoichiometric quantity should be added. Brooks Mass Flow Meters were used (Supplied by Emerson Electric Co.) to control the flow rate of gas that was fed into the system.

Staged injection of reactants: Based on earlier published work, there is a distinct advantage in being able to add oxygen in a staged manner. This has the effect of reducing the local velocity of the two-phase mixture as it flows through the reactor, and hence increasing the effectiveness of the reactor.

Pressure control: Based on earlier work (Kolaczkowski 2007), a minimum operating pressure of 8 bar(g) has been selected. This ensures that at an operating temperature of 110 ºC, the vaporization of: benzyl alcohol, benzaldehyde, dioxane, and water are suppressed in the liquid phase. Also, that the gas pressure is adequate to ensure that the oxygen is adequately dissolved in the liquid, and that the reaction is not limited by gas absorption.

Concentration of benzyl alcohol: Based on earlier published work (Kolaczkowski 2007), a concentration of 10 vol% benzyl alcohol will be used.

Selection of solvent: Based on earlier published work (Kolaczkowski 2007), a mixture of 90 vol% dioxane and 10 vol% water will be used. From work by Plucinski *et al*., (2005 b), it is known that the choice of solvent can have a strong effect on selectivity.

Liquid feed flow rate: Based on earlier work in the pilot-scale reactor (Kolaczkowski 2007), a feed flow rate of 4.2 L h^{-1} was used in a cross-sectional area equivalent to 339.29 mm^2 (with an average LHSV of 27 h^{-1}). Although in the earlier application, the mm-scale channels were packed with spherical beads of catalyst (150 μm), this ratio needs to be considered when considering what flow rate to use in a scaled-up version of the reactor. The outlet liquid flow rate was measured by collecting and measuring the outlet flow after 15 min and/or 30 min of operation at steady-state conditions.

Multi-stage sampling: It is believed that there are advantages in being able to take liquid samples at different sections along the reactor. This can help to optimize the operating conditions.

In the sections that follow, a description is provided of the ways in which the two different types of reactors were developed, and the way in which the Pt catalyst was made and recovered from a spent solution, and how it was coated onto a monolith support.

5.1.1 Single Tube Monolith Reactor (STMR)

Looking back at Figure 1.2 when the concept of 'methodology' was introduced, in order to help with the transition from Step 1 to Step 3, there is an intermediate Step 2 in the process.

It is for the purpose of implementing Step 2, that the concept of the 'Single Tube Monolith Reactor" (STMR) was developed. In this reactor, the catalyst is supported on a structured support (e.g. monolith), and sections of monolith are inserted into the tube. This concept is illustrated in the simplified schematic in Figure 5.1.

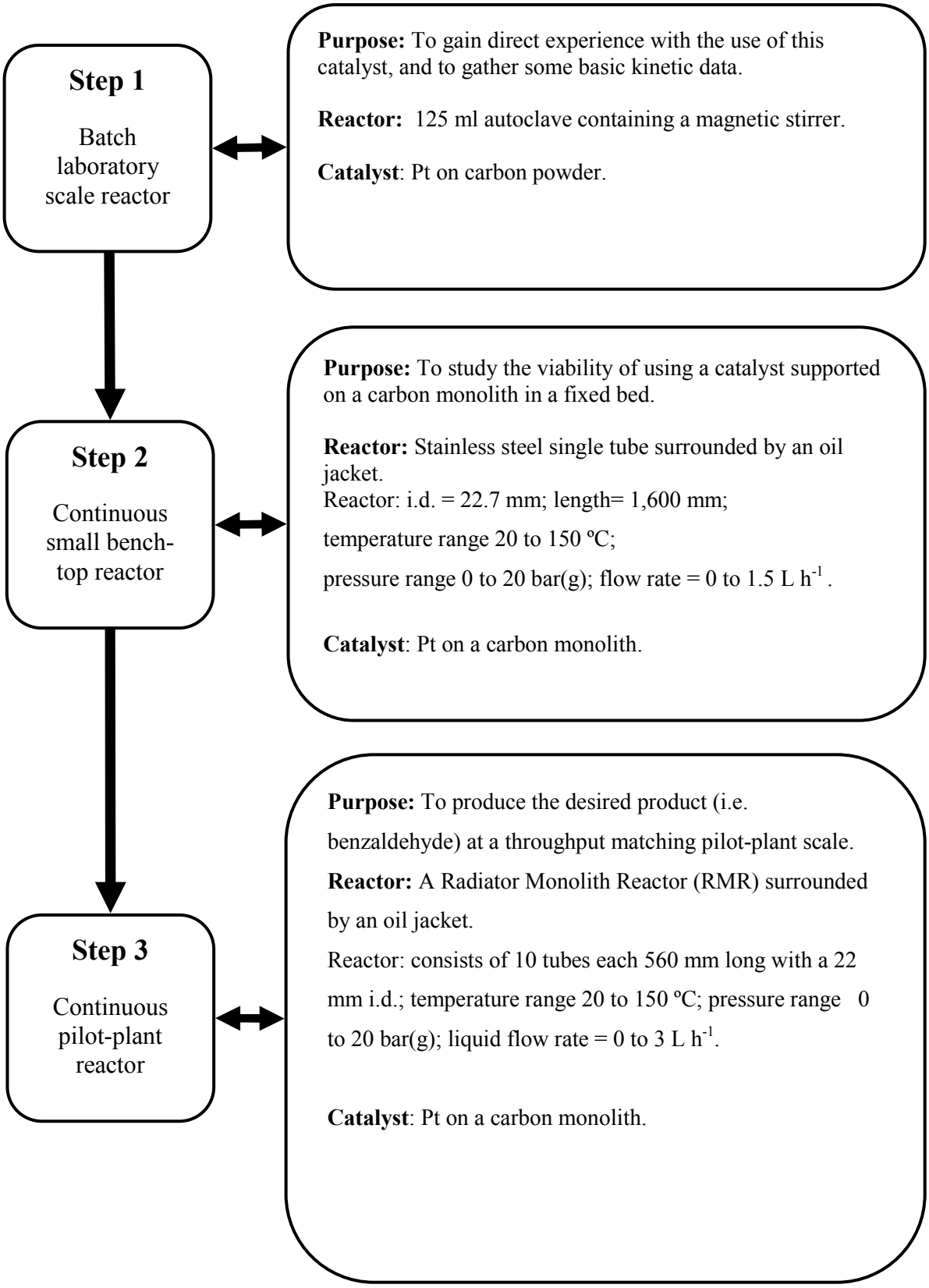

Figure 1.2: The scheme followed for the partial oxidation of benzyl alcohol.

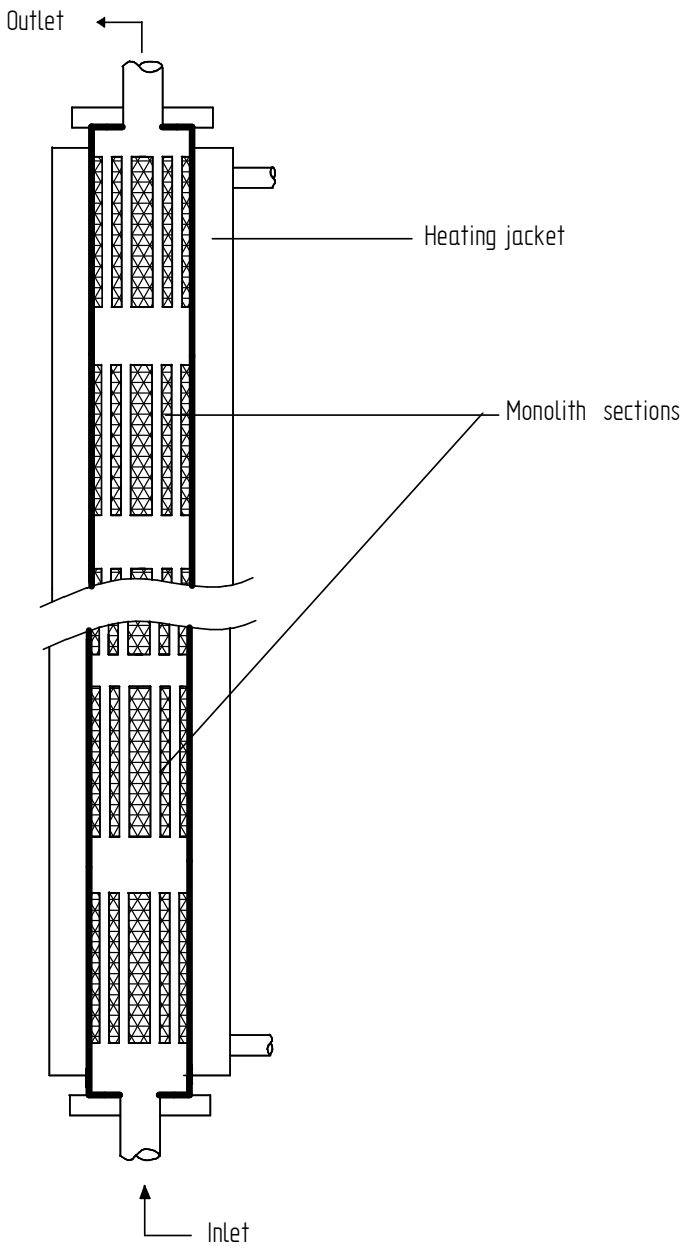

Figure 5.1: A schematic view of the Single Tube Monolith Reactor (STMR).

5.1.2 Design aspects of Single Tube Monolith Reactor (STMR)

In earlier unpublished work at the University of Bath (Wilson, 2007), a Single Tube Monolith Reactor (STMR) was constructed, and installed into the flow circuit where the partial oxidation of benzyl alcohol could be studied. A simplified schematic of this apparatus is illustrated in Figure 5.2. The reactor was surrounded by a heating jacket that contained high thermal resistance Dow corning silicon oil (210/H/100CS), which maintained the reaction temperature at the desired value. The jacket was connected to a thermostatic oil circulator bath (Grant GP100), maintained at 110 ºC. The temperatures inside the reactor are inferred from the surface temperatures measured on the outside of the metal surface of the heated jacket (T_1 to T_5). The outside metal surface has a layer of insulation on it.

The single tube contained carbon monoliths with a density of 400 cell per square inch (cpsi) (supplied by Mast Carbon Ltd. UK). Each monolith was ~ 20 ± 2 mm o.d. and 50 mm long. There were ~ 225 square channels (0.7 mm × 0.7 mm) with ~ 285 mm^2 cross sectional area of bed in each monolith, and an example is illustrated in Figures 5.3 to 5.5. The purpose of the monolith was to act as support for the Pt catalyst.

The 23 mm i.d. single-tube was 1600 mm long, and contained 18 monolith segments. Each monolith was separated by a stainless steel spacer (19 spacers in total). The spacers had an external diameter of 18 mm and their length was 30 mm, see Figure 5.4 b. The function of the stainless steel spacers was to direct the reaction mixture to the edges of the reactor wall, where the heat transfer process took place. In addition, the spacers played an important role in improving the effectiveness of local mixing.

Although Wilson (2007) performed experiments with air and water, the system was not tested under reaction conditions. However, Wilson (2007) did manage to coat the carbon monoliths with Pt, although at the time it was recognized that the coating technique employed had not worked very well. This was deduced from the final colour of the coated monoliths, which was very non-uniform, and visual observation that it was difficult to wet the surfaces of the carbon monolith (hence penetrate the solution into the pore structure).

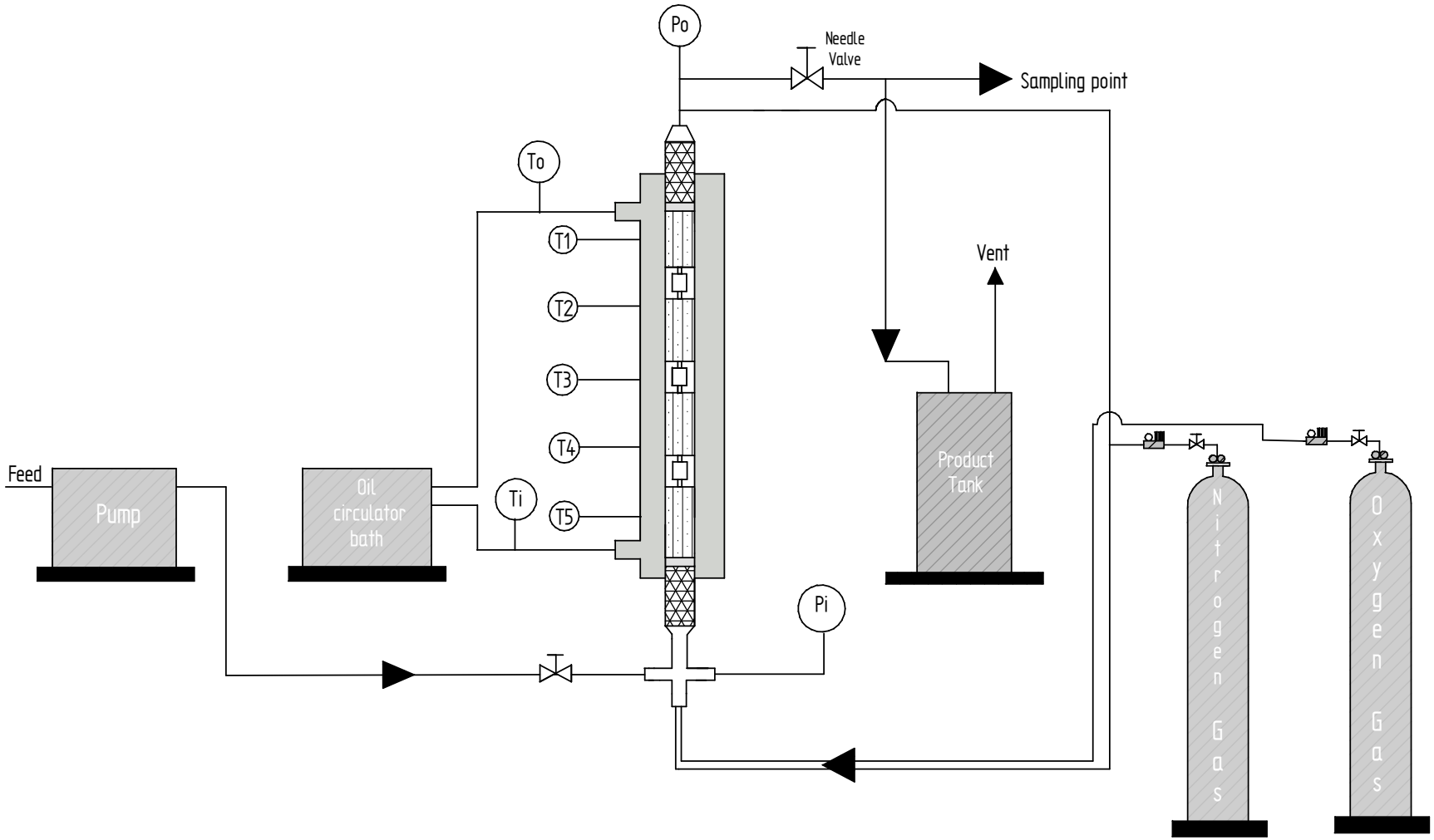

Figure 5.2: Schematic diagrams for the Single Tube Monolith Reactor (STMR).

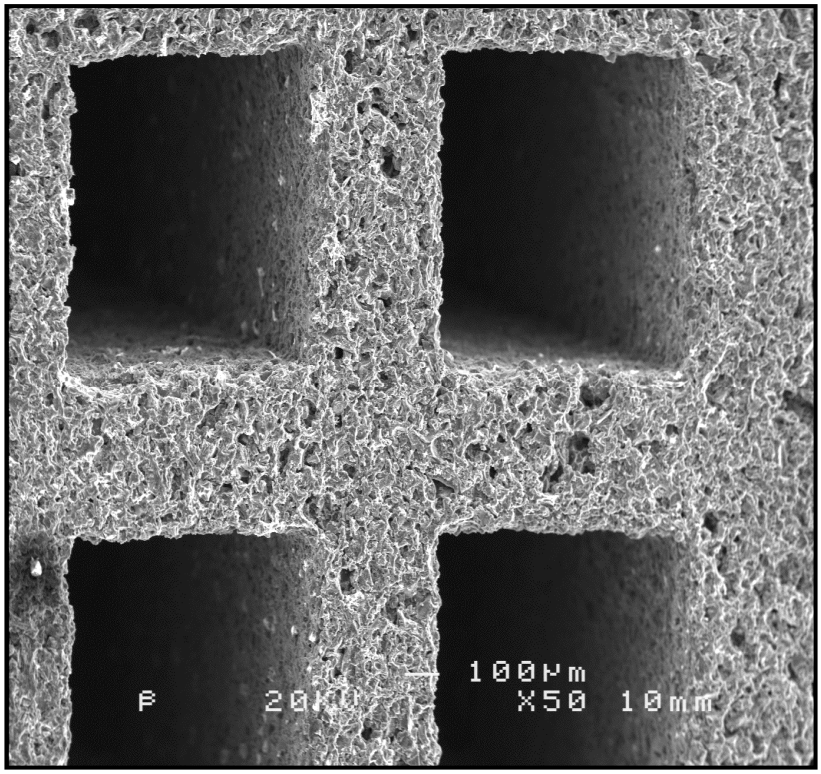

Figure 5.3: SEM image showing the porous nature of the micro channelled support.

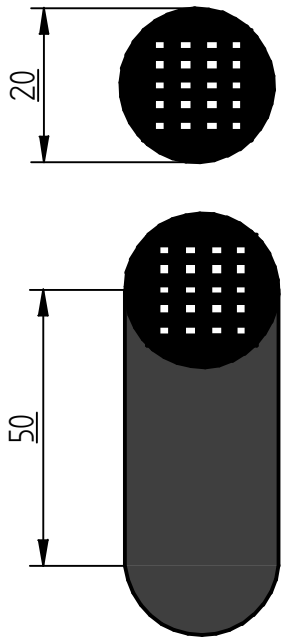

(a) Dimensions of a carbon monolith.

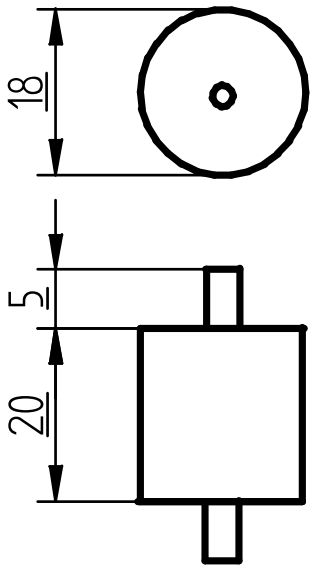

(b) Dimensions of a stainless steel spacer.

Figure 5.4: Dimensions of the stainless steel spacer and carbon monolith.

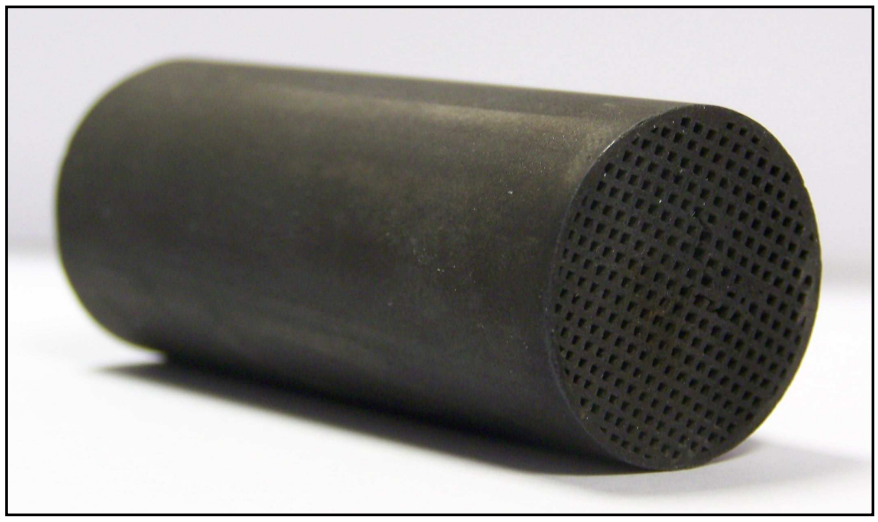

Figure 5.5: Image of carbon monolith.

In the next section an experiment is described that was performed as part of this research on this "Single Tube Monolith Reactor" (STMR).

5.1.3 Scoping study on Single Tube Monolith Reactor (STMR)

The reactor was tested, to explore the viability of this new design. The experimental conditions and results (% conversion) are summarised in Table 5.1. The samples from the reactor were taken every 15 min and analysed using a GC (Agilent 6890N Network) equipped with a 30 m HP-5 × 0.32 mm × 0.25 μm film thickness column to calculate the conversion of benzyl alcohol and the selectivity of the desired product benzaldehyde. The GC was calibrated for benzyl alcohol, benzylaldehde, and benzoic acid as the acid is one of the possible by-products for this type of reaction (description and sample calculations were shown in Sections 4.2.3 and 4.2.4).

For the set flow rate, the results in Table 5.1 show a reasonable conversion of benzyl alcohol (~ 19 %), which provides evidence that the bed was catalytically active and hence some platinum had been deposited on the surface of the carbon monoliths. Although the conversion did drop slightly with time, this may have occurred as a result of an increase in the liquid flow rate (from 3.13 L h^{-1} to 3.95 L h^{-1}). However, it was also very encouraging to observe that the pressure drop was low, and it did not increase significantly with time, and this was a big break-through.

After removing the catalyst from the tube, the following decisions were taken:

(a) To redesign the spacers to improve the heat transfer between the fluid and wall. These spacers also serve to improve the mixing process and mass transfer between the liquid and oxygen gas.

(b) To form a PTFE sleeve around the monolith to reduce wall slippage as there was a large gap (1 to 2 mm) between some of the carbon monoliths and the wall. Non-uniform flow around some of the monoliths may have contributed to variations in conversion during the course of the experiment. However, it is expected that the pressure drop will be higher, although conversion should also be higher as more of the fluid is forced through the channels in the carbon monolith.

(c) To re-coat the carbon support with fresh catalyst, as the first coating was known to have not been very successful. This should lead to a higher conversion.

(d) After modifications (a) to (c) have been implemented, the system should be tested under reaction conditions, and the variables explored to achieve high conversion and better selectivity.

(e) Longer term, after test (d) is complete, to design and test a new form of Single Tube Monolith Reactor (STMR), named the Radiator Monolith Reactor (RMR), in which multi-stage gas injection and liquid sampling could be used and a longer reaction zone achieved. This would represent a pilot-scale reactor (Step 3 in the methodology).

Table 5.1: Summary of experimental conditions and results from scoping study on Single Tube Monolith Reactor (STMR).

Time when sample was taken [h]	Feed* flowrate [L h^{-1}]	Excess O_2 = 180 %	Reactor temperature [ºC]							Pressure bar(g)			Conversion [%]
		Oxygen [L min^{-1}]	T_o oil outlet	T1 surface (top)	T2 surface	T3 surface	T4 surface	T5 surface (bottom)	T_i oil inlet	Pi	Po	ΔP bar	
0.5	3.13	1.225	117	114	114	114	114	121	120	12.4	12.2	0.0134	19.4
0.75	3.01	1.225	117	115	114	114	114	121	120	12.1	12.0	0.01	15.9
1.00	3.20	1.225	117	115	114	114	114	121	120	8.63	8.60	0.023	15.4
1.25	3.95	1.225	117	115	114	114	114	121	120	10.6	10.5	0.05	13.0

*Composition of feed: 10 vol% benzyl alcohol in a solvent of 90 vol% dioxane and 10 vol% water.

5.1.4 Design of improved Single Tube Monolith Reactor (STMR)

Spacer re-design: The stainless steel spacers have been re-designed, and these are illustrated in Figure 5.6. These spacers are a tighter fit in the tube, and they prevent the spacers from being wedged at an angle in the tube. The old and new spacers are illustrated in Figures 5.7 and 5.8. The new stainless steel spacers have a 22 mm o.d., and have sixteen 1.5 mm holes drilled at either end around the perimeter, to allow the fluid to flow in and out of the annular space. When the carbon monoliths have been recoated with Pt catalyst, then this reactor will be tested again.

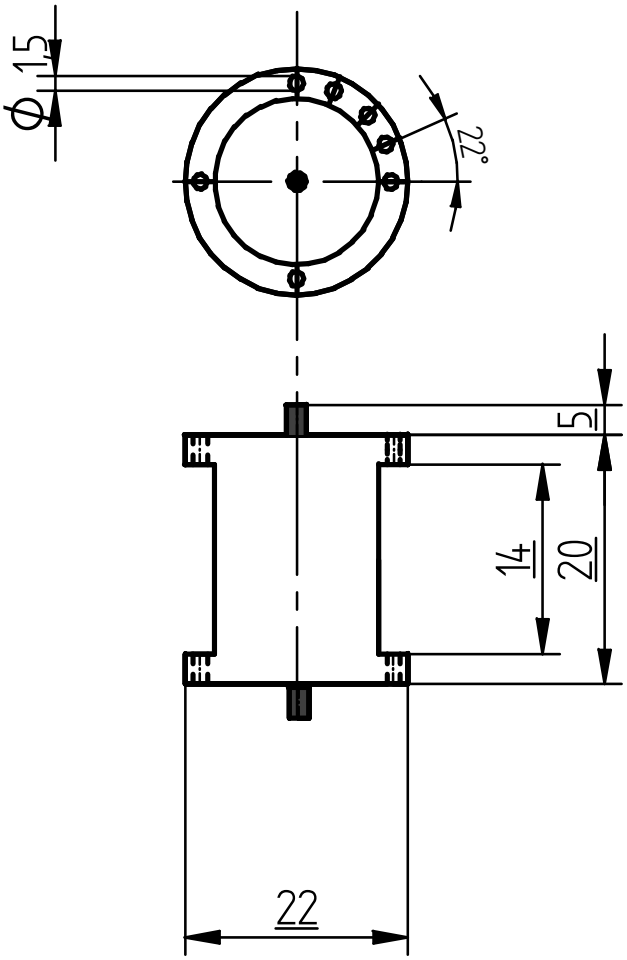

Figure 5.6: Dimensions for the new design of stainless steel spacer for STMR.

Figure 5.7: Image of the old design of the stainless steel spacer.

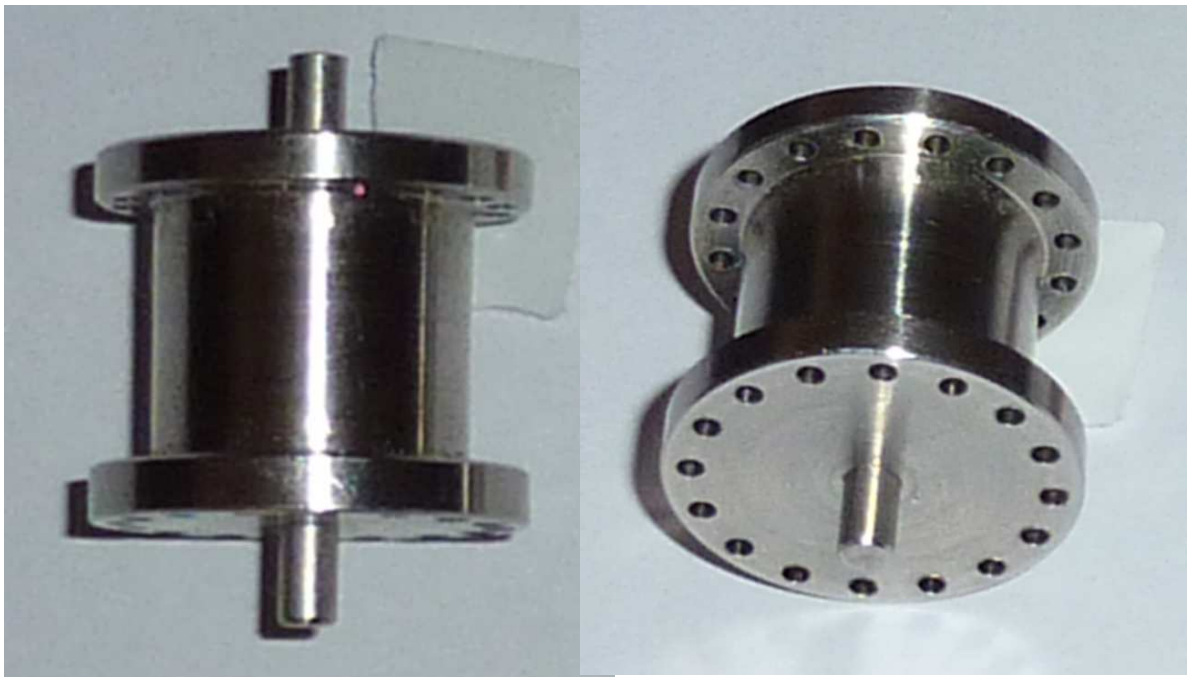

Figure 5.8: Image of the new design of the stainless steel spacer.

Forming a PTFE sleeve: Because of the way in which the monoliths are manufactured, they have a range of outside diameters (19 to 22 mm) which may lead to slippage of gas and liquid, as there was a large gap (1 to 2 mm) between some of the carbon monoliths and the inside tube wall. Therefore, a PTFE sleeve was formed from PTFE tape on each side of the monolith to seal the gap between the outside surface of the monolith and the inside tube wall, see Figure 5.9 and Figure 5.10. However, it was expected that the pressure drop would be higher, although conversion should also be higher as more of the fluid would be forced through the channels in the carbon monolith.

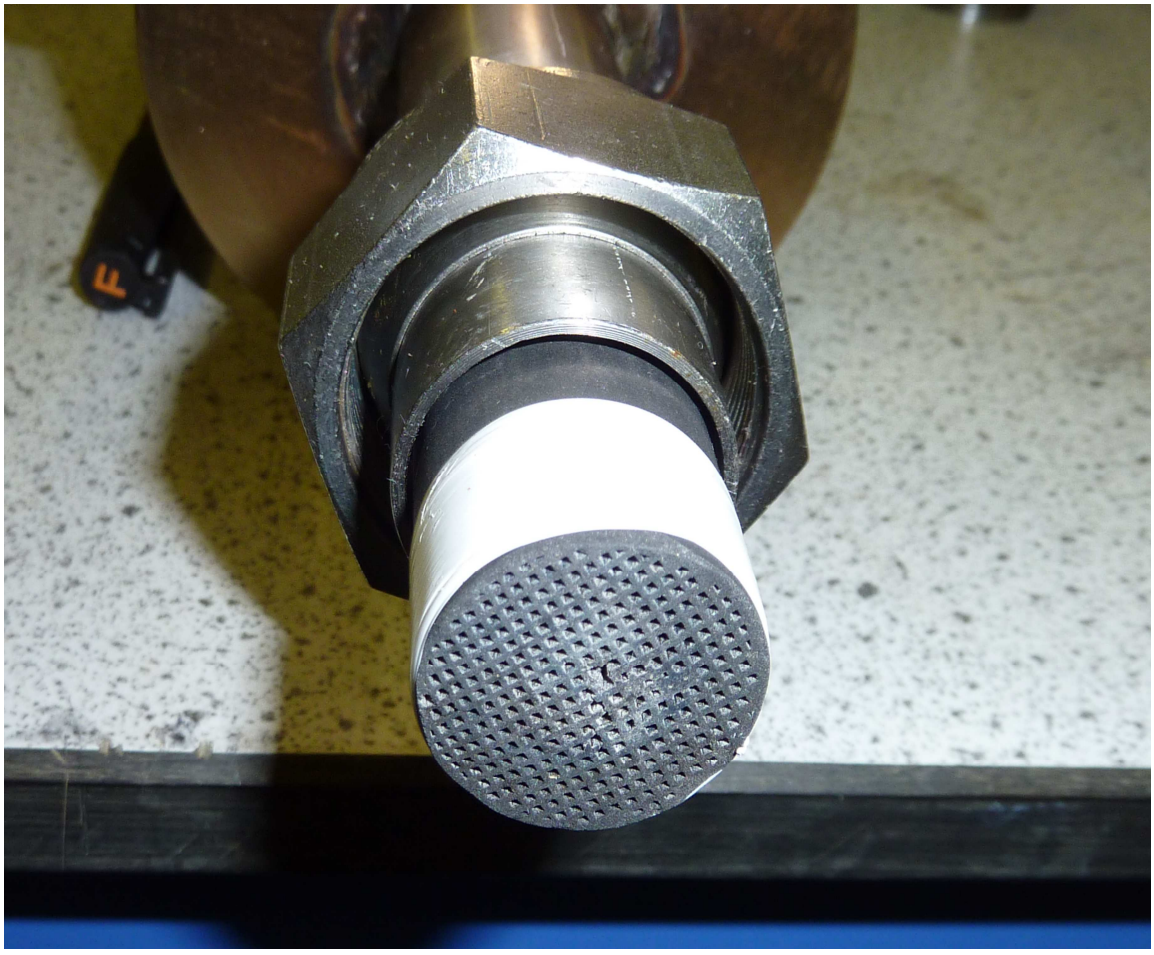

Figure 5.9: PTFE tape forming a sleeve at an end of a carbon monolith.

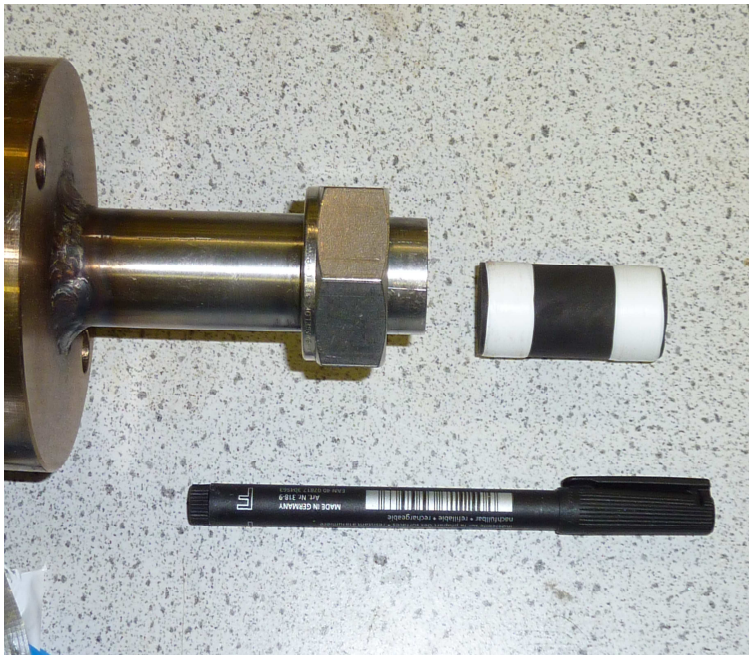

Figure 5.10: Monolith with PTFE sleeve about to be inserted into the STMR.

5.2 Catalyst

It was decided to use a carbon monolith as a support and this had to be coated with Pt which acted as a catalyst.

In this section the following tasks are described:

(a) The carbon monolith was coated with Pt catalyst using the impregnation-reduction method (described earlier in Section 4.2.2.4) in an ethanol media to overcome the surface wetability problem that had been encountered in the coating method in Wilson (2007).

(b) The catalyst was characterized using Transmission Electron Microscopy (TEM)

(c) A method of catalyst recovery from a spent solution was explored.

5.2.1 Coating procedure

The procedure was as follows:

(i) 20 g of $H_2PtCl_6.6H_2O$ was dissolved in 400 ml of ethanol and then it was sealed in a container.

(ii) 248 g of carbon monoliths (18 cylindrical sections, each one 50 mm long and 20 mm average diameter) were placed in a 5 litres round bottom flask and 2 litres of ethanol was added.

(iii) The monoliths were left to soak for 20 minutes under vacuum.

(iv) The flask was then fixed to a bench shaker to provide gentle mixing within the flask.

(v) The flask was then connected to an argon atmosphere.

(vi) The platinum solution was then added to the flask in drop-wise fashion and left in an argon atmosphere while it was mixed.

(vii) The concentration of platinum solution was measured using a UV-spectrophotometer at a wavelength of 460 nm (method described earlier in Section 4.2.2.3).

(viii) During course of 45 h, it was found that the concentration of platinum solution dropped from an initial concentration of 8.3 g L^{-1} to 0.75 g L^{-1}, resulting in ~ 90% of the Pt catalyst in the initial solution being loaded on the carbon monolith.

(ix) The flask was then cooled down to 0 ºC in an ice bath for one hour.

(x) When the contents of the flask were at 0 ºC, then 200 ml of formaldehyde was added in drop wise fashion to the flask.

(xi) Then 200 ml of 30 wt% of potassium hydroxide solution was added in drop-wise fashion to the flask.

(xii) The solution was then mixed in the flask for two days, at ambient temperature under an argon atmosphere; this provided the necessary reduction reaction.

(xiii) When the solution become visibly dark, the monoliths were taken out of the flask and they were washed with fresh ethanol twice.

(xiv) The coated monoliths were then dried overnight in a drying cupboard under ambient conditions.

5.2.2 Catalyst Characterization

The catalyst was characterized using Transmission Electron Microscopy (TEM) to identify the loading of platinum on the surface of carbon.
A TEM image of a sample of catalyst is shown in Figure 5.11 a, where small platinum particles can be seen dispersed on the surface of the carbon. The presence of platinum was then confirmed using x-ray diffraction spectrum and about 10 peaks of platinum were detected, see Figure 5.11 b.

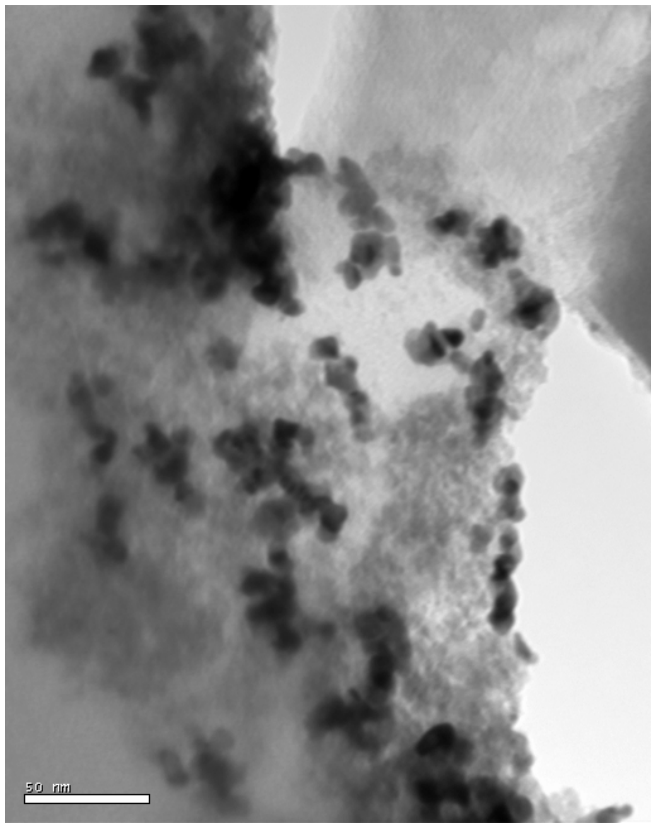

Figure 5.11 a: TEM micrograph of catalyst sample.

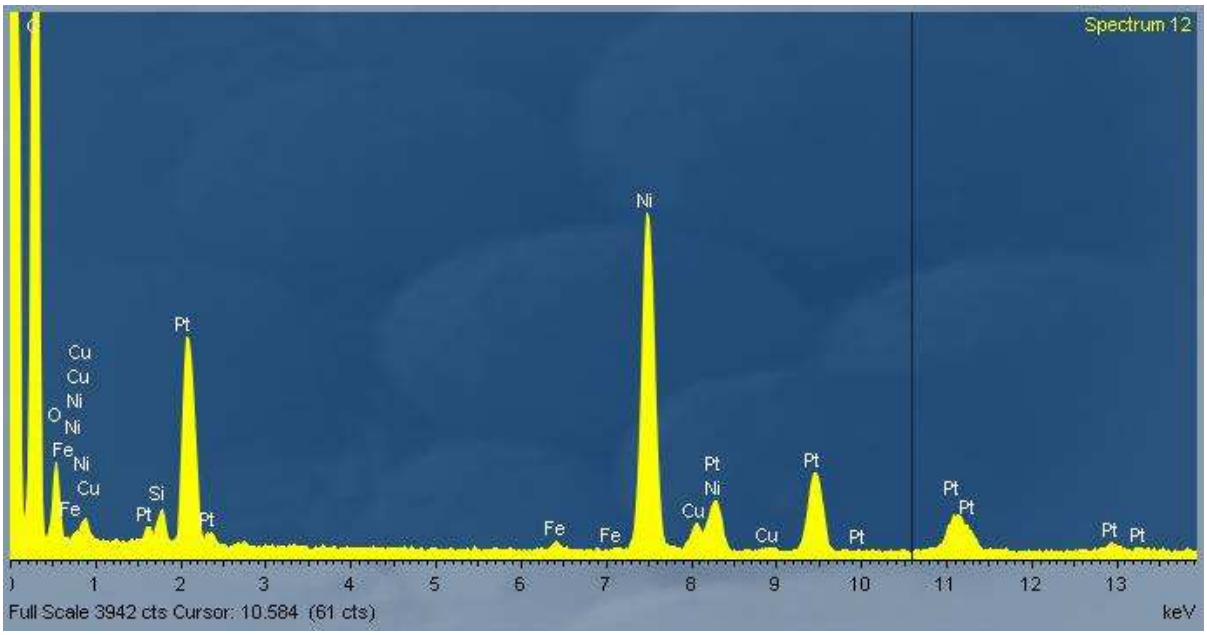

Figure 5.11 b: X-ray diffraction spectrum confirming the presence of Pt catalyst.

5.2.3 Recovery of Pt catalyst from spent solution

Catalyst recovery is an important issue, as the Pt catalyst is expensive to buy (e.g. 1g of $H_2PtCl_6.6H_2O$ costs £70), the material is scarce, and it also creates a disposal problem. This is important also from the point of developing the 'methodology'.

The Pt metal in the spent solution that had been produced during the earlier coating by Wilson (2007) was recovered in this section. The spent solution was based on hexachloroplatinic acid and contained a visible floating film of platinum (silver in appearance). It also contained fine particles of suspended and settled carbon (from previous coating of carbon monolith).

The recovery of platinum from the spent solution was performed as follows:

(i) The solution was first filtered, using glass microfibers fisher brand (FB 59391) paper. The filtered particles are illustrated in Figure 5.12 a.

(ii) The filter papers with the surface filter cake were then immersed in 250 ml of aqua regia (made up from 1:3 volumetric ratio of nitric acid and concentrated hydrochloric acid) for 2 h. During this period the solution was stirred and heated, maintaining a temperature of approximately 60 ºC.

(iii) When all of the carbon particles were washed from the surface of the paper, and the platinum was dissolved in the solution, the filter paper was washed with fresh acid and removed.

(iv) The resulting solution was then allowed to evaporate until it was dry, and then 5 ml of HCl and 0.1 g of NaCl were added.

(v) Again, the solution was allowed to evaporate and the residue was then dissolved in 20 ml of a 1:1 water/HCl solution. This was then diluted by adding deionized water forming 100 ml of solution.

(vi) This resulted in a bright yellow solution of platinum chloride, $PtCl_6^{-2}$, being formed, see Figure 5.12 b.

(vii) A volume of 10 ml from the produced solution in Step (v) was evaporated and the solid residue was washed with ethanol before it evaporated again.

(viii) 10 ml of ethanol was added to the residue and then the solution was analysed using UV-visible spectrophotometer SHIMADZU (UV-1601). The UV spectra were recorded (see Figure 5.13) between 190 to 900 nm to calculate the concentration of Pt and to indentify if there were any new peaks which might have been formed by new complexes. Figure 5.13 shows that no new peaks were formed comparing with a similar plot at 0.346 g L^{-1} in Figure 4.6.
The measurements were performed using a 1 cm quartz cell.

This technique was successful, and provides a method which can be used to recover Pt from a spent solution, however, the recovered Platinum needs to be coated again on fresh monoliths and tested in a reaction.

Figure 5.12 a: Glass microfiber filter paper with trapped platinum and carbon.

Figure 5.12 b: Platinum chloride solution recovered from the waste solution from the previous coating.

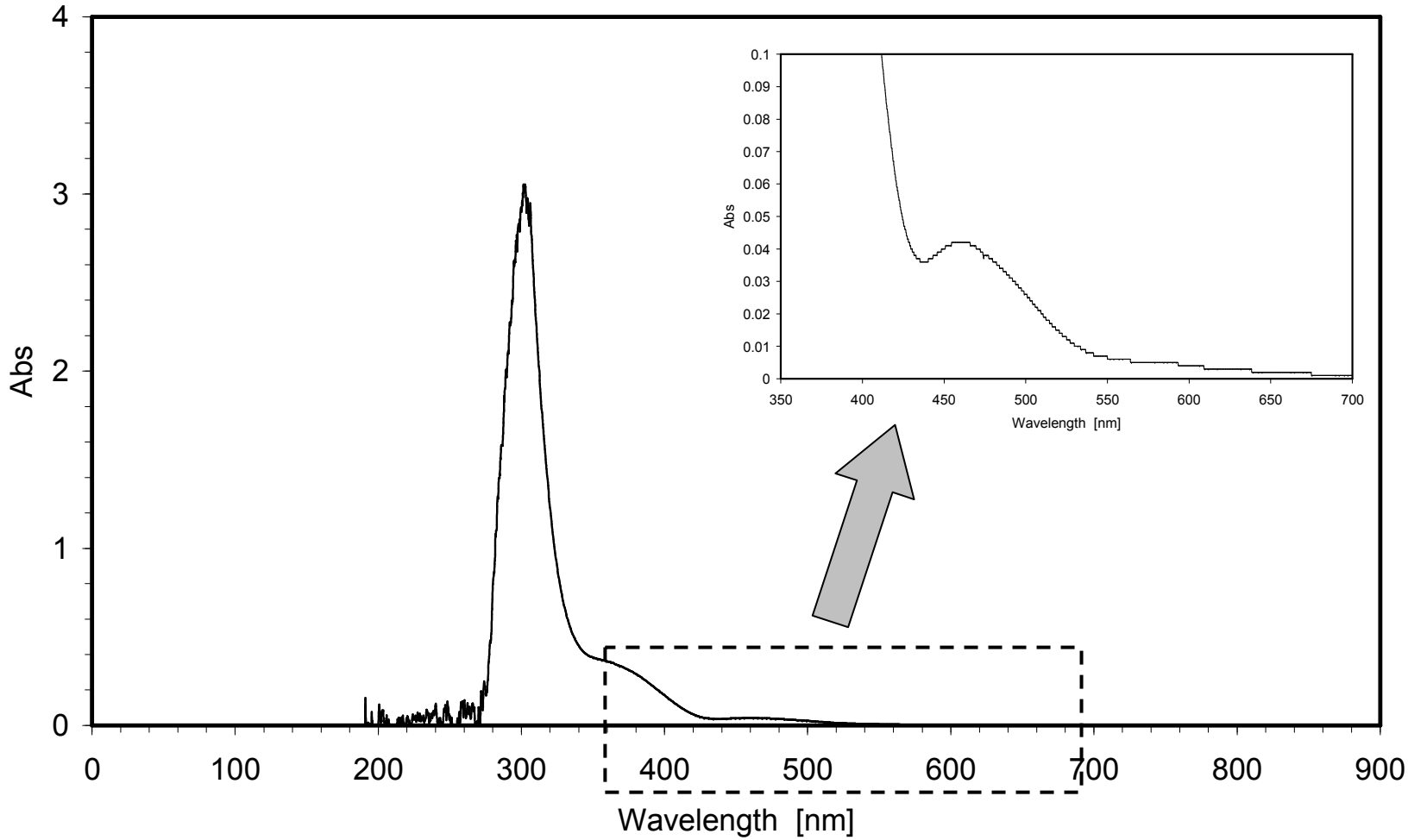

Figure 5.13: UV spectra for recovered Pt from a spent solution.

5.3 Experiments on an improved "Single Tube Monolith Reactor" (STMR)

5.3.1 First set of experiments

Having implemented the modifications described in Sections 5.1.4 and 5.2.1, the system was then tested under reaction conditions to look at the viability of the adjustments that been done and their effect on the STMR.

The experimental conditions and results (conversion and selectivity) are summarised in Table 5.2. The samples from the reactor were taken every 15 min and analysed using a GC (Aglient 6890N Network) equipped with a 30 m HP-5 × 0.32 mm × 0.25 μm film thickness column to calculate the conversion of benzyl alcohol and the selectivity of the desired product benzaldehyde.

The results of this preliminary set of experiments are shown in Table 5.2.
First, by looking at Set No 1.1, it can be seen that the conversion is increasing with time. This occurs because the reactor is first of all started with a flow of nitrogen and then the liquid feed pump is turned-on. After the desired operating pressure is reached, the flow of nitrogen is gradually replaced by the desired flow of oxygen. So, if samples are taken at regular intervals, the conversion will increase with time as more oxygen becomes available to take part in the reaction. Eventually steady-state conditions are achieved.

Comparing the results from Set No 1.3 experiments in Table 5.2, with the earlier results in Table 5.1, it is clear that for a similar set of conditions a higher conversion was obtained in the improved reactor (~ 34% compared with 15%). The pressure drop also remained low. Then as the liquid flow was reduced from 3 L h^{-1}, the conversion increased from ~ 34 to 60% (Set No. 1.3 compared with set No. 1.2). This experiment were performed at a range of LHSV of 6 to 12 h^{-1} and GHSV of 2640 to 3780 h^{-1}.
As the O_2 vol% was reduced, the conversion also decreased:

From ~ 34 to 26% (sets No 1.3 and 1.4), and

From ~ 60 to 44% (sets No 1.2 and 1.1).

In addition, it was very encouraging to observe that the pressure drop across the reactor was very small (< 0.02 bar) even after using the new designed spacers and PTFE sleeves around the monoliths.

However, during a course of six hours of continuous flow experiments, it was noticed that the pressure in the reactor could vary (e.g. 8 to 11 bar(g)), as it was not easy to maintain this constant by making manual adjustments with the needle valve. So it was decided to try to find a suitable back-pressure regulator.

After finishing these test runs, the following decisions were taken:

a) To replace the 16 turn needle valve with a back-pressure regulator to reduce the fluctuation in pressure, as pressure could have a significant effect on the solubility of oxygen in the liquid phase, which could be important in the mass transfer and reaction steps.

b) To perform experiments over a wider range of conditions, so that the performance of the reactor can be assessed.

Table 5.2: Summary of Set No 1 experimental conditions and results on an improved "Single Tube Monolith Reactor" (STMR).

Time [h]	Temperature [°C]	Pressure [bar(g)]	Liquid flow rate [L h^{-1}]	Gas flow rate [L min^{-1}]	O_2 vol%	Excess O_2 [%]	Conversion [%]	Selectivity [%]	Pressure drop bar
Set No 1.1									
0.50	110	8.8	1.5	1.75	70	359	17.96	99.97	0.0004
0.75	110	8.0	1.5	1.75	70	359	37.45	100	0.0004
1.00	110	9.7	1.5	1.75	70	359	38.22	100	0.0004
1.25	110	9.3	1.5	1.75	70	359	44.17	100	0.0004
1.50	110	10.0	1.5	1.75	70	359	43.98	100	0.0004
1.75	110	9.25	1.5	1.75	70	359	45.94	100	0.0004
2.00	110	9.75	1.5	1.75	70	359	48.84	100	0.0004
Set No 1.2									
2.50	110	8.86	1.5	1.225	100	359	56.9	99.68	0.0004
2.75	110	10.3	1.5	1.225	100	359	60.31	99.41	0.0004
3.00	110	9.80	1.5	1.225	100	359	66.94	98.07	0.0004
3.25	110	9.97	1.5	1.225	100	359	71.17	96.96	0.0004
Set No 1.3									
3.75	110	9.67	3	1.225	100	180	33.68	100	0.02
4.00	110	10.6	3	1.225	100	180	34.78	100	0.02
4.25	110	10.8	3	1.225	100	180	36.94	100	0.02
Set No 1.4									
4.75	110	10.3	3	1.75	70	180	26.69	100	0.02
5.00	110	10.5	3	1.75	70	180	26.73	100	0.02
5.25	110	10.0	3	1.75	70	180	26.39	100	0.02

5.3.2 Second set of experiments

In this section a range of experiments was carried out on the improved "Single Tube Monolith Reactor" (STMR) over the course of 160 h to assess the influence of a wider range of variables on the performance of the reactor and the longevity of the catalytic system.

The following variables were studied:

(a) Liquid flow rate at 0.5, 1.0 and 1.5 L h^{-1}.
(b) Total gas flow rate, ranged from 0.045 to 1.23 L min^{-1} ,
(c) The amount of oxygen, which is described as % excess oxygen ranged from -50% to +359%.
(d) Back-pressure ranged rom 8 to 14 bar(g).
(e) Temperature ranged from 90 to 130 ºC.
(f) The product was recycle through the reactor.
(g) Experiments were performed with the flow direction being upward, and also downward.

However, the concentration of feedstock was kept constant at 10 vol% of benzyl alcohol dissolved in a mixture of 10 vol% of water in 90 vol% dioxane, and the catalyst loading with 2.7 wt% of platinum metal.

The STMR contained 18 pieces Pt/C monoliths creating an effective catalytic length of 900 mm. Each pair of 50 mm long monoliths was separated by a 30 mm stainless steel spacer, creating a total bed length of 1140 mm.

5.4 Result and discussion from the second set of experiments

The results of Set No 2 experiments are presented in this section.

5.4.1 Effect of amount of oxygen

Figure 5.14 shows how varying the amount of oxygen that is added to the reactor affects the conversion of benzyl alcohol to benzaldehyde. These experiments were performed at 110 ºC with 100 vol% oxygen (in the gas feed) with an 8 bar(g) back-pressure. In the figure the amount of oxygen is described as % excess, referring to the amount of oxygen required for the stoichiometric oxidation of the benzyl alcohol to benzylaldehde:

$$C_6H_5CH_2OH_{(l)} + 1/2O_{2\ (g)} \rightarrow C_6H_5CHO_{(l)} + H_2O_{(l)} \qquad \Delta H_R \approx -210\ \text{kJ mol}^{-1} \qquad (5.1)$$

$$\%\ \text{excess}\ O_2 = \frac{\text{moles of}\ O_2\ \text{supplied in excess of stoichiometry}}{\text{moles of}\ O_2\ \text{required by stoichiometry}} \times 100 \qquad (5.2)$$

A negative % value (e.g. -50%), means that only 50% of the stoichiometric requirement had been supplied (see Appendix E). The effect of oxygen addition was also measured at different liquid flow rates with the total conversion of benzyl alcohol and the selectivity towards benzaldehyde being analysed by GC.

The results in Figure 5.14 show that increasing the % excess of oxygen in the system has a significant effect on the total conversion of benzyl alcohol. With a liquid flow rate of 1.0 L h^{-1} and a 0% excess of oxygen to benzyl alcohol, the conversion to benzaldehyde was 49%. However, increasing the excess of oxygen to 350% the total conversion had increased to 82%. This trend is reflected across the range of liquid flow rates tested (0.5, 1.0 and 1.5 L h^{-1}) with the liquid flow rates at 0.5 and 1.0 L h^{-1} giving much higher conversions than the faster flow rate of 1.5 L h^{-1}. This was because the residence time was less at 1.5 L h^{-1} than 1.0 L h^{-1}, however this effect was not noticeable when the flow rate was between 0.5 L h^{-1} and 1.0 L h^{-1}.

Figure 5.14 also shows that as the conversion increases, then the selectivity towards benzaldehyde decreases. However, it seems that even though the total conversion of benzyl alcohol at 0.5 L h^{-1} and 1.0 L h^{-1} are relatively similar (87 and 82% respectively) there is a marked difference in the observed selectivity. At the lower liquid flow rate of 0.5 L h^{-1} there is 83% selectivity towards benzaldehyde, whereas at 1.0 L h^{-1} a higher selectivity of 90% is achieved. The difference in the selectivity was believed to occur due to possible back-mixing which could be encountered at such low liquid flow rate of 0.5 L h^{-1}.

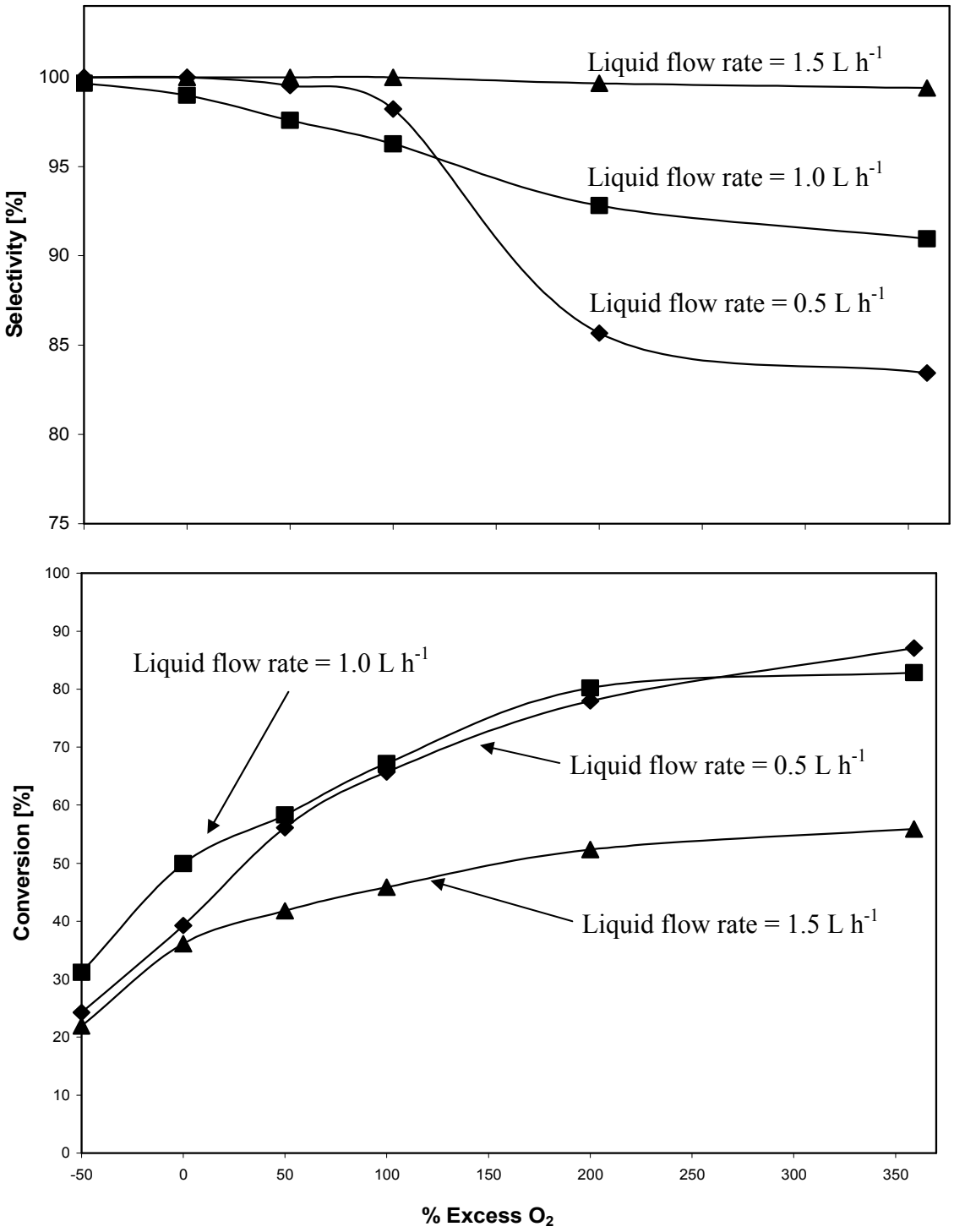

Figure 5.14: Effect of oxygen flow rate represented by excess O_2 [%] on the conversion of benzyl alcohol and selectivity of product benzaldehyde. Results obtained at temperature = 110 ºC, pressure = 8 bar(g).

Note: as the % excess of O_2 is increased, then the flow of gas is also increased.

5.4.2 Effect of varying the O_2 concentration at constant gas flow

The next set of experiments was carried out at 110 ºC with a back-pressure of 8 bar(g). Figure 5.15 shows the effect of varying the vol% oxygen in a gas feed of O_2 and N_2 whilst the overall gas flow was maintained constant (constant residence time). The results show that as the oxygen vol% is decreased in the feed, from 100 to 70, then the conversion of benzyl alcohol steadily decreases. At a 1.0 L h^{-1} liquid flow rate, this figure decreases from 82% to 61%. This experiment was repeated across a range of different liquid flow rates, all of which show a similar trend. The decreases in the conversion are likely to be linked to the decreases in the partial pressure of oxygen in the gas phase (see Henry's Law, equation 4.5). As when operating at :

100 vol% oxygen and 1 L h^{-1} liquid flow rate there is a 359% excess O_2,

and at:

70% vol% oxygen and 1 L h^{-1} liquid flow rate there is a 221% excess O_2.

It is interesting to note that at 70 vol% O_2 (value of O_2 vol% was suggested by GSK and used in Kolaczkowski 2007), although the conversion of benzyl alcohol has decreased, the system still achieves a reasonable level of conversion. This is a much more favourable condition for industrial operations, as when operating with a pure oxygen (100 vol%) feed there are additional safety features to considered. The results at 70 vol% O_2 also show remarkably high selectivity, which is greater than 97%.

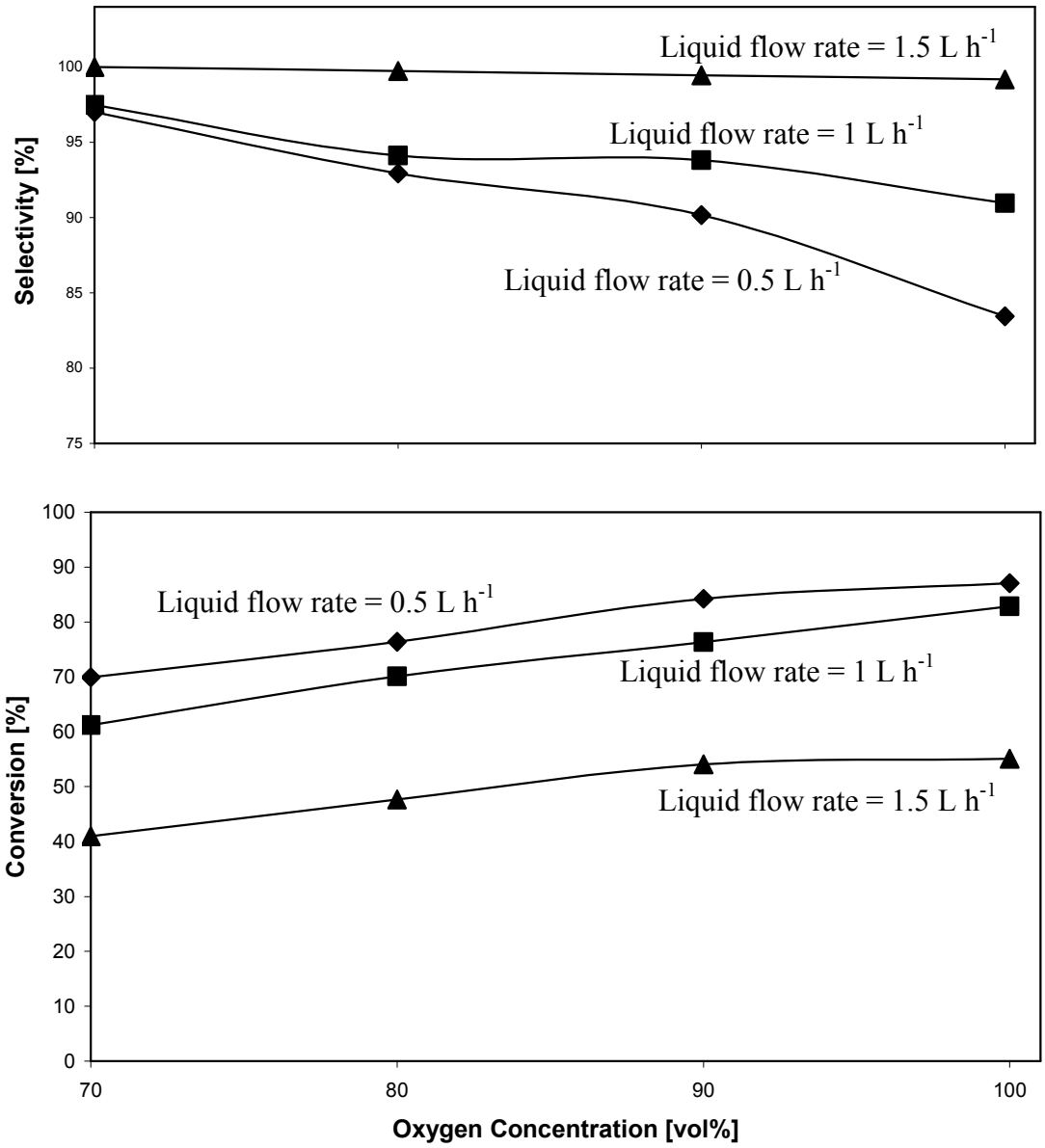

Figure 5.15: Dependence of the benzyl alcohol conversion and benzaldehyde product selectivity on the vol% of oxygen. Results obtained at: liquid flow rates = 1.5, 1 and 0.5 L h^{-1}, temperature = 110 ºC, pressure = 8 bar(g), total gas flow rate = 1.23, 0.818 and 0.409 L min^{-1}.

5.4.3 Effect of back-pressure

In Figure 5.16, one may observe the effect of increasing back-pressure within the system. Previously (at 110 ºC, 8 bar(g), 1.0 L h^{-1} liquid flow rate, and 70 vol% oxygen) the total conversion of benzyl alcohol was 61%. When the back-pressure within the system was increased, at intervals of 2 bar, up to a maximum of 14 bar(g), the total conversion increased steadily, levelling off at 12 to 14 bar(g).
This suggests that at low pressure zone between 8 and 10 bar(g) in Figure 5.16, the overall rate of reaction might be limited by the gas absorption and/or external mass transfer steps, as illustrated earlier in Figure 4.3.

At 14 bar(g) the total conversion had increased to 83%. This marked increased was also observed whilst using a lower excess of oxygen, with selectivities improving at higher pressures. At 8 bar(g) and >80% total conversion, the selectivity towards benzaldehyde had typically been approx. 80%. However, at higher pressures, even though the total conversion had been >80%, the selectivity had remained consistently higher at >90%.

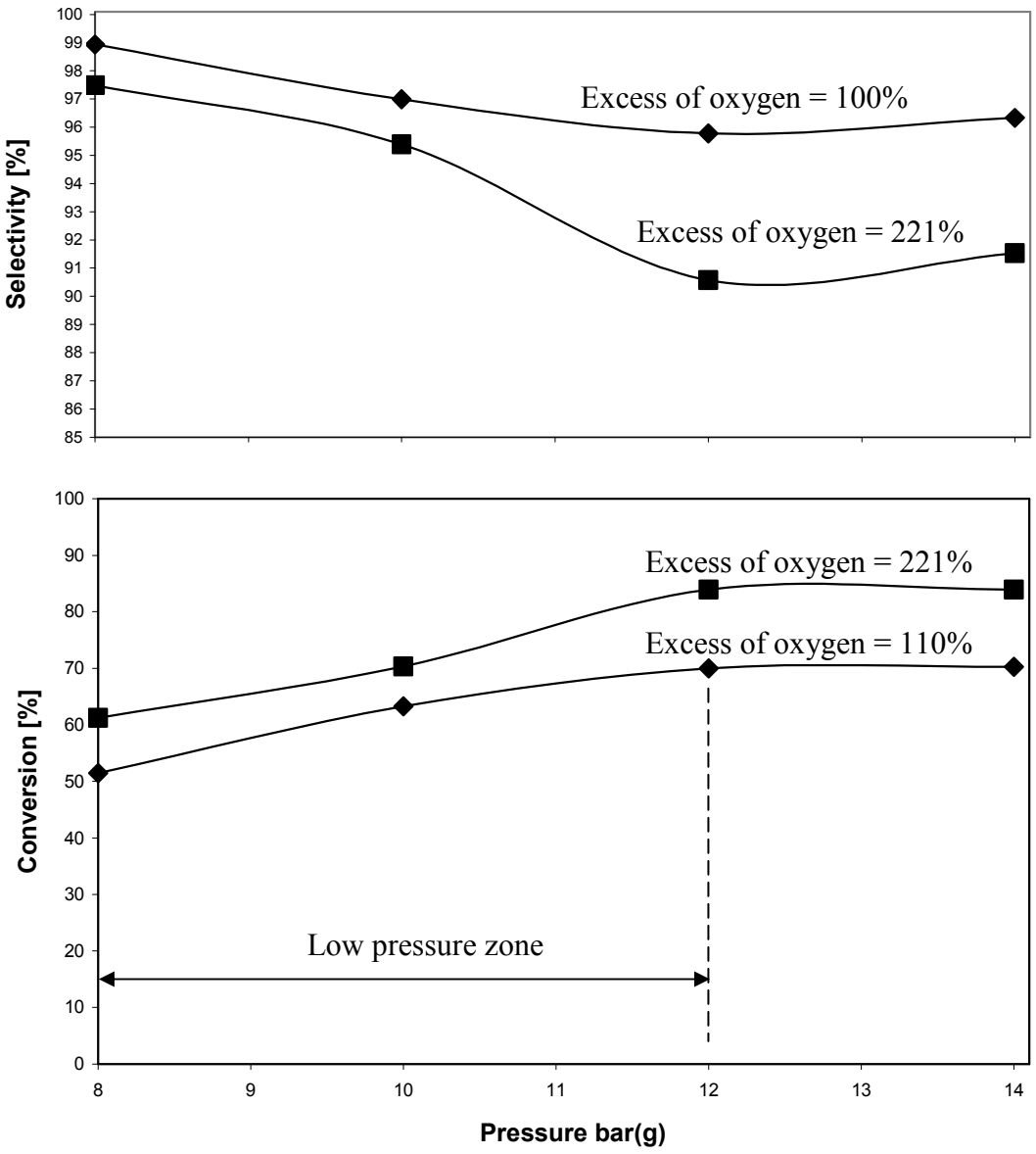

Figure 5.16: Conversion of benzyl alcohol and selectivity of benzaldehyde as a function of reaction pressure. Results obtained at: liquid flow rate = 1 L h^{-1}, temperature = 110 ºC, oxygen flow rate = 0.572 and 0.374 L min^{-1}, O_2 = 70 vol% in the O_2/N_2 mixture.

5.4.4 Effect of temperature

In order to assess the temperature sensitivity of the catalyst, the system was run at 20 ºC either side of the preferred operational temperature of 110 ºC. As the temperature was increased from 90 ºC to 110 ºC the total conversion of benzyl alcohol was observed to increase e.g. at 12 bar(g) and 70 vol% of oxygen the total conversion increased from 50% to 83% Figure 5.17. This suggests that the over all rate of reaction between 90 ºC to 110 ºC may be limited by the diffusion mass transfer step as the value of the activation energy was found to be between 23 kJ mol^{-1} to 29 kJ mol^{-1} (see Figure 5.17 a).

However, one may also observe in Figure 5.17 that from 110 ºC to 130 ºC and at 8 bar(g) there was no pronounced increase in the total conversion. For example, at 110 ºC the total conversion was 60%, and at 130 ºC this remained relatively unchanged at 61%. This suggests that the overall rate of reaction at ≥ 110 ºC may not be limited by the surface reaction step (activation energy $E_a = 0$), but it may be limited by the oxygen supply in the liquid phase as the solubility of the gas might have decrease by increasing temperature (see Table 4.4 p. 108 and/or value of Henry's constant in Figure 5.17). This was confirmed by increasing the pressure from 8 to 12 bar(g) at temperature of 110, 120, and 130 ºC as the conversion was increased by ~ 25% as more oxygen might be dissolved in the liquid phase

Once again at the higher pressure of 12 bar(g) the selectivity in favour of benzaldehyde remained greater than 90%, even though the system was operated at higher temperatures and with total conversions in excess of 80%.

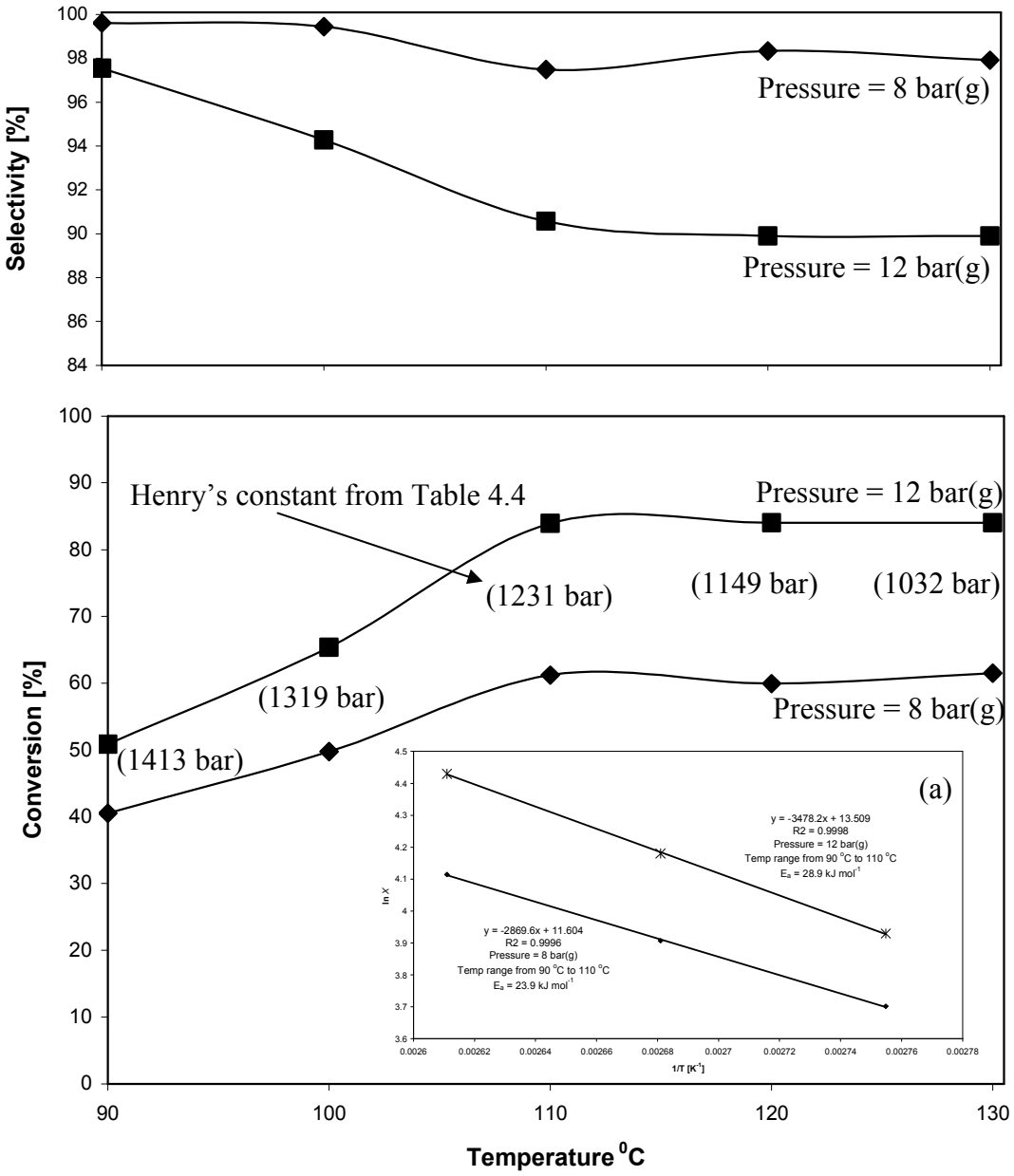

Figure 5.17: Influence of reaction temperature on the conversion of benzyl alcohol and selectivity of benzaldehyde. Results obtained at: liquid flow rate = 1 L h^{-1}, oxygen flow rate = 0.572 L min^{-1}, O_2 = 70 vol% in the O_2/N_2 mixture.

5.4.5 Recycle

Figure 5.18 shows the results of an experiment designed to investigate whether the total conversion of benzyl alcohol could be pushed to completion or whether there were unseen factors that may limit this in some way. This was achieved by running the reactor under a set of optimal/desirable conditions (110 ºC, 1 L h^{-1}, 12 bar(g) and 70 vol% oxygen) for a period of 7 h, after which the solution that had collected was recycled back into the reactor. After each hour, samples were taken and analysed using GC chromatography, showing a steady conversion of ~73% over the course of the first 7 h. Once the solution had been recycled one may observe an increase in the total conversion of benzyl alcohol up to >99%, which again remained steady over the course of the following 4 hours. Associated with this increase in conversion is a dramatic falling in the selectivity (down to 65%) for benzaldehyde, with the remaining 35% being the over oxidised product, benzoic acid. Therefore, this experiment clearly shows that there is no limiting factor to the oxidation of benzyl alcohol, with conversions of over 99% being achieved.

Therefore it is envisaged that with a longer catalyst bed, high conversion could be achieved.

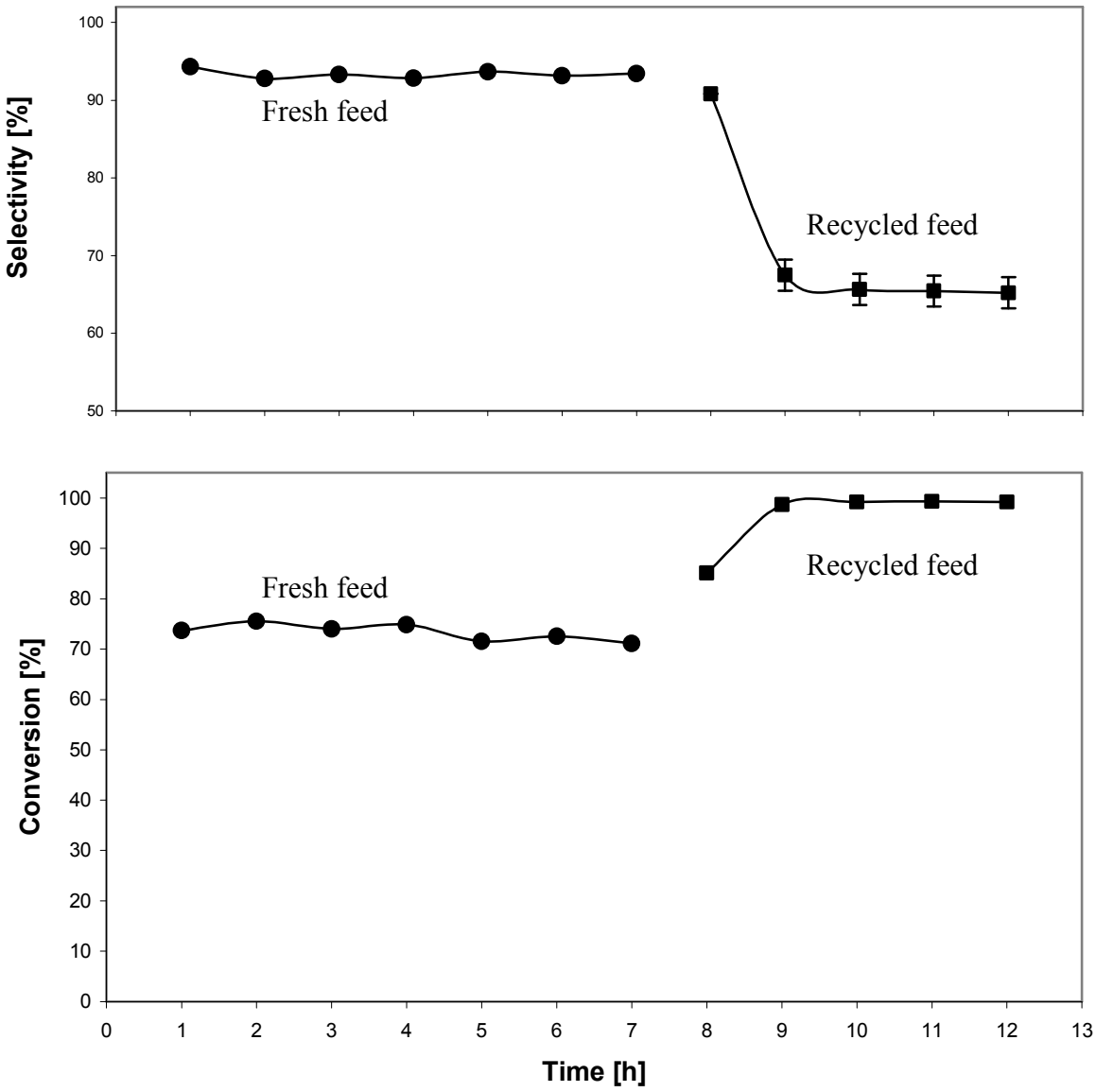

Figure 5.18: Influence of product recycling on the conversion of benzyl alcohol and selectivity of product benzaldehyde. Results obtained at: liquid flow rate = 1 L h^{-1}, temperature = 110 ºC, pressure = 12 bar(g), O_2 = 70 vol% in the O_2/N_2 mixture.

5.4.6 Catalysis stability assessment

Over the course of the 160 h of experimental time in the STMR, a high Turn Over Number (TON) >2600 was achieved. It was also interesting to look at the overall stability of the catalyst and the system as a whole. Figure 5.16 shows a relation between logarithmic Turn Over Frequency (TOF) [h^{-1}] and catalyst life time [h].
The TOF is calculated using:

$$\text{TOF} = \frac{C_{BH} \,.\, F_L \,.\, Mw_{Pt}}{m_{Pt}} \tag{5.3}$$

where:

TOF is the Turn Over Frequency, h^{-1},

C_{BH} is the concentration of the product benzaldehyde in the outlet of the reactor, mol L^{-1},

F_L is the volumetric liquid flow rate of the reactant, L h^{-1},

Mw_{pt} is the atomic weight of platinum, g mol^{-1}, and

m_{Pt} is the mass of metallic platinum on the catalyst, g.

The rate of catalyst deactivation is calculated (Bavykin, *el al*., 2005) using:

$$\text{TOF} = \text{TOF}_{(0)} \times e^{-kt} \tag{5.4}$$

where:

TOF is the Turn Over Frequency, h^{-1},

$\text{TOF}_{(0)}$ is the Turn Over Frequency at time zero,

k is the catalyst deactivation rate, h^{-1}, and

t is the catalyst life time, h.

Looking at Figure 5.19, the rate of catalyst deactivation was estimated to be equal to (0.0002 h^{-1}) which is a very small rate of deactivation.

There are several possible reasons for the deactivation of the platinum on carbon catalyst. These include leaching of the platinum. An Atomic Absorption Spectroscopy (AAS) test was performed on more than 80 samples and Pt was below the detectable limits of <2 ppm.

Example calculations To determine the TON, TOF, and catalyst deactivation rate (k).

No 3 (a): Turn Over Number (TON): for a Pt/C catalyst after of 160 h of operation:

$$\text{TON} = \frac{\text{mole of limiting reactant}}{\text{mole of catalyst}} \times \text{fractional conversion}$$

mole of limiting reactant (BA that was used in 160 h) = 157.03 mol
average fractional conversion = 58.2 %
mole of the catalyst (Pt) = 0.0347 mol

$$\text{TON} = \frac{157.03 \times 0.582}{0.0347}$$

$$= 2{,}634$$

No 3 (b): Turn Over Frequency (TOF): this was calculated using equation 5.3 for a feed stock of 10% vol of benzyl alcohol.

$$\text{TOF} = \frac{C_{BH} \,.\, F_L \,.\, Mw_{Pt}}{m_{Pt}}$$

C_{BH} = 0.6418 mol L^{-1}
F_L = 1 L h^{-1}
Mw_{Pt} = 195.086 g mol^{-1}
m_{Pt} = 6.78 g

$$TOF = \frac{0.6418 \times 1 \times 0.1 \times 195.086}{6.78}$$

$$TOF = 1.85\ h^{-1}$$

No 3 (c): Catalyst deactivation rate: this was calculated by plotting the relation between ln TOF *vs* t, see Figure 5.19 and equation 5.4.

In Figure 5.19, the slope is equal to -0.0002; this means that the catalyst deactivation rate (k) is equal to 0.0002 h^{-1}.

End of the Example

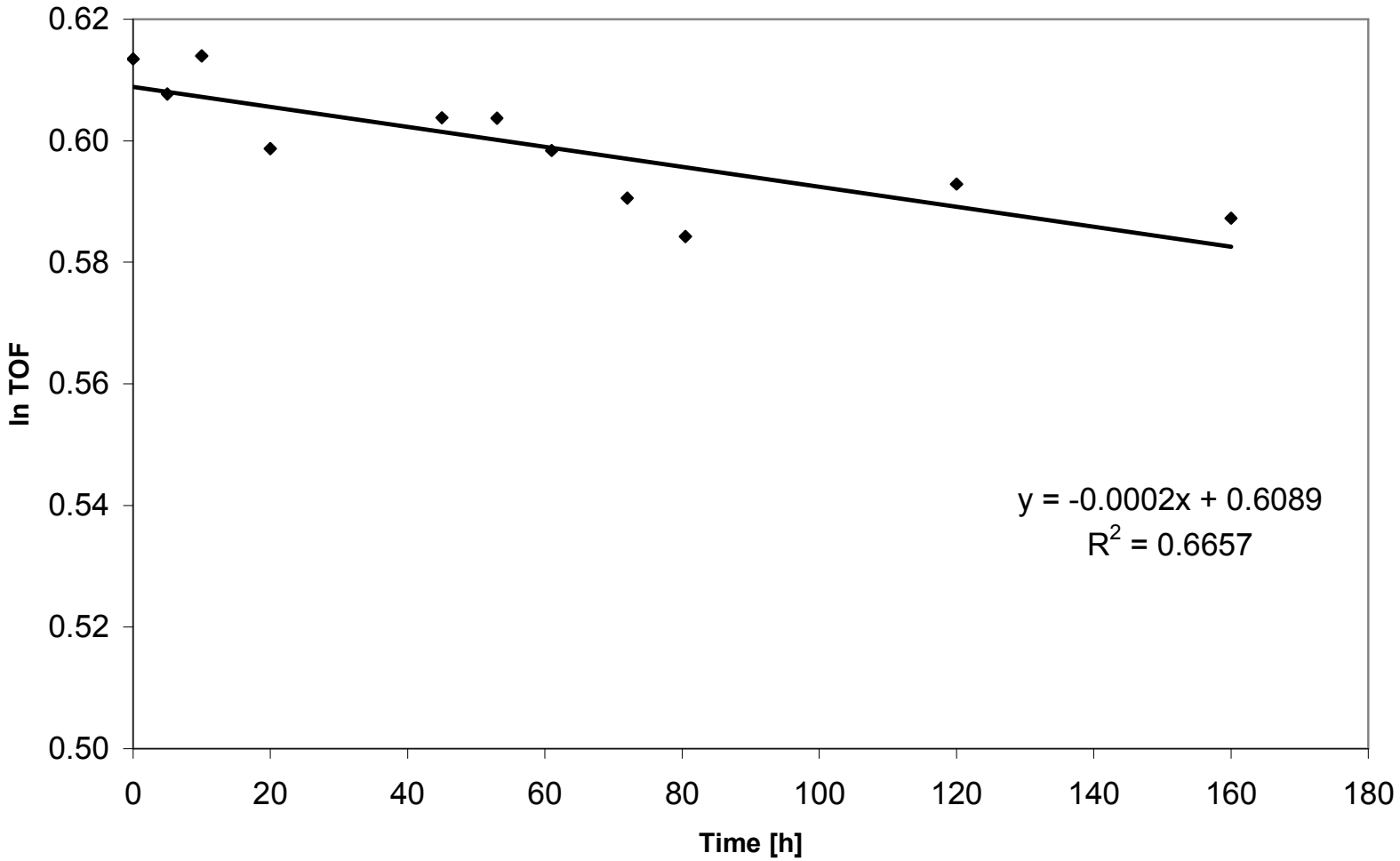

Figure 5.19: The deactivation rate of Pt/C catalyst over 160 h.

5.4.7 Gas-Liquid flow direction

It was decided to investigate the performance of the Single Tube Monolith Reactor (STMR) when the gas and the liquid were fed into the top "downward flow" rather than into the bottom "upward flow", which was used in all the previous experiments. Therefore, an experiment was performed applying downward flow at: 1 L h^{-1} of liquid, 0.818 L min^{-1} total gas, and O_2 at 70 vol% of the O_2/N_2 mixture. The results in Figure 5.20 show a dramatic drop in both conversion and selectivity in downward flow mode. They also demonstrate consistency in the data.

To explore this further, it was decided to perform some Residence Time Distribution (RTD) studies using a glass tube to represent the reactor.

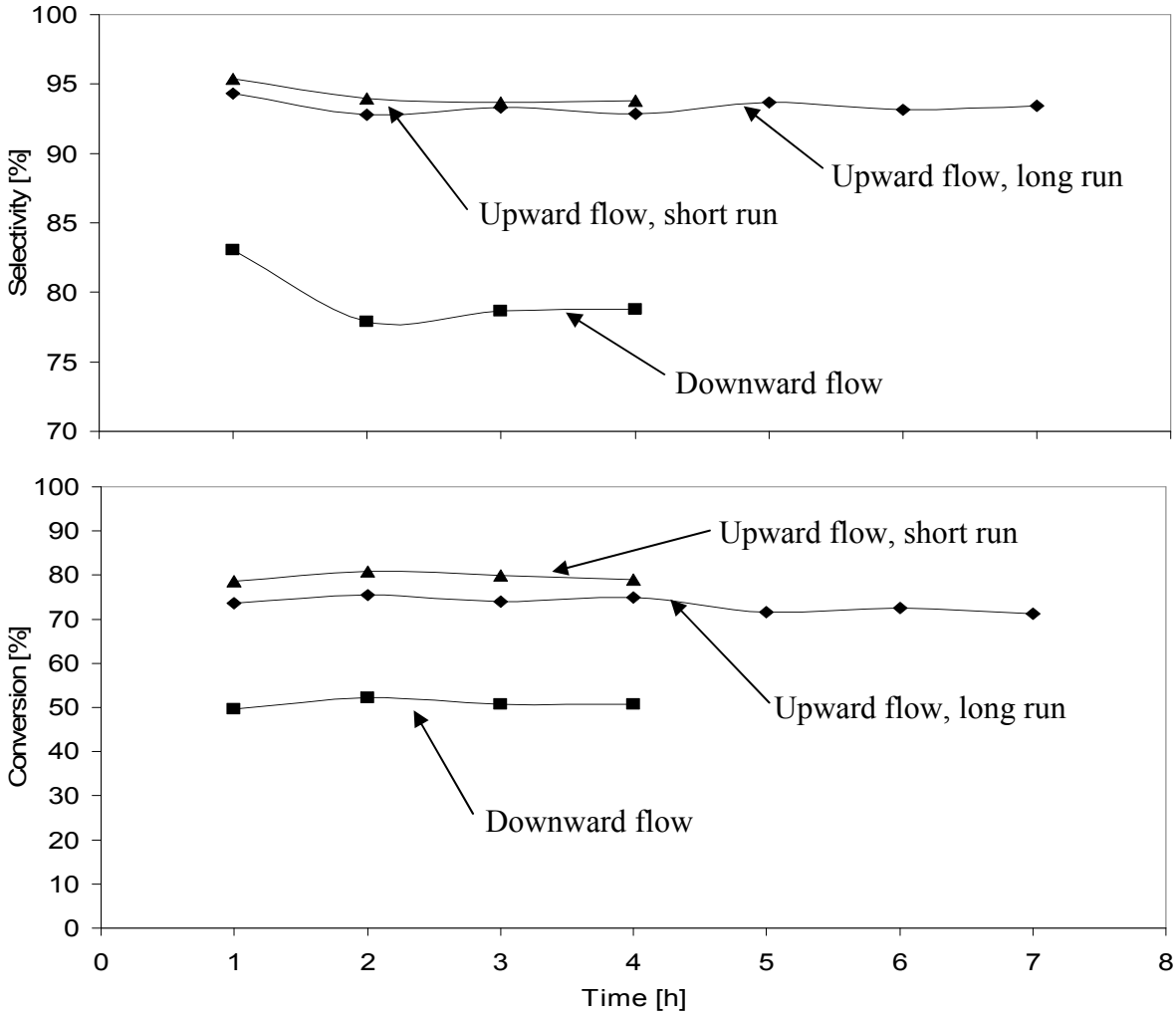

Figure 5.20: Influence of the feedstock inlet direction on the conversion of benzyl alcohol and selectivity of product benzaldehyde. Results obtained at: liquid flow rate = 1 L h^{-1}, temperature = 110 ºC, pressure = 12 bar(g), gas flow rate = 0.818 L min^{-1}, O_2 = 70 vol% in the O_2/N_2 mixture.

5.5 Residence Time Distribution (RTD) and flow visualisation

It was decided to explore further, if information could be obtained on the nature of flow in the Single Tube Monolith Reactor (STMR) during flow in the 'upward' and 'downward' directions in the reactor. So a glass tube column was used, into which the monoliths were inserted, and visual observations could also be made. The glass tube was packed with blank carbon monoliths (uncoated with catalyst). The following experimental set-ups were considered:

(a) Upward flow in a blank column.
(b) Upward flow in a monolith packed column.
(c) Downward flow in a monolith packed column.

5.5.1 Theoretical background

This is discussed in a number of classic textbooks e.g. Levenspiel (1999) and Fogler (1999). Residence time distribution (RTD) is a key tool to characterize the mixing and flow within reactors and to compare the behavior of real reactors with their ideal models. The RTD can be determined experimentally, by injecting an inert tracer into the reactor at some time t = 0 and then measuring the tracer concentration in the exit stream as a function of time.

5.5.2 Experimental set-up

Residence time distribution measurements were performed by injecting into the inlet section of the glass tube a known quantity of tracer (e.g. 5 ml of potassium chloride salt solution, at 5 mol L^{-1}) and then measuring the concentration of the tracer in the outlet stream. A schematic of the apparatus used for this experiment is shown in Figure 5.21. A metering pump (Bison Gear & Engineering Corp) was used to pump deionised water through the system. Nitrogen gas was fed into the system using a digital mass flow controller (Brooks). An inline conductivity cell was used to measure the concentration of the tracer in the outlet stream; the cell was connected to a conductivity meter (YSI 3200).

The column consisted of a 22 mm i.d. glass tube and was 700 mm high. Inside this column, 8 sections of 50 mm cylindrical monoliths were inserted, and between each pair of neighbouring monoliths, a 30 mm stainless steel spacer was inserted (see Figure 5.21), following the pattern in the STMR. Experimental conditions are summarized in Table 5.3.

To prevent the tracer from being absorbed by the carbon monoliths, the monoliths were pre-treated with a commercial sealant (Thompson‘s Water Seal brand) to seal the monolith pores. The monolith sections were soaked in a sealant solution overnight and under vacuum conditions, and then dried using a cold air blower to remove any excess solution from the channels. In order to make sure the monoliths were fully dried, they were left in the fume cupboard overnight.

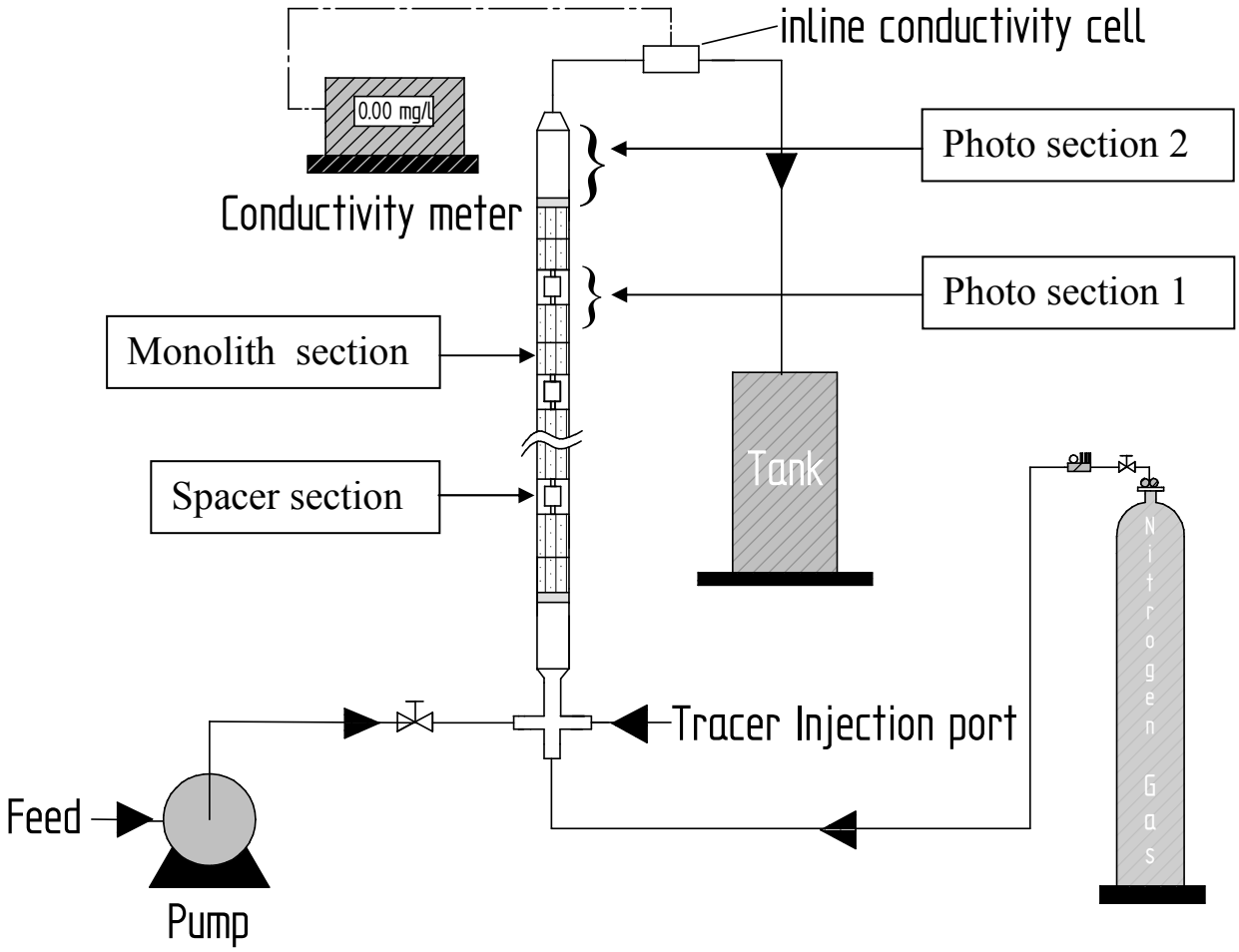

Figure 5.21: Schematic diagram of the RTD apparatus.

5.5.3 Experimental procedure for the RTD and flow visualisation experiment

The following experimental procedure was followed:

For upward flow experiments

(a) Switch on the conductivity meter.

(b) Switch on the liquid pump, and feed the deionised water from the water reservoir to the bottom of the column.

(c) Open the nitrogen gas valve and adjust the flow of gas to obtain 0.25 L min^{-1}, into the bottom of the column.

(d) Once the column was completely filled with water and gas, the liquid flow rate was adjusted using the metering pump. The outlet liquid flow rate was measured by collecting the liquid for 15 min at steady-state conditions.

(e) When the column reached steady-state conditions (constant outlet liquid flow rate), 5 ml of tracer was then injected into the inlet using a hypodermic syringe.

(f) The measurement of the outlet conductivity (concentration) was then recorded every 0.5 min until the outlet conductivity (concentration) returned to its original value.

For downward flow experiments

(a) The same sequence was followed, except that the gas and liquid were fed into the top of the glass tube.

Table 5.3: Conditions for RTD and flow visualisation experiments.

EXPERIMENT	Liquid flow rate $L\ h^{-1}$	Gas flow rate $L\ min^{-1}$	Tracer conc. $mol\ L^{-1}$	Tracer volume ml
Upward flow, blank column.	1.29	0.25	0.3	5
Upward flow, column was packed with monolith.	1.29	0.25	0.5	5
Downward flow, column was packed with monolith.	1.29	0.25	0.5	5

5.5.4 Experimental results and analysis RTD

5.5.4.1 Preliminary observations

The results that were obtained are presented in Figure 5.22 in the form of concentration *versus* time curves, otherwise known as C curves (Levenspiel, 1999).

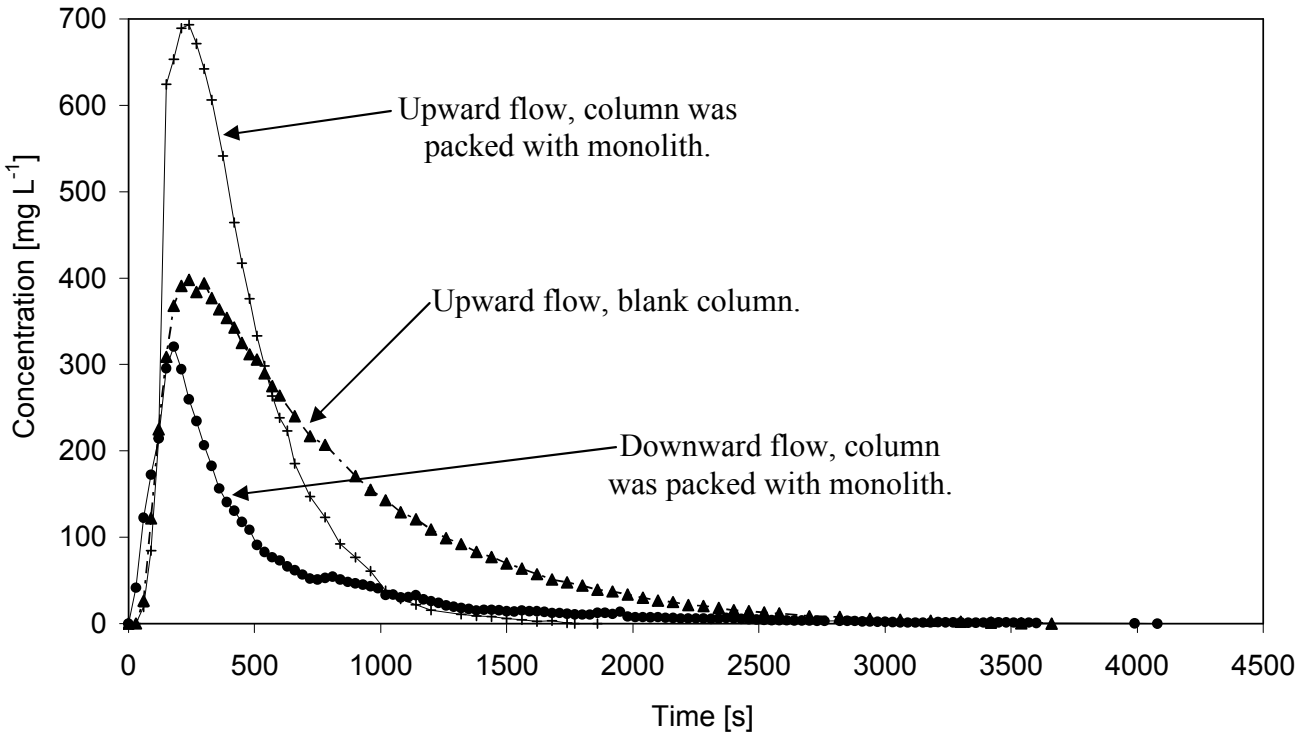

Figure 5.22: Comparison between C curves for upward and downward flow.

Mass balance on the amount of tracer: If the experiment was to prove to be useful for RTD analysis, then the amount of tracer that had been injected into the column must be close to the amount of tracer leaving the column. By looking at the areas under the individual C curves in Figure 5.22, it was suspected that that was not the case. This was confirmed, by calculating the total mass of tracer leaving the vessel, using the following equation (Fogler, 1999):

$$N_{tracer} = \int_0^{\infty} vC(t)\,dt \qquad 5.5$$

where:

N_{tracer} is the total amount of tracer in outlet stream, g,

v is the volumetric flow rate, L s^{-1},

$C(t)$ is the concentration of the outlet tracer as function of time, g L^{-1}, and

dt is the time interval, s.

This resulted in the mass balance presented in Table 5.4.

Table 5.4: Mass balance on the tracer in the inlet and in the outlet stream.

Experiment name	The amount of the tracer, mg		
	In	Out	% of the tracer detected
Upward flow in a blank column	112	120	107
Upward flow in a monolith packed column	186	110	59
Downward flow in a monolith packed column	186	51	28

From this material balance it is clear, that in the flow experiments in the blank tube, the technique worked reasonably well. However, with the carbon monoliths, the tracer was clearly being absorbed, and at a significant level making it very difficult to interpret the results from these tracer studies. Unfortunately, there was insufficient time to try to find an alternative method of sealing the carbon monolith, such that they did not retain the salt. Also, some of the salt may have been deposited on the surface of the monolith, possibly because of evaporation under the two-phase gas-liquid flow conditions. RTD is a specialist technique, and further work especially on this gas-liquid system was outside the scope of this thesis, especially as the tracer and method of analysis would probably need to be changed. Also, more work would need to be done to measure the RTD using fluids that more closely resembled the reacting environment, and this could require the development of a technique that would work even on the reactor.

Further work: It is recommended that RTD studies are performed on this system. Despite this set-back, this did provide an opportunity to make some interesting flow visualisation studies.

5.5.4.2 Visual observation

During the course of the attempted RTD experiments, photos were taken using a digital camera (set-up at in continuous shooting mode ~ 10.0 frames sec^{-1}). These shots were taken at two transparent sections of the tube, marked as: Photo section 1, and Photo section 2, in Figure 5.21.

Upward flow without monoliths: Examples of some of these snap-shots on the blank tube in upward flow are shown in Figures 5.23. The position on the photo marked as a_{S1} is before the last two monoliths, and the photo marked as a_{S2} is after the last monolith at the top of the column. Comparing this flow pattern with typical flow patterns (see Figure 5.26) in vertical tubes, it appears to correspond to “slug flow”.

Upward flow with monoliths: Examples of some of these snap-shots are shown in Figure 5.24 (b_{S1} & b_{S2}). From these it can be seen most clearly, that both the presence

of the channels in the monolith, and the holes in the spacers, are affecting the flow-pattern. This is leading to "dispersed bubble gas flow", which is clearly beneficial from a mass transfer perspective. The flow across the cross-sectional area of the tube also looks relatively uniform, without any significant channelling occurring either at the walls, or on one side of the monolith. These observations proved to be most useful.

Downward flow without monoliths: There was no point in doing these experiments, as the tube would contain either just a mist of liquid in gas, or liquid droplets falling through a flowing gas (depend on distributor). This was also not relevant to this study.

Downward flow with monoliths: Examples of some of these snap-shots are shown in Figure 5.25 (c_{S1} & c_{S2}), these two photos show a completely different type of flow pattern (than in upward flow). The column appears to be nearly empty of liquid, with a trickle of liquid on the sides of the tube, and also on the surface of the monolith. The gas is clearly pushing the liquid out of the column, and liquid hold-up in the column is low (see Figure 5.25). This helps to explain why low levels of conversion were obtained in the downward flow reaction experiments, as liquid residence time is low. The liquid also appears to be retained as a film in certain parts of the reactor, and this may also create conditions when the selectivity to form the aldehyde is reduced due to a longer residence time which might be accrued (Figure 5.22).

Further work: It was not possible to distinguish the type of flow pattern inside the monolith channels, and this is clearly something for further work together with the RTD studies.

Figure 5.23: Flow visualization for the upward flow without monoliths.

Figure 5.24: Flow visualization for the upward flow with monoliths.

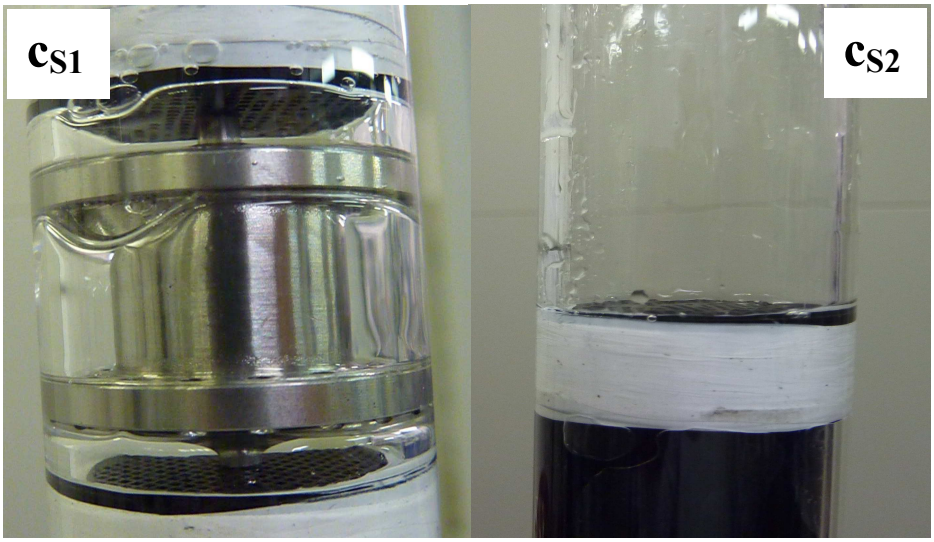

Figure 5.25: Flow visualization for the downward flow with monoliths.

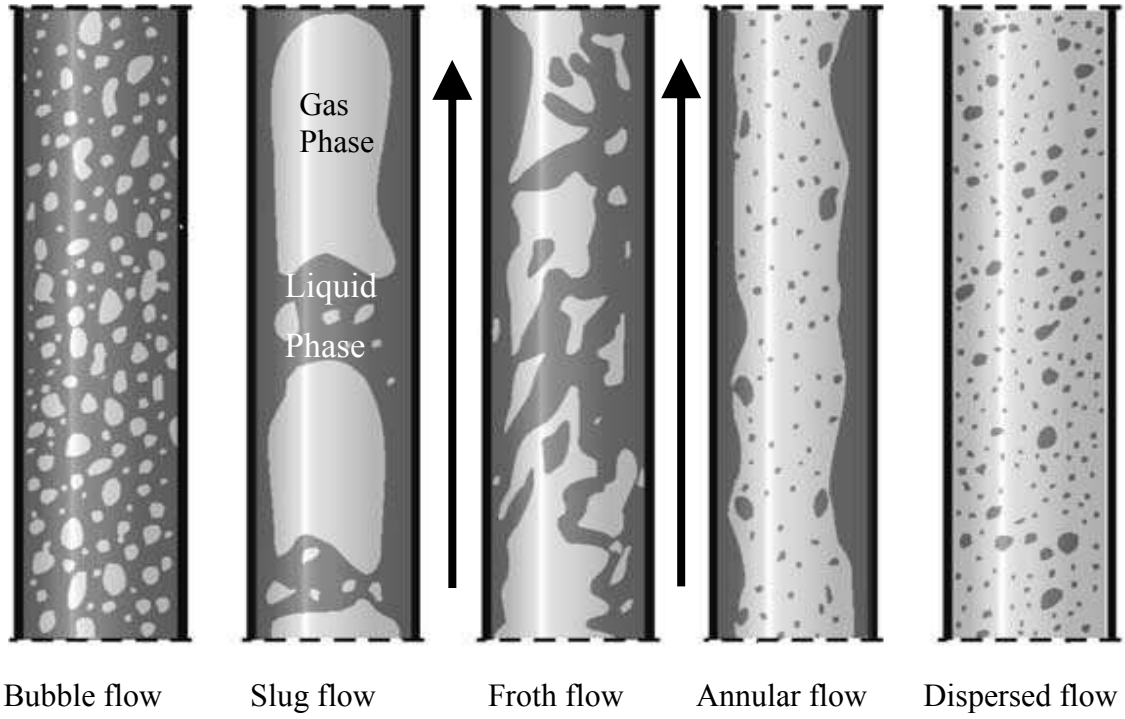

Figure 5.26: Basic flow patterns in vertical upward two phase flow system. (adapted from Dziubinski *et al*., 2004).

5.5.5 General discussion of experimental errors

In this section experimental errors are reviewed, so that their impact on the key conclusions presented at the end of this chapter may also be taken into account.

5.5.5.1 Experiments in the continuous flow STMR

Temperature: This was measured with K type thermocouples, and when measuring 110 ºC, this type of measurement is generally within ± 2.2 ºC. However, temperature would have varied between the base and the top of the reactor (along its length), and this was estimated to vary by ± 0.5 ºC. The value assigned to an experiment was based on measuring the temperature at the outer surface of the oil shell. This error would have no significant impact on the conclusions formed.

Analysis of the composition of the liquid phase: This was performed using a GC and as discussed in the pervious chapter (Example calculation No 2), the resulting errors in the values reported:

at a low conversion of 30 %, then the value could be expressed as = 30 ±2%, and
at a high conversion of 90 % then the value could be expressed as = 90 ±1%.

at a low selectivity of 60 %, then the value could be expressed as = 60 ±2%, and
at a high selectivity of 99 % then the value could be expressed as = 99 ±0.5%.

These errors would have no significant impact on the conclusions formed.

Liquid flow in the reactor: The fluid was pumped into the reactor by a positive displacement piston pump. At a prescribed setting on the pump a quantity of liquid was collected in a measuring cylinder over a known interval of time, and the liquid flow rate was calculated. For example, at a flow of 1 L h^{-1}, the error was estimated to be ±5 ml, which corresponds to ±0.5 % of the liquid flow. This would have no significant impact on the conclusions formed.

Pressure: This was measured with pressure transducers and a pressure gauge. In the early set of experiments on the STMR, the pressure was controlled in the reactor, by making manual adjustments to the needle valve on the outlet of the reactor. During these early experiments (as discussed in Section 5.3.1), while trying to maintain the

pressure constant, the pressure could vary for example from 8 to 11 bar(g). This problem was recognized, and a suitable back-pressure diaphragm valve (Tescom 44-2300 series supplied by Emerson Process) was found and installed. This was able to maintain better control over the desired set back-pressure. For example, operating at 8 bar(g), the pressure only varied by ±0.5 bar. This now has no significant impact on the conclusions formed.

Pressure drop: This was measured with a differential pressure transducer. For example, at a reading of 0.3 bar, the error was in the region of ±0.01 bar. This has no significant impact on the conclusions formed.

Gas flow: The flow of gas was controlled with a mass flow controller, and this had been calibrated at the operating conditions (see Appendix D) .
The error in flow was estimated to be: at a flow of 0.5 L min^{-1} of nitrogen, then the value = 0.5 ±0.004 L min^{-1}.
As significant amounts of excess air were used in this set of experiments, this would not have had any significant impact on the conclusions formed.

Monolith dimensions: There was a slight variation in the o.d. of the monoliths, and they were found to range from 19 to 22 mm. This was recognized, and a PTFE sleeve was used to reduce slippage at the wall (discussed in Section 5.1.4). Otherwise, this slight variation would not have had any significant impact on the conclusions formed.
Monolith length was 50 mm and varied by ±0.5 mm, again this would have little impact on final conclusions.

5.6 Pilot-scale reactor: the Radiator Monolith Reactor (RMR)

As the earlier reaction experiments in the Single Tube Monolith Reactor (STMR) had been very successful (Step 2 in the methodology, Figure 1.2), it was time to move to Step 3, and test the design at a scale more representative of pilot-plant scale.

The new design of reactor is called the "Radiator Monolith Reactor" (RMR). In the scaled-up design, the main difference is that a longer reaction zone is provided, and provision is made for the staged injection of reactants. All the other conditions and the design specifications were kept exactly the same as in STMR (e.g. size of monoliths, size of spacer, gas and liquid flow rate, temperature, feed concentration, and pressure), and this eliminates some of the uncertainty in scale-up.

Drawings were prepared for the design of the RMR by a 3rd year undergraduate Chemical Engineering student, Michael Johnston, who joined this PhD project for a short 9 week long research project. Then the designed RMR was manufactured by S&C Thermofluids Ltd.

In the section that follow:

- A detailed description is provided of the RMR.
- Experiments are then performed using the same catalyst and the same overall length of catalyst (18 monoliths, total catalytic bed length = 900 mm) to compare the performance of the RMR with the STMR.
- Results are then presented on the performance of the RMR with a longer catalytic bed (50 monoliths, total catalytic bed length = 2,500 mm).

5.6.1 Key design features in the RMR

The design evolved from the Single Tube Monolith Reactor (STMR), and the following key features were included into the design:

(a) The internal diameter of the reaction section in the RMR was maintained the same as the STMR, and the same size of carbon monolith was used.

(b) The overall catalytic bed length of the reactor was extended, so that high conversions could be achieved. This was an important consideration, and one that in the earlier European funded project, GSK said was an important requirement in order to demonstrate the viability of continuous flow reaction technology. GSK said that it was better to convert all of the benzyl alcohol into product (and even the by-product), rather than having to separate the benzyl alcohol from the finished product. So a design of reactor, in which high conversion (close to 99%) can be demonstrated in a once-through system, was an important objective.

(c) If operation at higher flow was required, then to ensure that the RMR reactor could be scaled-up easily, the number of RMR units would be increased, rather than increasing the cross-sectional area (i.e. diameter of monolith) of the reaction tube containing the monoliths.

(d) To ensure the catalyst section could be easily removed or replaced from the reaction tubes. This was a very important practical consideration. This is one of the reasons why the overall length of individual reaction tubes in the RMR was kept relatively short (about 600 mm).

(e) To be able to inject gas at various positions along the length of the reactor. In earlier work at the University of Bath, it was shown in Bavykin *et al*., (2005) that staged injection of oxygen was beneficial, as higher conversion can be achieved in the same overall length of catalyst bed.

(f) As a research tool, in this pilot-scale reactor it would be good to be able to take samples at different positions along the length of the reactor. Then the progress of the reaction can be monitored, as the effect of key variables is explored.

(g) As the overall length of the catalytic sections is extended, it is also important to ensure that isothermal conditions are maintained along the length of the reactor. That is why the outside of the reaction tubes was surrounded by a flowing heat transfer fluid. A heat transfer fluid was used rather than external electrical

heating, as heat transfer fluids are already used to heat and cool reactors in pharmaceutical plants. This is a safer option of heat transfer.

(h) As a research tool, and even when operating as a pilot-scale reactor, some flexibility in use was important e.g. ability to perform experiments in a shorter overall length of catalytic bed.

(i) It was necessary to provide easy access to the fittings on the reaction tubes, so that the catalytic monoliths could be easily inserted, and that the gas and liquid feed and exit ports on the reactor could also be easily fastened and disassembled. This all required some careful consideration. Also the need to use heavy lifting equipment to perform such basic operations was to be avoided, and this was a key design feature.

5.6.2 Description of the RMR

The RMR unit consisted of 10 catalytic tubes, which were welded inside a stainless steel frame, see Figure 5.27. At either end of each catalytic tube, there were male hexagonal plugs (¾" BSP), which enabled the carbon monoliths to be inserted or removed. At either end of each tube, there was a port on the side of the tube through which the fluid/gas could enter.

The catalytic tubes were made from stainless steel tube (22 i.d., 560 mm length, 2.5 mm wall thickness). The length of the reaction section enabled various combinations of monoliths and spacers to be installed (e.g. 7 monoliths × 50 mm long, with 6 spacers). The monoliths were held in position at either end by a stainless steel spring (supplied by Flexo Springs Ltd).

The catalytic tubes were contained within a metal plate box frame forming a rectangular shape, through which the heat transfer fluid flowed, and this acted just like a heat exchanger, see Figure 5.28.
The design information on the RMR is summarized in Table 5.5.

Fluid flow: The gas and liquid were first fed into the bottom (*via* the side) of the first reaction channel, and then the liquid/gas would flow upwards through the catalytic bed of monoliths. From the side at the top of the first channel, the fluid flowed *via* a ¼" stainless steel tube into the bottom of the neighbouring reaction tube. This was then repeated, depending on the number of tubes that were being utilized. This arrangement is shown in the left-hand photo in Figure 5.29, for a reaction system which is making use of 3 catalytic tubes. This configuration could be varied, and experiments could be performed in any combination of catalytic tubes from 1 to 10.

On the sides, at the top and bottom of the reaction tubes, were cross-shaped fittings, which could be used for the staged injection of reactant(s), or local sampling.

Heat transfer oil (glycerol) was circulated through the shell-side of the RMR *via* a 2×2 kW heated oil bath. The oil was pumped with a Weldon 9200-A high temperature oil transfer pump (supplied by Demon Tweeks), which had a maximum flow rate of 8 L min^{-1}, a maximum supply pressure of 4 bar(g) and a max operating temperature of 150 ºC.
Different views of the RMR are shown in Figures 5.29.

General views: In Figure 5.30, a general view of the RMR is provided in its operating position inside the walk-in fume cupboard. On the left, is a PC and this was used to view much of the data that was measured. An example view of the screen during an experiment is shown in Figure 5.31. Data was obtained making use of LabView 7.1, and this was arranged by the author. On the screen:

- temperatures were measured at key positions using K type thermocouples, and their readings were displayed on the screen,
- the flow of gas and the ratio of oxygen to nitrogen was controlled, and
- the operating pressure and the overall pressure drop were displayed.

Safety considerations:

- Prior to start-up, the reactor was purged with nitrogen using the gas feed lines.
- The feed supply tank to the reactor and also the product tank were both purged with nitrogen.

- A small purge of nitrogen was also supplied into the vent line from the product feed tanks. This was to ensure that as the liquid was pumped from the supply tank, then nitrogen occupied the void space formed in the tank.
- After the reactor had been brought up to its operating temperature (e.g. 110 ºC, using the heat transfer oil), then a flow of nitrogen was set in the gas feed line(s) to match the total gas flow that was required at that point.
- Nitrogen was also fed into the line at the outlet of the reactor, so as to reduce the concentration of oxygen in the gas leaving the reactor.
- An in-line gas analyser (Kane 400 Combustion Gas Analyser) was used to estimate the oxygen concentration in the vent line that discharged the gas into the fume cupboard. As nitrogen was added at various stages to purge the lines, then this provided a good indication that the oxygen content was being reduced in the vented gas. This provided more of a qualitative indication of oxygen concentration, rather than a quantitative one.
- Cooling water was turned on, to cool the two phase gas/liquid mixture leaving the reactor down to a temperature of about 20 ºC.
- Then the liquid feed pump, a single acting plunger pump fitted with a pulsation damper was turned on, and this supplied the benzyl alcohol solution into the base of the reactor. The pump was Bison Gear & Engineering Corp. with max pressure 56 bar(g) and 6.24 L h^{-1} , supplied by Cole-Parmer.
- The pressure in the reactor was controlled with a Tescom (44-2300 series) back-pressure valve supplied by Tescom Corporation UK.
- After a period of 15 min, the supply of gas to the catalytic stage(s) was gradually adjusted, so that the appropriate ratio of oxygen and nitrogen was fed into the reactor (e.g. to achieve 100 vol% oxygen, or 70 vol% oxygen).
- From the top of the reactor, the two-phase gas/liquid mixture flowed though a water cooled tube, and then to a gas-liquid separator. From the separator, the liquid was fed by gravity into a sealed and vented storage tank, *via* a dip tube to the bottom of the tank, and below a liquid seal to avoid splashing.
- Two pressure safety valves were installed in the rig. The first safety valve was installed before the reactor and it is outlet was connected to the feed stock tank and the second safely valve was installed after the reactor and it is outlet was connected to the waste tank.

-

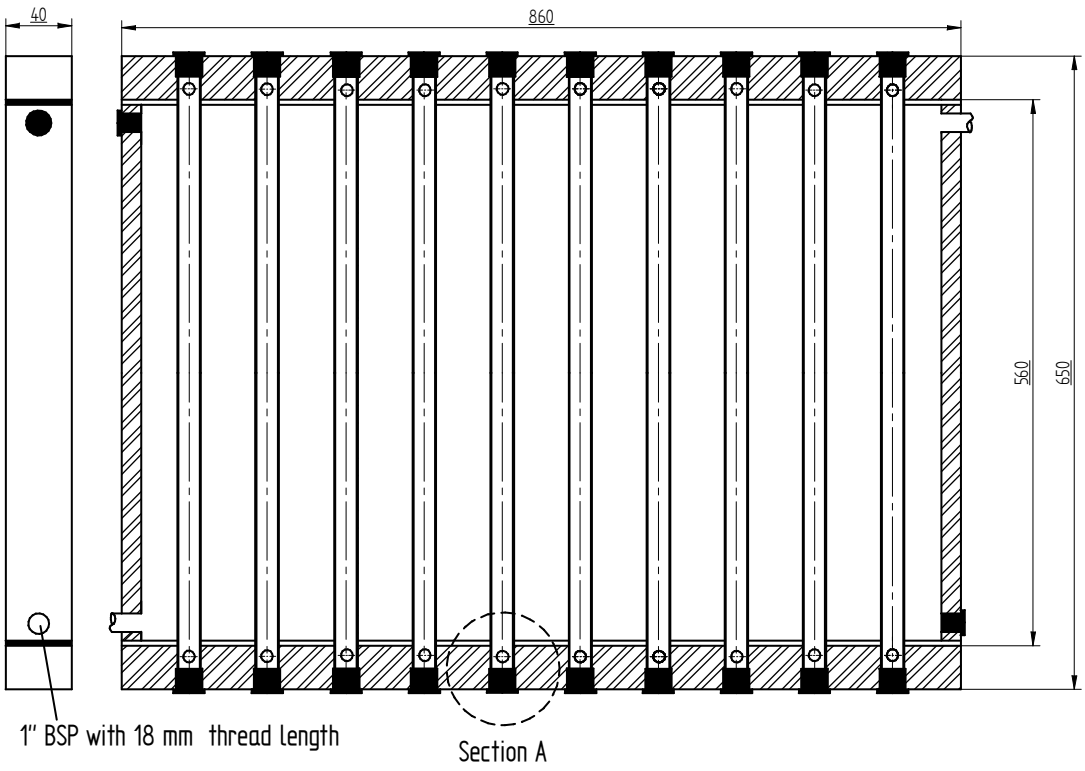

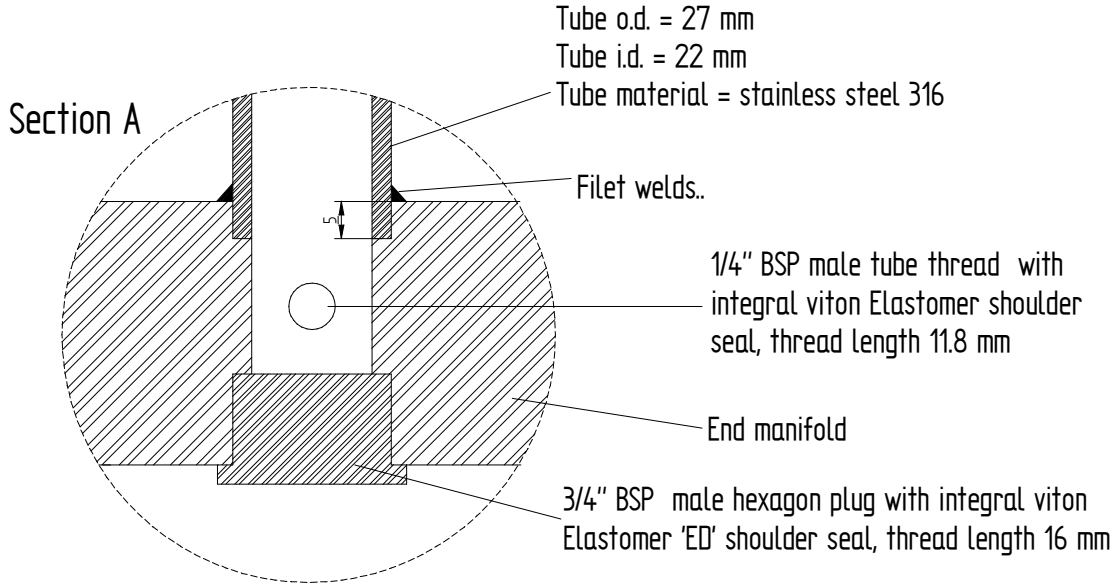

Figure 5.27 Schematic of the RMR.

Table 5.5: Design information on the RMR.

Item	Description	Range or value
1	Design pressure (reaction tube):	20 bar(g)
2	Design Temperature:	150 ºC
3	Pressure control valve (max pressure 24 bar(g))	Set to operate between: 1 to 15 bar(g)
4	Reaction tube wall thickness:	2.5 mm
5	Volume of single reaction tube:	0.235 L
6	Pressure classification of single reaction tube:	4.7 bar.L @ 20 bar(g)
7	Ratio between i.d. and wall thickness of reaction tube:	8.8 (this is classified as a thick wall pressure vessel, Sinnott (2005))
8	Overall external dimensions: length x height x width:	860 mm x 650 mm x 40 mm
9	Weight of RMR empty:	45.3 kg
10	Weight of RMR with heat transfer fluid:	60 kg
11	Volume of heat transfer fluid:	13.0 kg

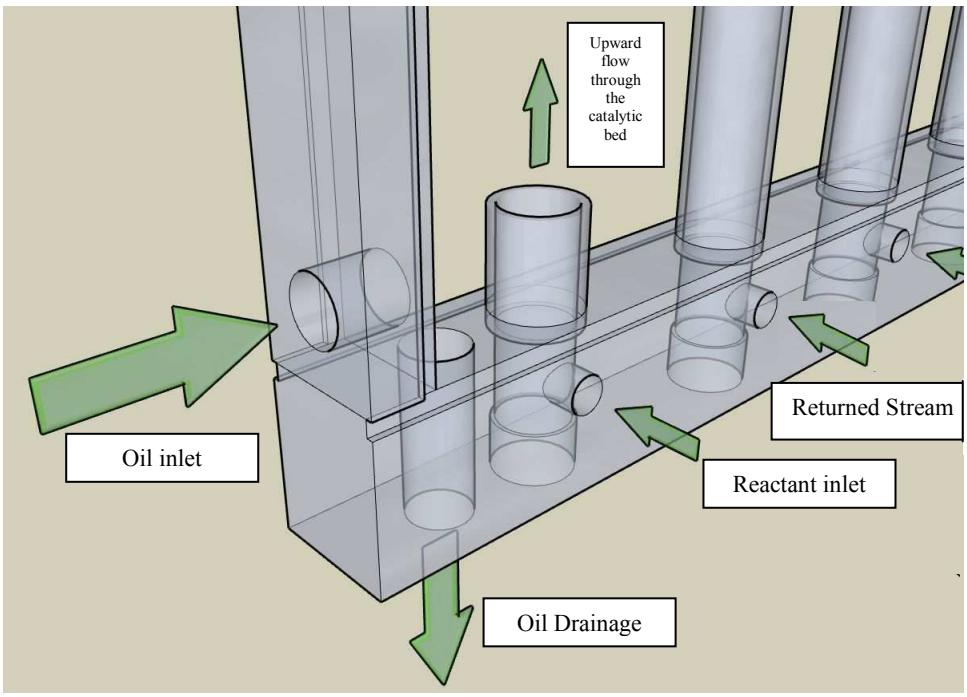

Figure 5.28: 3D drawing of the RMR.

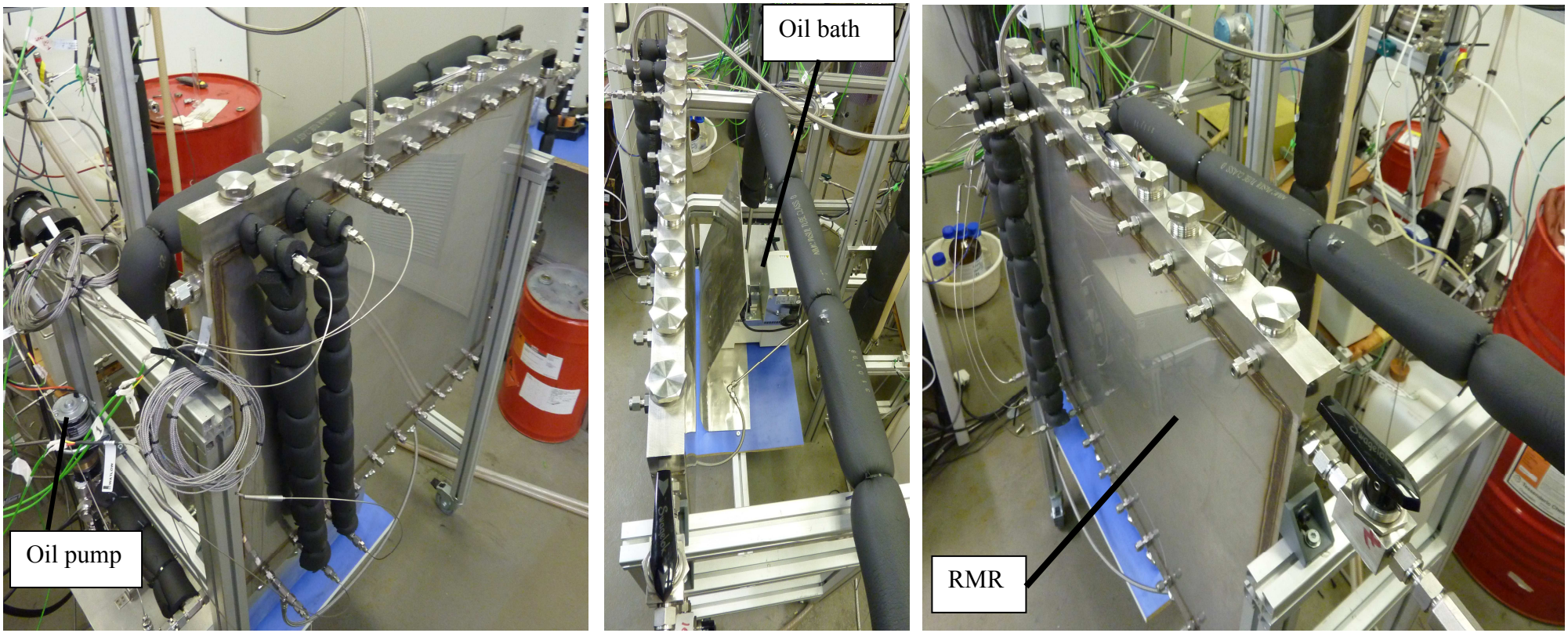

Figure 5.29: Different views of the RMR.

Figure 5.30: The pilot-scale rig showed the RMR.

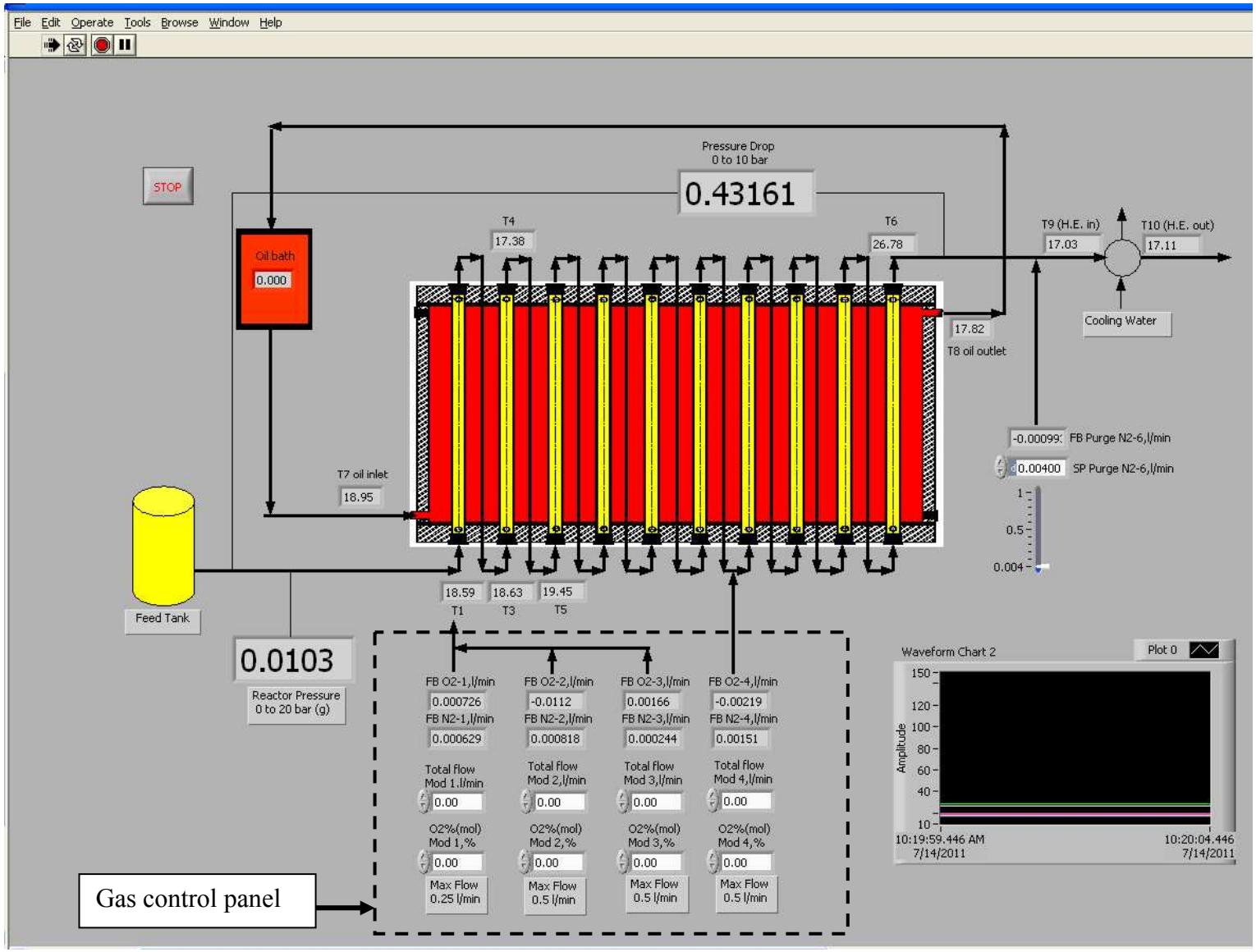

Figure 5.31: View of screen on Pc, using LabView 7.1 to monitor and control the RMR.

5.6.3 Experiments on the RMR to compare performance with STMR

In order to compare the performance of the RMR with the STMR, two different sets of experiments were performed:

(a) **First set:** In these the catalyst was removed from the STMR, and then it was inserted into the RMR. This ensured that exactly the same form of catalyst and the same overall length of catalyst (18 monoliths, total catalytic bed length = 900 mm) was used. As a reminder, the catalyst loading was about 2.7 wt% Pt, and this catalyst had already been in use for 160 h. This test was also selected, to ensure that by putting the catalyst into 3 shorter tubes in the RMR (rather than one long tube in STMR), that the overall performance in terms of conversion and selectivity would not change.

(b) **Second set**: In these, the old coated monoliths were removed, and 18 sections of Pt coated carbon monoliths from a freshly prepared batch were inserted into the RMR. The Pt loading for this batch of catalyst was measured to be about 2.5 wt% Pt, and this was slightly lower than that used in the first set of experiments. However, the same number of monoliths was used as in the first set.

Experiments were then performed over the following set of conditions:

(a) Liquid flow rate = 1.0 L h^{-1}.

(b) Total gas flow rate = 0.818 L min^{-1}.

(c) The oxygen concentration in the O_2/N_2 gas mixture was:

(i) 70 vol% (corresponding to 221% excess oxygen), and

(ii) 100 vol% (corresponding to 359% excess oxygen).

(d) The backpressure on the reactor was set at = 12 bar(g).

(e) Operating temperature = 110 ºC.

(f) The concentration of feed stock was 10 vol% of benzyl alcohol dissolved in a solvent of 90% dioxane and 10% water. This corresponds to approximately

1 mol L^{-1}, a concentration that was known to be of interest to the pharmaceutical industry (based on discussions with GSK).

(g) After the reactor reached its operating temperature and pressure, and being fed with the reactants, a period of 2h was allowed for the reactor to reach steady-state conditions before any samples were taken. These samples were then analyzed using the GC.

The results of these experiments are presented in Figure 5.32 (for the 70 vol% oxygen gas feed), and in Figure 5.33 (for the 100 vol% oxygen gas feed). From the pair of bar charts on the left and middle in Figure 5.32, it is very clear that a good match is obtained when exactly the same catalyst was used in the two different reaction systems. The same applies when the data in Figure 5.33 is considered, when 100 vol% oxygen was used in the gas feed. This is very encouraging, as it shows that the way in which the single long catalytic tube in the STMR, had been split into 3 shorter tubes in the RMR, had not affected the performance of the reactor - neither the conversion nor the selectivity had been changed.

Next, to compare the performance of the used and fresh batch of catalyst, the pair of bar charts on the right and middle in Figures 5.32 and 5.33 are compared. From these it is clear that there is a slight reduction in conversion, but also a small increase in selectivity. The slight reduction in conversion is not surprising; as the catalyst loading was slightly lower (i.e. 2.5 *versus* 2.7 wt% Pt). This slight variation was not of any concern.

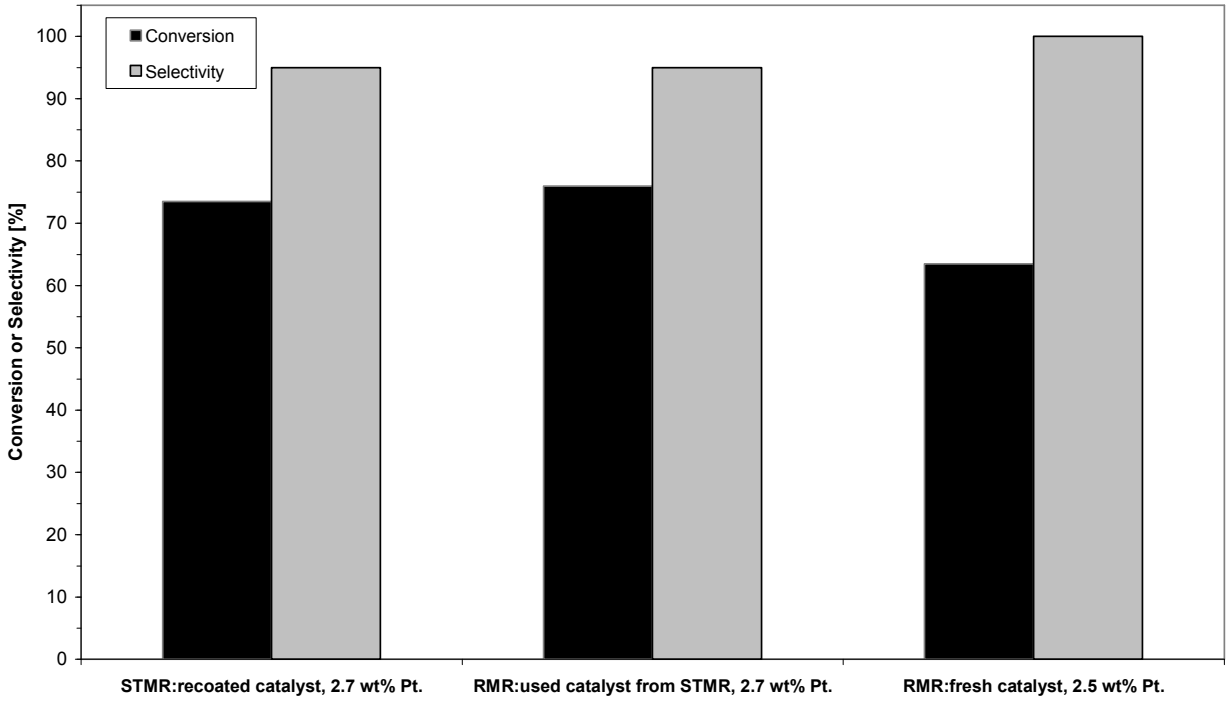

Figure 5.32 Comparing performance of the STMR and RMR. Results obtained at: liquid flow rate = 1 L h^{-1}, gas flow rate = 0.818 L min^{-1}, O_2 in the gas feed = 70 vol%, temperature = 110 ºC, pressure = 12 bar(g).

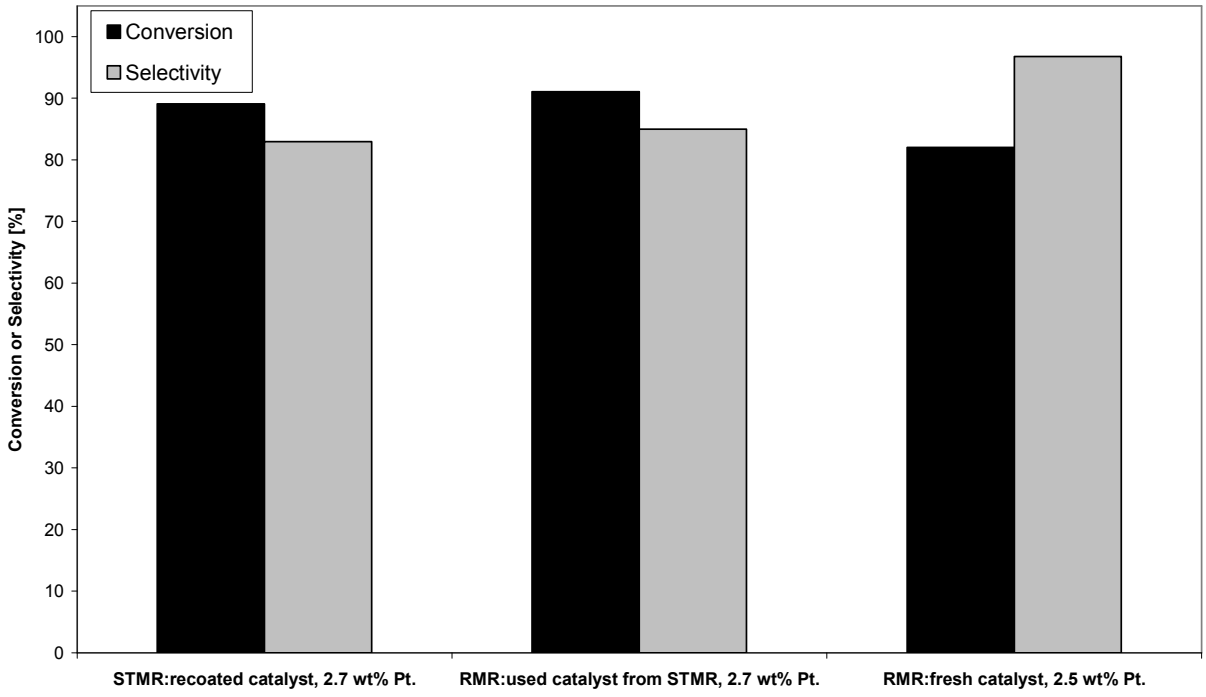

Figure 5.33 Comparing performance of the STMR and RMR. Results obtained at liquid flow rate = 1 L h^{-1}, gas flow rate = 0.818 L min^{-1}, O_2 in the gas feed = 100 vol%, temperature = 110 ºC, pressure = 12 bar(g).

5.6.4 Experiments on the RMR with a longer catalytic bed

For this set of experiments, freshly prepared catalyst was used and a total of 50 monoliths were required. This quantity was prepared in two batches of 25 monoliths using the same method that had been described earlier in Section 5.2.1. The average platinum loading for these two batches was = 2.5 wt% Pt .

For the experiment with the 50 monoliths this filled 8 of the 10 catalytic tubes, so there were still two spare catalytic tubes in the RMR.

Oxygen concentrations: In this section, experiments were performed with a 70 vol% and a 100 vol% oxygen in the gas feed.

Multi-stage sampling: Three sampling points were installed along the reactor:

(a) the first sampling point was after 18 sections of monolith (only used when steady-state conditions are reached),
(b) the second sampling point was after 32 sections of monolith (only used when steady-state conditions are reached), and
(c) the last sampling point was after the last monolith (50^{th}).

Experiments with <u>70 vol%</u> oxygen in the gas feed: During the course of the experiment, in the first 140 minutes (min), samples were taken every 20 min, but just from the outlet stream (after 50^{th} monolith). These results are shown in Figure 5.34 a. As expected, the conversion is seen to increase with time as the reactor approaches steady-state conditions after 100 min of operation. After 120 min, the conversion was 89%. It is interesting to note, that as soon as the reactant starts to become converted (e.g. data point at 40 min), the selectivity is high and remains so (close to 100%)

At the end of the 140 min steady-state conditions were clearly reached, so samples were then taken from the intermediate sampling points (after 18^{th} and 32^{nd} monoliths). These results are shown in Figure 5.34 b. These results are consistent with what had been observed when the fluid was recycled in the STMR (to explore if higher conversions could be achieved). As expected, as the conversion of benzyl alcohol decreases along the length of the reactor, the rate of reaction decreases and this is consistent with the

form of rate expression determined in Chapter 4. Nevertheless, this was a very exciting achievement, as it was shown that when steady-state conditions are reached, high conversion (89.3% after 120 min) and a high selectivity (100% after 120 min) can indeed be obtained in this type of reactor. As a reminder, as discussed earlier, this was seen as a key test that that had to be demonstrated, if a company like GSK was to take more of a serious interest in this approach. From the shape of the data in Figure 5.34 b, it is also very likely that with a longer length of reactor, then a higher conversion could be achieved.

Also, it is useful to note from an operational point of view that at these test conditions, the reactor reached steady-state conditions relatively quickly, and only 2.0 litres of solution (20 ml of benzyl alcohol) would need to be diverted to a waste tank, before useful product was formed. Pharmaceutical reactants can also be very expensive, especially if they contain the API, so this is an important factor in reactor design.

Experiments with <u>100 vol%</u> oxygen in the gas feed: The same experimental procedure was followed (as for 70 vol% oxygen), and the results are shown in Figure 5.35 a and Figure 5.35 b.

Looking at the conversion data in Figure 5.35 a, it is clear that with the higher concentration of oxygen in the gas feed, then higher conversions were achieved (93.6% after 140 min), however, the selectivity decreased down to 57% (after 140 min) due to the formation the acid. The data in Figure 5.35 b, shows the expected trend along the length of the reactor, however, it appears that a longer length of catalytic bed may not provide any significant benefits in terms of conversion as the conversion increases significantly between the entrance of the reactor and the 32 monoliths section however small value of conversion (e,g, 10% in Figure 5.34 b) was seen between the 32 monoliths and 50 monoliths (final product).

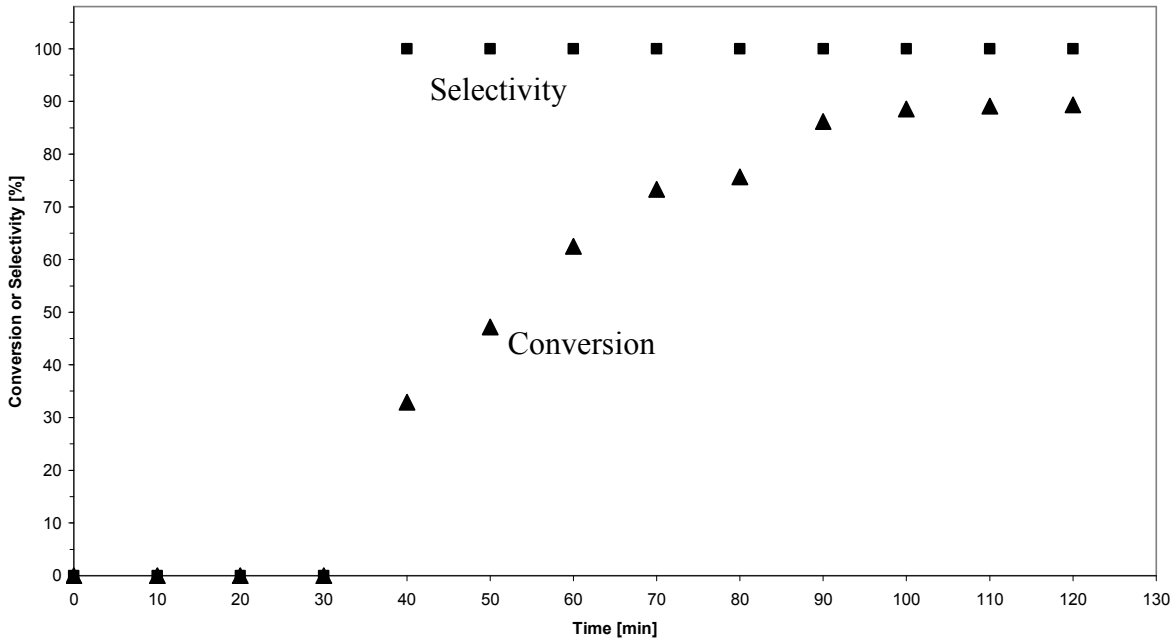

Figure 5.34 a: Conversion and selectivity *vs* time in RMR. Results obtained at liquid flow rate = 1 L h^{-1}, gas flow rate = 0.818 L min^{-1}, O_2 in the gas feed = 70 vol%, temperature = 110 ºC, pressure = 12 bar(g).

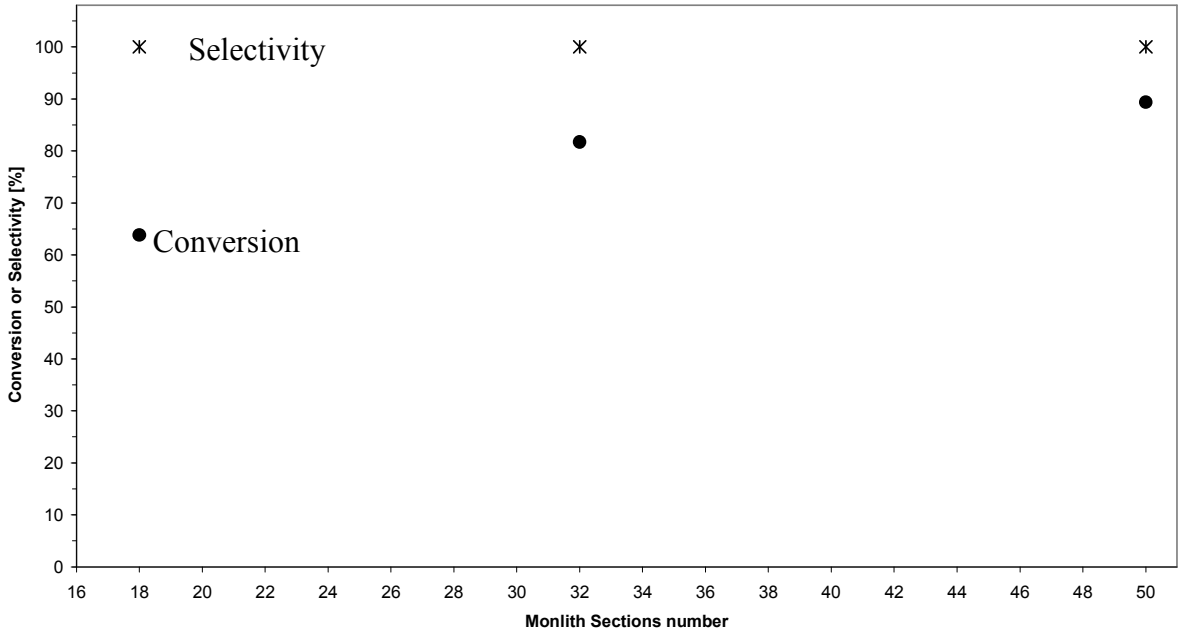

Figure 5.34 b: Conversion and selectivity at three different positions a long side the RMR. Results obtained at liquid flow rate = 1 L h^{-1}, gas flow rate = 0.818 L min^{-1}, O_2 in the gas feed = 70 vol%, temperature = 110 ºC, pressure = 12 bar(g).

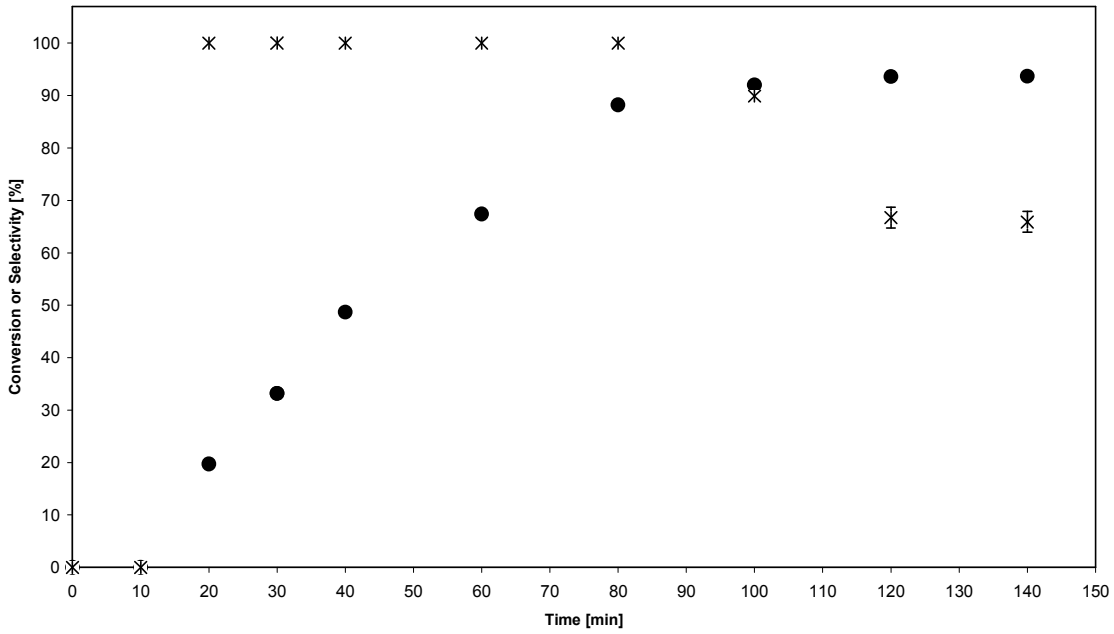

Figure 5.35 a: Conversion and selectivity *vs* time in RMR. Results obtained at liquid flow rate = 1 L h^{-1}, gas flow rate = 0.818 L min^{-1}, O_2 in the gas feed = 100 vol%, temperature = 110 ºC, pressure = 12 bar(g).

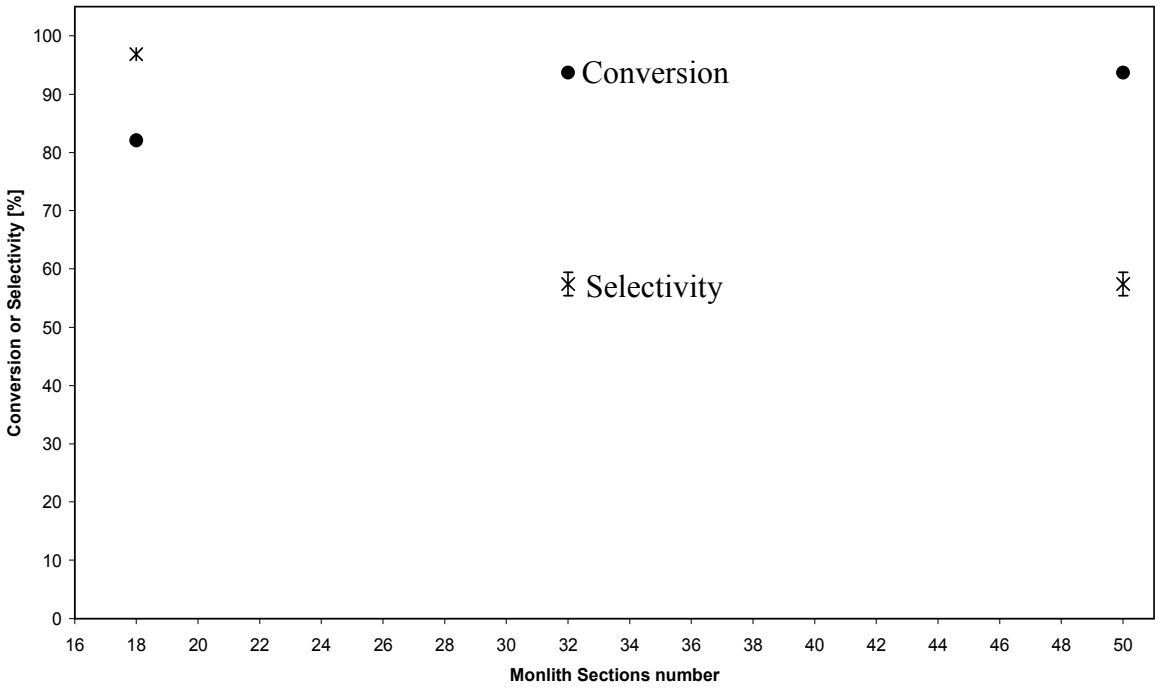

Figure 5.35 b: Conversion and selectivity at three different positions along the RMR. Results obtained at liquid flow rate = 1 L h^{-1}, gas flow rate = 0.818 L min^{-1} , O_2 in the gas feed = 100 vol%, temperature = 110 ºC , pressure = 12 bar(g).

5.6.5 Experiments on the RMR with a longer catalytic bed and staged injection

To illustrate the benefits of gas injection along the reactor, this technique was tried on the RMR, by injecting gas at two positions as follows:

(a) The first injection port was at entrance to the 1st monolith.

(b) The second inject port was after the 25th monolith.

Experiments with <u>70 vol%</u> oxygen in the gas feed: The flow rate of gas at each injection port is illustrated in Table 5.6. Two experiments were performed (Case 1 and Case 2) and the results are compared in Figures 5.36 and 5.37, and also with earlier data obtained during a single point of gas injection (from Figure 5.34).

Table 5.6: Gas flows at the injection ports (with 70 vol% oxygen in the gas feed).

	Injection Port 1	**Injection Port 2**	**Total**
	entrance to 1st monolith	after 25th monolith	Port 1 + Port 2
	Gas flow (L min^{-1})	Gas flow (L min^{-1})	Gas flow (L min^{-1})
Case 1:	0.5 (61% of flow)	0.318	0.818
Case 2:	0.318 (39% of flow)	0.5	0.818

In Figure 5.36 it is clear that in Case 1, higher levels of conversion are achieved along the length of the reactor and a final exit conversion of 95% was achieved. In Case 2, the final exit conversion was 91%, which was close to the single point injection outcome (89%).

The selectivity in Case 1 and also in Case 2 decreased to ~ 55 Figure 5.37. This had also been shown earlier in Figure 5.35 a, so this is not surprising.

In conclusion, the main advantage from this short set of experiments was the benefit of being able to push the reaction to a higher conversion, with a shorter length of reactor.

This is consistent with the findings in Bavykin *et al*., (2005), but this has now been shown:

- on a pilot-scale reactor,
- at high conversions,
- and using monolith catalysts,

as opposed to an experimental laboratory bench top reactor using powdered catalyst.

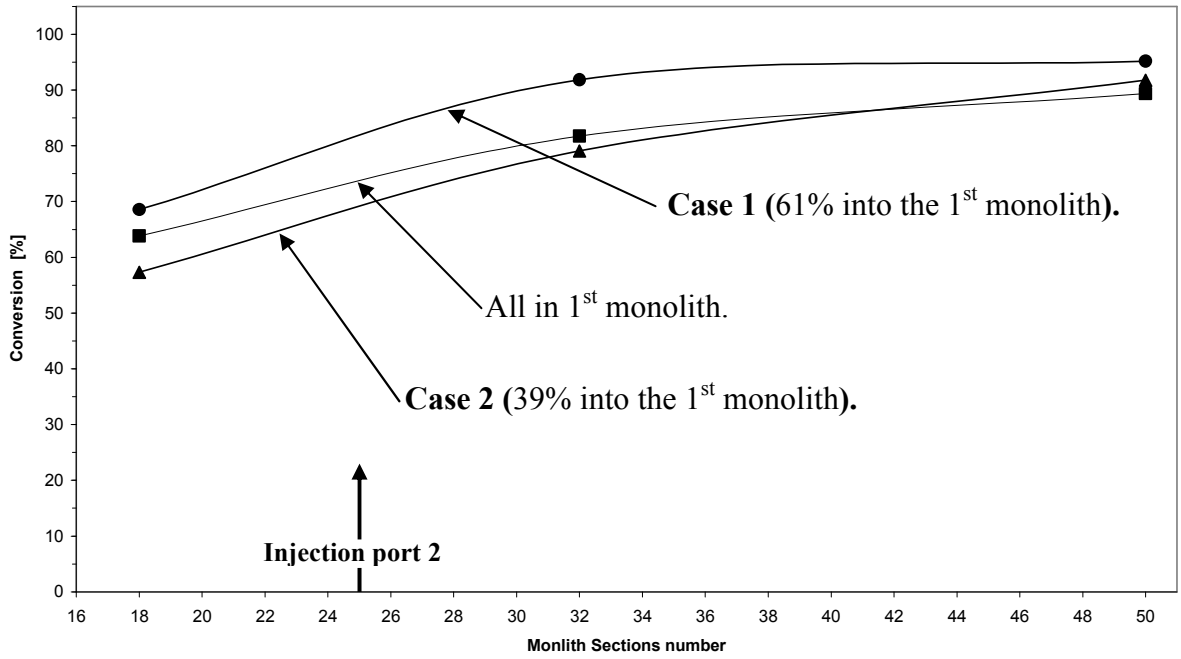

Figure 5.36: Conversion at three different positions along the RMR. Results obtained at liquid flow rate = 1 L h^{-1}, gas flow rate = 0.818 L min^{-1}, O_2 in the gas feed = 70 vol%, temperature = 110 ºC, pressure = 12 bar(g).

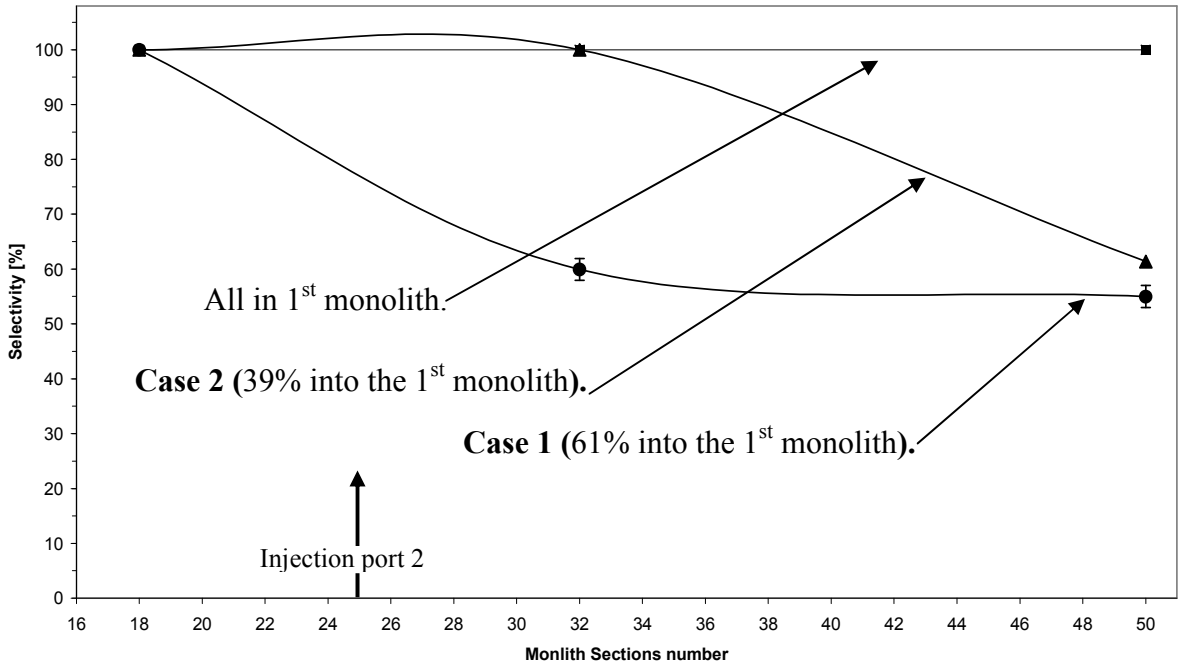

Figure 5.37: Selectivity at three different positions along the RMR. Results obtained at liquid flow rate = 1 L h^{-1}, gas flow rate = 0.818 L min^{-1}, O_2 in the gas feed = 70 vol%, temperature = 110 ºC, pressure = 12 bar(g).

5.6.6 Test for catalyst leaching

Samples were taken from the reactor(s) and tested for catalyst leaching using Atomic absorption spectroscopy (AAS). During the course of experiments in the STMR and RMR, a total 90 samples were tested, and Pt could not be detected (detection limit of 2 ppm).

5.6.7 Pressure drop across the RMR

Across catalytic section: Throughout the experiments, the pressure drop across the catalytic tubes in the RMR remained relatively low and steady during the various experiments. For example, in experiments with 50 monoliths and 60 spacers, using 8 catalytic tubes, the maximum pressure drop was 0.3 bar. This was a great achievement, as pressure drop was the main reason why the earlier attempts (in the EU project) of using powdered catalysts in a fixed bed pilot-scale reactor had failed.
The earlier problems identified at the start of this PhD work which had been suspected of causing the excessive pressure drop build-up, had clearly now been overcome.

Across heating oil side: As illustrated in Figure 5.39, heating oil was pumped into the outer casing of the RMR *via* the side port (valve 1). Two ½" ports were used to return the circulated oil to the heating oil bath. The pressure in the oil loop was measured using a pressure gauge.

Two different start-up procedures were tried and these are summarized in Table 5.7.

Procedure (1): Using this method, the maximum pressure reached 0.4 bar(g), with a steady-state pressure of 0.3 bar(g). However, this took 2 h to reach steady-sate conditions.
Procedure (2): Using this method, the maximum pressure reached 2.9 bar(g), with a steady-state pressure of 0.5 bar(g) after 1 h of operation.

Although 1 h can be saved using Procedure 2, the peak pressure of 2.9 bar(g) is too high for a commercial application, as it will increase the capital cost of the reactor (thicker outer plates to contain the oil around the reaction tubes). It was also observed, that at the end of the experiments with the RMR that the tubes had been slightly bowed, and the outer plates had also been bowed under the forces that resulted from higher pressures on the oil side. This aspect is now being investigated further, and it was decided to cut the existing RMR in half, to make two smaller RMRs with 5 reaction tubes (instead of 10) in each unit. This is now being implemented.

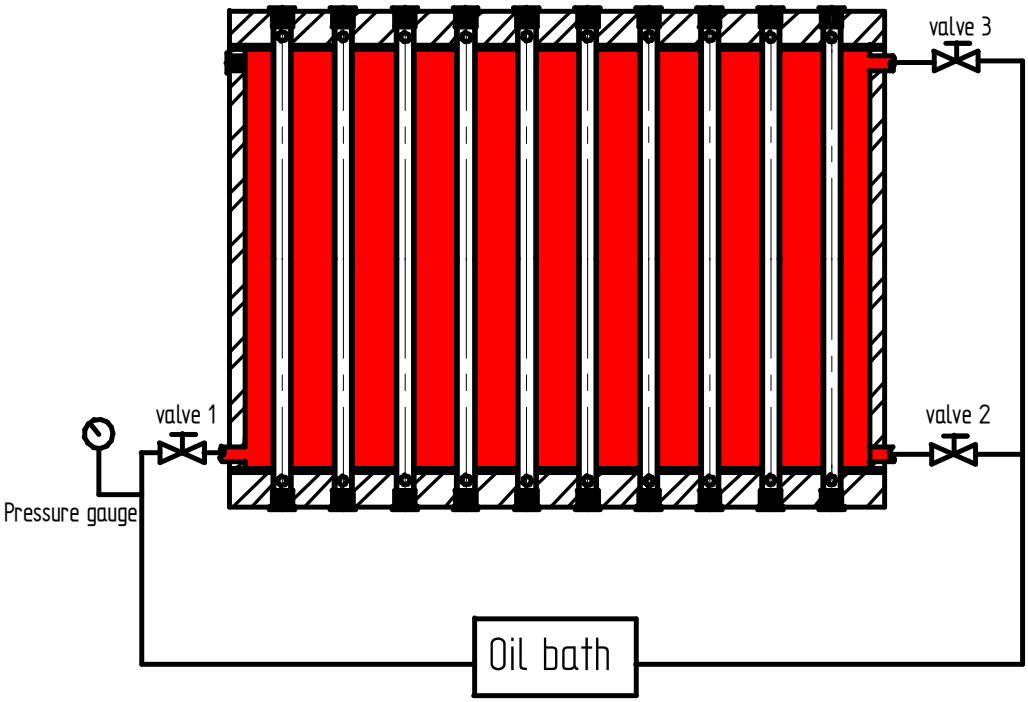

Figure 5.38: The heating oil loop in the RMR.

Table 5.7: Description of two different start-up heating procedures for the RMR

Procedure (1)					
Steps	**Time [min]**	**Valve 1**	**Valve 2**	**Valve 3**	**Pressure bar(g)**
1	0	Open	Open	Open	**0.3**
2	20	Open	Partially closed	Open	**0.4**
3	120	Open	Partially closed	Open	**0.3**

Steady state conditions were achieved after ~ 2 h.

Procedure (2)					
Steps	**Time [min]**	**Valve1**	**Valve 2**	**Valve 3**	**Pressure bar(g)**
1	0	Open	Open	Open	**0.3**
2	20	Open	Closed	Open	**2.5-2.9**
3	90	Open	Closed	Open	**0.5**

Steady state conditions were achieved after ~ 1 h

5.7 General discussion of experimental errors

In this section experimental errors are reviewed, so that their impact on the key conclusions presented at the end of this chapter may also be taken into account.

5.7.1 Experiments in the continuous flow RMR

Temperature: This was measured with K type thermocouples, and when measuring 110 ºC, this type of measurement is generally within ± 2.2 ºC. However, temperature could have varied along the length of the RMR by ± 10 ºC, which would drop to ±3 ºC after the first reaction section. The value assigned to an experiment was based on the measured the fluid temperature inside the reaction sections. To pre-heat the fluid 60% of the first reaction section was filed with just spacers.
These errors would have no significant impact on the conclusions formed.

Analysis of the composition of the liquid phase: The same comments apply, as discussed earlier in Section 5.5.5.1
The resulting errors in the values reported:

at a low conversion of 30 %, then the value could be expressed as = 30 ±2%, and
at a high conversion of 90 % then the value could be expressed as = 90 ±1%.

and

at a low selectivity of 60 %, then the value could be expressed as = 60 ±2%, and
at a high selectivity of 99 % then the value could be expressed as = 99 ±0.5%.

This level of error could affect the interpretation of some of the data in Figures 5.36 and 5.37, as the difference in performance between the cases studied for some of the conditions is small. Otherwise, these errors would have no significant impact on the conclusions formed.

Liquid flow in the reactor: The fluid was pumped into the reactor, by a positive displacement piston pump. At a prescribed setting on the pump a quantity of liquid was collected in a measuring cylinder over a known interval of time, and the liquid flow rate was calculated. For example, at a flow of 1 L h^{-1}, the error was estimated to be ±5 ml, which corresponds to ±0.5% of the liquid flow. This would have no significant impact on the conclusions formed.

Pressure: This was measured with pressure transducers and a pressure gauge.
A back-pressure valve was used to control the pressure. For example, operating at 12 bar(g), the pressure only varied by ±0.5 bar.
This error has no significant impact on the conclusions formed.

Pressure drop: This was measured with a differential pressure transducer. For example, at a reading of 0.3 bar, the error was in the region of ±0.01 bar.
This has no significant impact on the conclusions formed.

Gas flow: The flow of gas was controlled with a mass flow controller, and this had been calibrated at the operating conditions. The error in flow was estimated to be:
at a flow of 0.818 L min^{-1} of oxygen, then the value = 0.818 ±0.002.

This would not have had any significant impact on the conclusions formed, especially as under most conditions, excess air was used.

Monolith dimensions: There was a slight variation in the o.d. of the monoliths. This variation was less than in the first batch of monolith used in the STMR.
For the RMR the monolith o.d. was found to range from 21.9 to 22 mm. This slight variation would not have had any significant impact on the conclusions formed.
Monolith length was 50 mm and varied by ±0.5 mm, again this would have little impact on final conclusions.

5.8 Interim summary conclusion

(a) Based on the work in this chapter, scale-up from the Single Tube Monolith Reactor (STMR) to the pilot-scale RMR preceded relatively smoothly, and the method of coating a large number of monoliths with the Pt catalyst for pilot-scale work was a great success.

(b) It was demonstrated that the catalyst system was robust, with little loss in activity even after 160 h of operation, with many start-ups and shut-downs of the reactor (approximately 25). This was very encouraging.

(c) The transition from Step 2 to Step 3 in the methodology developed in this thesis was demonstrated, and considered a success.

(d) The pilot-scale RMR reactor was successfully operated, and as the length of catalytic zones in the reactor was extended, high conversions could be achieved. The pressure drop was also relatively low and constant during the course of extended runs (e.g. maximum of 0.3 bar(g)). These were all significant achievements at this scale of operation.

(e) Based on the work, there were also some recommendations. The most important, was to split the RMR into two smaller sections, so as to reduce the stress from pressure on the hot-oil side of the RMR. The length of the catalytic tubes will be maintained the same, but each unit will consist of 5 catalytic tubes (rather than 10). This is now being implemented.

References

Bavykin, D.V., Lapkin, A.A., Kolaczkowski, S.T. and Plucinski, P.K., 2005. Selective Oxidation of Alcohols in a Continuous Multifunctional Reactor: Ruthenium Oxide Catalysed Oxidation of Benzyl Alcohol. *Applied Catalysis A: General,* 288, pp. 175-184.

Sinnott R.K., 2005. In: Coulson & Richardson's chemical engineering, ed. Voulme 6. 4th ed. Oxford: Elsevier's Science & Technology

Dziubinski, M., Fidos, H., and Sosno, M., 2004. The flow pattern map of a two phase non- Newtonian liquid-gas flow in the vertical pipe. *International Journal of Multiphase Flow.* 30, pp. 551-563.

Fogler, H.S. 2006. *Elements of Chemical Reaction Engineering*. 4th ed. United States of America: Pearson Education International.

Kolaczkowski, S., Pluncinski, P. and lapkin, A., 2007. Selective Oxidation of Benzyl Alcohol in a Pilot Scale Multichannel Reactor. Proceeding on *1st International Congress on Green Process Eng.*, Toulouse,April 2007. Paris, France, pp.1-8.

Kolaczkowski, S.T, 2008. *Apparatus and Process for use in three-Phase Catalytic Reactions.* International Application Published Under The Patent Cooperation Treaty (PCT), WO2008/040999 A2.

Levenspiel, O. 1999. *Chemical Reaction Engineering*. 3rd ed. United States of America: John Wiley & Sons.

Plucinski, P.K., Bavykin, D.V., Kolaczkowski, S.T and Lapkin, A.A., 2005 a. Application of a structured multifunctional reactor for the oxidation of a liquid organic feedstock. *Catalysis Today*, 105, pp. 479-483.

Plucinski, P.K., Bavykin, D.V., Kolaczkowski, S.T and Lapkin, A.A., 2005 b. Liquid-Phase Oxidation of organic Feedstock in a Compact Multichannel Reactor. Ind. *Eng.Chem. Res*., 44, pp. 9683-9690.

MAST Carbon, http://www.mastcarbon.co.uk/, (3st August 2011)

Wilson, T., and Kolaczkowski, S.T., 2007. Partial oxidation for the pharmaceutical industry. CE30122 MEng Research Project. University of Bath, Chemical Engineering Department.

CHAPTER 6

CONCLUSIONS AND RECOMMENDATIONS FOR FURTHER WORK

6.1 Conclusions

6.1.1 In this thesis a methodology has been described, developed and tested, to illustrate how a new form of continuous flow reactor could be developed, as an alternative to the traditional batch reaction system used in the pharmaceutical industry. Any new approach involving a flow reactor, should be used at an early phase in the production of new drugs, as this influences the way in which such processes are then scaled-up.

6.1.2 There are a number of interesting approaches in the literature, which include the use of micro-channels in compact reactors and magnetic catalytic particles. However, in this thesis, the use of 'mm to cm' scale reaction systems was explored, using mm scale channels in monolith supports.

Based on the work described in Chapter 3 on 'borrowing hydrogen':

6.1.3 It was shown that the novel homogeneous catalytic pathway, based on 'borrowing hydrogen' could be extended and used to make amines in a continuous process, with the catalyst retained and fixed in a packed bed. This was clearly a major achievement and one on which other researchers working on pharmaceutical applications can build.

(a) In the batch experiments, it was not easy to detect if catalyst leaching was going to be a major problem. This is an important observation from a 'methodology' perspective.

(b) The Ru catalyst was clearly very active as a 70% conversion with 100% selectivity was achieved. Unfortunately catalyst leaching occurred under certain conditions. It was postulated that this was due to interaction between morpholine and Ru in the liquid phase.

(c) In batch experiments, the use of Pt/C catalyst showed some interesting initial results, however, the transfer of this particular system from batch to continuous was found to have complications and catalyst leaching.

(d) Unfortunately, a point was reached with this reacting system, where it was not possible to proceed further to Step 3 (pilot-scale), as the chosen combination of catalyst/support and reactants/solvent was shown to be insufficiently robust. This also reflects the reality of developing a system in a batch reactor which appears to work, and then problems are noticed at the Step 2 stage (small continuous-flow). It is far better to realize the problem in Step 2, rather than in Step 3 (pilot-plant), where the costs are significantly higher.

Based on the work described in Chapter 4 on the benzyl alcohol to aldehyde kinetics on Pt/C catalyst:

(e) For the Pt/C catalyst (with a loading of 2.7 wt% Pt), and for the reaction conditions studied in Chapter 4, the reaction rate expression was of the following form:

$$r_{BA} = -\frac{dC_{BA}}{dt} = k_s \times [C_{BA,s}]^{0.442} \times [C_{O_2,s}]^{0.005}$$

where:

$$k_s\,|_{atT_1} = 0.019 \exp\left(-\frac{24.4\times10^3}{RT}\right) \qquad T \text{ range from 130 ºC to 110 ºC}$$

or

$$k_s\,|_{atT_2} = 0.016 \exp\left(-\frac{49.6\times10^3}{RT}\right) \qquad T \text{ range from 100 ºC to 80 ºC}$$

An activation energy of 24.4 ± 0.1 kJ mol^{-1} (for a temperature range 130 ºC to 110 ºC) and 49.6 ± 0.1 kJ mol^{-1} (for a temperature range 100 ºC to 80 ºC)

were determined for the Pt, and the reaction order with respect to benzyl alcohol = 0.442. As excess oxygen was used, it is not surprising to find the order with respect to oxygen = 0.005, which is close to zero.

Based on the work described in Chapter 5 on the STMR & RMR:

(f) The Single Tube Monolith Reactor (STMR) was shown to be a very useful experimental reactor to test catalysts at the Step 2 phase in the methodology developed in this thesis. The implemented design modifications (improvement in spacer design, and PTFE sleeves on monoliths), proved beneficial. This was also illustrated in the visual flow experiments (air/water), where the gas/liquid flow was seen to be relatively uniform, and the spacers and monoliths created fine gas bubbles in the liquid phase.

(g) Scale-up from the STMR to the RMR proceeded relatively smoothly, and the design of the RMR was flexible, and enabled the catalyst to be inserted and removed relatively easy.

(h) For the range of conditions tested, flow direction in the reactor was found to be important, and the upward flow direction was preferred. This ensured that high conversions were achieved in the reactor, with a higher level of selectivity.

(i) The catalyst system was tested in the STMR for a period of 160 h, and this is a significant run-time relative to many experiments that are described on such catalysts in the literature. The TON was estimated to be > 2,600, and catalyst deactivation was very low at 0.0002 h^{-1}. Tests for catalyst leaching into the liquid phase (using Atomic Absorption Spectroscopy), could not detect the presence of Pt at a detection limits of 2 ppm..

(j) A catalyst coating method was developed, which was successfully applied to a large quantity of monoliths (in batches of 25). This enabled testing at a pilot-plant scale to be progressed in the RMR.

(k) The maximum conversion of benzyl alcohol to benzylaldehde at the specified conditions that was achieved was:

~ 95% in a single pass run in the RMR, and

~ 99% in the STMR in a recycle run.

This suggests that equilibrium thermodynamics are not limiting the reaction, and it is possible to achieving very high conversions. However in both cases at such high conversions, selectivity also decreases down to ~ 60%.

(l) Experiments were performed at pilot-scale in the RMR, demonstrating not only the possibility of high conversions, but also the opportunity for multi-stage sampling and gas injection in such a design.

(m) Throughout the experiments, the pressure drop across the catalytic tubes in the RMR remained relatively low and steady during the various experiments (e.g. with 50 monoliths and 70 spacers, using 8 catalytic tubes, $\Delta P = 0.3$ bar). This was a great achievement, as pressure drop was the main reason why the earlier attempts (in the EU project) of using powdered catalysts in a fixed bed pilot-scale reactor had failed.

6.2 Recommendations for the further work

Based on the work described in Chapter 3

(i) Although a catalytic pathway, based on 'borrowing hydrogen' is clearly very promising and it provides a greener and more atom efficient route for the production of secondary and tertiary amines, further work is necessary to identify a more robust catalyst system.

Based on the work described in Chapter 5

(ii) It would be interesting to perform RTD studies on the RMR. However, this will not be an easy task. It would also be interesting to learn more about the actual two-phase flow patterns inside the monolith channels.

(iii) Although a method of catalyst recovery from a spent solution was tested at a significant scale – it would be interesting to test the catalytic activity of the recovered Pt, when used as a catalyst.

(iv) There is clearly much work that could be done, to explore further the performance of the RMR, across a wider range of flow and operating conditions.

(v) Further work could also be done to explore the effect of channel size in the monoliths used as catalyst supports. Many variations could be studied in the choice of catalyst support.

(vi) It was recommended to split the present size of RMR into two smaller sections, so as to reduce the stress from pressure on the hot-oil side of the RMR. The length of the catalytic tubes should be maintained the same, but each unit should consist of 5 catalytic tubes (rather than 10). This is now being implemented.

(vii) Finally, based on a visit to GSK and discussions with Lilly, it was decided, that a bench-top continuous flow reactor, in which smaller diameter (4 to 7 mm) catalytic monoliths could be tested, in a bench-top scale rig, would be very useful at the start of Step 2 work. This would also help to engage the chemists developing the new formulations at an early stage in the process. By retaining the same size of channel inside the monolith, scale-up to the RMR would also then be easier. An outline idea of what this type of reactor may look like is shown in Figure 6.1 and Figure 6.2.

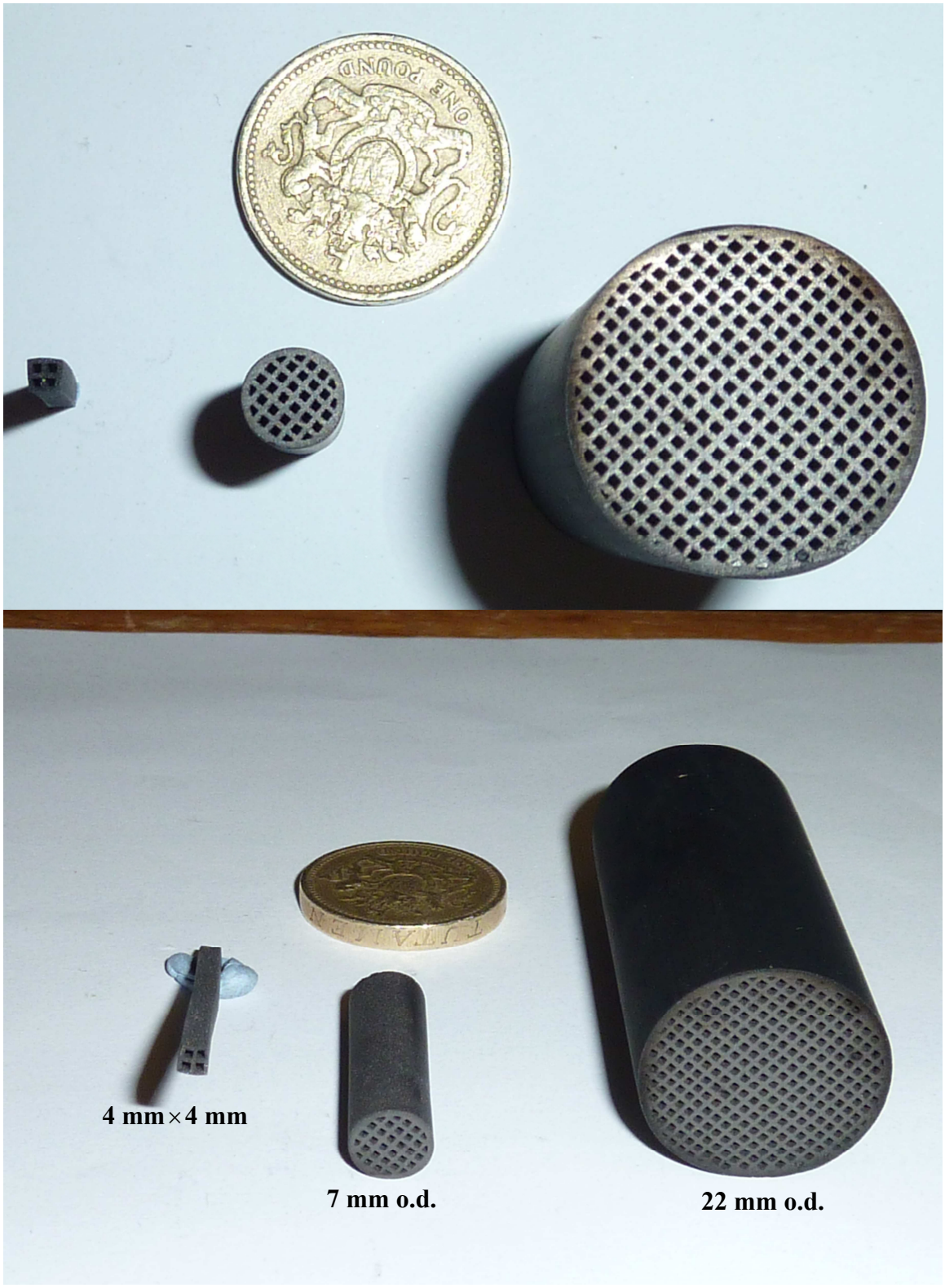

Figure 6.1: Images of three different sizes of carbon monoliths.

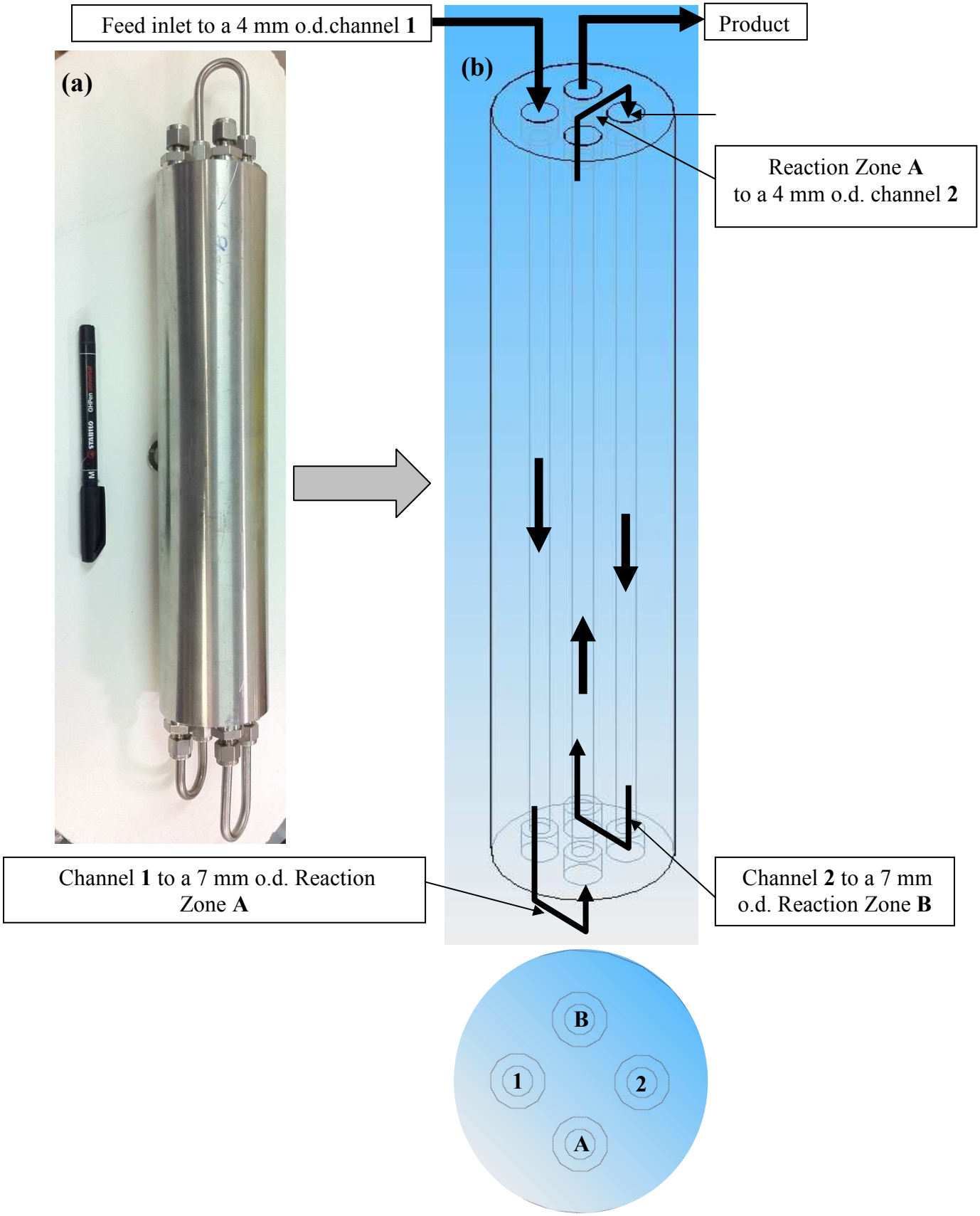

Figure 6.2: The design of the new bench-top monolith reactor "Mini-Mo": (a) Side view of the Mini-Mo, (b) 3D drawing of the Mini-Mo.

Appendix A

A copy of paper on “Production of pharmaceuticals: amines from alcohols in a continuous flow fixed bed catalytic reactor”
Published in: Chemical Engineering Research and Design, 2010

Appendix B

B-1 Calculating Henry's constant

In the literature there is a lack of information as to the value of Henry's constant for oxygen in a feed mixture of: benzyl alcohol, dioxane and water. However it was possible to make use of the simulation package, known as ASPEN+, in order to:

- perform a hypothetical flash calculation (to determine the mole fractions of species in the liquid and vapour phases), and
- then to back-calculate Henry's constant from such data.

In Aspen, the Henry's constant model is used when Henry's Law is applied to calculate the solubility (K-value) for dissolved gas components in a liquid mixture. It is available in active coefficient property methods, such as the WILSON property method.

The model calculates Henry's constant for a dissolved gas component (i), in a solvent that could consists of one or more components. For a single component, A, acting as the solvent, then:

$$\ln(H_{i,A}) = a_{i.A} + b_{i,A}\mathrm{T}^{-1} + c_{i,A}\ln\mathrm{T} + d_{i,A}\mathrm{T} + e_{i,A}\mathrm{T}^{-2} \qquad \text{(B-1)}$$

where:

T is the temperature

$a_{i.A}, b_{i,A}, c_{i,A}, d_{i,A}, e_{i,A}$ are coefficients, specified for each solute-solvent pair.

The coefficients can be obtained from regression of experimental gas solubility data. According to (Aspen+ User Guide, 2000) the Aspen Physical Property System has a large number of built-in Henry's constants for many solutes in solvents. These

parameters were obtained using data from the Dortmund Databank, and outside the available temperature range, Aspen uses a method of linear extrapolation (based on $\ln(H_{i,A})$ *versus* T).

Before calculating the value of Henry's constant for the feed stock mixture, Aspen was tested using a mixture of oxygen/water, and a mixture of nitrogen/water, for which there is published data. This was performed as a check on the way in which this program was used.

(a) Oxygen/water: In the first run, a flash simulation was constructed to estimate the mole fraction of species in the liquid and vapour phases (x_i and y_i) at 25ºC and 1 atm , see Figure B1, and the results are shown in Table B1.

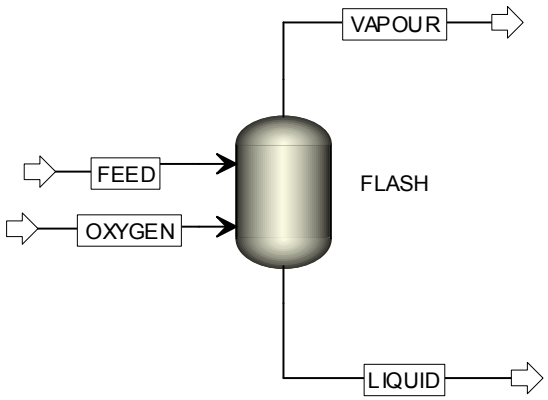

Figure B1: A flash drum simulation to estimate the mole fractions in the vapour and liquid phases.

Table B1: Mole fractions in both liquid and vapour phases determined using Aspen (at 25ºC and 1 atm).

Species	Feed (mol%)	Liquid (mol fraction)	Vapour (mol fraction)
Oxygen	10	2.226569×10^{-5}	0.9687114
Water	90	0.99997778	0.031289

The values in the table were then used to back-calculate Henry's constant using:

$$H_{O_2} = \frac{P_T y_{O_2}}{x_{O_2}} \qquad \text{(B-2)}$$

where:

P_T is the total pressure, atm,

y_{O_2} is the mole fraction of oxygen in the vapour phase, and

x_{O_2} is the mole fraction of oxygen in the liquid phase.

Therefore:

$$H_{O_2} = \frac{1 \times 0.9687114}{2.226569 \times 10^{-5}} = 43{,}507 \text{ atm.}$$

The calculated values were then compared with Henry's constant published in Perry *et al*. (2008), see Table B3. A good match was obtained.

(a) Nitrogen/water: This second simulation was performed at 25ºC and 1 atm, and the results are presented in Table B2.

Table B2: Mole fractions in both liquid and vapour phases determined using Aspen (at 25ºC and 1 atm).

Species	Feed (mol%)	Liquid (mol fraction)	Vapour (mol fraction)
Nitrogen	10	1.136473×10^{-5}	0.9687111
Water	90	0.9999886	0.03128892

From these:

$$H_{N_2} = \frac{1 \times 0.9999886}{1.136473 \times 10^{-5}} = 87{,}991 \text{ atm}$$

Comparing this in Table B3 with published data, a reasonable match has also been obtained.

Table B3: A comparison between calculated values of Henry's constant with data in Perry *et al*. (2008), at 25ºC and 1 atm.

System	Feed (mol%)	Calculated value (atm)	Value from literature (atm)
Oxygen-Water	10% oxygen	43506.91	43400
Nitrogen-Water	10% nitrogen	87990.52	84600

(c) Example calculation for reaction feed mixture: An example of a simulation using Aspen for the feed mixture is illustrated in Table B4.

Table B4: Example of a simulation using Aspen (at 110ºC and 8 bar).

Components	Feed (mol h^{-1})	Liquid (mol fraction)	Vapour (mol fraction)
Oxygen	3.87	0.0064143	0.9875868
Water	5	0.0034408	0.0027117
Dioxane	10.4	0.0348354	0.0056889
Benzyl alcohol	0.97	0.9553096	0.0040126
Nitrogen	0.00	0.0000000	0.0000000

The data from Table B4, was then used to back-calculate Henry's constant as follows:

$$H_{O_2} = \frac{8 \times 0.9875868}{0.0064143} = 1{,}232 \text{ bar}$$

References

Perry, R. H. and Green, D.W. 2008. *Perry's Chemical Engineering Handbook*. Physical and chemical data, 8th ed. United States of America: McGraw-Hill.

Aspen Plus User Guide., 2000. Physical Property Parameters and Data.Version 10.2. Aspen Technology, Inc.

Appendix C

C-1 Experimental data

Raw data for the experiments performed in Chapter 5 are listed in this appendix. The location of the points where the temperature and pressure were measured is illustrated in Figures C-1 and C-2.

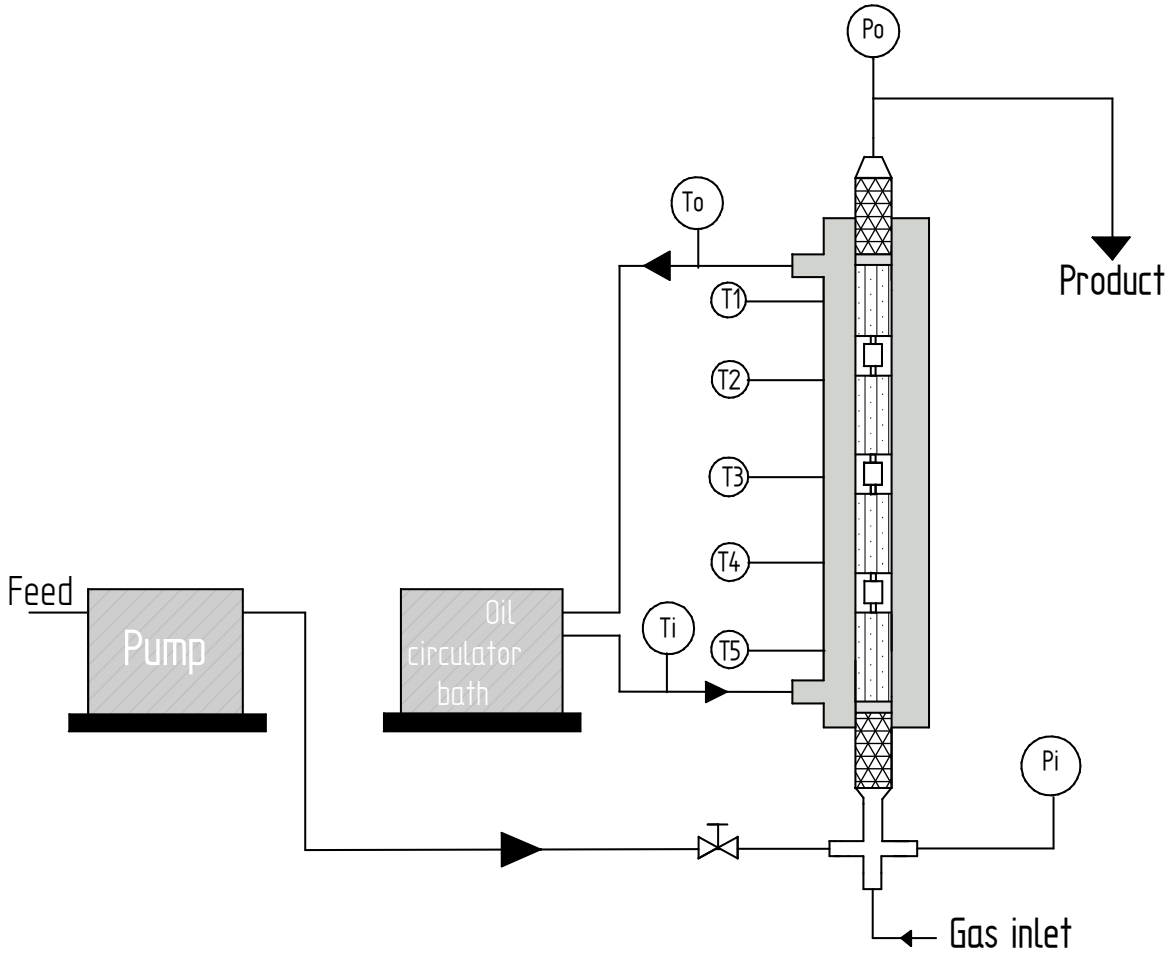

Figure C-1: Schematic diagram of the STMR.

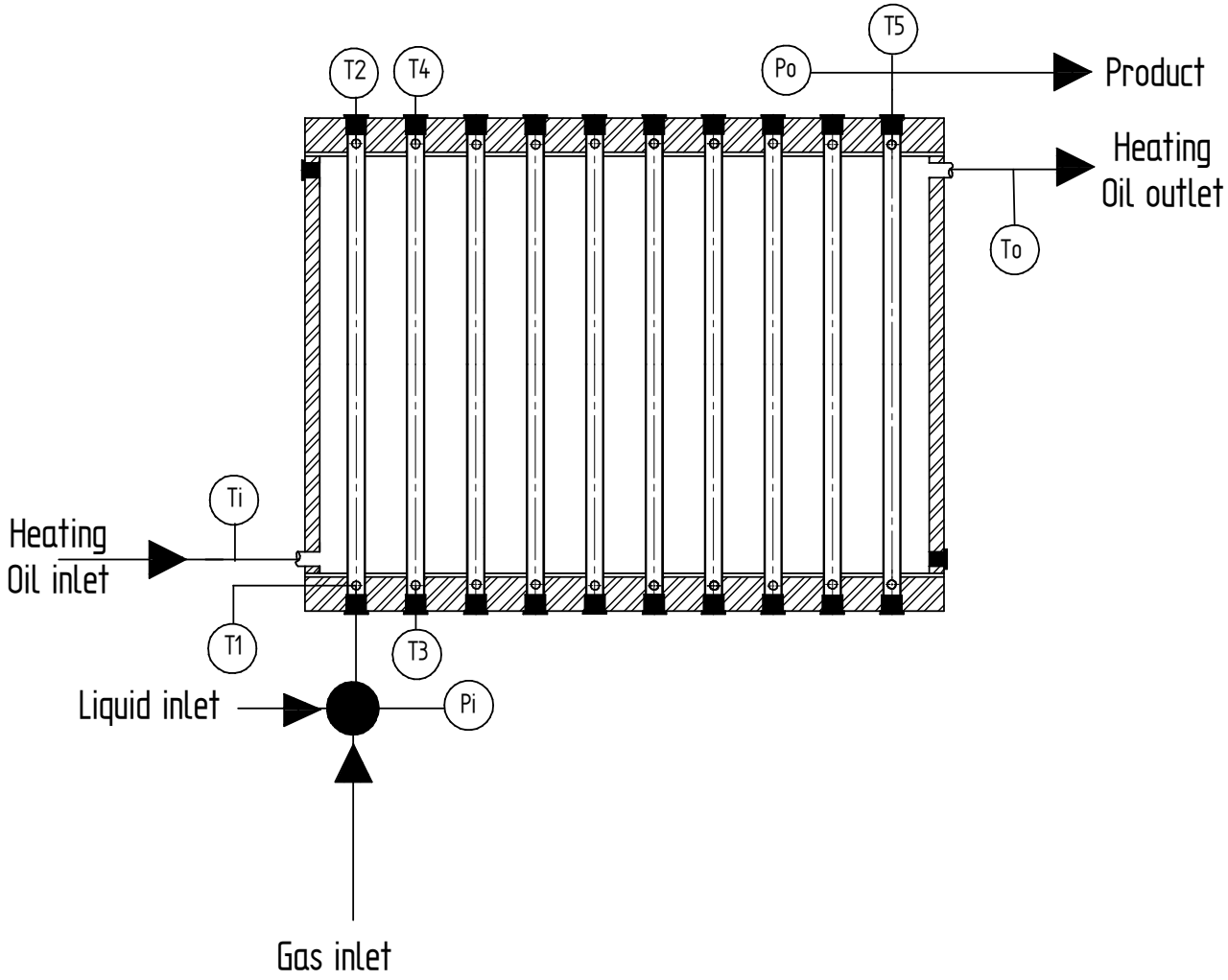

Figure C-2: Schematic diagram of the RMR.

Table C-1: Data for Figure 5.14

Time at which sample was taken[(a)] [h]	O_2 vol% = 100		Liquid feed flow rate[(b)] [L h^{-1}]	Reactor temperature [°C]							Pressure bar(g)			Conversion [%]	Selectivity [%]
	Total gas feed flow rate [L min^{-1}]	Excess O_2 [%]		T_o oil outlet	T1 surface (top)	T2 surface	T3 surface	T4 surface	T5 surface (bottom)	T_i oil inlet	P inlet	P outlet	ΔP [bar]		
1.5	0.13	-50	0.5	113	110.8	110.4	110.3	110.4	110.7	112.4	8.4	8.39	0.01	24.22	100
3.0	0.27	0	0.5	112.9	110.7	110.4	110.3	110.3	110.7	112.4	8.4	8.4	0	39.23	100
4.5	0.40	50	0.5	112.9	110.8	110.4	110.1	110.4	110.7	112.3	8.5	8.46	0.04	56.09	99.53
6	0.53	100	0.5	113	110.7	110.4	110.3	110.4	110.7	112.4	8.4	8.4	0	65.73	98.22
7.5	0.80	200	0.5	112.9	110.8	110.4	110.3	110.4	110.7	112.4	8.3	8.28	0.02	77.95	85.67
9	1.23	359	0.5	112.9	110.8	110.4	110.2	110.4	110.7	112.4	8.4	8.39	0.01	87.09	83.43
10.5	0.13	-50	1.0	113.1	110.8	110.4	110.3	110.4	110.7	112.3	8.32	8.31	0.01	31.18	99.67
12	0.27	0	1.0	113	110.7	110.4	110.2	110.4	110.7	112.4	8.4	8.4	0	49.90	98.99
13.5	0.40	50	1.0	113	110.8	110.4	110.3	110.4	110.7	112.3	8.0	8.0	0	58.30	97.58
15	0.53	100	1.0	112.8	110.7	110.4	110.3	110.4	110.7	112.4	8.35	8.34	0.01	67.21	96.27
16.5	0.80	200	1.0	113	110.8	110.4	110.3	110.4	110.7	112.4	8.41	8.40	0.01	80.22	92.81

Continue Table C-1, data for Figure 5.14

Time at which sample was taken[(a)] [h]	O_2 vol% = 100		Liquid feed flow rate[(b)] [L h^{-1}]	Reactor temperature [°C]							Pressure bar(g)			Conversion [%]	Selectivity [%]
	Total gas feed flow rate [L min^{-1}]	Excess O_2 [%]		T_o oil outlet	T1 surface (top)	T2 surface	T3 surface	T4 surface	T5 surface (bottom)	T_i oil inlet	P inlet	P outlet	ΔP [bar]		
18	1.23	359	1.0	113	110.8	110.4	110.3	110.4	110.7	112.4	8.3	8.3	0	82.88	90.96
19.5	0.13	-50	1.5	113	110.8	110.1	110.3	110.4	110.7	112.4	8.41	8.4	0.01	22.1	100
21	0.27	0	1.5	112.9	110.8	110.4	110.1	110.4	110.7	112.4	8.41	8.4	0.01	36.5	100
22.5	0.40	50	1.5	113.1	110.8	110.3	110.3	110.4	110.7	112.4	8.1	8.0	0.1	42.2	100
24	0.53	100	1.5	113.1	110.8	110.3	110.3	110.4	110.7	112.4	8.2	8.0	0.2	46.12	100
25.5	0.80	200	1.5	113.1	110.8	110.4	110.3	110.4	110.7	112.4	8.3	8.30	0	52.21	100
27	1.23	359	1.5	113.1	110.8	110.4	110.3	110.4	110.7	112.4	8.25	7.9	0.35	56.41	99.1

(a) For each set of experiments, samples were taken every 0.5 h. However, conditions at 1.5 h onwards were plotted in Figure 5.14, this represents steady-state.

(b) Composition of feed mixture: 10 vol% benzyl alcohol in a solvent of 90 vol% dioxane and 10 vol% water.

Note: the oxygen concentration in the purge gas stream after the separator was <10 vol%. this was low number because of the extra nitrogen that was added for safety reasons.

Table C-2: Data for Figure 5.15

Time at which sample was taken[(a)] [h]	Total gas feed flow rate [L min^{-1}]	Excess O_2 [%]	Liquid feed flow rate [L h^{-1}]	O_2 vol% in the feed	Reactor temperature [ºC]							Pressure bar(g)			Conversion [%]	Selectivity [%]
					T_o oil outlet	T1 surface (top)	T2 surface	T3 surface	T4 surface	T5 surface (bottom)	T_i oil inlet	P inlet	P outlet	ΔP [bar]		
1.5	0.409	359	0.5	100	113	110.7	110.4	110.2	110.4	110.7	112.4	8.4	8.4	0	87.09	83.43
3.0	0.409	310	0.5	90	113	110.8	110.4	110.3	110.4	110.7	112.3	8.6	8.6	0	84.25	90.17
4.5	0.409	264	0.5	80	112.8	110.7	110.4	110.3	110.4	110.7	112.4	8.35	8.34	0.01	76.41	92.93
6	0.409	219	0.5	70	113	110.8	110.4	110.3	110.4	110.7	112.4	8.4	8.4	0	69.93	97.01
7.5	0.818	359	1.0	100	112.9	110.8	110.4	110.3	110.4	110.7	112.4	8.3	8.28	0.02	82.88	90.96
9	0.818	310	1.0	90	112.9	110.8	110.4	110.2	110.4	110.7	112.4	8.4	8.39	0.01	76.39	93.81
10.5	0.818	264	1.0	80	113.1	110.8	110.4	110.3	110.4	110.7	112.3	8.32	8.31	0.01	70.11	94.12
12	0.818	219	1.0	70	113	110.7	110.4	110.2	110.4	110.7	112.4	8.5	8.5	0	61.22	97.49
13.5	1.23	359	1.5	100	113	110.8	110.4	110.3	110.4	110.7	112.3	8.0	8.0	0	55.09	99.18
15	1.23	310	1.5	90	113.1	110.8	110.4	110.3	110.4	110.7	112.3	8.3	8.28	0.02	54.04	99.45
16.5	1.23	264	1.5	80	113	110.7	110.4	110.2	110.4	110.7	112.4	8.4	8.39	0.01	47.65	99.72
18	1.23	219	1.5	70	113	110.8	110.4	110.3	110.4	110.7	112.3	8.32	8.31	0.01	40.97	100.00

Continue Table C-2, data for Figure 5.15

(a) For each set of experiments, samples were taken every 0.5 h. However, conditions at 1.5 h onwards were plotted in Figure 5.14, this represents steady-state.

(b) Composition of feed mixture: 10 vol% benzyl alcohol in a solvent of 90 vol% dioxane and 10 vol% water.

Note: the oxygen concentration in the purge gas stream after the separator was <10 vol%. this was low number because of the extra nitrogen that was added for safety reasons.

Table C-3: Data for Figure 5.16

Time at which sample was taken[(a)] [h]	O_2 vol% = 70		Liquid feed flow rate[(b)] [L h^{-1}]	Reactor temperature [°C]							Pressure bar(g)			Conversion [%]	Selectivity [%]
	Total gas feed flow rate [L min^{-1}]	Excess O_2 [%]		T_o oil outlet	T1 surface (top)	T2 surface	T3 surface	T4 surface	T5 surface (bottom)	T_i oil inlet	P inlet	P outlet	ΔP [bar]		
1.5	0.818	221	1.0	112.9	110.8	110.4	110.2	110.4	110.7	112.4	8.46	8.46	0	61.22	97.49
3.0	0.818	221	1.0	113.1	110.8	110.4	110.3	110.4	110.7	112.3	10.2	10.19	0.01	70.31	95.39
4.5	0.818	221	1.0	113	110.7	110.4	110.2	110.4	110.7	112.4	12.0	11.99	0.01	83.91	90.57
6	0.818	221	1.0	112.9	110.8	110.4	110.2	110.4	110.7	112.4	14.1	14.07	0.03	83.95	91.53
7.5	0.534	110	1.0	113	110.7	110.4	110.2	110.4	110.7	112.4	8.5	8.48	0.02	51.47	98.93
9	0.534	110	1.0	113	110.8	110.4	110.3	110.4	110.7	112.3	10.4	10.39	0.01	63.24	96.99
10.5	0.534	110	1.0	113.1	110.8	110.4	110.3	110.4	110.7	112.3	12.2	12.17	0.03	70.01	95.78
12	0.534	110	1.0	113	110.7	110.4	110.2	110.4	110.7	112.4	14.0	14.0	0	70.26	96.33

(a) For each set of experiments, samples were taken every 0.5 h. However, conditions at 1.5 h onwards were plotted in Figure 5.14, this represents steady-state.

(b) Composition of feed mixture: 10 vol% benzyl alcohol in a solvent of 90 vol% dioxane and 10 vol% water.

Note: the oxygen concentration in the purge gas stream after the separator was <10 vol%. this was low number because of the extra nitrogen that was added for safety reasons.

Table C-4: Data for Figure 5.17

Time at which sample was taken[(a)] [h]	O_2 vol% = 70		Liquid feed flow rate[(b)] [L h^{-1}]	Reactor temperature [°C]							Pressure bar(g)			Conversion [%]	Selectivity [%]
	Total gas feed flow rate [L min^{-1}]	Excess O_2 [%]		T_o oil outlet	T1 surface (top)	T2 surface	T3 surface	T4 surface	T5 surface (bottom)	T_i oil inlet	P inlet	P outlet	ΔP [bar]		
1.5	0.818	221	1.0	112.9	110.8	110.4	110.2	110.4	110.3	112.4	8.2	8.199	0.001	40.51	99.61
3.0	0.818	221	1.0	113	110.7	110.4	110.2	110.4	110.7	112.4	8.1	8.09	0.01	49.73	99.44
4.5	0.818	221	1.0	113	110.8	110.4	110.3	110.4	110.2	112.3	8.0	7.98	0.02	61.22	97.49
6	0.818	221	1.0	113.1	110.8	110.4	110.3	110.4	110.7	112.3	8.4	8.39	0.01	59.91	98.34
7.5	0.818	221	1.0	112.9	110.8	110.4	110.2	110.4	110.6	112.4	8.5	8.5	0	61.49	97.92
9	0.818	221	1.0	113.1	110.8	110.4	110.3	110.4	110.7	112.3	12.4	12.4	0	50.87	97.56
10.5	0.818	221	1.0	113	110.7	110.4	110.2	110.4	110.7	112.4	12.1	12.09	0.01	65.37	94.28
12	0.818	221	1.0	113	110.8	110.4	110.3	110.4	110.4	112.3	12	12	0	83.91	90.57
13.5	0.818	221	1.0	113.1	110.8	110.4	110.3	110.4	110.7	112.3	12.8	12.8	0	84.0	89.9
15	0.818	221	1.0	113	110.7	110.4	110.2	110.4	110.7	112.4	12.1	12.1	0	84.18	89.9

(a) For each set of experiments, samples were taken every 0.5 h. However, conditions at 1.5 h onwards were plotted in Figure 5.14, this represents steady-state.

(b) Composition of feed mixture: 10 vol% benzyl alcohol in a solvent of 90 vol% dioxane and 10 vol% water.

Note: the oxygen concentration in the purge gas stream after the separator was <10 vol%. this was low number because of the extra nitrogen that was added for safety reasons.

Table C-5: Data for Figure 5.18

Time at which sample was taken[(a)] [h]]	Total gas feed flow rate [L min^{-1}]	Excess O_2 [%]	Liquid feed flow rate[(b)] [L h^{-1}]	O_2 vol% in the feed	Reactor temperature [ºC]							Pressure bar(g)			Conversion [%]	Selectivity [%]
					T_o oil outlet	T1 surface (top)	T2 surface	T3 surface	T4 surface	T5 surface (bottom)	T_i oil inlet	P inlet	P outlet	ΔP [bar]		
Fresh feed																
1	0.818	221	1.0	70	113	110.7	110.4	110.2	110.4	110.1	112.4	12.4	12.39	0.01	73.69	94.30
2	0.818	221	1.0	70	113	110.8	110.4	110.3	110.4	110.2	112.3	12.32	12.31	0.01	75.53	92.80
3	0.818	221	1.0	70	112.8	110.7	110.4	110.3	110.4	110.7	112.4	12.35	12.34	0.01	74.00	93.30
4	0.818	221	1.0	70	113	110.8	110.4	110.3	110.4	110.3	112.4	12.4	12.4	0	74.86	92.83
5	0.818	221	1.0	70	112.9	110.8	110.4	110.3	110.4	110.7	112.4	12.3	12.28	0.02	71.57	93.68
6	0.818	221	1.0	70	112.9	110.8	110.4	110.2	110.4	110.4	112.4	12.4	12.39	0.01	72.51	93.14
7	0.818	221	1.0	70	113.1	110.8	110.4	110.3	110.4	110.7	112.3	12.32	12.31	0.01	71.13	93.44
Recycled feed																
8	0.818	221	1.0	70	113	110.7	110.4	110.2	110.4	110.4	112.4	12.3	12.28	0.02	85.11	90.83
9	0.818	221	1.0	70	113	110.8	110.4	110.3	110.4	110.4	112.3	12.0	12.0	0	98.70	67.48
10	0.818	221	1.0	70	113.1	110.8	110.4	110.3	110.4	110.7	112.3	12.3	12.28	0.02	99.19	65.64

Continue Table C-5, data for Figure 5.18

11	0.818	221	1.0	70	113	110.7	110.4	110.2	110.4	110.7	112.4	12.35	12.34	0.01	99.31	65.43
12	0.818	221	1.0	70	113	110.8	110.4	110.3	110.4	110.2	112.3	12.4	12.4	0	99.22	65.21

(a) Samples were taken every 1h over 7 h, then the product (7 L) was recycled and samples were taken ever 1 h over 4 h.

(b) Composition of feed mixture: 10 vol% benzyl alcohol in a solvent of 90 vol% dioxane and 10 vol% water.

Note: the oxygen concentration in the purge gas stream after the separator was <10 vol%. this was low number because of the extra nitrogen that was added for safety reasons.

Table C-6: Data for Figure 5.20

Time at which sample was taken[(a)] [h]	Total gas feed flow rate [L min^{-1}]	Excess O_2 [%]	Liquid feed flow rate[(b)] [L h^{-1}]	O_2 vol% in the feed	Reactor temperature [ºC]							Pressure bar(g)			Conversion [%]	Selectivity [%]
					T_o oil outlet	T1 surface (top)	T2 surface	T3 surface	T4 surface	T5 surface (bottom)	T_i oil inlet	P inlet	P outlet	ΔP [bar]		
Upward flow, long run																
1	0.818	221	1.0	70	113	110.7	110.4	110.2	110.4	111	112.4	12.4	12.39	0.01	73.69	94.30
2	0.818	221	1.0	70	113	110.8	110.4	110.3	110.4	110.2	112.3	12.32	12.31	0.01	75.53	92.80
3	0.818	221	1.0	70	112.8	110.7	110.4	110.3	110.4	110.5	112.4	12.35	12.34	0.01	74.00	93.30
4	0.818	221	1.0	70	113	110.8	110.4	110.3	110.4	110.7	112.4	12.4	12.4	0	74.86	92.83
5	0.818	221	1.0	70	112.9	110.8	110.4	110.3	110.4	111	112.4	12.3	12.28	0.02	71.57	93.68
6	0.818	221	1.0	70	112.9	110.8	110.4	110.2	110.4	110.6	112.4	12.4	12.39	0.01	72.51	93.14
7	0.818	221	1.0	70	113.1	110.8	110.4	110.3	110.4	110.7	112.3	12.32	12.31	0.01	71.13	93.44
Upward flow, short run																
1	0.818	221	1.0	70	113	111	110	110.6	110.2	110.1	112.4	12.1	12.1	0	78.66	95.35
2	0.818	221	1.0	70	113.1	111	110	110.4	110.2	110.2	112.4	12.4	12.4	0	80.81	93.94
3	0.818	221	1.0	70	113	111	110	110.4	110.2	110.2	112.4	12.4	12.38	0.02	79.91	93.65

Continue Table C-6, data for Figure 5.20

Time at which sample was taken[(a)] [h]	Total gas feed flow rate [L min^{-1}]	Excess O_2 [%]	Liquid feed flow rate[(b)] [L h^{-1}]	O_2 vol% in the feed	Reactor temperature [ºC]							Pressure bar(g)			Conversion [%]	Selectivity [%]
					T_o oil outlet	T1 surface (top)	T2 surface	T3 surface	T4 surface	T5 surface (bottom)	T_i oil inlet	P inlet	P outlet	ΔP [bar]		
4	0.818	221	1.0	70	113	111	110	110.4	110.1	110.2	112.4	12.0	12.0	0	78.89	93.78
Downward flow, short run																
1	0.818	221	1.0	70	114	110.5	110.1	110.2	110.3	110.9	113.4	12.71	12.7	0.01	49.65	83.07
2	0.818	221	1.0	70	113	110.4	110.1	110.3	110.3	110.9	112.3	12.31	12.3	0.01	52.20	77.88
3	0.818	221	1.0	70	113.4	110.5	110.1	110.3	110.3	110.9	113	12.8	12.79	0.01	50.77	78.69
4	0.818	221	1.0	70	113.1	110.3	110.1	110.3	110.3	110.9	112.4	12.71	12.69	0.01	50.66	78.80

(a) Samples were taken every 1h for each set of experiment.

(b) Composition of feed mixture: 10 vol% benzyl alcohol in a solvent of 90 vol% dioxane and 10 vol% water.

Note: the oxygen concentration in the purge gas stream after the separator was <10 vol%. this was low number because of the extra nitrogen that was added for safety reasons.

Table C-7 a: Data for the first pair of bars in Figure 5.32 and Figure 5.33

Time at which sample was taken[(a)] [h]			Liquid feed flow rate[(b)] [L h^{-1}]		Reactor temperature [°C]							Pressure bar(g)			Conversion [%]	Selectivity [%]
	Total gas feed flow rate [L min^{-1}]	Excess O_2 [%]		O_2 vol% in the feed	T_o oil outlet	T1 surface (top)	T2 surface	T3 surface	T4 surface	T5 surface (bottom)	T_i oil inlet	P inlet	P outlet	ΔP [bar]		
STMR: recoated catalyst, 2.7 wt% Pt and 70 vol% O_2																
2	0.818	221	1.0	70	113	110.8	110.4	110.3	110.4	110.7	112.4	12.4	12.4	0	74.86	92.83
STMR: recoated catalyst, 2.7 wt% Pt and 100 vol% O_2																
2	0.818	359	1.0	100	114	110.5	110.1	110.2	110.3	110.9	113.4	12.7	12.7	0	89.23	83.27

(a) Samples were taken after 2 h for each set of experiment.

(b) Composition of feed mixture: 10 vol% benzyl alcohol in a solvent of 90 vol% dioxane and 10 vol% water.

Note: the oxygen concentration in the purge gas stream after the separator was <10 vol%. this was low number because of the extra nitrogen that was added for safety reasons.

Table C-7 b1: Data for the second and the third pair of bars in Figure 5.32

Time at which sample was taken[(a)] [h]	Total gas feed flow rate [L min^{-1}]	Excess O_2 [%]	Liquid feed flow rate[(b)] [L h^{-1}]	O_2 Vol% in the feed	Reactor temperature [ºC] T_i oil inlet	T_o oil outlet	T1	T2	T3	T4	T5	Pressure bar(g) P inlet	P outlet	ΔP [bar]	Conversion [%]	Selectivity [%]
RMR : used catalyst from STMR, 2.7 wt% Pt																
2	0.818	221	1.0	70	130.2	112	64	97	116	114	112	12.1	12	0.101	76.42	95.2
RMR : fresh catalyst from, 2.5 wt% Pt																
2	0.818	221	1.0	70	131	112.5	68	98	119	113	111.8	12.4	12.29	0.11	63.4	100

(a) Samples were taken after 2 h for each set of experiment.

(b) Composition of feed mixture: 10 vol% benzyl alcohol in a solvent of 90 vol% dioxane and 10 vol% water.

Note: the oxygen concentration in the purge gas stream after the separator was <10 vol%. this was low number because of the extra nitrogen that was added for safety reasons.

Table C-7 b2: Data for the second and the third pair of bars in Figure 5.33

Time at which sample was taken[(a)] [h]	Total gas feed flow rate [L min^{-1}]	Excess O_2 [%]	Liquid feed flow rate[(b)] [L h^{-1}]	O_2 vol% in the feed	Reactor temperature [ºC]							Pressure bar(g)			Conversion [%]	Selectivity [%]
					T_i oil inlet	T_o oil outlet	T1	T2	T3	T4	T5	P inlet	P outlet	ΔP [bar]		
RMR : used catalyst from STMR, 2.7 wt% Pt																
2	0.818	359	1.0	100	130.2	112	63.5	99	115	114	112	12.3	12.2	0.1	91.4	85.2
RMR : fresh catalyst from, 2.5 wt% Pt																
2	0.818	359	1.0	100	131	112.5	67	98	118	113	111.8	12.5	12.45	0.15	82.3	96.4

(a) For each set of experiments, samples were taken every 0.5 h. However, conditions at 2 h was plotted in Figure 5.33, this represents steady-state.

(b) Composition of feed mixture: 10 vol% benzyl alcohol in a solvent of 90 vol% dioxane and 10 vol% water.

Note: the oxygen concentration in the purge gas stream after the separator was <10 vol%. this was low number because of the extra nitrogen that was added for safety reasons.

Table C-8: Data for Figure 5.34 a

Time at which sample was taken[(a)] [min]	Total gas feed flow rate [L min^{-1}]	Excess O_2 [%]	Liquid feed flow rate[(b)] [L h^{-1}]	O_2 vol% in the feed	Reactor temperature [ºC]							Pressure bar(g)			Conversion [%]	Selectivity [%]
					T_i oil inlet	T_o oil outlet	T1	T2	T3	T4	T5	P inlet	P outlet	ΔP [bar]		
0	0.818	221	1.0	70	130.2	113	64.5	95.5	115	113	112	12.5	12.19	0.31	0.00	0
10	0.818	221	1.0	70	130	113.5	64.4	95	115	114.5	112	12.3	12.00	0.31	0.00	0
20	0.818	221	1.0	70	130	112	63.5	94	115	113.8	112	12.5	12.19	0.31	0.00	0
30	0.818	221	1.0	70	130.3	113	64.4	94.8	115	113.8	112	12.4	12.09	0.31	0.00	0
40	0.818	221	1.0	70	130.1	112	63.5	96	115	114.1	112	12.11	11.79	0.32	32.94	100
50	0.818	221	1.0	70	130.2	112.2	63.7	96	115	113.8.	112	12.4	12.07	0.33	47.18	100
60	0.818	221	1.0	70	130.1	112	63.5	96	115	114.2	112	12.5	12.09	0.41	62.53	100
70	0.818	221	1.0	70	130.2	112	63.8	96	115	114.1	112	12.5	12.19	0.31	73.35	100
80	0.818	221	1.0	70	130.3	112.3	63.5	96	115	114.1	112	12.3	11.99	0.31	75.68	100
90	0.818	221	1.0	70	130.1	112	63.3	96	115	114	112	12.4	12.10	0.30	86.19	100
100	0.818	221	1.0	70	130.2	112	63.5	96.3	115	114.2	112	12.4	12.09	0.31	88.55	100
110	0.818	221	1.0	70	130.1	112	63.8	96	115	114	112	12.4	12.09	0.31	89.14	100

Continue Table C-8, data for Figure 5.34 a

120	0.818	221	1.0	70	130.2	112	63.5	96	115	114.2	112	12.4	12.09	0.31	89.35	100

(a) Samples were taken every 10 min for each set of experiment.

(b) Composition of feed mixture: 10 vol% benzyl alcohol in a solvent of 90 vol% dioxane and 10 vol% water.

Note: the oxygen concentration in the purge gas stream after the separator was <10 vol%. this was low number because of the extra nitrogen that was added for safety reasons.

Table C-9: Data for Figure 5.34 b

Time at which sample was taken[(a)] [min]	70 vol% O_2 in the feed		Liquid feed flow rate[(b)] [L h^{-1}]		Reactor temperature [ºC]							Pressure bar(g)			Conversion [%]	Selectivity [%]
	Total gas feed flow rate [L min^{-1}]	Excess O_2 [%]		Monolith number	T_i oil inlet	T_o oil outlet	T1	T2	T3	T4	T5	P inlet	P outlet	ΔP [bar]		
120	0.818	221	1.0	18	130.2	112	63.5	96.2	115	114.2	112	12.4	12.09	0.31	63.84	100
120	0.818	221	1.0	32	130.2	112	63.5	96.1	114	114.2	112	12.4	12.09	0.31	81.72	100
120	0.818	221	1.0	50	130.2	112	63.5	96	115	114.2	112	12.4	12.09	0.31	89.35	100

(a) Samples were taken after 120 min for each set of experiment.

(b) Composition of feed mixture: 10 vol% benzyl alcohol in a solvent of 90 vol% dioxane and 10 vol% water.

Note: the oxygen concentration in the purge gas stream after the separator was <10 vol%. this was low number because of the extra nitrogen that was added for safety reasons.

Table C-10: Data for Figure 5.35 a

Time at which sample was taken [min]	Total gas feed flow rate [L min^{-1}]	Excess O_2 [%]	Liquid feed flow rate[(a)] [L h^{-1}]	O_2 vol% in the feed	Reactor temperature [ºC]							Pressure bar(g)			Conversion [%]	Selectivity [%]
					T_i oil inlet	T_o oil outlet	T1	T2	T3	T4	T5	P inlet	P outlet	ΔP [bar]		
0	0.818	359	1.0	100	130.2	112	63.5	96	115	113	112	12.5	12.19	0.31	0.00	0.00
10	0.818	359	1.0	100	130	112	63.4	94.1	114	114.5	112	12.3	12.00	0.31	0.00	0.00
20	0.818	359	1.0	100	130	112	63.5	93	114	113.8	112	12.5	12.19	0.31	19.74	100.00
30	0.818	359	1.0	100	130.3	112	63.4	96.2	115	113.8	112	12.4	12.09	0.31	33.21	100.00
40	0.818	359	1.0	100	130.1	112	63.5	96.3	114.2	114.1	112	12.11	11.79	0.32	48.70	100.00
60	0.818	359	1.0	100	130.2	112	63.7	96	115	113.8.	112	12.4	12.07	0.33	67.41	100.00
80	0.818	359	1.0	100	130.1	112	63.5	96	114.5	114.2	112	12.5	12.09	0.41	88.21	100.00
100	0.818	359	1.0	100	130.2	112	63.8	96.1	115	114.1	112	12.5	12.19	0.31	92.03	89.90
120	0.818	359	1.0	100	130.3	112	63.5	96	115.3	114.1	112	12.3	11.99	0.31	93.60	66.74
140	0.818	359	1.0	100	130.1	112	63.3	96.3	115	114	112	12.4	12.10	0.30	93.70	57.41

(a) Composition of feed mixture: 10 vol% benzyl alcohol in a solvent of 90 vol% dioxane and 10 vol% water.

Note: the oxygen concentration in the purge gas stream after the separator was <10 vol%. this was low number because of the extra nitrogen that was added for safety reasons.

Table C-11: Data for Figure 5.35 b

Time at which sample was taken[(a)] [min]	100 vol% O_2 in the feed		Liquid feed flow rate[(b)] [L h^{-1}]		Reactor temperature [ºC]							Pressure bar(g)			Conversion [%]	Selectivity [%]
	Total gas feed flow rate [L min^{-1}]	Excess O_2 [%]		Monolith number	T_i oil inlet	T_o oil outlet	T1	T2	T3	T4	T5	P inlet	P outlet	ΔP [bar]		
140	0.818	359	1.0	18	130.2	112	63.5	96.1	115	114.2	112	12.4	12.09	0.31	82.05	96.86
140	0.818	359	1.0	32	130.2	112	63.5	96.2	114.8	114.2	112	12.4	12.09	0.31	93.56	57.90
140	0.818	359	1.0	50	130.1	112	63.3	96.1	115	114	112	12.4	12.10	0.30	93.70	57.41

(a) Samples were taken after 140 min for each set of experiment.

(b) Composition of feed mixture: 10 vol% benzyl alcohol in a solvent of 90 vol% dioxane and 10 vol% water.

Note: the oxygen concentration in the purge gas stream after the separator was <10 vol%. this was low number because of the extra nitrogen that was added for safety reasons.

Table C-12: Data for Figure 5.36 and Figure 5.37

Time at which sample was taken [h]	70 vol% O_2 in the feed		Liquid feed flow rate[(b)] [L h^{-1}]		Reactor temperature [ºC]							Pressure bar(g)			Conversion [%]	Selectivity [%]
	Total gas feed flow rate [L min^{-1}]	Excess O_2 [%]		Monolith number	T_i oil inlet	T_o oil outlet	T1	T2	T3	T4	T5	P inlet	P outlet	ΔP [bar]		
One stage gas injection																
2	0.818	221	1.0	18	130	112	63.5	96	115	114.2	112	12.4	11.7	0.3	63.84	100
2	0.818	221	1.0	32	130.2	112	63	96.2	114.8	114.4	111	12.5	12.18	0.32	81.72	100
2	0.818	221	1.0	50	130	112	63.3	96.1	115.1	114	112	12.5	12.2	0.3	89.35	100
Two stages gas injection, Case 1																
2	0.818	221	1.0	18	130.3	112	63.4	96.2	115	113.8	112	12.1	11.8	0.31	68.57	100
2	0.818	221	1.0	32	130.1	112	63.5	96.3	114.2	114.1	112	12.4	12.1	0.3	91.82	59.95
2	0.818	221	1.0	50	130.2	112	63.7	96	115	113.8.	112	12.5	12.1	0.4	95.19	54.97
Two stages gas injection, Case 2																
2	0.818	221	1.0	18	130.2	112	63.7	96	115	113.8.	112	12.4	12.1	0.3	57.32	100
2	0.818	221	1.0	32	130.2	112	63	96.2	114.8	114.4	130.2	12.4	12.1	0.3	79.09	100
2	0.818	221	1.0	50	130	112	63.3	96.1	115.1	114	112	12.5	12.19	0.31	91.76	61.39

Continue Table C-12, data for Figure 5.36 and Figure 5.37

(a) Samples were taken after 2 h for each set of experiment.

(b) Composition of feed mixture: 10 vol% benzyl alcohol in a solvent of 90 vol% dioxane and 10 vol% water.

Note: the oxygen concentration in the purge gas stream after the separator was <10 vol%. this was low number because of the extra nitrogen that was added for safety reasons.

Appendix D

D-1 Calibration plot and error plot for the mass flow meters

The calibration plots were produced using a bubble flow meter to measure gas flow.

Gas: O_2, Figures D-1 and D-2

Temperature: 22 ºC

Inlet pressure: 20 bar(g)

Outlet pressure: 8 to 12 bar(g)

Number of the mass flow meters: 4 (connected in parallel)

Full scale flow: 1.75 L min^{-1}

Flow ranges of the mass flow meters were as follow:

Brooks mass flow meter No 1 = 0.25 L min^{-1}

Brooks mass flow meter No 2 = 0.5 L min^{-1}

Brooks mass flow meter No 3 = 0.5 L min^{-1}

Brooks mass flow meter No 4 = 0.5 L min^{-1}

Gas: N_2, Figures D-3 and D-4

Temperature: 22 ºC

Inlet pressure: 20 bar(g)

Outlet pressure: 8 to 12 bar(g)

Number of the mass flow meters: 4 (connected in parallel)

Full scale flow: 1.75 L min^{-1}

Flow ranges of the mass flow meters were as follow:

Brooks mass flow meter No 5 = 0.25 L min^{-1}

Brooks mass flow meter No 6 = 0.5 L min^{-1}

Brooks mass flow meter No 7 = 0.5 L min^{-1}

Brooks mass flow meter No 8 = 0.5 L min^{-1}

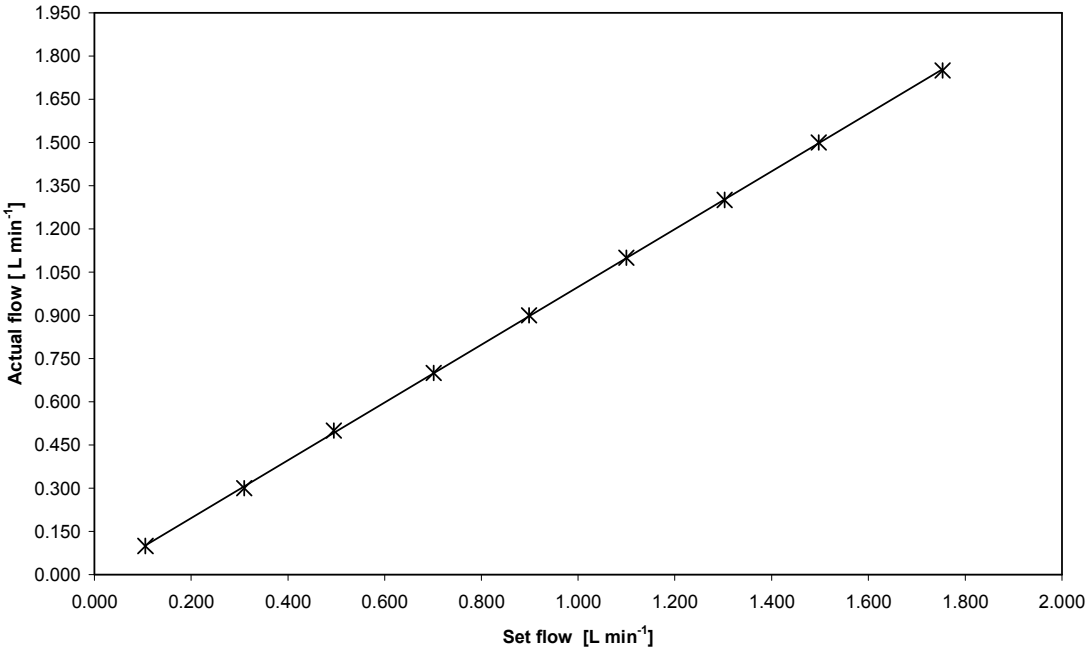

Figure D-1: Calibration curve for oxygen.

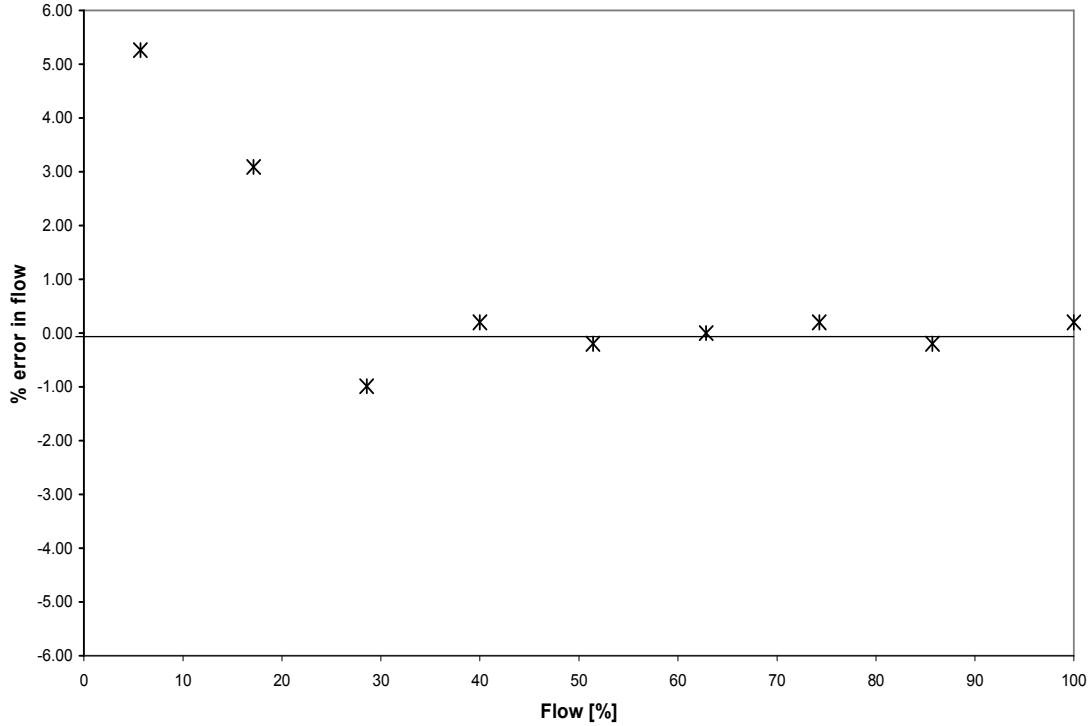

Figure D-2: Calculated error for oxygen.

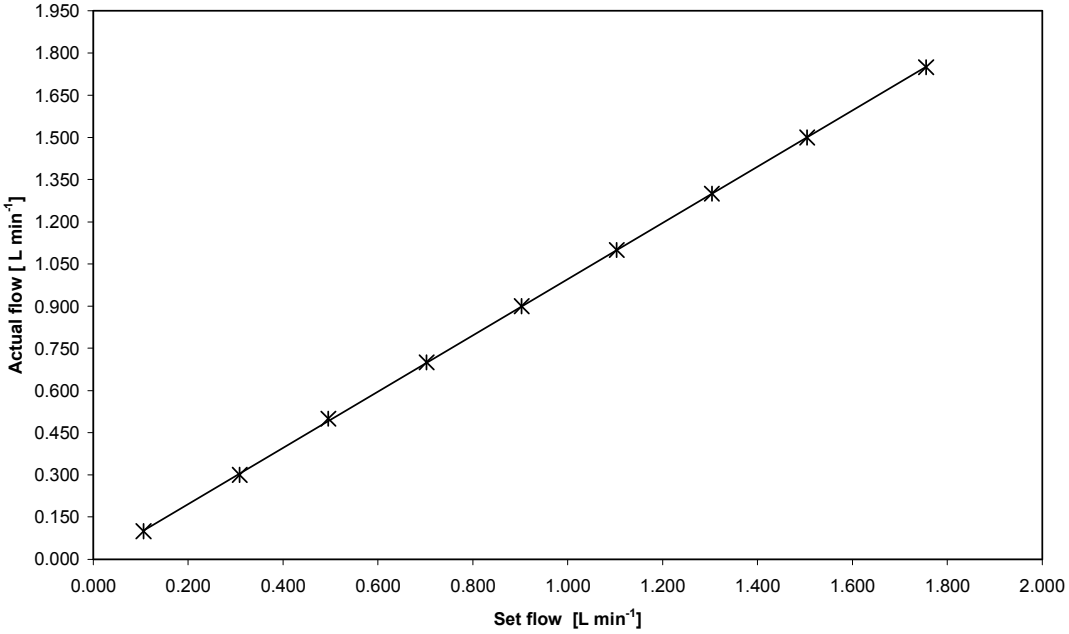

Figure D-3: Calibration curve for nitrogen.

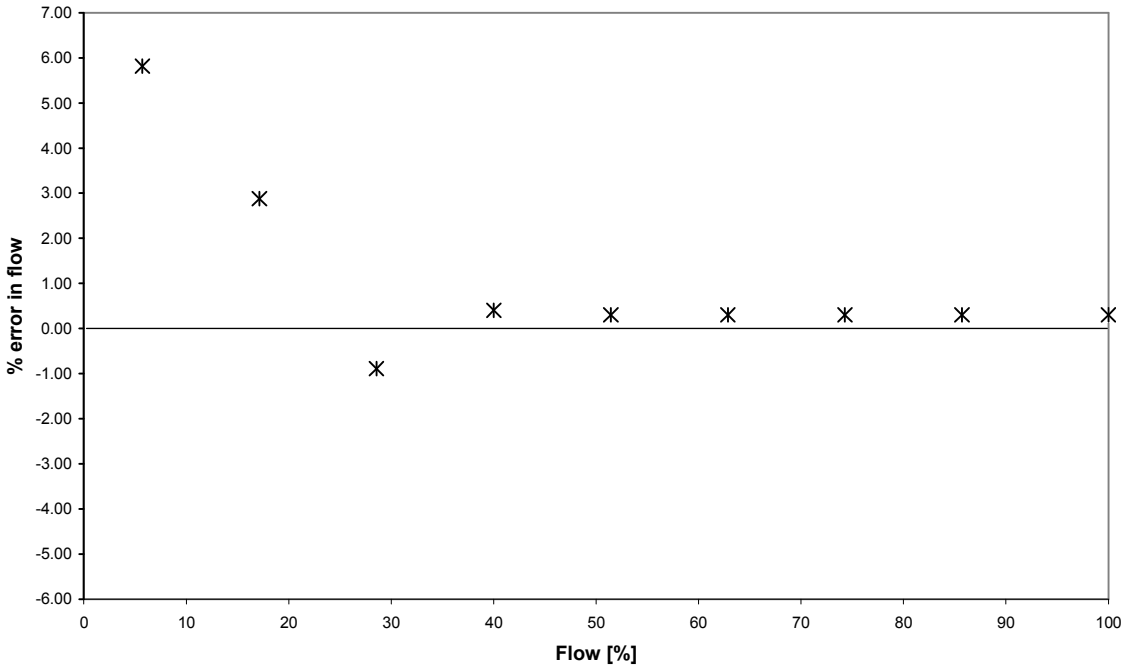

Figure D-4: Calculated error for nitrogen.

Appendix E

D-1 Example calculation to determine the % excess of O_2

For a 10 vol% solution of BA in the solvent (10 vol% water and 90 vol% dioxane), then for a volume of 1 L of solution then the quantities illustrated in Table E-1 are calculated.

Table E-1: Calculating the number of moles in 1 L of solution.

Component	Volume [L]	Density [g L^{-1}]	Mass [g]	Molar mass [g mol^{-1}]	Component mole [mol]
BA	0.1	1044	104.4	108.14	0.97
DX	0.09	1030	916.7	88.11	10.40
W	0.89	1000	90	18.00	5.00

From table E-1, if the volumetric flow rate of solution is 0.5 L h^{-1}, then this corresponds to a molar flow of:

$$\text{molar flow of BA} = 0.483 \text{ mol h}^{-1}$$
$$= 0.008 \text{ mol min}^{-1}$$

Then for the reaction:

$$C_6H_5CH_2OH_{(l)} + 1/2O_{2\,(g)} \rightarrow C_6H_5CHO_{(l)} + H_2O_{(l)} \qquad \Delta H_R \approx -210 \text{ kJ mol}^{-1} \quad (5.1)$$

$$\%\text{ excess } O_2 = \frac{\text{moles of } O_2 \text{ supplied in excess of stoichiometry}}{\text{moles of } O_2 \text{ required by stoichiometry}} \times 100 \qquad (5.2)$$

At 0.5 L h^{-1} liquid feed:

mole flow rate of the benzyl alcohol in the liquid feed = 0.008 mol min^{-1}

mole flow rate of the O_2 required by stoichiometry = 0.004 mol min^{-1}

If the actual volumetric flow rate of O_2 feed to the reactor = 0.4 L min^{-1}, then as 1 mol occupies 22.41 L at STP, then this corresponds:

mole flow rate of O_2 fed to the reactor = 0.018 mol min^{-1}

$$\% \text{ excess } O_2 = \frac{0.018 - 0.004}{0.004} \times 100$$

$$= 350\%$$

The same method was applied for liquid flow rate at 1.0 L h^{-1} and 1.5 L h^{-1}. The summary of the calculation was plotted in Figure E-1 and E-2.

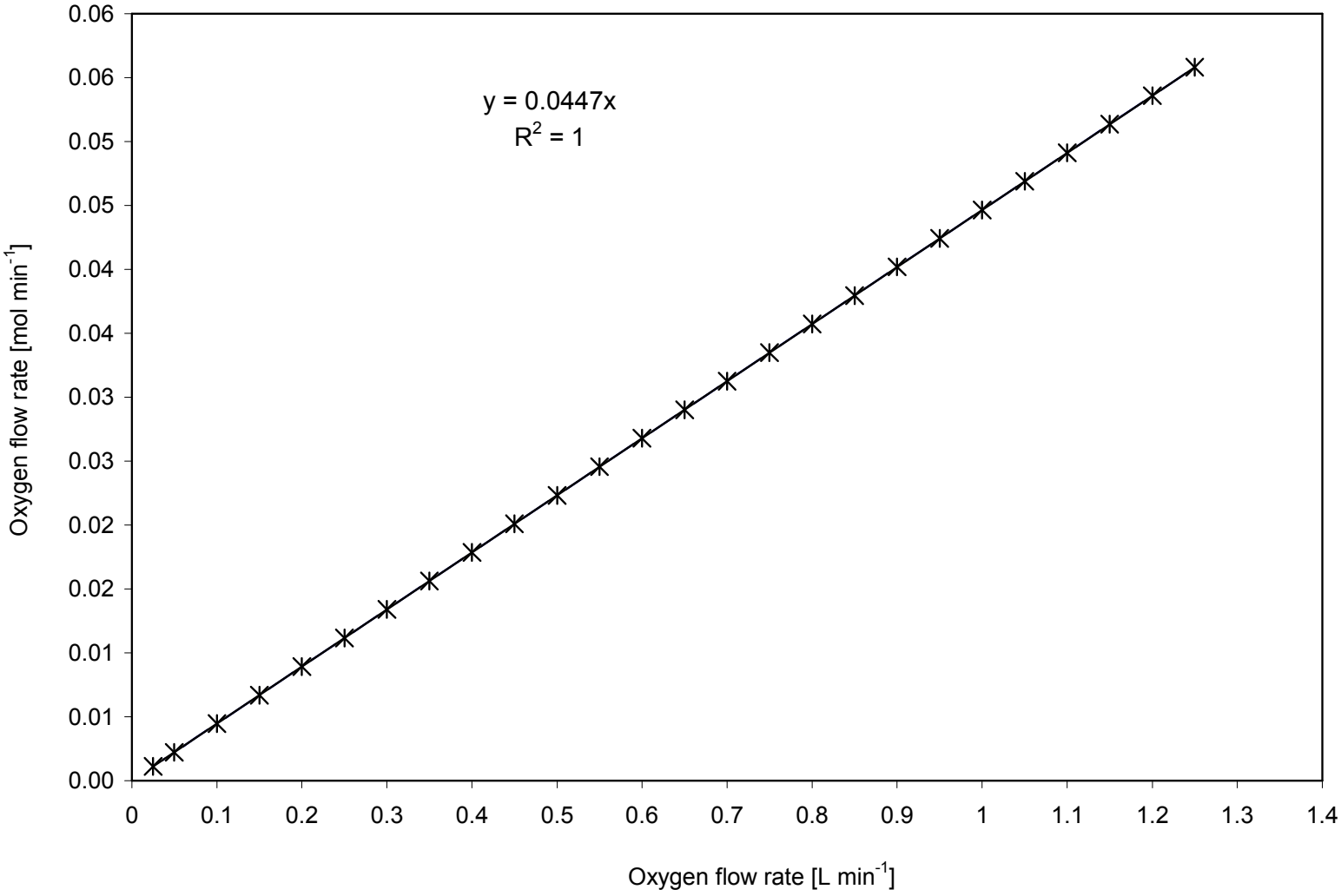

Figure E-1: Plot for the relation between the volumetric flow rate and the mole flow rate of oxygen